



University "Ss Cyril and Methodius"

Institute of Earthquake Engineering and Engineering

Seismology, IZIS, Skopje, Republic of Macedonia

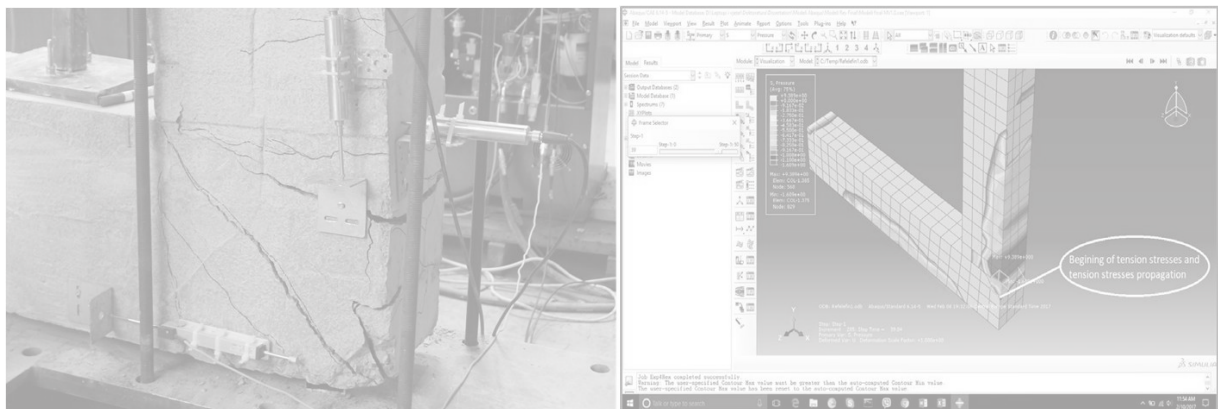


## DOCTORAL DISSERTATION

*Performance of innovative beam-to-column connections in precast industrial buildings*

Veton PIRA,

graduate civil engineer, master of technical science



Skopje, April 2018

## Апстракт

**Клучни зборови: префабрикувана армиранобетонска конструкција, "суви" врски греда – столб отпорни на моменти, анкери, доверливост.**

Неодамна случените земјотреси покажаа дека најслабата точка кај постојните префабрикувани конструкции се врските и дека најголемиот процент на оштетувања кои се јавуваат кај овие системи е директна последица на оштетувањата на врските. Посебно компликувани се врските греда-столб, со акцент на "сувите" врските, за кои во праксата има многу малку примери за соодветни решенија.

Овој проблем е идентификуван и во рамките на докторската дисертација предложени се иновативни проектни решенија на "суви" префабрикувани врски греда-столб, отпорни на моменти кои, од една страна имаат степен на доверливост близок до монолитните армиранобетонски врски, а од друга страна, од конструктивен аспект се доволно едноставни и лесни за примена во градежното инженерство.

Во истражувањата е применет комбиниран експериментално-аналитички пристап. Експерименталните истражувања се реализирани на десет модели, од кои осум се иновативни решенија на "сува" префабрикувана врска греда-столб отпорна на моменти, и два се референтни монолитни армиранобетонски модели. Предложени се три генерални типа на проектни решенија за овие врски кои се релативно едноставни за примена во секојдневната инженерска пракса и тоа: (1) врска во која се предвидени само анкери и отворите се залееани со високовреден цементен материјал; (2) врска кај која анкерите изложени на товар на затегнување се зајакнати со поединечни челични плочи за спречување на лом од извлекување на истите анкери и последователно на врските; (3) врска кај која сите анкери се зајакнати со заедничка челична плоча за да се избегнат сите можни механизми на лом на врската.

Предложените врски се тестирани во случаи на: доминантно свиткување (коефициент на свиткување/смолкнување = 1.5), ист интензитет на свиткување и смолкнување (коефициент на свиткување/смолкнување = 1.0) како и доминантно смолкнување (коефициент на свиткување/смолкнување од 0.5), со цел да се тестира врската со различни можни комбинации на товарење и во услови кога врските се реализираат со вертикално или хоризонтално поставени анкери. Моделите се изложени на соодветно проектиран полу-цикличен програм на товарење и дефинирани се нивните јакостни и деформабилни карактеристики.

Добиените експериментални резултати покажуваа дека: (1) врската греда – столб која беше конструирана само со анкери претрпе крт лом поради ломот на извлекување на анкерите во услови на товар на затегнување; (2) врската греда – столб зајакната со челични плочи покажа дуктилно однесување со значително подобрување на капацитетот за деформабилност во однос на врската која беше конструирана само со анкери. Овој ефект е уште поизразен кај проектните решенија зајакнати со една заедничка плоча; (3) предложените иновативни врски имаат многу поголема јакост на смолкнување од силите на смолкнување кои дејствуваат врз истите и последователно на тоа нивното однесување се карактеризира со свиткување дури и во услови на доминантно смолкнување (коефициент на свиткување/смолкнување = 0.5).

Во рамки на аналитичките истражувања направено е нумеричко микромоделирање на врските со примена на 3D конечни елементи и софтвер посебно развиен за механички врски и склопови (Abagus/CEA V.14). Овој софтвер е селектиран бидејќи врските кај префабрикувани бетонски згради можат да се третираат, со голема доверливост како механички врски поради процесот на монтирање на истите.

Резултатите од нумеричките истражувања покажаа дека дистрибуцијата на напрегањата во врските и во нивните составни компоненти конзистентно ја следи шемата на пукнатини и деформации кај тестираните примероци.

Генерално, добиените резултати се добра основа за примена на предложените иновативни “суви” врски греда-столб, отпорни на моменти, кај префабрикуваните конструкции, со што на истите им се обезбедува поголема робустност и се зголемува нивната компетитивност во споредба со монолитните армиранобетонски конструкции. Треба да се напомене дека реализираниот експериментален програм наметнува одредени ограничувањата врзани со поширока примена на предложените решенија и во тој контекст во дисертацијата се дадени насоки за понатаможни истражувања.

## **ABSTRACT**

**Keywords:** precast reinforced concrete structures, moment-resistant “dry” beam-column connections, dowels, reliability.

Recent earthquakes have shown that the weakest points of existing precast structures are the connections and that the greatest percentage of damage to these systems is a direct consequence of damage to the connections. Beam-column connections, particularly “dry” connections, are considerably complicated. Very few examples of appropriate solutions of these connections are found in practice.

This problem has been identified and innovative design solutions for moment-resistant “dry” precast beam-column connections have been proposed within the frames of the doctoral dissertation. On one hand, these connections are reliable to the extent close to monolith RC connections, while on the other hand, from structural aspect, they are sufficiently simple and easy for application in structural engineering.

A combined experimental-analytical approach has been used in the investigations performed within the doctoral study. The experimental investigations have been realized on ten models out of which eight represent innovative solutions for precast moment-resistant “dry” beam-column connection and two represent referent monolith RC models. There have been proposed three general types of design solutions for these precast connections that are relatively simple for application in everyday engineering practice: (1) a connection with dowels only and openings grouted with high strength cement material; (2) a connection in which the dowels exposed to tensile loads are strengthened by individual steel plates to prevent pullout failure of these dowels and consequently of the connections; (3) a connection in which all dowels are strengthened by a common steel plate to avoid all possible failure mechanisms of the connection.

The proposed connections have been tested in the case of: dominant flexure (flexure/shear ratio = 1.5), flexure and shear of the same intensity (flexure/shear ratio = 1.0) as well as dominant shear (flexure/shear ratio of 0.5) for the purpose of testing the connection under different possible load combinations and in conditions of connections realized by vertically or horizontally placed dowels. The models have been subjected to appropriately designed half-cyclic programme of loading and their strength and deformability characteristics have been defined.

The obtained experimental results have shown that: (1) the beam-column connection constructed of dowels only has suffered brittle failure due to the pullout failure of the dowels under tensile load; (2) the beam-column connection strengthened by steel plates has exhibited a ductile behavior with considerable improvement of the deformability capacity in respect to that of the connection constructed of dowels only. This effect has even been more pronounced in the design solutions strengthened by a common plate; (3) the proposed innovative connections have exhibited a shear strength greater than the shear forces acting upon them and consequently, their behaviour has been characterized by flexure even in conditions of dominant shear (flexure/shear ratio = 0.5).

Numerical micro-modeling of the connections has been made within the analytical investigations by application of 3D finite elements and a software specially developed for mechanical connections and assemblages (Abagus/CEA V.14). This software has been selected since the connections in precast

concrete buildings can be reliably treated as mechanical connections due to the process of their assemblage.

The results from the numerical investigations have shown that the distribution of stresses in the connections and in their constituent components has consistently followed the scheme of cracks and deformations of the tested specimens.

Generally, the obtained results represent a good basis for application of the proposed innovative moment-resistant “dry” beam-column connections in precast structures by which they are provided a greater robustness and a greater competitiveness compared with the monolith reinforced concrete structures. It should be noticed that the realized experimental programme imposes certain limitations associated with the wider application of the proposed solutions and, within that context, directions for further investigations are also given in the dissertation.

## ACKNOWLEDGEMENT

*I would like to thank the Institute of Earthquake Engineering and Engineering Seismology (IZIIS) – Skopje as a scientific institution as well as all the academic staff for accepting me and supporting me during all the phases of my postgraduate studies, including this dissertation thesis work.*

*The greatest gratitude I would like to express to the Supervisor of this dissertation thesis, Prof. Dr. Roberta APOSTOLSKA, who continuously supported and guided me throughout my doctoral studies, starting from the first phase of preparing proposal for dissertation, research work, and experimental program and all the way to dissertation composition. Prof. Roberta's constant support and high professionalism was a key factor for completion of this dissertation.*

*Furthermore, I would like to thank the Laboratory Staff of the University of Pristina, Faculty of Civil Engineering and Architecture, Prof. Dr. Naser Kabashi and Dr. Sc. Arton Dautaj for making possible to conduct actual experiments of the specimens. In specific and especially I would like to thank Dr. Sc. Cenë Krasniqi and Dr. Sc. Lavdim Kurtaj for providing technical support during the experimental programme.*

*Finally and most importantly, I would like to thank my family for being there for me in all aspects during all the time.*

*Veton Pira*

## Contents

<b>List of figures</b> .....	<b>xi</b>
<b>List of tables</b> .....	<b>xx</b>
<b>CHAPTER 1 - Introduction</b> .....	<b>1</b>
1.1 Introduction .....	1
1.2 Objective and Methodology of research.....	4
1.3 Organization of dissertation .....	7
<b>CHAPTER 2 - General Overview of Application of Precast Buildings in Seismic Regions</b> .....	<b>9</b>
2.1 Scope.....	9
2.2 General overview of application of precast buildings.....	9
2.3 Connections in the precast building structures.....	10
2.3.1 Structural type of precast connections.....	11
2.3.1.1 Pinned connections.....	11
2.3.1.2 Fixed connections .....	11
2.3.2 Connections in regard to construction methodology.....	12
2.3.2.1 Wet connections .....	12
2.3.2.2 Dry Connections.....	15
2.4 General behavior of precast building structures with dry connections– weak points.....	17
2.4.1 Typical damages to single story structures under various earthquakes.....	17
2.4.2 Weakness of single story precast structure with pinned beam-to-column connections .....	20
2.4.3 Failure mechanism of dry beam-to-column connections .....	22
2.4.3.1 Failure of the dowel/s .....	23
2.4.3.2 Failure of concrete in the connection.....	23
2.5 Moment resisting connections.....	27
2.5.1 Moment resisting connections constructed as wet connections .....	27
2.5.2 Recent research investigations and publications on moment resisting beam-to-column dry connections conducted under quasi-static loading conditions .....	32
2.5.2.1 Recent investigation performed on dry connections under quasi-static loading conditions .....	32
2.5.2.2 Recent investigation performed on hybrid connections .....	36
2.5.3 Summary of current state regarding moment resisting precast connection .....	40
2.5.4 Coverage of precast moment resisting connections by Eurocode .....	41
2.6 Shaking table experiments of precast frames realized with prefabricated beam-to-column connections .....	42
2.6.1 “Shaking table tests on precast reinforced concrete and engineered cementitious composite/reinforced concrete composite frames”; [Ref.:040].....	42

2.6.2	“Assessment of the seismic design of precast frames with pinned connections from shaking table tests”, [Ref.: 024].....	46
2.7	<i>Gap to be filled</i> .....	51
<b>CHAPTER 3 - Numerical Modeling of Experiments Performed at UL under SAFECAST Project.....</b>		<b>53</b>
3.1	<i>Scope</i> .....	53
3.2	<i>SAFECAST project, description and goals [Ref.: 027]</i> .....	54
3.3	<i>Description of experiments performed at UL under SAFACAST project</i> .....	54
3.4	<i>Analysis of performance of connections</i> .....	57
3.4.1	Analysis of behavior in experiment S 1-1.....	57
3.5	<i>Calibration of non-linear parameters for numerical model</i> .....	59
3.5.1	Selection of non-linear model, type of hysteresis for numerical model .....	59
3.6	<i>Calibration of non-linear parameters of numerical model</i> .....	61
3.6.1	Experiment S1-1, pinned connection with single centric dowel, push-pull loading .....	61
3.6.2	Experiment S1-2, pinned connection with single centric dowel, cyclic loading .....	61
3.6.3	Experiment S-2, pinned connection with single centric dowel, cyclic loading .....	62
3.6.4	Experiment S3-1, pinned connection with single centric dowel, push-pull loading .....	63
3.6.5	Experiment S3-2, pinned connection with single centric dowel, cyclic loading .....	63
3.6.6	Experiment S4, pinned connection with single centric dowel, cyclic loading .....	64
3.6.7	Experiment S5-2, pinned connection with single centric dowel, cyclic loading .....	65
3.6.8	Experiment S6-1, top eccentric connection, push-pull loading .....	65
3.6.9	Experiment S6-2, top eccentric connection, cyclic loading .....	66
3.6.10	Experiment S7-2, intermediate story connection, strong column, cyclic loading .....	66
3.6.11	Experiment S8-1, intermediate story connection, weak column .....	67
3.7	<i>Verification of application of simplified linear hinge for beam-to-column connection with single dowel</i> .....	68
3.7.1	Verification of application of hinge in experiment S1-1 .....	68
3.7.2	Verification of application of hinge in experiment S1-2 .....	69
<b>CHAPTER 4 – Design and testing of innovative moment resisting beam to column dry connection</b>		<b>71</b>
4.1	<i>Objective</i> .....	71
4.2	<i>Proposed moment resisting beam to column dry connections</i> .....	71
4.2.1	Brief description of application of beam-to-column connections.....	71
4.2.2	Justification of investigating dry connections.....	72
4.2.3	Overview of proposed connections.....	72
4.2.3.1	Anticipated behavior of precast beam-to-column dry connection constructed by dowels .....	73
4.2.4	Possibilities for improving performance of connections and options adopted for the tests .....	76



4.2.4.1	Connection upgrading for preventing dowel pullout failure .....	76
4.2.4.2	Connection upgrading for preventing dowel pullout failure and concrete spalling failure .....	77
4.2.4.3	Connection upgrading by a steel plate for preventing dowel pullout failure and concrete spalling failure .....	79
4.3	<i>Experimental program</i> .....	79
4.3.1	Design of the experimental program .....	79
4.3.2	Type of connections tested .....	82
4.4	<i>Preliminary design of precast connection</i> .....	84
4.4.1	Case study .....	85
4.4.2	Details of the elements for testing .....	89
4.4.3	Construction methodology .....	91
4.5	<i>Experiment set-up</i> .....	96
4.5.1	Boundary conditions .....	96
4.5.2	Loading Programme .....	101
4.5.3	Description of equipment and sensors used in the experimental program .....	102
4.5.3.1	Positioning of LVDT's .....	104
4.6	<i>Results from experiments</i> .....	105
4.6.1	Specimen "S 1, V.D." .....	105
4.6.1.1	Description of the specimen performance .....	107
4.6.2	Specimen "S 2, V.D." .....	109
4.6.2.1	Description of the specimen performance .....	111
4.6.3	Specimen "S 3, V.D." .....	113
4.6.3.1	Description of the specimen performance .....	115
4.6.4	Specimen "S 4, R.M." .....	117
4.6.4.1	Description of the specimen performance .....	119
4.6.5	Specimen "S 5, H.D." .....	120
4.6.5.1	Description of the specimen performance .....	121
4.6.6	Specimen "S 6, V.D." .....	123
4.6.6.1	Description of the specimen performance .....	125
4.6.7	Specimen "S 7, V.D." .....	126
4.6.7.1	Description of the specimen performance .....	129
4.6.8	Specimen "S 8, H.D." .....	130
4.6.8.1	Description of the specimen performance .....	131
4.6.9	Experiment "S 9, H.D." .....	133
4.6.9.1	Description of the specimen performance .....	135
4.6.10	Specimen "S 10, R.M." .....	136
4.6.10.1	Description of the specimen performance .....	137
4.7	<i>Comparison of the performance of the tested specimens</i> .....	138
4.7.1	Comparison of overall performance of the specimens .....	138
4.7.1.1	Comparison of specimens "S 2, V.D.", "S 3, V.D.", "S 4, R.M." and "S 7, V.D." .....	138
4.7.1.2	Comparison of specimens "S 1, V.D.", "S 5, H.D." and "S 8, H.D." .....	141
4.7.1.3	Comparison between specimens "S 9, H.D." and "S 10, R.M." .....	143

4.7.2	Summary of the results.....	143
<b>CHAPTER 5 - Numerical modeling of moment resisting beam to column dry connections.....</b>		<b>147</b>
5.1	<i>Objective</i> .....	147
5.2	<i>Challenges in modeling precast beam-to-column connections and possible options</i> .....	147
5.2.1	Application of macro-modelling for beam-to-column moment resisting connections.....	148
5.2.2	Application of micro -modelling for beam-to-column moment resisting connections.....	149
5.3	<i>Micro-modelling procedure adopted for this research program</i> .....	149
5.3.1	Procedure of modeling specimens in Abaqus [Ref.: 001].....	150
5.4	<i>Theoretical background of features of applied model [Ref.:002], [Ref.:003]</i> .....	154
5.4.1	Solid Elements.....	155
5.4.2	Beam Elements.....	157
5.4.3	Rebar modeling in three dimension solid element.....	158
5.4.4	Procedure for modeling reinforced concrete elements model used for reinforcement and concrete.....	158
5.4.4.1	Metal elasto-plasticity model.....	159
5.4.4.2	Inelastic model for concrete – Concrete damage plasticity.....	160
5.4.5	Contact modeling.....	162
5.5	<i>Results from micro-modelling and comparison with experimental results</i> .....	162
5.5.1	Results of stress distribution.....	163
5.5.2	Results of global behavior.....	172
<b>CHAPTER 6 - Conclusions and Recommendations for Further Research.....</b>		<b>173</b>
6.1	<i>Conclusions referring to modeling procedure of connections realized with single centrally positioned dowel</i> .....	173
6.2	<i>Conclusions on developed innovative dry moment resisting beam-to-column connections</i> ..	174
6.2.1	Conclusions based on experimental results.....	175
6.2.1.1	Connections implemented by dowels only.....	175
6.2.1.2	Connections with dowels strengthened by individual steel plates.....	176
6.2.1.3	Connections with dowels strengthened by single large steel plate.....	177
6.2.1.4	<i>Impact of flexure/shear ratio on precast dry moment resisting beam-to-column connections</i> .....	177
6.2.1.5	<i>Impact of axial force on the precast dry moment resisting beam-to-column connections</i> ..	177
6.2.2	<i>Conclusions based on numerical analyses</i> .....	178
6.3	Limitations of the drawn conclusions.....	178
6.4	<i>Recommendations for further research</i> .....	179
6.4.1	Recommendation for further investigation of connections strengthened by a single large steel plate.....	179

6.4.2	Recommendation for further investigation of connections strengthened without any steel plates , .....	180
6.4.3	Recommendation for further investigation of connections regarding their seismic performance .....	181
<b>List of references .....</b>		<b>182</b>

## List of figures

- Figure 2.1 Illustration of application of precast structure buildings: a) Typical precast concrete structure building in UK, b) Precast concrete high-rise building in USA, c) Brunel University, Uxbridge, Middlesex – 1400 Students Room, d) Budenberg building in UK.
- Figure 2.2 Typical fixed column - foundation connection
- Figure 2.3 Examples of beam-to-column fixed (moment resisting) connection realized as wet connection
- Figure 2.4 Typical example of partially cast-in-situ beam-to-column fixed (moment resisting) connection
- Figure 2.5 Example of beam-to-column dry connection, a) outer connection, b) inner connection.
- Figure 2.6 Example of beam-to-column dry connection with eccentric position of dowel
- Figure 2.7 Example of beam-to-column dry connection with possible degree of fixity
- Figure 2.8 Example of beam-to-column dry connection with two dowels
- Figure 2.9 Collapsed industrial building near Adapazari – Turkey. Failure of a connection, mostly beam-to-column connections
- Figure 2.10 Collapse of a precast building due to the Kocaeli earthquake, where damages to beam-to-column connections are visible.
- Figure 2.11 Collapse of beam-to-column connections of a precast building due to the Kocaeli earthquake, structural pinned connections
- Figure 2.12 Collapse of a precast building due to the Emilia-Romagna earthquake, mainly due to failure of beam-to-column connections
- Figure 2.13 Collapse of a precast building due to various earthquakes, mainly due to failure of beam-to-column connections.
- Figure 2.14 Possible location of plastic hinges formation in the structure with fixed connections.
- Figure 2.15 Static scheme of a typical single story precast frame
- Figure 2.16 Possible location where plastic hinge could be created at a column base
- Figure 2.17 Potential failure mechanism due to increase of displacement of a mechanically unstable frame should plastic hinge is created as in fig. 2.16
- Figure 2.18 Precast dry beam-to-column connection with T beam section
- Figure 2.19 Stress distributions in the concrete element from the dowel (a), concrete crushing with hinge creation at the dowel (b) [Ref.: 035]

- Figure 2.20 Stress distributions on the concrete element from the dowel due to three-axial compression [Ref.:035]
- Figure 2.21 Splitting failure of the concrete, a) potential splitting plane when the dowel is located further deep into the section of the element, b) splitting plane when the dowel is located close to the edge of the element, and c)strut and tie method of force transfer [Ref.:035].
- Figure 2.22 Pullout (concrete cone) failure of concrete [Ref.: 029]
- Figure 2.23 Type of wet connections of precast structures, equivalent to cast in situ connections presented in FIB bulletin 27, 2003 [Ref.: 034]
- Figure 2.24 Type of dry connections of precast structures, with performance equivalent to cast in situ connections in regard to moment resistance, presented in FIB bulletin 27, 2003 [Ref.: 034]
- Figure 2.25 Recommended moment resisting connections presented in “Design Guidelines for Connections of Precast Structures under Seismic Action” publication of 2012, with cast-in-situ.
- Figure 2.26 Recommended moment resisting connections presented in “Design Guidelines for Connections of Precast Structures under Seismic Action” publication of 2012, with partial cast-in-situ.
- Figure 2.27 Recommended moment resisting connections presented in “Design Guidelines for Connections of Precast Structures under Seismic Action” publication of 2012, with mechanical couplers, top and side view of a connection, b) details of mechanical couplers
- Figure 2.28 Details of experiment, a) referent model and b) proposed moment resisting connection conducted within “BEHAVIOUR OF PRECAST BEAM-COLUMN TIE-ROD CONNECTION UNDER CYCLIC LOAD; researchers: R. Vidjeapriya and K.P. Jaya, published in 2012” [Ref.:037]
- Figure 2.29 Results, F-D diagram from experiment, a) referent model and b) proposed moment resisting connection conducted within “BEHAVIOUR OF PRECAST BEAM-COLUMN TIE-ROD CONNECTION UNDER CYCLIC LOAD; researchers: R. Vidjeapriya and K.P. Jaya, published in 2012”[Ref.:037]
- Figure 2.30 Details of experiment, a) PC1 and b) PC2 of proposed moment resisting connection conducted within “BEHAVIOUR OF PRECAST BEAM-COLUMN MECHANICAL CONNECTIONS UNDER CYCLIC LOAD; researchers: R. Vidjeapriya and K.P. Jaya, published in 2011”[Ref.:038]
- Figure 2.31 Results of experiments on: a) Monolithic specimen (ML), b) PC1 specimen and c) PC2 specimen of the research “BEHAVIOUR OF PRECAST BEAM-COLUMN MECHANICAL CONNECTIONS UNDER CYCLIC LOAD; researchers: R. Vidjeapriya and K.P. Jaya,” [Ref.:038]
- Figure 2.32 Test specimen within the research “Hybrid Moment Frame Joints Subjected to Seismic Type Loading” by M. I. Pastrav and C. Enyedi, presented at 15WCEE-Lisboa 2012”, [Ref.:023]

- Figure 2.33 Detail of connections tested within the research “Hybrid Moment Frame Joints Subjected to Seismic Type Loading” by M. I. Pastrav and C. Enyedi, presented at 15WCEE-Lisboa 2012 [Ref.:023]
- Figure 2.34 Force-Deformation diagram for joint N1 and N2 [Ref.: 023]
- Figure 2.35 Details of realization of connections tested within the research: “Experimental Study on a New Precast Post-Tensioned Concrete Beam Column Connection System” by Do Tien THINH, Koichi KUSUNOKI and Akira TASAI , presented at 14WCEE-Beijing 2008 [Ref.: 033]
- Figure 2.36 Results of experiment, Moment-Story Drift diagram of: a) Connection SP1-A, b)Connection SP1-A, and c) Connection SP3-A.
- Figure 2.37 Geometric properties of the testes specimens: a) Floor layout of RC structure, b) Floor layout of ECC/RC structure, c) Cross-section of RC structure, d) Cross-section of ECC/RC structure [Ref.: 040]
- Figure 2.38 Section details of the elements following design; a) beam, b) column, c) beam base [Ref.: 040]
- Figure 2.39 Detail of connections of the elements, column-to-column and beam-to-column, [Ref.: 040]
- Figure 2.40 Crack patterns after completion of experiments of tested specimens, a) RC frame, b) ECC/RC frame, [Ref.: 040]
- Figure 2.41 Total global displacement of specimens, a) RC frame and b) ECC/RC frame under different PGA values, [Ref.: 040]
- Figure 2.42 Experimental set-up of a half of frame [Ref.: 024]
- Figure 2.43 Experimental set-up details; a) Overall specimen, b) detail of sliding achievement on the middle beam [Ref.: 024]
- Figure 2.44 Shear force versus joint slip diagrams for ST-4 specimen (SS column) subjected to Petrovac earthquake in the horizontal direction for stepwise increasing pga and comparison with the corresponding cyclic response (Psycharis and Mouzakis 2012); d backbone envelope of the cumulative response. [Ref.: 024].
- Figure 2.45 Shear force versus joint slip diagrams for the ST-6 specimen (FS column) subjected to Petrovac earthquake applied in the horizontal and the vertical directions for stepwise increasing pga and comparison with the corresponding cyclic response (Psycharis and Mouzakis 2012). [Ref.: 024].
- Figure 2.46 a–c Shear force versus joint slip diagrams for the ST-8 specimen (FS column, connection made of one dowel) subjected to Petrovac earthquake applied in the horizontal direction for stepwise increasing pga and comparison with the corresponding cyclic response (Psycharis and Mouzakis 2012); d backbone envelope of the cumulative response. [Ref.: 024].

- Figure 3.1 Top centric connection,[Ref.: 027]
- Figure 3.2 Top eccentric connection, [Ref.: 027]
- Figure 3.3 Intermediate story connection, [Ref.: 027]
- Figure 3.4 Force-deformation relationship – push/pull test of specimen S1
- Figure 3.5 Actual photos of a broken dowel after the test completed for specimen S1,[Ref.: 027]
- Figure 3.6 Stress distribution within dowel loaded in flexure
- Figure 3.7 Pivot model shape
- Figure 3.8 Graphical presentation of numerical model vs experimental results of S1-1 experiment
- Figure 3.9 Graphical presentation of numerical model vs experimental results of S1-2 experiment
- Figure 3.10 Graphical presentation of numerical model vs experimental results of S2 experiment
- Figure 3.11 Graphical presentation of numerical model vs experimental results of S3-1 experiment
- Figure 3.12 Graphical presentation of numerical model vs experimental results of S3-2 experiment
- Figure 3.13 Graphical presentation of numerical model vs experimental results of S3 experiment
- Figure 3.14 Graphical presentation of numerical model vs experimental results of S3 experiment
- Figure 3.15 Graphical presentation of numerical model vs experimental results of S6-1 experiment
- Figure 3.16 Graphical presentation of numerical model vs experimental results of S6-2 experiment
- Figure 3.17 Graphical presentation of numerical model vs experimental results of S7-2 experiment
- Figure 3.18 Graphical presentation of numerical model vs experimental results of S7-2 experiment
- Figure 3.19 Comparison of bending moments at the base of column in experiment S1-1 from non-linear analysis with non-linear link element (N.L.L.E.) vs linear analysis with elastic hinge element
- Figure 3.20 Comparison of bending moments at the base of the column in experiment S1-15 from non-linear analysis with non-linear hinge element vs linear analysis with elastic hinge element
- Figure 4.1 Possible use of connection performed with a) vertical dowels and horizontal dowels in b) single story structure and b) multi-story structures
- Figure 4.2 Potential flexural behavior of precast beam-to-column connection
- Figure 4.3 Behavior of dowel in pullout [Ref.: 012]

- Figure 4.4 Possible dowel pullout failure in the case of a short anchorage height
- Figure 4.5 Upgrading of the connection with steel plates to prevent pullout failure
- Figure 4.6 Upgrading of a connection strength with carbon fiber strips for preventing concrete spalling
- Figure 4.7 *Strengthening dowels by a large steel plate to prevent all failure modes*
- Figure 4.8 Connection performed with vertically positioned dowels where dowels are anchored with grout only (a), connection performed with vertically positioned dowels where two dowels in tension are strengthened with individual plates (b), cast-in-situ connection (c), connection performed with horizontally positioned dowels where two dowels in tension are strengthened with individual plates (d), connection performed with vertically positioned dowels where all dowels are strengthened with one large plate (e), connection performed with horizontally positioned dowels where all dowels are strengthened with one large plate (f).
- Figure 4.9 Position of dowel within the cross-section
- Figure 4.10 Connection of precast elements, a) with rubber between elements and b) direct contact.
- Figure 4.11 Case study building drawing, a) Layout, b) section B-B, c) section A-A
- Figure 4.12 Cross-section properties of the referent model (a), precast model (b), M-f diagram for the referent model (c) and M-f diagram for the precast model (d).
- Figure 4.13 Monolithic side of the joint
- Figure 4.14 Details of the referent cast-in-situ model
- Figure 4.15 Details of precast element with vertical dowels
- Figure 4.16 Details of precast element with horizontal dowels
- Figure 4.17 Photo taken during construction of the column of connection performed with vertically positioned dowel; a) dowels inserted in column prior to concreting, b) sleeves preserved in beam by steel pipes prior to concreting for performing the connection.
- Figure 4.18 Photo taken during connection of elements with vertically positioned dowels
- Figure 4.19 Photo taken during construction of elements with horizontally positioned dowel, a steel pipe being inserted for sleeve preservation
- Figure 4.20 Positioning the dowel within the sleeve; a) longitudinal view of the dowel within the connection, b) cross-section view of the dowel within the sleeve
- Figure 4.21 Photo taken during performance of a connection with horizontally positioned dowels; a) filling of the upper sleeves, b) filling of the upper and the lower sleeves
- Figure 4.22 Method used for treating sleeve walls for adequate roughness



Figure 4.23 Boundary conditions

Figure 4.24 Test set-up of the specimen with vertical dowels

Figure 4.25 Test set-up for the specimen with horizontal dowels

Figure 4.26 Loading programme adopted for performing experiments

Figure 4.27 Photo of items used for the experiments; a) Multifunctional Control Console (MCC 8), b) Hydraulic Cylinder, c) Force Transducer, d) Linear Potentiometer Transducer and e) Displacement Transducer

Figure 4.28 F-D diagram of global displacement of specimen "S.1 V.D."

Figure 4.29 F-D diagram of opening of section at connection level of specimen "S.1 V.D."

Figure 4.30 F-D diagram of opening of section at the monolithic part of the joint (beam face) of specimen "S.1 V.D."

Figure 4.31 F-D diagram of shear slip of the connection of specimen "S.1 V.D."

Figure 4.32 Cracks in the specimen after the sixth loading cycle applied on specimen "S.1 V.D."

Figure 4.33 The specimen after the last loading cycle, failure state of specimen "S.1 V.D."

Figure 4.34 F-D diagram of global displacement of specimen "S.2 V.D."

Figure 4.35 F-D diagram of opening of section at the connection level of specimen "S.2 V.D."

Figure 4.36 F-D diagram of opening of section at the monolithic part of the joint (beam face) of specimen "S.2 V.D."

Figure 4.37 F-D diagram of shear slip of the connection of specimen "S.2 V.D."

Figure 4.38 Crack pattern of the specimen at the last loading cycle -photo from experiment of specimen "S.2 V.D."

Figure 4.39 Rotation of the section of specimen "S.2 V.D."

Figure 4.40 F-D diagram of global displacement of specimen "S.3 V.D."

Figure 4.41 F-D diagram referring to the connection level of specimen "S.3 V.D."

Figure 4.42 F-D diagram referring to the monolithic part of the joint (beam phase) of specimen "S.3 V.D."

Figure 4.43 F-D diagram of shear slip of the connection of specimen "S.3 V.D."

Figure 4.44 Crack pattern of the specimen under the last loading cycle - photo from the experiment on specimen "S.3 V.D."

- Figure 4.45 Deformation of the connection/joint at the last loading cycle applied on specimen "S.3 V.D."
- Figure 4.46 F-D diagram of global displacement of specimen "S.4 R.M."
- Figure 4.47 F-D diagram referring to the column face of the joint of specimen "S.4 R.M."
- Figure 4.48 F-D diagram referring to the beam face of the joint of specimen "S.4 R.M."
- Figure 4.49 F-D diagram of shear slip of the joint (column face vs joint) of specimen "S.4 R.M."
- Figure 4.50 Photo of the specimen after the last loading cycle applied on specimen "S.4 R.M."
- Figure 4.51 Deformation of the connection/joint at the last loading cycle of specimen "S.4 R.M."
- Figure 4.52 F-D diagram of global displacement of specimen "S.5 H.D."
- Figure 4.53 F-D diagram referring to the connection level of specimen "S.5 H.D."
- Figure 4.54 Crack pattern of a joint of an element of specimen "S.5 H.D."
- Figure 4.55 Photos after the last loading cycle applied on specimen "S.5 H.D."
- Figure 4.56 F-D diagram of global displacement of specimen "S.6 V.D."
- Figure 4.57 F-D diagram referring to the connection level of specimen "S.6 V.D."
- Figure 4.58 F-D diagram referring to the monolithic part of the joint (beam phase) of specimen "S.6 V.D."
- Figure 4.59 Crack pattern of specimen "S.6 V.D."
- Figure 4.60 Photo taken after the last loading cycle applied on specimen "S.6 V.D."
- Figure 4.61 Eccentric position of the dowels in the sleeve of specimen "S.6 V.D."
- Figure 4.62 F-D diagram of global displacement of specimen "S.7 V.D."
- Figure 4.63 F-D diagram referring to the connection level of specimen "S.7 V.D."
- Figure 4.64 F-D diagram referring to the monolithic part of the joint (column face) of specimen "S.7 V.D."
- Figure 4.65 F-D diagram of shear slip of the connection of specimen "S.7 V.D."
- Figure 4.66 Main crack after the last loading cycle applied on specimen "S.7 V.D."
- Figure 4.67 Photos of the specimen after the last loading cycle applied on specimen "S.7 V.D."
- Figure 4.68 F-D diagram of global displacement of specimen "S.8 H.D."
- Figure 4.69 F-D diagram referring to the connection level of specimen "S.8 H.D."

- Figure 4.70 F-D diagram referring to the monolithic part of the joint (column face) of specimen "S.8 H.D."
- Figure 4.71 Main critical crack of specimen "S.8 H.D."
- Figure 4.72 Photos of the specimen at the last loading cycle applied on specimen "S.8 H.D."
- Figure 4.73 Failure of the joint after the last cycle applied on specimen "S.8 H.D."
- Figure 4.74 F-D diagram of global displacement of specimen "S.9 H.D."
- Figure 4.75 F-D diagram referring to the connection level of specimen "S.9 H.D."
- Figure 4.76 F-D diagram referring to the monolithic part of the joint (column phase) of specimen "S.9 H.D."
- Figure 4.77 F-D diagram of shear slip of the connection of specimen "S.9 H.D."
- Figure 4.78 Photo of the specimen after the last loading cycle applied on specimen "S.9 H.D."
- Figure 4.79 F-D diagram of global displacement of specimen "S.10 R.M."
- Figure 4.80 F-D diagram referring to the connection level of specimen "S.10 R.M."
- Figure 4.81 Photo of the specimen after the last loading cycle applied on specimen "S.10 R.M."
- Figure 4.82 Comparison of global behavior of specimens "S2, V.D." and "S3, V.D."
- Figure 4.83 Comparison of global behavior of specimens "S2, V.D." and "S3, V.D." with "S4, R.M."
- Figure 4.84 Comparison of global behavior of specimens "S3, V.D." and "S7, V.D." with "S4, R.M."
- Figure 4.85 Comparison of global behavior of specimens "S1, V.D." and "S5, H.D."
- Figure 4.86 Comparison of global behavior of specimens "S5, H.D." and "S8, H.D."
- Figure 4.87 Comparison of global behavior of specimens "S9, H.D." and "S10, R.M."
- Figure 5.1 Presentation of independent elements, column, beam, steel plate and sleeve elements for composing the model
- Figure 5.2 Presentation of reinforcement assembling
- Figure 5.3 Graphic presentation of assembling column, sleeve elements, column reinforcement and dowels
- Figure 5.4 Graphic presentation of assembling beam, steel plate, and their connection with dowels
- Figure 5.5 Graphic presentation of the complete assembled model, the column-sleeve element and the beam-plate element are presented in blue color, while the steel reinforcement rebar and the dowels are presented in red color
- Figure 5.6 Print screen shot of the modeling of the beam element

- Figure 5.7 Print screen shot of the modeling of the rebar element
- Figure 5.8 Isometric parametric elements
- Figure 5.9 Response of concrete to uniaxial loading in tension (a) and compression (b)
- Figure 5.10 Tension stress distribution on referent model specimen S4
- Figure 5.11 Crack distribution on Specimen S4 after failure
- Figure 5.12 Stress distribution on the cross-section of connection of specimen "S 2, V.D."
- Figure 5.13 Photo of specimen "S 2, V.D." after failure indicating the failure mode of dowel pullout
- Figure 5.14 Concrete spalling in specimen "S 2, V.D." due to rotation of the dowel
- Figure 5.15 Tension stress distribution on specimen "S 2, V.D." due to rotation of the dowel
- Figure 5.16 Tension stress distribution on specimen "S3, V.D." in x-y cross-section plane
- Figure 5.17 Crack distribution on specimen "S 3, V.D." after failure
- Figure 5.18 Tension stress distribution on concrete element of specimen "S7, V.D." at the grout sleeve cross-section
- Figure 5.19 Crack distribution on specimen "S 7, V.D." after failure
- Figure 5.20 Tension of dowels on model specimen "S 7, V.D."
- Figure 5.21 Tension stress distribution on concrete element of specimen "S 9, H.D."
- Figure 5.22 Crack distribution on specimen "S 9, H.D." after failure
- Figure 5.23 Stress on tension and compression dowels of specimen "S 9, H.D."
- Figure 5.24 Results of force-deformation plot of global displacement from modeling and comparison with results from experiment of specimen "S2, V.D"
- Figure 5.25 Results of force-deformation plot of global displacement from modeling and comparison with results from experiment of specimen "S10, R.M"

## List of tables

Table 2.1	Beam moment strength and story drift of experiments [Ref.: 033]
Table 2.2	Detail of specimen of experiment [Ref.:024]
Table 2.3	Loading details and material properties of the specimen [Ref.: 024]
Table 3.1	Detail of experiments on elements conducted under the UL program, [Ref.: 027]
Table 4.1	Description of type of experimental tests under this research thesis
Table 4.2	Maximum member forces on the frame elements and the flexural strength at yielding point of designed section
Table 4.3	Boundary conditions for the specimens tested under this research thesis
Table 4.4	Summary of results, flexural strength (at yielding and ultimate points), total deformability and the lateral displacement of the specimens
Table 4.5	Comparison of results of precast connections vs cast-in-situ connection

## CHAPTER 1 - Introduction

### 1.1 Introduction

In the construction industry, precast buildings have started to be used since the middle of the last century. They won a high reputation among investors and contractors due to the simplicity and speed of construction. Another high advantage of precast structures is the high quality control during the production of the construction elements and good control during the construction process.

In the beginning of application, precast structures were used mainly for industrial buildings and other types of buildings with long spans.

Nowadays, due to their advantages, precast structures are mass applied in: infrastructures, e.g., bridges, tunnels, culverts, administrative and office buildings, hotels, schools and universities, sport and recreational centers, typical residential buildings, parking garages, warehouses, retail buildings, agricultural facilities such as barns, etc.

Due to their advantages, precast structures tend to be increasingly used and replace the cast-in-situ structures. The advantages of precast structures are:

- with the increase of the cost of workmanship, the reduction of construction has a direct impact on the final cost of the structure;
- with the increase of the worldwide concern for environmental issues, the simplicity of demolition of precast buildings makes this type of construction more desirable;
- whenever there is a limitation of construction time, for different kinds of reasons, precast buildings are one of the favorable structural systems.

The biggest constraint in the wide application of precast structures is the limited knowledge on the behavior of the connections of precast structures. Recent earthquakes have proved that the weakest point of the already constructed precast structures are the connections and most of the damages that have occurred in precast structures have been directly related to their connections.

Precast reinforced concrete structures, like monolithic structures, are of various structural systems:

- Frame structural systems,
- Shear wall structural systems,
- Combined, or dual structural systems

The connections of precast structures are unique regarding each structural system. Realization, design and construction of connections depend directly on the type of elements that are being connected, the position of the connection (outer connection or inner connection), the elevation of the building in regard to the number of floors, etc.

Considering that the subject of this research has been the performances of the connections in precast industrial buildings, the focus herein has been placed on critical connections of industrial buildings.

Industrial buildings are mostly constructed as a large span frame. In a typical frame, there are two connections:

- Column to foundation, and
- Beam to column.

Column to foundation connections are quite simple connections to be realized and constructed whereas beam-to-column connections are considered to be more complicated. This has also been proved by observation of damages from earthquakes where the beam-to-column connection has been the weak link of the structure and most of the damages have occurred directly to the beam-to-column connection. From the structural point of view, beam-to-column precast connections are two primary types, pinned connections and moment resisting (fixed) connections.

#### **a) Beam-to-column pinned connections**

In almost all cases in practice, beam-to-column connections are realized with one dowel in the middle of the connection, which is a dry connection. This connection is structurally considered as pinned connection. Dry connections are more feasible for the construction process.

Pinned dry beam-to-column connections have been applied for more than half a century and the procedure for design, strength calculation, and construction has already been developed and studied to the point that it has become a regular applicable procedure.

Even though there have been studies on beam-to-column pinned connections and there are formulas for calculating the strength of such a connection, and there has been a general belief among engineers that behavior of beam-to-column pinned connections is understood and successfully controlled, recent earthquakes have proved that beam-to-column pinned connections are the weakest link in precast structures.

The most recent thorough research on behavior of beam-to-column pinned connections was performed by the University of Ljubljana (UL), under SAFECAST Project [Ref.: 027] and enabled acquiring of a good and deep knowledge on the capacity of beam-to-column pinned connections and their behavior.

The accuracy of the expressions that are existing today for calculation of the capacity of beam-to-column pinned connections has been the subject of many researches including the UL SAFECAST research program. However, they have not been the subject of this research. This research has dealt with verification of whether beam-to-column connections implemented with centrally located dowels can be considered as pinned connections from structural modeling aspect.

Understanding this element is very important for structural analysis and design of a structure since member forces on the structure have a direct impact on the behavior of a connection.

In addition, this research will analyze and confirm whether the beam-to-column pinned connections are, in fact, structural pinned connections. For analyzing this, the results from the UL SAFECAST program have been made available by the University of Ljubljana [Ref.: 027].

**b) Beam-to-column moment resisting (structurally fixed) connections**

Moment resisting beam-to-column connections of precast structures have not been used much. In fact, up to the best knowledge of the author of this research, based on the researches in previous studies, there are no moment resisting connections performed as dry connections in industrial buildings. This is due to lack of guidelines on the procedures of design, strength verification and calculation and lack of unified realized procedures. This is a big gap in structural engineering in general and especially in the field of precast structures.

The biggest challenge in moment resisting connections is that there is not one way to realize such a connection, whereas in pinned connections, there is one way, which is considered standard.

In the recent decade there has been an ongoing tendency of various researches to develop moment resisting beam-to-column connection (see, the following references: [Ref.: 009], [Ref.: 032], [Ref.: 037], [Ref.: 023], [Ref.: 033]) knowing the high advantage that moment resisting connections have for seismic resistance of structures. When compared to pinned connections, where a pinned connection is simply realized by putting a dowel through a sleeve and filling the sleeve with grout and there is no other way, in the case of the moment resisting connections, this is the only way that a moment resisting connection cannot be realized.

Since there is no standard way for realizing moment resisting connections, each connection is innovative. This element of unspecified realization method is a big problem and it is the main constraint in developing a generalized method for realization of a moment resisting connection, including a calculation method and a construction methodology.

Until general and unified method for realization of moment resisting connections is achieved, it would not be possible to have a standardized and codified method for design and construction of such a connection. For this very reason, today, there are no standards for developing moment resisting beam-to-column connections. Such design and construction of such connection is not in any construction codes and this is the main obstacle in application of moment resisting connections in the engineering field.

Since there are no guidelines for designing moment resisting beam-to-column connections, especially dry connections, in order to be confident about the fixity of a developed moment resisting beam-to-column connection, an experimental program has to be performed for each developed connection. Considering the financial implication of conducting an experimental program, the use of moment resisting beam-to-column connections in engineering practice is even more difficult.

Another big obstacle for application of moment resisting beam-to-column connections are the complications that exist in developing and constructing such a connection. Some of the developed and experimentally tested moment resisting connections where this element is evident are presented in Chapter 2.

Considering the above mentioned facts on moment resisting beam-to-column connections, especially dry connections, the goal of this research has been to make a contribution to moment resisting connections by developing innovative as well as simple, beam-to-column moment resisting connections.



Such a contribution has been focused on:

1. Developing a connection that behaves as a full moment resisting connection,
2. Definition of a procedure for designing and calculating the strength of such a connection, and
3. Making the connection simple and easy for practical application.

In addition, Chapter 5 displays a numerical/simulation model that exhibits the best behavior of a connection and the elements constituting the connection.

## **1.2 Objective and Methodology of research**

The main goal of the research within the doctoral dissertation has been to investigate performance of dry precast beam-to-column connections, especially moment-resisting ones, by applying scientific approach and using science tools. Practitioner engineers in the field of precast structures and the construction industry in general, should benefit from the outcomes of this research.

The objectives of this research has been to fill the existing gap on:

- a) Modeling procedure for design and analysis of precast structures when the beam-to-column connection is realized with single dowel centrally positioned.
- b) Develop innovative dry precast beam-to-column moment resisting connections, simple for construction but reliable, that could be easily by design engineers in everyday practice.

In order to achieve these goals complex research programme has been designed comprised of full scale experimental testing of developed innovative precast dry moment resisting beam-to-column connections and appropriate non-linear analyses using 3D finite elements.

### **a) Beam-to-column connections realized with single dowel centrally positioned– numerical modeling procedure**

The connections realized with single dowel centrally positioned are the most widely used type of beam-to-column connections in industrial precast buildings. From the structural analysis and design point of view these type of connections in general have been considered as hinge connections.

The purpose of this part of the numerical research has been to verify/confirm that the above consideration could be used with reliability for general engineering practices.

In order to make this verification, the results of the experiments performed at UL under SAFECAST Project [Ref.: 027] have been used for further analytical research. For this research, specimens with centrally positioned dowels have been used since such a connection exhibits the same behavior in both directions of force acting (push and pull), specifically in the elastic range.

The following methodology has been adopted for this analytical research:

**First step** - Non-linear modeling of single dowel precast connections has been performed where respective numerical model parameters of the adopted hysteretic model have been properly calibrated using the experimental results as a benchmark.

**Second step** - Non-linear dynamic analysis has been performed of experimentally tested beam-to-column connection using calibrated non-linear hysteretic model were performed and bending moments at the end column section (connection of the column with the foundation) were calculated.

**Third step** - Dynamic linear analysis of the beam-to-column connection using an elastic hinge were carried out and again the bending moments at the columns base have been obtained.

Analyzing the results from both, non-linear dynamic analysis with non-linear model for the connection and linear dynamic analysis with applying elastic hinge as a beam-to-column connection and comparing time history of the calculates bending moments the following conclusion was drawn:

*Beam-to-column connections implemented with a dowel positioned vertically and in the center of the connection in regards to structural modeling are to be considered as pinned connections.*

## **b) Beam-to-column moment resisting dry connections**

### **i. General behavior of a connection**

The objective of this part of the research has been to develop a precast beam-to-column dry moment resisting connection with properties (moment resistance and deformability capacity) similar to those of a cast-in-situ moment resisting connection. In addition, the developed connections should be simple enough for construction in order to be considered for practical application in precast industrial buildings.

The presented research has been based on a full scale experimental program. The experiments have been conducted on ten specimens (8 specimens with innovative precast beam-column connections and 2 reference specimens) in quasi-static (half-cycle) loading conditions.

Initially, the simplest connection, a connection realized by dowels only, has been experimentally tested. Based on the outcome of the experiments, the anticipated failure modes of such connection are confirmed, and the appropriate methods for improvement of the behavior of the connections are adopted for further testing. The suggested mode of improving performance of a connection were:

- Confining dowels loaded in tension due to flexure by small (individual) steel plates. The confinement has been implemented from the top of the dowel. These plates have been intended for prevention of failure of the dowel in pullout, as one of the main failure mechanisms of the initial connection;
- Confining all four dowels of the connection by a one large plate. This behavior improvement method should prevent any possible failure mechanism of a connection.

For comparison purposes, as an indicator for determining whether the proposed connections are to be considered as cast-in-situ connections, referent cast-in-situ specimens have been constructed. These cast-in-situ referent specimens have been constructed to have the same flexural strength as the connecting section of the precast beam-to-column connection.

**ii. Behavior of connection under different member force intensities**

Since in a real situation in engineering practice, a precast connection could be subject to different loading conditions the critical section within the element could be subject to different intensities of bending moments and shear forces as the result of the influence of many external factors. In such a case, predominant flexural forces, predominant shear forces or equally predominant flexure and shear may occur at the critical section.

For this reason, the experimental program has been designed to test the proposed beam-to-column connection under various loading conditions. The connection has been tested in the case of predominant flexure (Flexure/Shear=1.5), predominant shear (Flexure/Shear=0.5) and the possible case of equally predominant flexure and shear (Flexure/Shear=1.0).

The tests on the connections under the above conditions enabled an insight into the behavior of a connection under different loading situations in real practice.

**iii. Behavior of connection under different construction orientation**

Further, in real practical situations, a connection could be realized with vertically positioned dowels (V.D.) and horizontally positioned dowels (H.D.). These connections vary from each other from two aspects:

- The flexure/shear ratio could vary due to various intensities of all load actions (gravity vs. lateral)
- The construction methodology for realization of these two types of connection is different.

The first varying aspect between V.D. and H.D. has been clarified through the tests performed under different intensities of member forces (as explained in item ii above)

The second varying aspect, the construction methodology, both type of connections i.e. with VD and HD dowels are tested simulating in such a way different design solutions in real engineering practice.

Considering the complexity of realization of beam-to-column moment resisting dry connections and the high impact that the precision of construction could have on their performance, such experimental testing could provide valuable information.

**c) Numerical modeling of beam-to-column moment resisting dry connections**

The objective of this part of the research has been to define a numerical modeling procedure that will simulate in a proper way behavior of the connection, including the elements composing the connection. The defined numerical modeling procedure is intended to be use, with acceptable reliability, in research programs or in engineering practice.

Since moment resisting beam-to-column connection is a connection assembled of several elements/components, such a connection could easily be considered as a “mechanical connection”. For this reason, it is also important to define a numerical modeling procedure by considering the connection as a “complex mechanical connection”.

The suitable procedure for reflecting the behavior of a precast connection as a whole and the connecting elements individually is to define a modeling procedure that will enable, as an outcome, stress distribution within the connection and the connecting elements.

The ability to follow the stress distribution within the elements (beam, column, dowel, steel plates etc.) as a part of a connection could provide a very good indication of the possible behavior of each specific moment resisting beam-to-column connection by observing the behavior (stress distribution) of each element constituting that connection.

The appropriate modeling method for achieve such a goal is micro-modeling with 3D finite element. Such a modeling approach has recently begun to be widely used, especially in mechanical engineering connections, since through micro-modeling, there is a possibility to follow stress and deformation, including the failure mechanism of each element that constitutes the connection.

The tool/software used for performing the numerical model, micro model, has been Abaqus V14 [Ref.: 001].

### **1.3 Organization of dissertation**

This doctoral dissertation consists of 6 Chapters.

#### **Chapter 1 - Introduction**

#### **Chapter 2 - General Overview of Application of Precast Buildings in Seismic Regions**

This chapter deals with application of precast structures in general, weak points of precast structures identified by some recent earthquakes with emphasis on industrial buildings, overview on connections of precast structures with focus on beam-to-column connections and some studies and recent researches on precast connections with focus on beam-to-column moment resisting connections.

#### **Chapter 3 - Numerical Modeling of Experiments Performed at UL under SAFECAST Project**

The goal of this chapter is to determine the connection performed by a dowel, considered and applied as a pinned connection and whether it is also a structural pinned connection. In order to verify this on the targeted connections, a non-linear numerical modeling will be adopted and the adopted numerical model with the respective calibrated parameters will be used to further verify whether this connection can be considered structurally as a pinned connection. The methodology applied is further elaborated in this chapter.

#### **Chapter 4 - Design and Testing of Innovative Moment Resisting Beam to Column Dry Connection**

This chapter shows the developed three general innovative moment resisting connections, designed within the frames of this dissertation with the goal of behaving as a moment resisting connection. The proposed connections were experimentally tested. This chapter further contains explanations as to the details of the proposed connections, the adopted construction methodology, the testing methodology and procedure as well as the results from the experimental testing of the proposed connections.

#### **Chapter 5 - Numerical Modeling of Moment Resisting Beam to Column Dry Connections**

The numerical model adopted and considered the most appropriate for defining the behavior of moment resisting beam-to-column connections is presented in this Chapter. Herein, the justification for the use of the micro-model and its benefits in regard to other possible macro-models is elaborated to more details.

## **Chapter 6 – Conclusion and Recommendations for Further Research**

This chapter contains the main conclusions drawn from the research and the recommendations for further research based on the results of these investigations.

## CHAPTER 2 - General Overview of Application of Precast Buildings in Seismic Regions

### 2.1 Scope

The scope of this chapter involves an overview of the general application of precast building structures in practice, the methodology for their construction with emphasis on connections, the existing applicable procedures for design and realization of connections, and particularly, recent research findings regarding moment resisting beam-to-column connections.

### 2.2 General overview of application of precast buildings

In the construction industry, precast buildings have started to be used since the middle of the last century. They have gained a high reputation among investors and contractors due to their high advantages in construction. The main advantages of application of precast structures are mostly due to the simplicity and speed of construction, as well as, high quality control during production of construction elements.

In the beginning of application, precast structures were used mainly for industrial buildings and other types of buildings with long spans.

Nowadays, due to their advantages, precast structures are mass applied for: infrastructures, e.g., bridges, tunnels, culverts, etc; administrative and office buildings, hotels, schools and universities, sport and recreational centers, typical residential buildings, parking garages, warehouses, retail building, agricultural facilities such as barns, etc.

With the increase of the workmanship costs, precast buildings are increasingly becoming the chosen type of construction as the most feasible ones. Also, with the increase of the worldwide concerns about environmental issues, the simplicity of demolition of precast buildings makes this type of construction more desirable.

Furthermore, in certain circumstances where there is a limitation of the construction time, for different kinds or reasons, precast buildings are among the favorable structural systems, along with steel and timber structures.

Fig. 2.1 shows photos of some precast buildings constructed worldwide.



Fig.2.1. Illustration of application of precast structure buildings: a) Typical precast concrete structure building in UK, b) Precast concrete high-rise building in USA, c) Brunel University, Uxbridge, Middlesex – 1400 Students' Room, d) Budenberg building in UK.

- Structural configuration/systems of precast building structures

Just as cast-in-situ structures, the precast building structures can be designed and constructed as:

- o Structural frame systems
- o Structural wall systems
- o Structural dual systems
- o Structural hybrid systems and structural systems with incorporation of steel elements mainly on the floor systems (composite elements), etc.

### 2.3 Connections in the precast building structures

Connections in the precast building structures serve as link elements for transferring loads from one structural element to another and ultimately from the structure to the foundation/ground. Connections have always been the most complicated part of precast structures and also the most vulnerable elements especially in earthquake prone areas.

A general division of precast connections can be done in regard to:

- a) Structural aspect, and
- b) Construction methodology

### **2.3.1 Structural type of precast connections**

From structural aspect, in general, despite the type of elements that are connected (for example, slab-to-beam, beam-to-column, column-to-foundation), there are two types of connections:

- Pinned connection,
- Fixed connection (moment resisting connection).

Application of the respective types of connections depends on the type and the location of the building, whether the building is a single story or multi story building, single span or multi span structure, high or low redundancy structure, etc.

#### **2.3.1.1 Pinned connections**

Pin connections are the mostly connections in construction of precast industrial buildings. Pinned connections are generally being used in the following cases:

- o Connecting floor elements, whether slab-to-slab or slab-to-column;
- o In beam-to-column connections, mostly in single story and single span buildings, such as: industrial buildings, warehouses, sport halls, or in other structure with a low redundancy requirement;
- o Connection of precast cladding elements to structural elements, etc.

In recent period many researches, experimental and numerical, have been performed for the purpose of understanding the behavior of pinned connections under dynamic loadings, [Ref.: 008], [Ref.: 011], [Ref.: 015], [Ref.: 022], [Ref.: 024] and [Ref.: 036].

Understanding in depth behavior of pinned connections is key factor for developing successful moment resisting connection since all the failure modes of pinned connections are present in moment resisting connections.

#### **2.3.1.2 Fixed connections**

Fixed connection is general are being used as wet-connections. Fixed connections (moment resisting connection) can be fully fixed or partially fixed connections. Fixed connections in precast building structures are mostly used in:

- Column to foundation connection
- Beam-to-column connections in following structures:
  - o Multi story structures,
  - o Multi span structures,
  - o Seismic resistant structures especially in zones of high seismicity (they should be designed with maximum structural redundancy which enables high energy absorbing capacity).



The degree of redundancy of a structure is related to the type of connections that are used. A precast structure with fully fixed connections will possess a maximum redundancy. This kind of a precast structure can be considered as a monolithic structure (cast-in-situ structure).

In the opposite case, more pinned connections in precast structures lead to a lesser redundancy of the structure. The major setback for the wide application of precast structures in earthquake prone areas is the fact that most of the connections, especially beam-to-column connections are realized as pinned connections.

Considering importance of redundancy on the seismic resistant structures, achieving moment resistant beam-to-column connections has become an important research topic. In recent period many experimental investigations have been performed for achieving moment resisting beam-to-column connections, [Ref.: 004], [Ref.: 006], [Ref.: 010], [Ref.: 013], [Ref.: 014], [Ref.: 016], [Ref.: 017], [Ref.: 018], [Ref.: 019], [Ref.: 020], [Ref.: 030] and [Ref.: 039].

### 2.3.2 Connections in regard to construction methodology

In regard to construction methodology, connections are divided into:

- Wet connections
- Dry connections

#### 2.3.2.1 Wet connections

Wet connections are type of connections where part of the connection is concreted on site after the elements are fixed in place. Wet connections can be applied in all connections of all structural elements.

- Column to foundation connection

Wet connections are used mostly for column-to-foundation connection when fixed (moment resisting) connections are required. A common example is presented in fig 2.2.

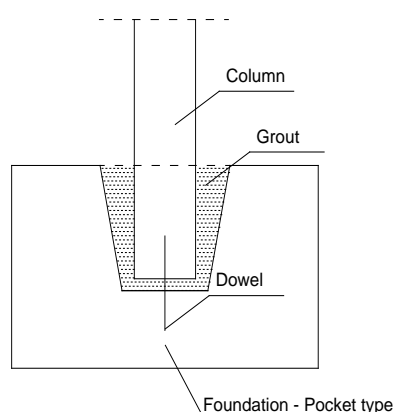


Fig 2.2. Typical fixed column - foundation connection

In this type of connection, (fig 2.2), a pocket type of foundation is constructed to allow for the column to be positioned properly. The foundation can be precast and just placed on the ground or can be cast-in-situ. Usually, there is a dowel that is also used for initial positioning of the column on the

foundation. Finally, for providing respective fixed connection of the column with the foundation, the space between these two elements is filled with cement gout.

This type of connection is mostly used for single story, single span structures, such as industrial buildings, sport centers, barns, etc.

However, from structural point of view, there are no limitations for this type of connection to be used in any type of RC structure.

- Beam to column wet connection

Wet connections are also broadly used in beam to column connections. Usually, for beam to column connections, wet connections are used when fixed connections (moment resisting) are required.

In most cases, this connection is applied in multi-story and multi span building structures (fig 2.3.a,b, c and d).

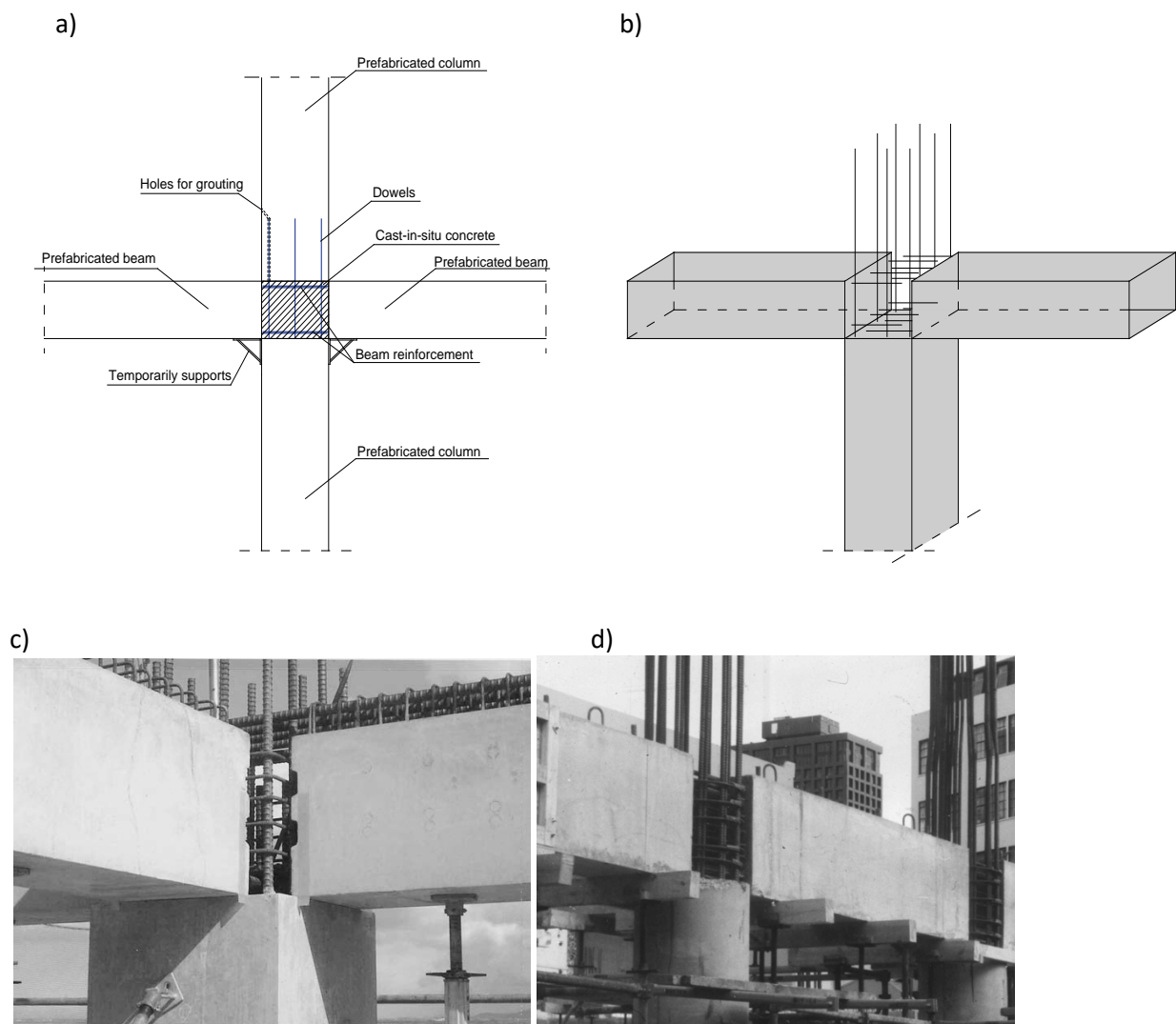


Fig 2.3. Examples of beam-to-column fixed (moment resisting) connection realized as wet connections

The beam-to-column connection presented in fig. 2.3 is the most common connection used in precast multi story and multi span structures, but it is also used in single story structures when moment

resisting connections are required/provided. The main reason for the common application of this connection is the fact that it is the easiest way to achieve a moment resisting connection.

This connection has certain requirements that need to be fulfilled. The most important one is that the width of a connection that needs to be cast-in-situ should be determined by the required length of lap splices, in order for elements to be properly anchored to the joint. For this connection, limited formworks are required. If the connection is in the 3D joint and if the length of the lap splices equals the length of the connection, then no formworks are required.

The negative side of this type of connection is that it is significantly difficult to place stirrups in the joint, which is a requirement for seismic resisting structures. If insertion of stirrups into the joint is impossible to realize, then the connection should not be used in seismically resistant structures. Wet connections (semi-wet connections) are also used in cases where only some cast-in-situ concreting is required for achieving a moment resisting connection. An example of this kind of connection is presented in fig. 2.4.

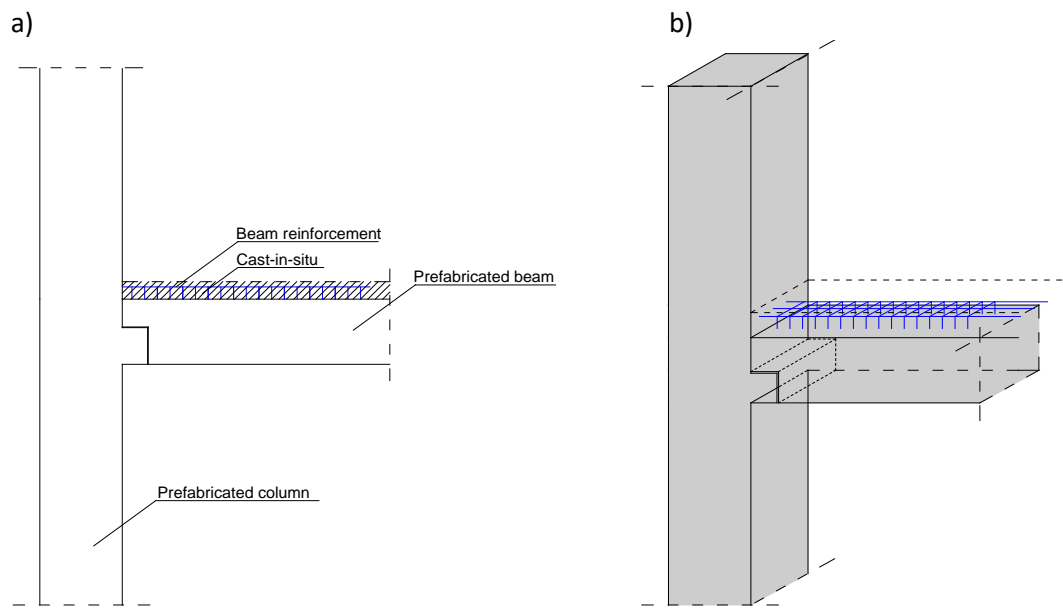


Fig 2.4. Typical example of partially cast-in-situ beam-to-column fixed (moment resisting) connection.

This connection (fig. 2.4. a,b) is mostly used in multi-story structures, but it can also be used in single story structures with moment resisting connections. Columns in this connection are completely precast. Columns are constructed with the corbel where the beam will be placed. The corbel should be designed to sustain the shear forces from the gravity loads.

The beam is generally precast, except in the upper zone which is left to be cast-in-situ. After the beam is positioned, the reinforcement in the upper zone is anchored to the column and then, that part of the beam is cast in situ. This ensures continuity of the beam and fixity of the connection. In this type of connection, some formworks are required, as well.

### 2.3.2.2 Dry Connections

Dry connections are connections achieved by using only dowels, where no additional concreting is required.

Dry connections in precast structures can be used to connect all elements of the structure, such as:

- Beam-to-column,
- Column-to-foundation,
- Slab-to-beam,
- Claddings-to-structure, etc.

Due to the purpose of this research only, only beam-to-column connections are discussed herein.

Dry connections are mostly used in single story structures for beam-to-column connections. Due to the difficulty in the realization of fixed connections, most of the connections performed with dowels are pinned connections.

Dry connections are used generally in structures that are configured with plane (uniaxial) frames, respectively in structures where gravity loads paths are directed in one direction. These structures are used mostly in industrial buildings, sport centers, etc.

A typical dry connection is presented in fig. 2.5.

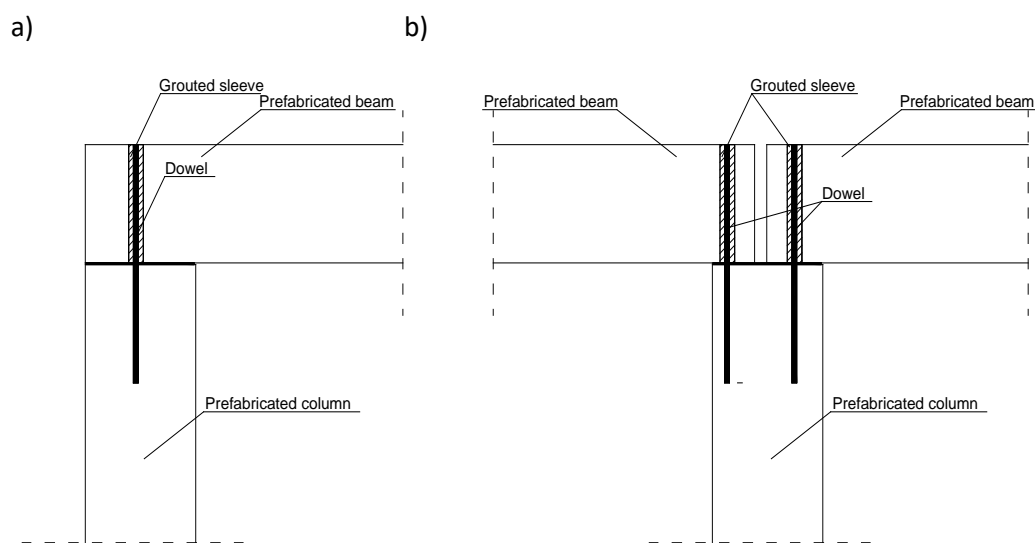


Fig 2.5. Example of beam-to-column dry connection, a) outer connection, b) inner connection

Fig. 2.5 shows the most common pinned connections used in construction. Both elements, column and beam, are precast. The connecting element is the dowel, where usually a simple reinforced bar of a large diameter is used. The dowel is usually placed in the column and is concreted inside the column, but can also be left to be inserted after the column is concreted. On the construction site, then the beam is positioned by being centered on the dowel. For easy operation, the sleeve is left on the beam for the dowel to be inserted. The sleeve is left wider and then once the elements are in place, the sleeve is filled with cement grout. Sometimes, the sleeve is formed by inserting a steel tube which is left inside the beam.

Between the column and the beam, a rubber element with sufficient thickness of 10mm is usually placed. This element helps for easy installation, but also prevents edges of column to be crushed during an earthquake, which normally happens if there is no rubber plate.

In most of the cases, the dowel is centered in the middle of the column (centric connection), however, there are cases where the dowel is inserted eccentrically, (fig 2.6). The position of a dowel can be on both sides of the column center.

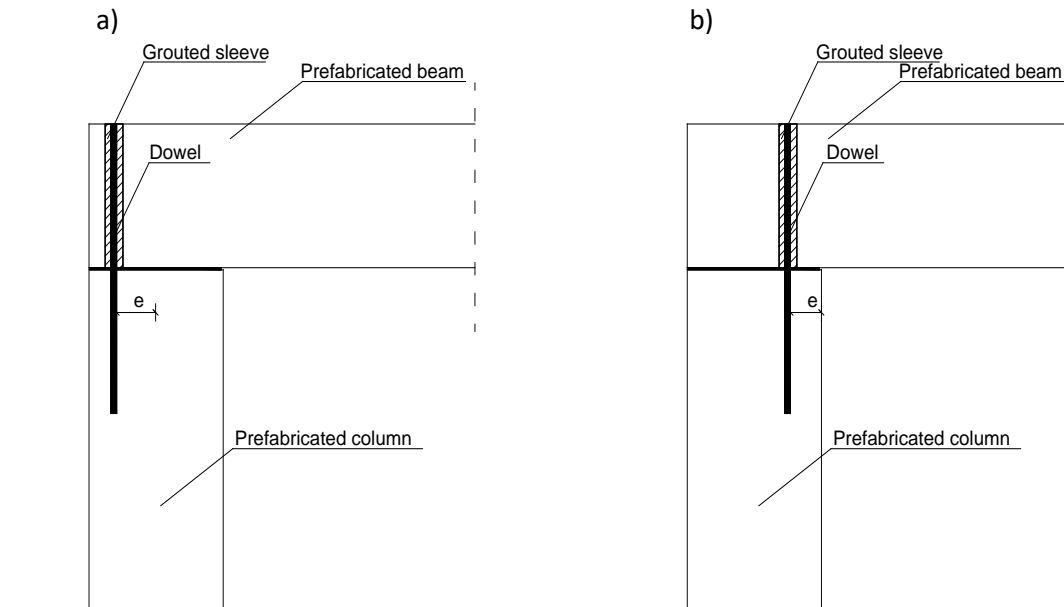


Fig 2.6. Example of beam-to-column dry connection with eccentric position of dowel

Due to the eccentric position of the dowel and depending on the rotation forces acting on the joint, this type of connection, fig. 2.6, can provide a certain degree of fixity. It is very important to be aware of the fact that eccentric connection is not always a pinned connection. In situations when this connection provides a certain degree of fixity, this should be taken into account during the design of the structure and the structural elements.

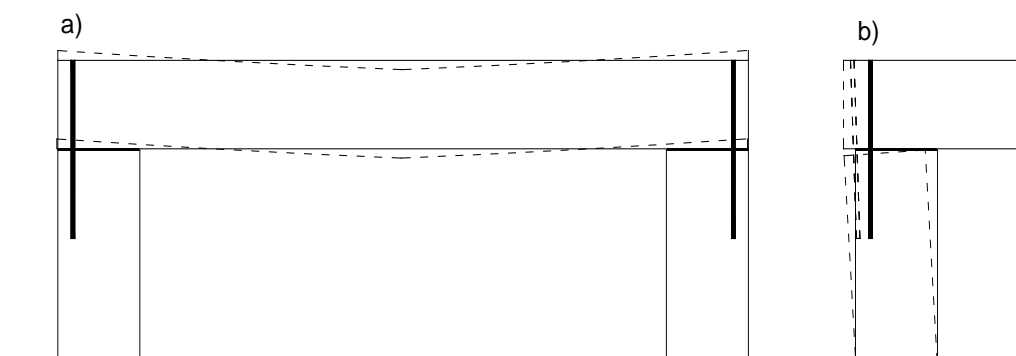


Fig 2.7. Example of beam-to-column dry connection with possible degree of fixity

For example, for the gravity loads, the dowel located on the left side of the column face (fig.2.6.a)) will also provide some degree of fixity since it will prevent, to a certain extent, the rotation of the beam caused by vertical deflections, fig, 2.7. Depending on the intensity of loads and the diameter of the

dowel (and also other aspects such as length of anchorage, concrete strength, etc.), the degree of fixity of this dowel can vary. In this case, the design engineer should account for the bending moments on the upper side of the beam and provide adequate longitudinal reinforcement on this side. Otherwise, if the elements are designed considering this connection to be a purely pinned connection, in that case, there will be a risk for the beam to crack on the upper side near the connection due to the existence of bending moments and lack of proper longitudinal reinforcement.

One dowel is usually used for a pin connection, especially in a single story structure. However, depending on the safety factor desired for earthquake resistance, or depending on the seismicity zone, etc., more dowels can be used, (fig.2.8).

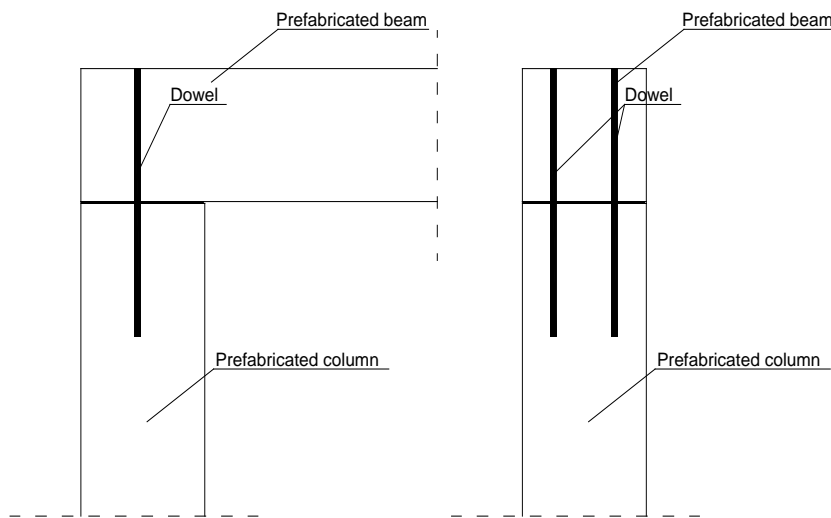


Fig 2.8. Example of beam-to-column dry connection with two dowels

This connection with two dowels is considered as pinned connection in the plane of the frame, but in the orthogonal direction, it can be considered as a fixed connection, similarly to the case presented in fig. 2.6.a).

## 2.4 General behavior of precast building structures with dry connections– weak points

During earthquakes, like any other structures, precast structures have also experienced significant damages and collapse.

The connections, mainly dry connections, have also been the major cause of total collapse of precast structures.

### 2.4.1 Typical damages to single story structures under various earthquakes

Single story structures account for the vast majority of damages to precast structures that have occurred during earthquakes. This happened because most of the connections, especially beam-to-column connections, were pinned connections, in which case the structures did not have enough redundancy.

The probability of single story structures with pinned connections to experience significant damages or collapse is much higher. A possible location that can experience failure is the beam-to-column connection. A numerous of investigations have been conducted on damages on industrial buildings during the earthquake, [Ref.: 021], [Ref.: 005], [Ref.: 007]

The subsequent fig.2.9, fig.2.10, fig.2.11, fig. 2.12 and fig. 2.13 show failures of connections in precast industrial buildings.



*Fig. 2.9. Collapsed industrial building near Adapazari – Turkey. Failure occurred at the connection, mostly at beam-to-column connections.*



*Fig. 2.10 Collapse of a precast building due to the Kocaeli earthquake, where damages at the beam-to-column connections are visible.*



*Fig. 2.11 Collapse of beam-to-column connections of precast building due to the Kocaeli earthquake, structural pinned connections.*



*Fig. 2.12 Collapse of a precast building due to the Emilia-Romagna earthquake, mainly due to failure of beam-to-column connections.*





Fig. 2.13 Collapse of a precast building due to various earthquake, mainly due to failure of beam-to-column connections

#### 2.4.2 Weakness of single story precast structure with pinned beam-to-column connections

Compared to cast-in-situ structures, precast structures are more vulnerable structures and, in principle, have a lower seismic resistance capacity and less energy absorption capacity.

In the case of standard cast-in-situ frames with high redundancy, there is a possibility for multiple plastic hinges in the structure, whereas the structure still remain mechanically stable. In such situation, the structure has the capacity to absorb more energy transferred by the earthquake excitations. Fig. 2.14 shows a single story single span structure. Although there are possibilities for occurrence of two plastic hinges in this structure, it will still remain functional after an earthquake (if the structure is properly designed and constructed). The locations where plastic hinges can be formed depend on the flexural strength of the elements. In the case when the flexural strength of the column is higher than that of the beam (strong column - weak beam design philosophy), the plastic hinges will be formed in the beam, (fig.2.14.a). On the contrary, if the flexural strength of the column is less than that of the beam, the plastic hinge will be formed in the column, more likely, near the connection with the beam, (fig. 2.14.b). In both cases, the structure remains stable.

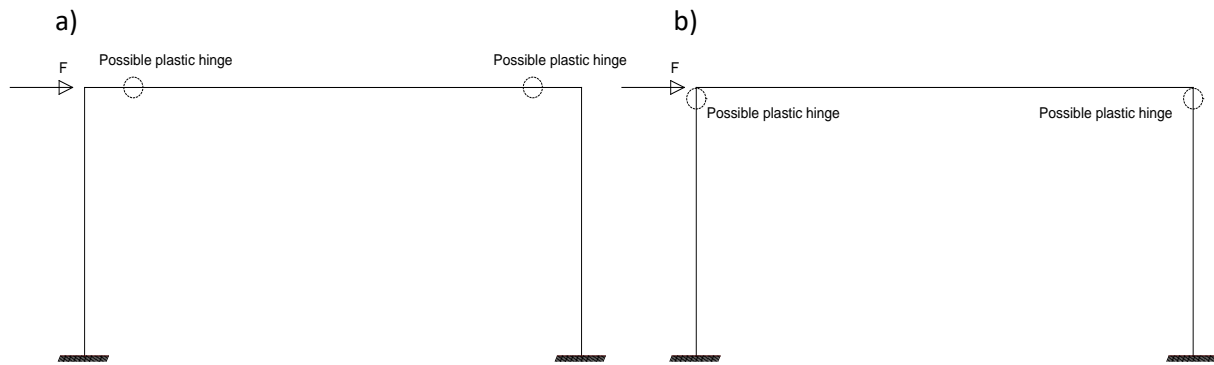


Fig.2.14. Possible location of plastic hinges formation in the structure with fixed connections

In precast structures, the static scheme of a frame, which is generally adopted and realized is presented in fig. 2.15.

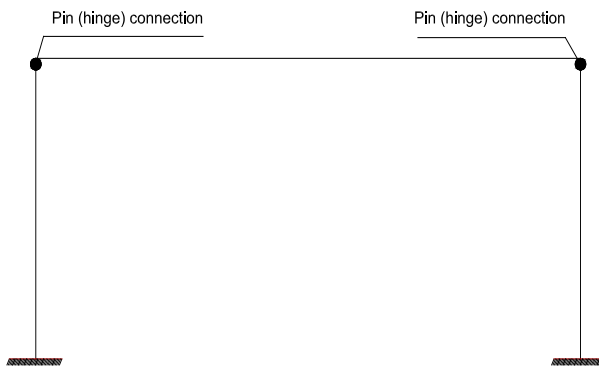


Fig.2.15. Static scheme of a typical single story precast frame

Since all the structures, following the design codes, are designed to possess energy absorption capacity in the non-linear range of behavior (unless a structure is designed to exhibit elastic behavior under an earthquake and to absorb energy in the elastic state) and if a connection is designed to have a higher bearing capacity than the other elements of the structure, plastic hinges will be created in the structure, inevitably.

In the situation where the beam to column connection is adopted as a purely hinged connection, fig. 2.5, then plastic hinges will be formed at the column base, as presented in fig. 2.16. In such a scenario, the structure becomes mechanically unstable, in which case, the horizontal displacements are continuously increased until collapse of the structure, fig.2.17.

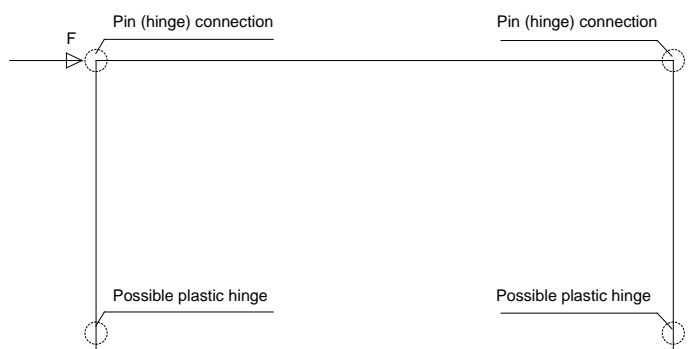


Fig. 2.16 Possible location where plastic hinge could be created on the column base



Fig. 2.17 Potential failure mechanism due to increase of displacement of a mechanically instable frame should plastic hinge is created as in fig. 2.16

Unless the structure is designed to behave fully elastically, precast structures of single story frames with pinned beam-to-column connections are not suitable for earthquake areas and are characterized by a very high probability of failure. Even if the connection is designed strong enough to sustain earthquakes, the lack of redundancy of the structure will make the structure to collapse, as illustrated above.

For this reason, due to high risk of collapse under an earthquake, this type of a structure should be avoided in seismically prone areas.

In addition to the risk for human lives, an additional reason for not constructing this kind of structures is the very low possibility for the continuation of serviceability of such structures after an earthquake that represents a big financial loss to the industry and an overall loss.

Considering the high advantages of precast structures, in order to be able to apply these structures in seismically prone areas, the solution is to make them with a high redundancy. The only way to make these structures with a high redundancy is to apply moment resisting beam-to-column connections in addition to the moment resisting column to foundation connections.

**The above said has been the main motivation for the research within this dissertation, with the main goal of designing reliable moment resisting beam-to-column connections.**

### 2.4.3 Failure mechanism of dry beam-to-column connections

Understanding of possible failure mechanisms of beam-to-column dry connection is a key factor for developing/designing successful moment resisting connection.

The most common types of failure of dry beam-to-column connections are:

- Failure of dowel/s
- Failure of concrete in the connection

### 2.4.3.1 Failure of the dowel/s

The most vulnerable element of the beam-to-column dry connection is the dowel. It has been proved, by observing damages from previous earthquakes, as well as experimentally, that the main cause of failure of such a connection is actually failure of the dowel.

The main failure mechanisms of the dowel in pinned connections are:

- Dowel failure in shear
- Dowel failure in flexure due to shear

#### a) Failure of dowel in shear

In the situations where the strength of a dowel is less than the crushing concrete strength where the dowel is anchored, the dowel will fail in pure shear.

#### b) Dowel failure in flexure due to shear

For the other situations where the dowel strength is high enough to sustain loads while the concrete around dowel crushes, the dowel will fail in flexure due to shear.

### 2.4.3.2 Failure of concrete in the connection

The other type of failure of connections in precast structures is due to the failure of concrete in the connection.

Failure of concrete can occur at the following places and in the following situations:

- Crushing of concrete around the dowel
- Splitting failure
- Pullout failure

#### a) Crushing of concrete around the dowel

Crushing of concrete around the dowel is a very common situation in the precast connections, loaded in shear. This type of failure of concrete mostly occurs in beam-to-column dry connections.

In most cases, this happens when:

- the sleeve is grouted with cement grout of a lower strength than that of the concrete of the element (fig. 2.5a),
- when the concrete precast element is thin, which is usually when the beam has a T section (fig. 2.18),
- in rectangular type of a beam of relatively proper dimensions, but with no proper confinement.

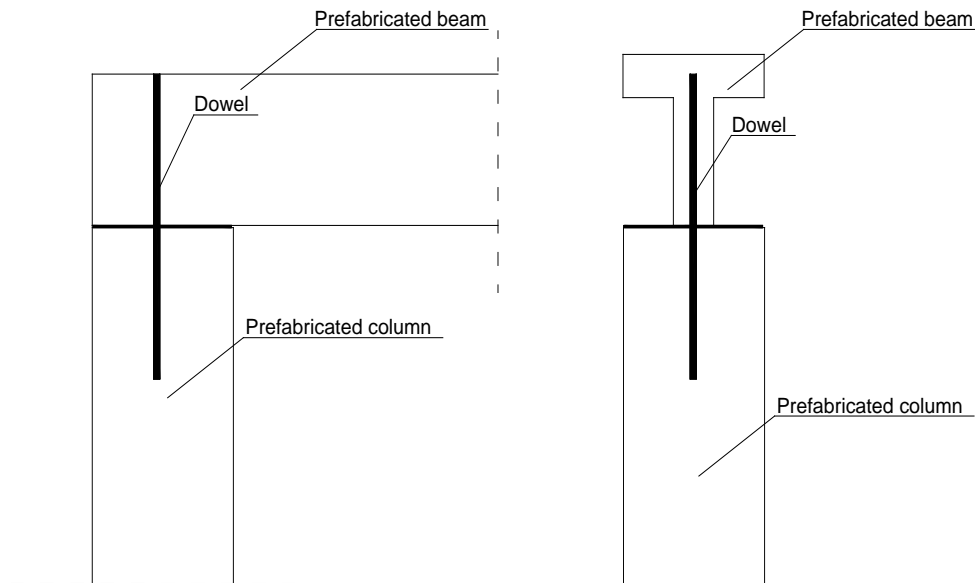


Fig. 2.18 Precast dry beam-to-column connection with T beam section

Even though the crushing of the concrete around the dowel as isolated fact may not cause great damage to the structure as a whole, it can lead to other situations which can jeopardize the integrity of the connection and the stability of the structure, such as:

- The crushing of the concrete around the dowel will create a gap between the dowel and the concrete element which can allow for larger displacement of the structure.
- This gap can create pounding forces from the concrete elements to the dowel which can lead to failure of the dowel and of the connection.

Crushing of the concrete can happen almost always in situations when the dowel is placed eccentrically in the element (fig. 2.6 presents the eccentric position of a dowel).

This could happen because:

- The distribution diagram of the stresses from the dowel loaded in shear to the concrete element as presented in fig. 2.19, is significantly higher in the upper side of the contact face with the concrete and much higher than the compression strength of the concrete. Under these stresses, the concrete always crushes in that part, which in fact, allows for hinge to be created in the dowel. This mechanism (crushing of the concrete on the edge of the dowel) is the cause of the failure mechanism of the dowel referred to as shear-flexure mechanism, which decreases the connection shear bearing strength under lateral forces. This crushing of the concrete can become disfavor in the situation when the dowel is located eccentrically and very close to the edge of the element.
- Even in the cases when the dowel is located eccentrically, not so close to the edge of the element, concrete crushing can still happen due to three-axial compression stresses. The three-axial compression and the distribution of the stresses are presented in fig. 2.20.

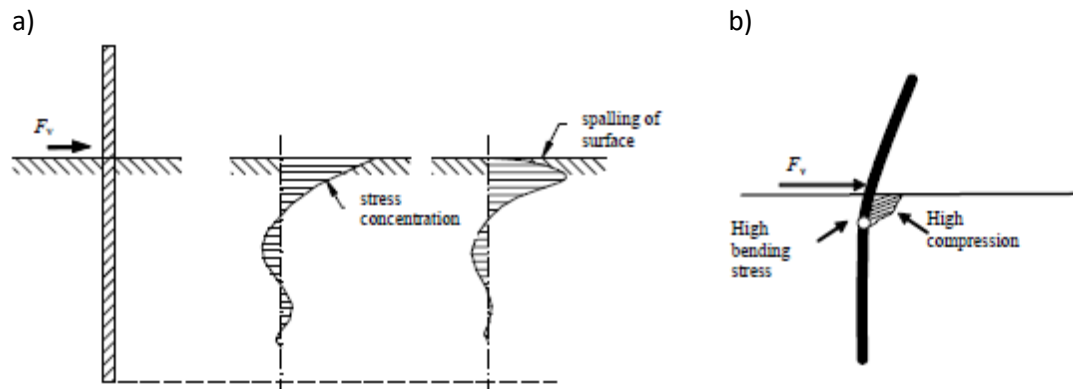


Fig. 2.19 Stress distributions in the concrete element from the dowel (a), concrete crushing with hinge creation at the dowel (b) [Ref.: 035]

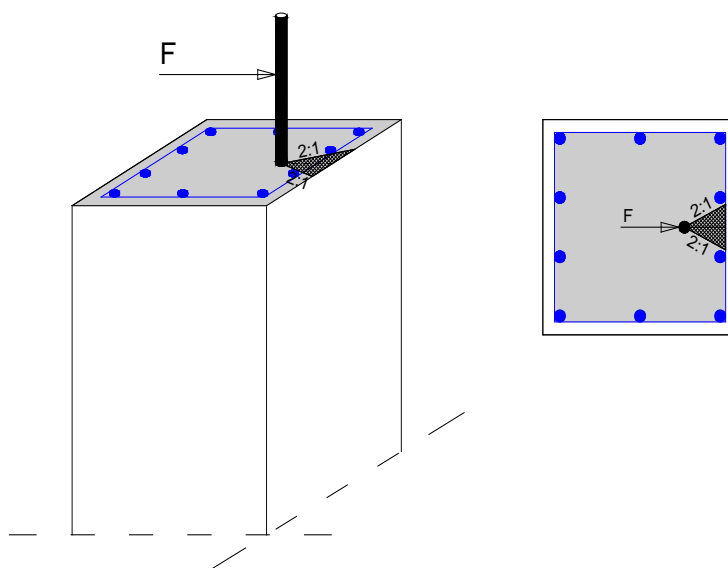


Fig.2.20. Stress distributions on the concrete element from the dowel due to three-axial compression [Ref.:035].

### b) Splitting failure

The splitting of the concrete is a phenomenon that occurs due to a large concentrated force on the element.

Depending on the position of the concentrated force, the splitting can be spread differently. Fig.2.21 a) shows a graphic presentation of the potential splitting plane when the dowel is located deeper into the volume of the elements, whereas fig. 2.21 b) shows the potential splitting plane when the dowel is located close to the edge of the element.

In both cases, the splitting of the concrete can be controlled though reinforcement, shear reinforcement, by applying the strut and tie method, (fig. 2.21, c).

Design of the shear reinforcement is governed by the following design criteria:

- If crack splitting of concrete is allowed, design of reinforcement should be done by simplified design procedures.

- If splitting of concrete is not allowed, then shear reinforcement should be designed in such a way that the deformation (strains) of the reinforcement should be limited with the maximum elastic deformation (strains) of the concrete.

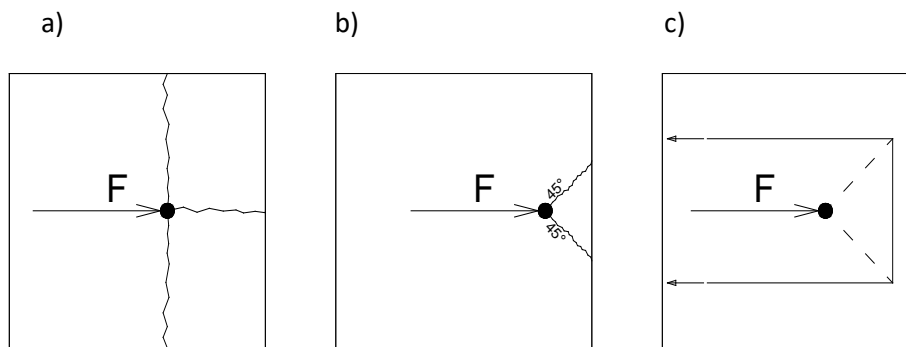


Fig. 2.21. Splitting failure of the concrete, a) potential splitting plane when the dowel is located further deep into the section of the element, b) splitting plane when the dowel is located close to the edge of the element, and c) strut and tie method of force transfer [Ref.:035].

### c) Pullout failure (concrete cone failure)

The pullout failure is the type of failure that is directly related to the anchorage length of the dowel in to the concrete mass.

If the anchorage length is not sufficient, then the part of the concrete, in the conic shape, will be pulled out from the concrete mass together with the dowel. This is because the pullout strength, in the case of short length of anchorage, is less than the tension strength of the dowel, wherefore, before the dowel fails, the concrete around the dowel will break. The pullout failure is another shear type failure of concrete.

For the last decade, there have been many researches on the mode of concrete pullout failure. Here is presented the failure shape from one research [Ref: 029], fig. 2.22.

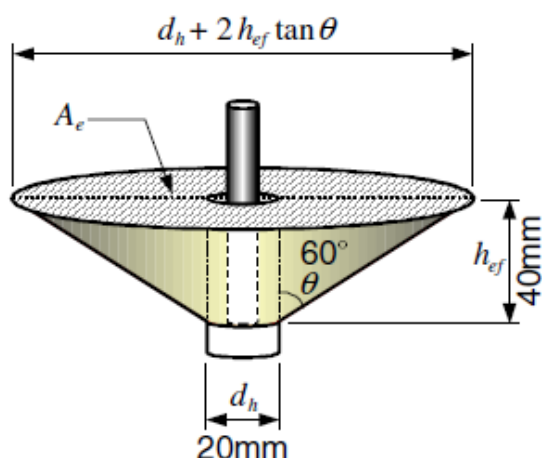


Fig. 2.22. Pullout (concrete cone) failure of concrete [Ref.: 029]

## 2.5 Moment resisting connections

In different documentation, regardless whether guideline publications or research documents (some of which are elaborated herein), there are instructions on realization of moment resisting beam-to-column connections in precast structures.

In guideline documentation, realization of moment resisting connections is suggested to be performed with wet connections. The reason is that with wet connections it is possible to meet required length of lap splice in order for a connection to be realized as a moment resisting connection.

The realization of dry moment resisting connections achieving the requirement for the lap splices in connecting elements/dowels is the main obstacle in the realization of moment resisting connections. Since the requirement for lap splices is not achievable, most of the researches have been focused on different approaches, some of which are presented herein.

### 2.5.1 Moment resisting connections constructed as wet connections

An independent European scientific entity, “The International Federation for Structural Concrete (FIB)” has published a series of publications for the connections of precast structures with the aim to serve as a guideline for design and construction of wet connections, [Ref.: 034] and [Ref.: 035] where are presented some guidelines on realization of moment resisting connections. Also under a EU Commission financed project, a document was published “Design Guidelines for Connections of Precast Structures under Seismic Action”– Editors: Paolo Negro and Giandomenico Toniolo [Ref.: 025], presenting in more detail recommendations for realization of moment resisting connections. Presented in more details further in the text is the general outcome of these two documents in regard to moment resisting connections.

#### *a) Seismic design of precast concrete building structures – bulletin 27, 2003 [Ref.: 034]*

The main requirement in this publication is that precast structures should exhibit the same performances as cast-in place structures. Therefore, the recommendations presented herein are in line with this requirement, namely, the connections constructed by following these criteria should exhibit the same performances as cast-in place connections.

Fig.2.23 shows some details of a possible method, which is not the only one, for realization of moment resisting wet connections, which in this document are referred to as equivalent cast-in place (monolithic) connections.



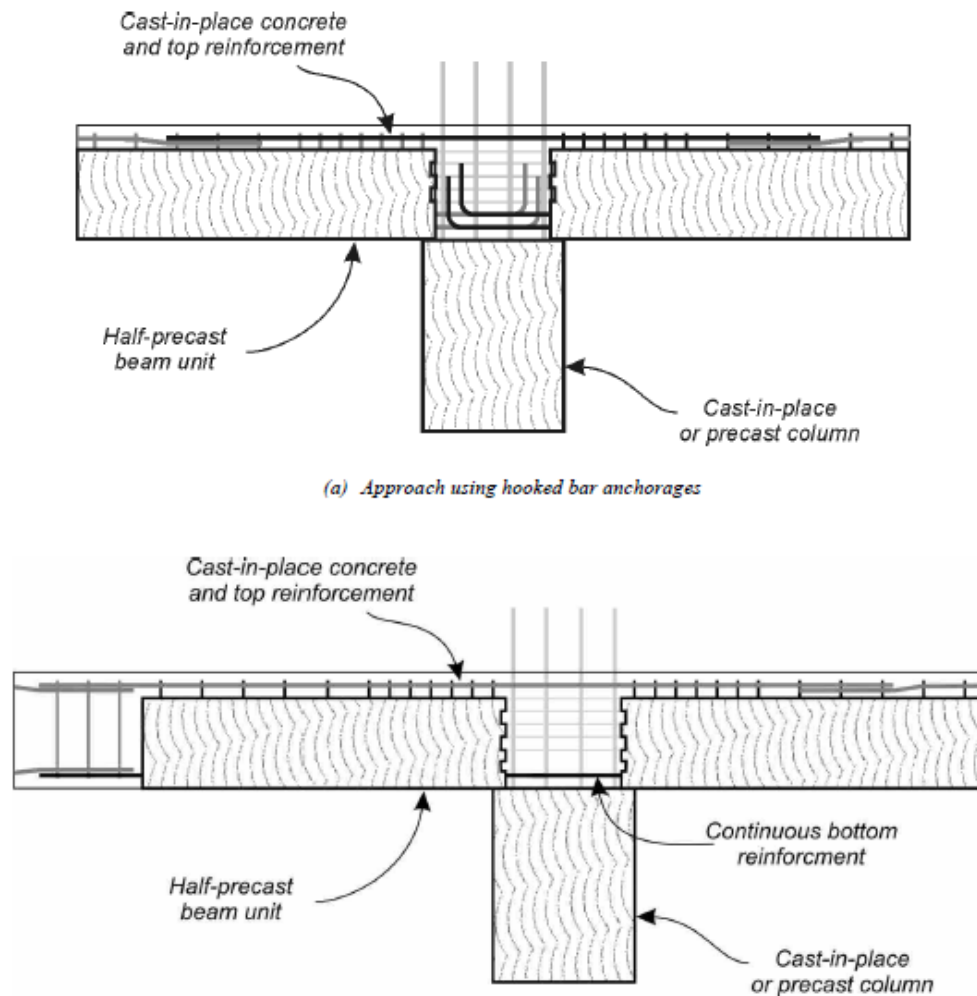
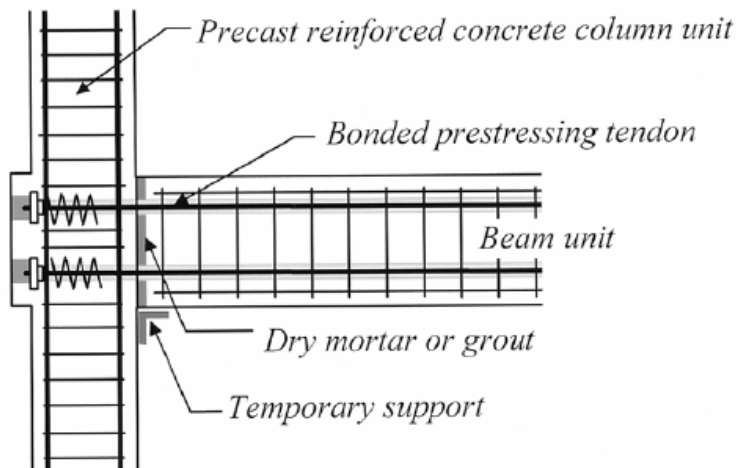


Fig. 2.23. Type of wet connections of precast structures, equivalent to cast in situ connections presented in FIB bulletin 27, 2003 [Ref.: 034]

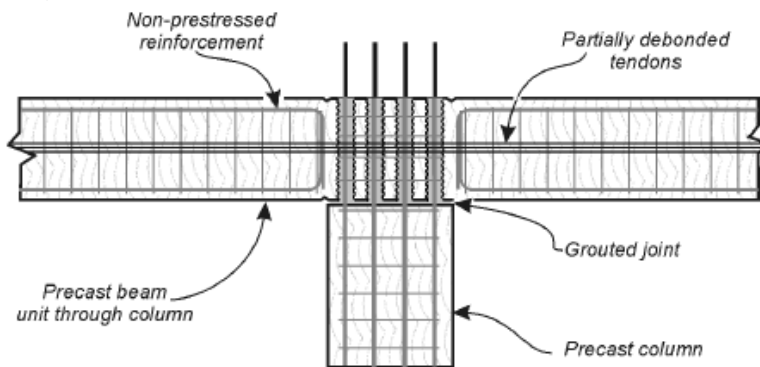
In addition to the guidelines for realization of moment resisting wet connections, this document also contains recommendations for dry moment resisting connections, which have proved (based on this document) to exhibit good behavior as moment resisting beam-to-column connections.

Fig. 2.24 shows some of the beam-to-column dry connections presented in this document.

a)



b)



c)

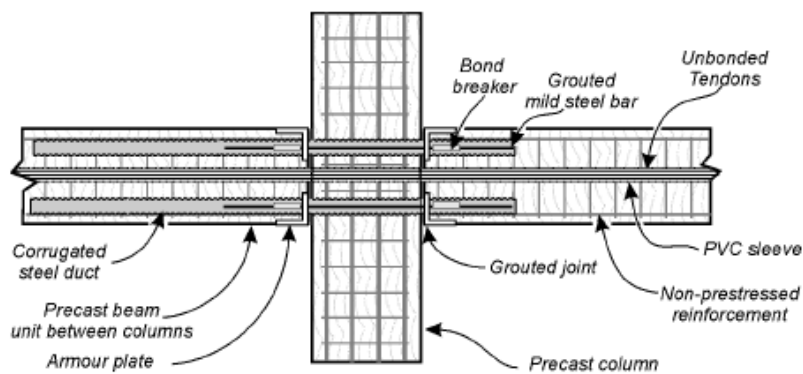


Fig. 2.24. Type of dry connections of precast structures, with performance equivalent to cast in situ connections in regard to moment resistance, presented in FIB bulletin 27, 2003 [Ref.: 034]

As illustrated in fig. 2.24, these connections are dry connections, but they require some post tensioning or pre-stressing. For this reason, these connections are called Hybrid Connections.

As presented in this publication, in Japan, there are some criteria for considering a precast connection as a moment resisting one. The following is a citation from this document:

“in Japan, a precast concrete system is considered to be equivalent to a monolithic system if the drift of the precast system is within 80 to 120 percent of the cast-in-place counterpart and if the energy dissipation in the second loading cycle is no less than 80 percent of that obtained from the response of the cast-in-place counterpart”.

**b) Design Guidelines for Connections of Precast Structures under Seismic Action, – Editors: Paolo Negro and Giandomenico Toniolo, project financed by EU Commission, 2012 [Ref.: 025]**

Also in this publication, the presented moment resisting beam-to-column connections require cast in situ concreting, which means that they are wet connections. As presented in figures 2.25, this type of connections are simple cast in situ connections with various possible behavior and structure configuration.

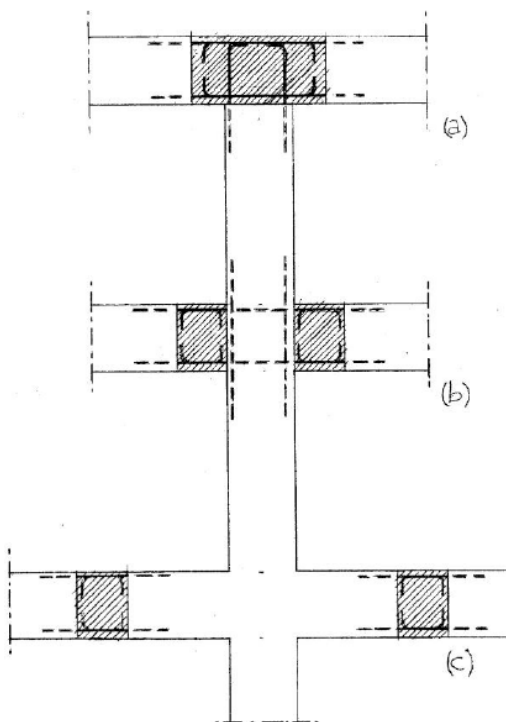


Fig.2.25. Recommended moment resisting connections presented in “Design Guidelines for Connections of Precast Structures under Seismic Action” publication of 2012, with cast-in-situ.

Fig. 2.25 a) shows a cast-in situ connection for a single story structure. The consideration in this connection should be that the length of the connection should be adequate in order to enable the lap splices as in the cast-in situ connection.

Fig. 2.25 b) displays a cast-in situ connection for a multi-story structure. The connection is done outside the column joint, respectively at the column face. Similar to the previous case, the length of the connection should be enough to accommodate lap splices as in the cast-in situ connection.

Presented in fig. 2.25 c) is a cast-in situ connection for a single and a multi-story structure. This connection is done in the beam and outside the critical zone of the plastic hinge.

Another possible type of moment resisting connection/cast in situ connection is presented in fig.2.26.

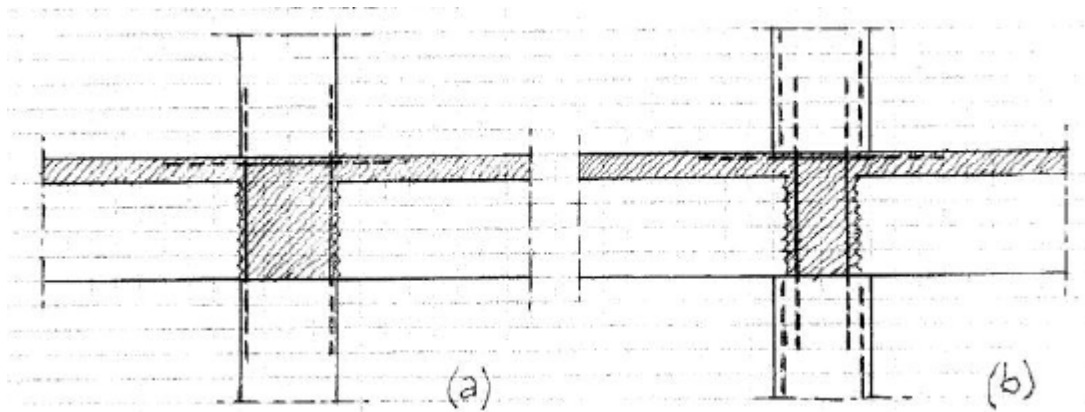


Fig.2.26 Recommended moment resisting connections presented in “Design Guidelines for Connections of Precast Structures under Seismic Action” publication of 2012, with partial cast-in-situ.

These are connections used for multi-story buildings. In these connections, continuity of the columns is enabled by extension of the longitudinal bars from the column of the story below through the connection on the column of the story above.

Fig. 2.26 a) shows the case where the connection is of the same width as the column, whereas in fig. 2.26 b), the connection enters inside the width of the column.

Besides realizing moment resisting beam-to-column connections by casting in situ, there are also some details on realizing connections with mechanical couplers, fig. 2.27.

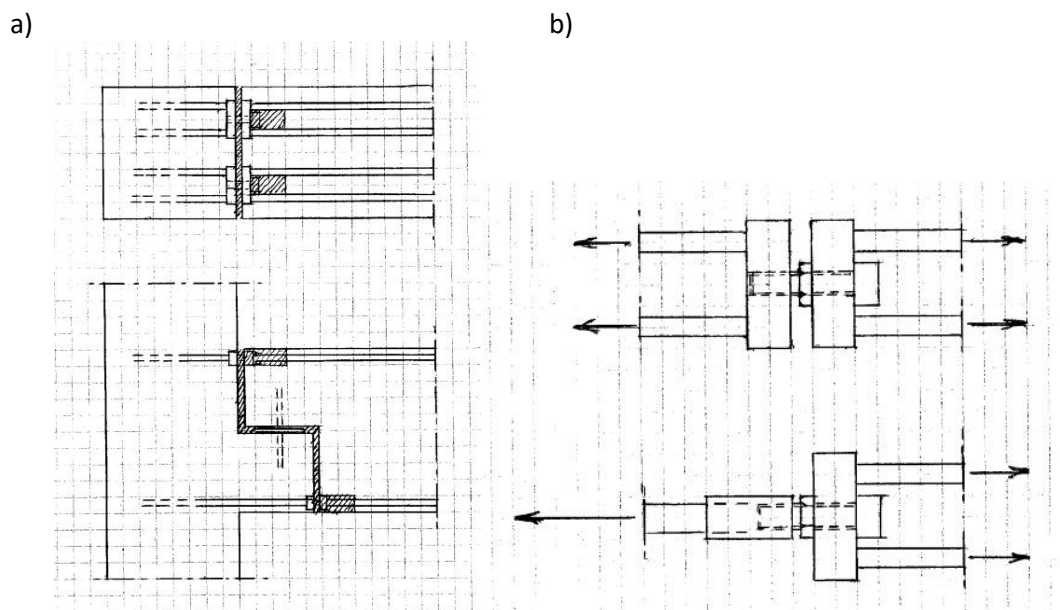


Fig.2.27 Recommended moment resisting connections presented in “Design Guidelines for Connections of Precast Structures under Seismic Action” publication of 2012, with mechanical couplers, top and side view of a connection, b) details of mechanical couplers .

## **2.5.2 Recent research investigations and publications on moment resisting beam-to-column dry connections conducted under quasi-static loading conditions**

In quasi-static loading conditions it is possible to be tested the behavior of the beam-to-column connection only. In this way with quasi-static loading conditions the effect of the behavior of the connection on the global deformation of the elements, respectively frame, will be determined. Therefore the quasi-static loading conditions are more practical experimental procedure to determine deformability capacity of the beam-to-column connection only since wit this loading conditions it is possible to test the connection only.

Considering the advantages of dry connections, in the recent decade, there have been numerous scientific studies and research investigations aimed at designing innovative moment resisting beam-to-column connections and experimentally verifying their behavior.

### **2.5.2.1 Recent investigation performed on dry connections under quasi-static loading conditions**

Achieving moment resistance of dry beam-to-column connections is considered a difficult task wherefore not many researches have been conducted on these type of beam-to-column connections.

Below are presented two experimental studies on beam-to-column dry connections.

#### **a) Research: “BEHAVIOUR OF PRECAST BEAM-COLUMN TIE-ROD CONNECTION UNDER CYCLIC LOAD”; researchers: R. Vidjeapriya and K.P. Jaya; published in 2012” [Ref.: 037]**

This research was conducted on an external joint of a possible multi-story building. The connection is realized with a tie rod and a steel plate, fig. 2.28b). The beam is connected to the column by a tie rod positioned horizontally for transferring (resisting) flexural strength, in which case, the tie road is placed on the top of the beam and also through the corbel by steel plates. Connection with the tie rod is performed by preserving sleeve in bothelements, beam and column, and then following the positioning of the elements, the rod is placed.

The connection of the beam with the column on the corbel is realized through steel plates, which are welded with each other after the elements are positioned. Prior to this, the plates are welded with the elements of the longitudinal reinforcement bars.

The results of the testing of this innovative connection were compared with the results obtained for the cast-in-place referent connection, fig. 2.28a)

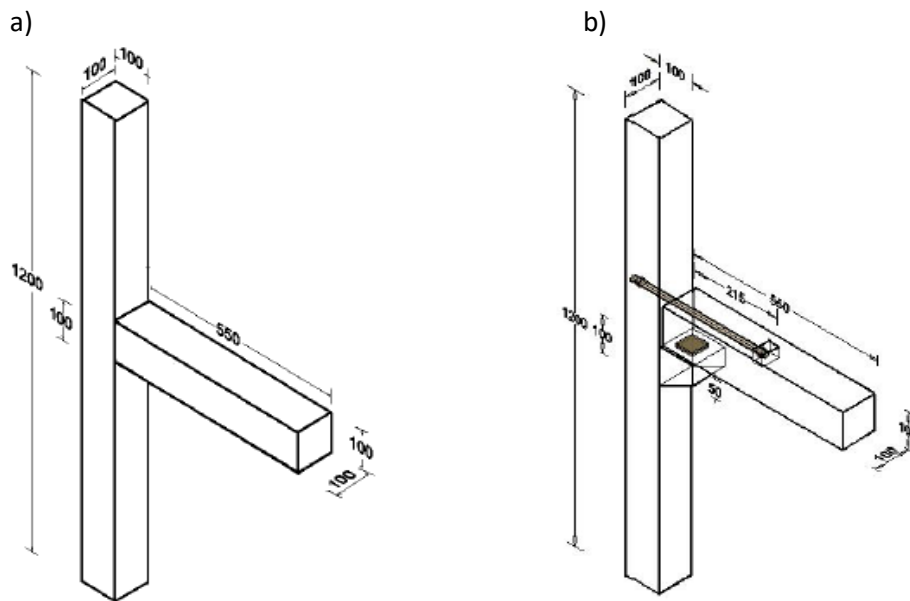


Fig.2.28.Details of experiment, a) referent model and b) proposed moment resisting connection conducted within “BEHAVIOUR OF PRECAST BEAM-COLUMN TIE-ROD CONNECTION UNDER CYCLIC LOAD; researchers: R. Vidjeapriya and K.P. Jaya, published in 2012” [Ref.:037]

Graphical presentation of the results on both specimens; the referent monolithic model (ML) and the proposed moment resisting tie-rod connection (PC-TR) are presented in fig. 2.29 in a Force-Displacement format.

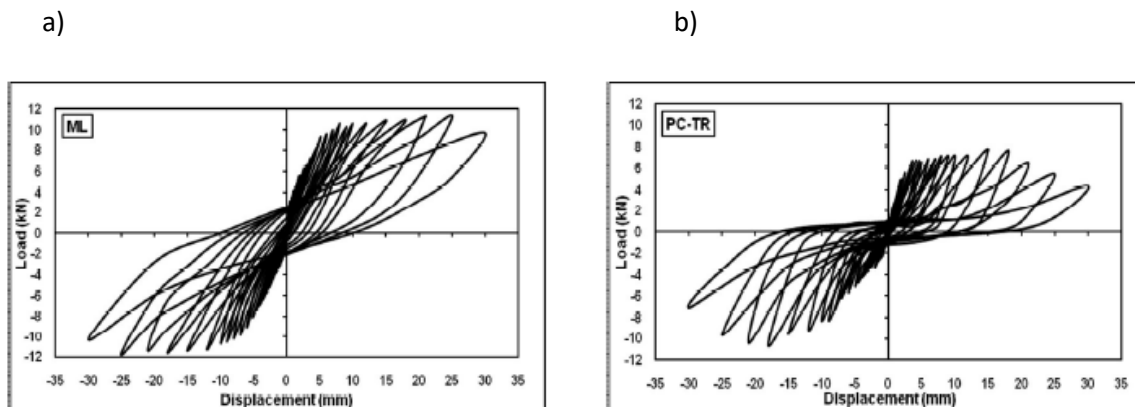


Fig. 2.29. Results, F-D diagram from experiment, a) referent model and b) proposed moment resisting connection conducted within “BEHAVIOUR OF PRECAST BEAM-COLUMN TIE-ROD CONNECTION UNDER CYCLIC LOAD; researchers: R. Vidjeapriya and K.P. Jaya, published in 2012”[Ref.:037]

From observing the behavior of both ML and PC-TR specimens, the following conclusion is drawn (the same conclusion is also presented in the referent paper):

*In positive direction, the PC-TR specimen has less load bearing capacity for 32.55% compared to the ML, whereas in negative direction, the reduction in load bearing capacity is 8.42%.*

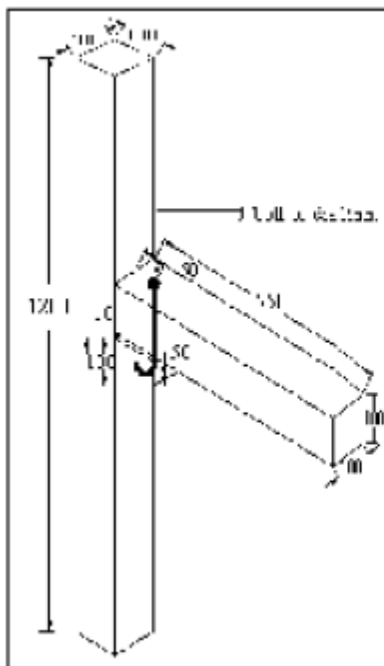
The following are the general comments and conclusions in regard to this innovative moment resisting connection:

- Positive side of this innovative connection:
  - o This connection is a dry connection and its realization on the construction site is manageable, despite the welding requirements;
  - o The proposed connection does provide a considerable amount of deformability, which is a key property regarding the seismic behavior of a structure.
- Potential negative side of this innovative connection:
  - o Strength reduction of this innovative connection for 32% can be considered significant setback for considering it as moment resisting connection, even though having 68% moment resistance of the referent cast-in-situ specimen can still be considered an achievement.

**b) Research: “BEHAVIOUR OF PRECAST BEAM-COLUMN MECHANICAL CONNECTIONS UNDER CYCLIC LOAD; researchers: R. Vidjeapriya and K.P. Jaya, published in 2011” [Ref.: 038]**

This research was conducted on an outer joint of a multi-story building. Within the scope of this research, two innovative connections were tested, PC1 and PC2, as presented in fig 2.30 a) and b).

a)



b)

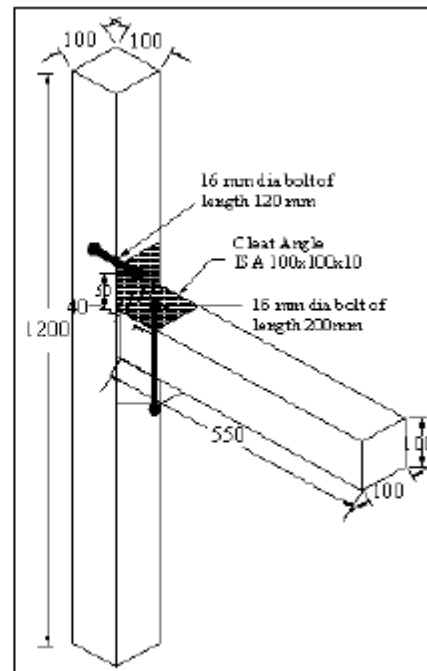


Fig.2.30. Details of experiment, a) PC1 and b) PC2 of proposed moment resisting connection conducted within “BEHAVIOUR OF PRECAST BEAM-COLUMN MECHANICAL CONNECTIONS UNDER CYCLIC LOAD; researchers: R. Vidjeapriya and K.P. Jaya, published in 2011” [Ref.:038]

- Connection “PC 1”

In this connection, the beam was supported by a concrete corbel using a J-bolt. This connection transmits vertical shear forces. The J-bolt with a diameter of 16 mm was kept inside the corbel and cast

by keeping its straight portion protruding outside. The beam was inserted into the J-bolt and the nut was tightened. Iso-resin grout was used to fill the gap between the J-bolt and the hole in the beam. The schematic representation of the isometric view of precast concrete column with corbel and the beam connected using a J-bolt is shown in Figure 2.30<sup>1</sup>.

- Connection "PC 1"

*In this type of connection, two 16mm diameter bolts were used, in which one bolt connects the cleat angle with the column and the other connects the cleat angle with both the beam and the corbel. Figure 3 shows the schematic representation of the isometric view of the precast beam-column connection using cleat angle. The cleat angle used for the connection is ISA 100x100x10. The bolts used are high tensile friction grip bolts. The gap between the bolts and the groove was filled using iso-resin grouts.*"<sup>2</sup>

The results of this specimen and the referent monolithic specimens are presented in fig. 2.31 a), b) and c).

- Results on connection PC1

*In positive direction, the PC 1 specimen has less load bearing capacity for 51.99% compared to the ML, whereas in negative direction, the reduction in load bearing capacity is 61.11%.*

- Results on connection PC2

*In positive direction, the PC 2 specimen has less load bearing capacity for 61.65% compared to the ML, whereas in negative direction, the reduction in load bearing capacity is 69.53%.*

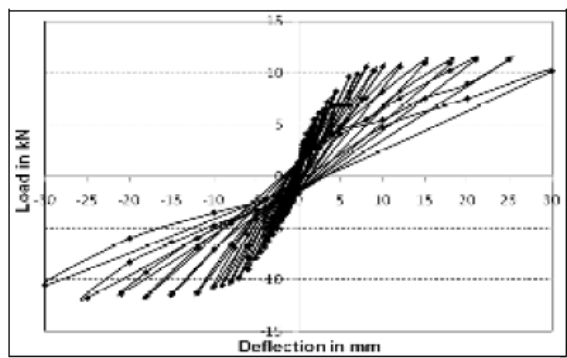
---

<sup>1</sup> This citation is extracted from the referent paper.

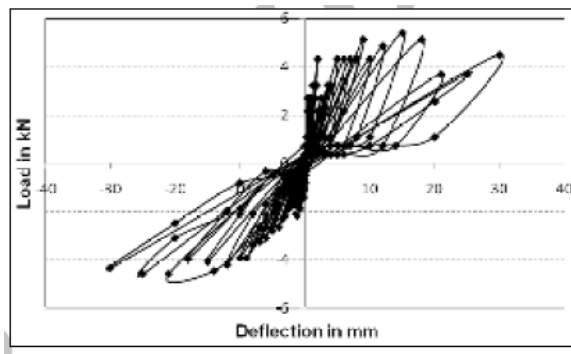
<sup>2</sup> This citation is extracted from the referent paper



a)



b)



c)

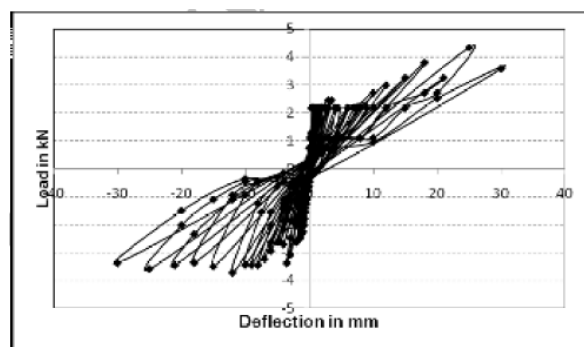


Fig.2.31. Results of experiments on: a) Monolithic specimen (ML), b) PC1 specimen and c) PC2 specimen, within the research "BEHAVIOUR OF PRECAST BEAM-COLUMN MECHANICAL CONNECTIONS UNDER CYCLIC LOAD; researchers: R. Vidjeapriya and K.P. Jaya, [Ref.:038]

### 2.5.2.2 Recent investigation performed on hybrid connections

The hybrid moment resisting joints are the joints that are combined with ordinary reinforcement of member elements and post-tension elements introduced in joints.

As illustrated in FIB Bulletin 27 [Ref. 034] in the Kobe earthquake of 1995, most of the precast structures with post-tension connection have shown very good performance and, as such, this type of connection is highly recommended.

Recently, numerous investigations and studies have been performed on hybrid beam-to-column connections for specifying a beam-to-column hybrid connection methodology and determining their behavior, [Ref.:024], [Ref.:040], [Ref.:015], [Ref.:011]

Below are presented two recent studies/experiments on hybrid beam-to-column connections. There have also been researches other than these two, but these are presented for a representative hybrid beam-to-column connection since the concept of beam-to-column hybrid connection is generally the same.

a) Research: “Hybrid Moment Frame Joints Subjected to Seismic Type Loading” by M. I. Pastrav and C. Enyedi, presented at 15WCEE-Lisboa 2012 [Ref.:023]

The subject of this research was investigation of the performance of a hybrid joint in typical precast multi-story frame.

Under this research study, two types of joints (N1 and N2) were investigated.

The test specimen and details of joints are presented in fig.2.32 and fig. 2.33 a) and b).

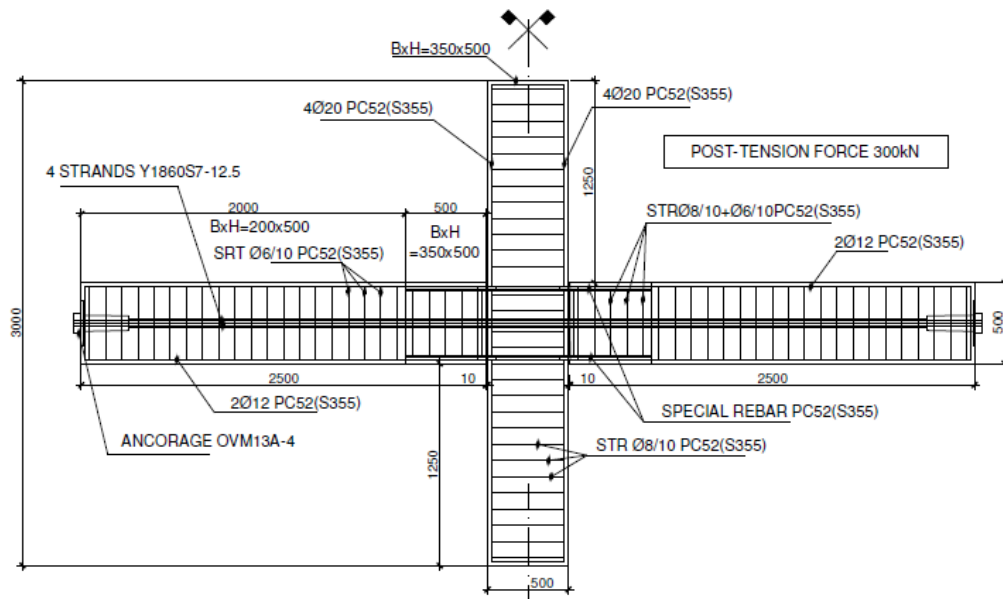


Fig 2.32 Test specimen within the research “Hybrid Moment Frame Joints Subjected to Seismic Type Loading” by M. I. Pastrav and C. Enyedi, presented at 15WCEE-Lisboa 2012”, [Ref.:023]

a) Hybrid joint N1

b) Hybrid joint N2

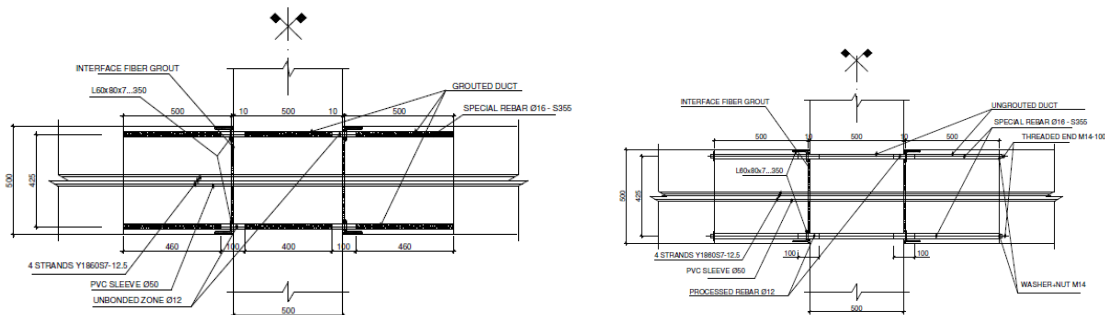
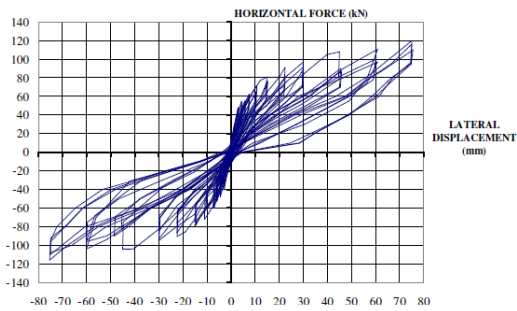


Fig 2.33 Detail of connections tested within the research “Hybrid Moment Frame Joints Subjected to Seismic Type Loading” by M. I. Pastrav and C. Enyedi, presented at 15WCEE-Lisboa 2012 [Ref.:023]

- Results of the experiment

The force-deformation relationship for both types of joints is presented in fig. 2.34 given below.

b) Hybrid joint N1



b) Hybrid joint N2

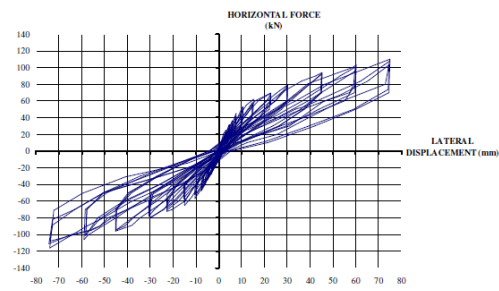


Fig. 2.34 Force-Deformation diagram for joint N1 and N2 [Ref.: 023]

The final results and conclusions after the testing are:

- In both types of joints, the cracks in the elements, except the interface opening, are less than 0.2mm;
- The estimated and actual flexural strength of the joints are as follows:

N1 Model		N2 Model	
Estimated flexural strength (kNm)	Test flexural strength* (kNm)	Estimated flexural strength (kNm)	Test flexural strength* (kNm)
157.6	150.6*	160.3	144.2*

\* = Flexural moment corresponding to the maximum lateral displacement of 75mm.

**b) Research: “Experimental study on a new precast post-tensioned concrete beam column connection system” by Do Tien THINH, Koichi KUSUNOKI and Akira TASAI , presented at 14WCEE-Beijing 2008 [Ref.: 033]**

The scope of this research was to investigate the performance of a hybrid joint of precast beam-column connection.

One connection with three types of shear force transfer was tested, fig. 2.35:

- Connection (SP1-A) designed without shear bracket in which case shear gravity forces from beam to column are transferred through the friction and the pre-stressed bars. Here the pre-stressed bars are designed to resist demand moment and shear force.
- Connection (SP2-A) with shear bracket to resist shear forces from gravity. Here the pre-stressed bars are designed to resist demand moment and shear force induced by seismic load.
- Connection (SP3-A) similar to SP2-A with shear bracket to resist shear forces from gravity only 1.5 higher than SP2-A.

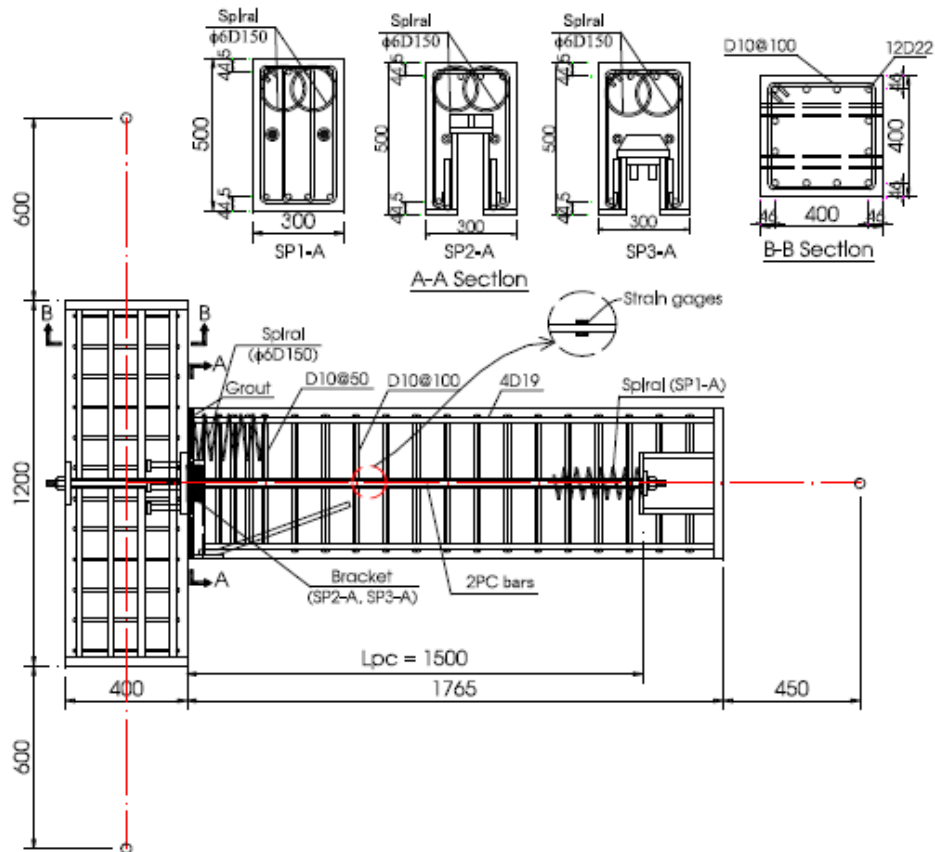


Fig. 2.35 Details of realization of connections tested within the research: “Experimental Study on a New Precast Post-Tensioned Concrete Beam Column Connection System” by Do Tien THINH, Koichi KUSUNOKI and Akira TASAI , presented at 14WCEE-Beijing 2008 [Ref.: 033]

- Results of the experiment

The moment- deformation relationship for three types of connections is presented in fig. 2.36 given below.

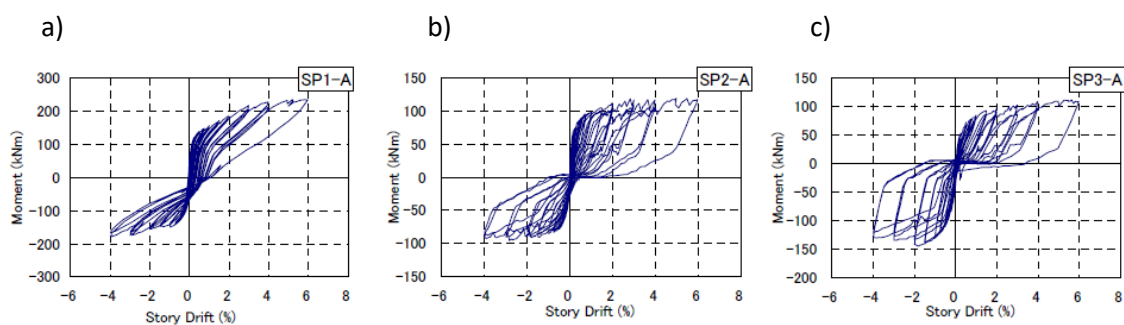


Fig. 2.36 Results of experiment, Moment-Story Drift diagram of: a) Connection SP1-A, b) Connection SP1-A, and c) Connection SP3-A.

The results on strength and story drifts are given in table 2.1

Table 2.1 Beam moment strength and story drift of experiments [Ref.: 033]

Specimens	Loading Direction	$M_d$ (kNm)	$R_d$ (%)	$M_y$ (kNm)	$R_y$ (%)	$M_{max}$ (kNm)	$R_{max}$ (%)
SP1-A	+	97.1	0.09	185.6	1.99	234.9	5.21
	-	-84.7	-0.20	-152.5	-1.74	-178.7	-4.0
SP2-A	+	52.7	0.09	109.4	3.82	118.7	4.97
	-	-50.3	-0.12	-94.2	-2.65	-95.4	-2.82
SP3-A	+	53.8	0.07	101.9	3.85	110.9	5.62
	-	-43.1	-0.15	-132.0	-2.61	-144.3	-1.82

The author of the research concluded that all three specimens provided story drift, 6% in positive direction and 4% in negative direction. Also, the specimen with shear bracket exhibited a much better behavior than the specimen without shear bracket.

### 2.5.3 Summary of current state regarding moment resisting precast connection

As presented in this chapter, moment resisting connections in precast structures are the best solution and, for seismic areas, they are the necessary solution for construction of connections.

#### a) Wet connections

Currently, the widely spread solution for realizing moment resisting beam-to-column connections in precast structures is the wet connection or partially wet connection. Wet connections are also presented as means for realizing moment resisting beam-to-column connection in many publications.

The only limitation for realizing moment resisting wet connection is that the length of the “connection” has to respect the requirement for length of lap splices. In all cases when this requirement is met, the connection behaves as a monolithic connection and, to confirm this, there is no need for any experimental investigation.

The downside (negative part) of the wet connections is that there is always a need for applying formworks and scaffoldings and the implication of concreting activities. This cast-in-situ concreting requirement is an obstacle for progress of the works on precast structures and, in a way, minimizes, to a certain degree, the benefit that precast structures have in regard to the construction speed. This is something that makes difference in decisions regarding choosing a structure type and connection type and most likely is one of the main reasons that most of the beam-to-column connections that are used in single story structures are dry pinned connections.

#### b) Hybrid connections

Recently, many investigations have been focused on realization of moment resisting connections through application of post tensioning of the connections.

Most of the hybrid connections studied have post tension tendon in the center of element. From the presented experiments, it is evident that the connection as a whole has good resistance under cyclic loading and is capable of sustaining a large number of load cycles.

The moment resistance offered with these hybrid connections is provided indirectly through axial tension on the beam-to-column connection. Without consideration of axial tension, these types of connections are hinged connections. Therefore, the only way to realize fixity in hybrid connections is through axial compression in the connection as a result of axial tension on the beam.

Even though hybrid connections can be designed to offer moment resistance, the wide application of such connections would still be difficult due to the complication that the execution of post tensioning makes.

#### 2.5.4 Coverage of precast moment resisting connections by Eurocode

The overall connections of prefabricated structures are only generally covered in EC2 and EC8. In regard to moment resisting connections, Eurocode (EC2 and EC8) provides more requirements for the anticipated behavior of the connection, but there are no technical guidelines on how to realize a moment resisting connection.

In **Eurocode 2**, there is one Chapter dedicated to precast structures, "*Chapter 10 - Additional Rules for Precast Concrete Elements and Structures*". In this chapter, article 10.9.4.5 - *Connections Transmitting Bending Moments or Tensile Forces* gives general recommendations/requirements for realizing a moment resisting connection, as follows:

1. Reinforcement shall be continuous across the connection and anchored in the adjacent elements.
2. Continuity may be obtained by, for example:
  - lapping of bars
  - grouting of reinforcement into holes
  - overlapping reinforcement loops
  - welding of bars or steel plates
  - pre-stressing
  - mechanical devices (threaded or filled sleeves)
  - swaged connectors (compressed sleeves)

In **Eurocode 8**, there is a sub-chapter dedicated to precast structures, "Chapter 5.11 – Precast Concrete Structures", whereas connections are covered in "Chapter 5.11.2 – Connection of Precast Elements". In most of the part of EC8 dedicated to connections, recommendations on values of parameters to be used and the procedure for evaluation of the resistance of non-seismically resistant connections are given.

In regard to the requirements for the connections with seismic resistance properties, and especially with regard to the requirements referring to the behavior of steel elements (sections or bars) fastened into the concrete, demonstration of seismic resistance of the connection is required both analytically and experimentally.

## 2.6 Shaking table experiments of precast frames realized with prefabricated beam-to-column connections

With shaking table experiments it is possible to determine behavior of the precast connection, including precast beam-to-column connection. However, shaking table experiments are the best experiments for determining the overall behavior of the reinforced concrete precast frame as a whole with considering impact of respective prefabricated connections.

In shaking table experiments for determining total global deformation of the frame, or element, other connections also will have impact.

### 2.6.1 “Shaking table tests on precast reinforced concrete and engineered cementitious composite/reinforced concrete composite frames”; [Ref.:040]

The purpose of this experiment has been to assess performance of the prefabricated structure with moment resisting connection under shaking table loading of a frames constructed as:

- i. Reinforced Concrete (RC) structure, and
- ii. Reinforced Concrete (RC) structure with replacing concrete with a high-performance fiber-reinforced cementitious composite (ECC) at the beam-to-column joints and at the bottom columns of precast RC frames.

#### a) Specimen details

This experiment is performed on the model, scaled by 3 (Dimension scale factor  $S=1/3$ ), of a prototype 4 floor building designed according to China Code. The building is square shape with symmetrical single-bay frames. The shape of the building is presented in the figure 2.37

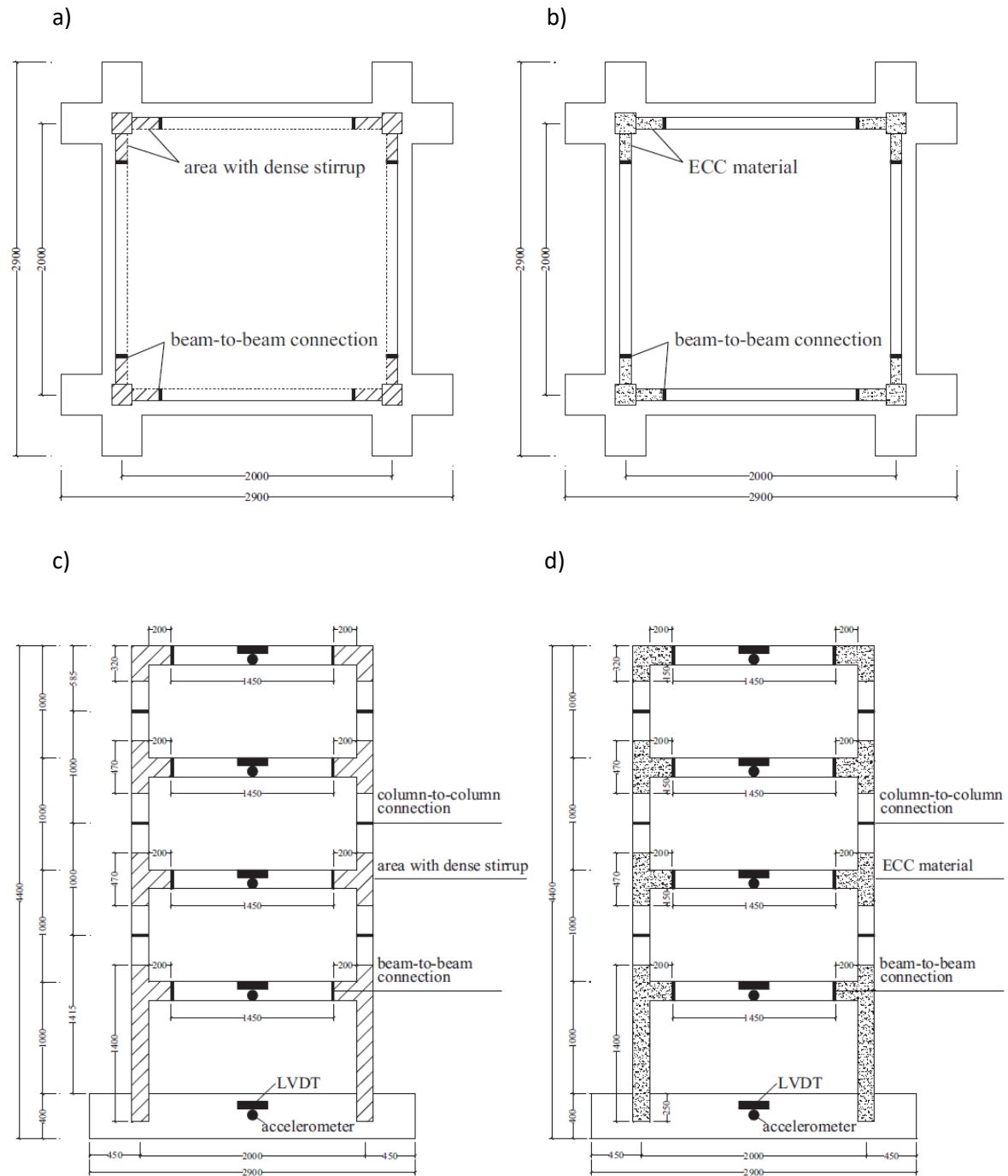


Fig 2.37 Geometric properties of the testes specimens: a) Floor layout of RC structure, b) Floor layout of ECC/RC structure, c) Cross-section of RC structure, d) Cross-section of ECC/RC structure [Ref.: 040]

Design parameters used for design are:

- PGA 0.10 g basic design acceleration which is magnified by 2
- imposed load (variable load) is  $2.0 \text{ kN/m}^2$  based on the load code for the design of building structures (China Ministry of Construction, 2012), and
- Additional dead load  $0.4 \text{ kN/m}^2$  which is considered as the finishes and screeding load.

The details of the section of the elements are presented in fig. 2.38



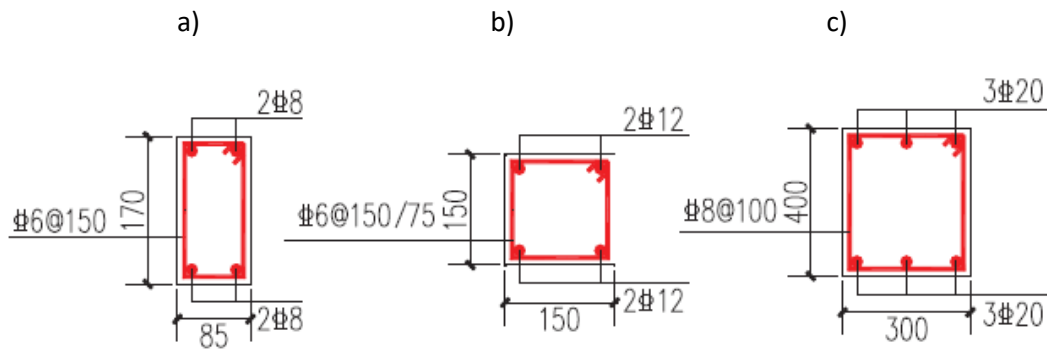


Fig. 2.38 Section details of the elements following design; a) beam, b) column, c) beam base [Ref.: 040]

### b) Connection details of precast elements

The connection of the elements are performed as follows, fig. 2.39:

- Colum-to-column is performed on the middle of the column height
- Beam-to-column is performed near to beam inflection point

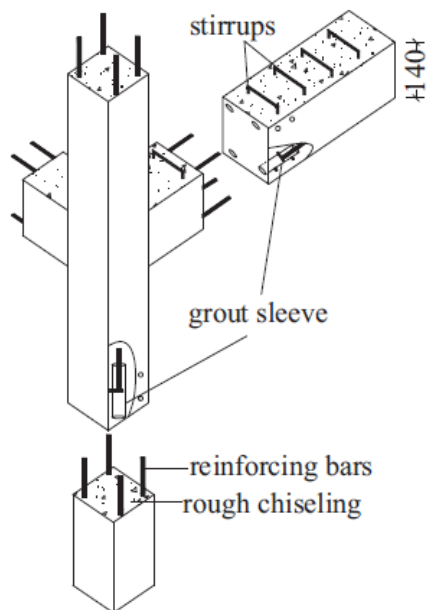


Fig. 2.39 Detail of connections of the elements, column-to-column and beam-to-column, [Ref.: 040]

The following loading programme is applied:

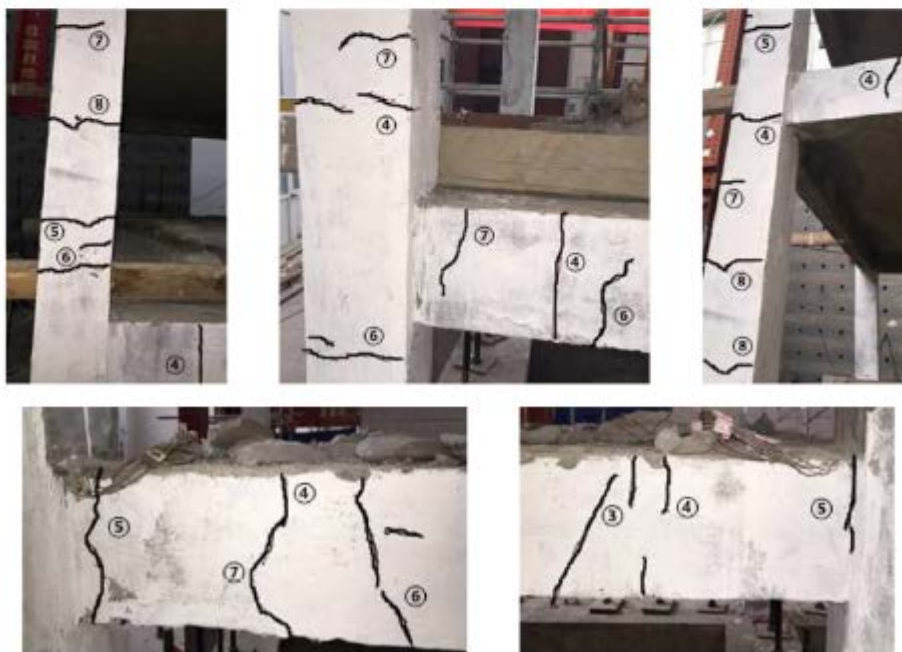
- the peak table acceleration progressively increased from 0.07 to 1.5 g for the eight loading conditions in the tests
- the predominant period of the recorded Castaic wave, Taft wave, and artificial wave is 0.32, 0.34, and 0.37 s respectively, which is very close to the characteristic period of the site 0.35 s

c) Results from experiments

In fig. 2.40 are presented final crack patterns of tested specimens, a) Crack pattern of RC frame, and b) Crack pattern of ECC/RC frame.



(a)



(b)

Fig. 2.40 Crack patterns after completion of experiments of tested specimens, a) RC frame, b) ECC/RC frame [Ref.: 040]

From crack pattern presented in fig. 2.40 it could be noted that the main damages on both specimens occurred away from the element connection point. This is a confirmation that when the beam-to-

column connection is performed near to inflection point than the connection point will not be subject to any flexural impact.

Following crack pattern from fig. 2.40 further it could be noted than in the specimen ECC/RC on the area around joint where the concrete is replaced with ECC no cracks have developed.

The results of global performance of the specimen, presented by total global displacement, are presented in fig. 2.41.

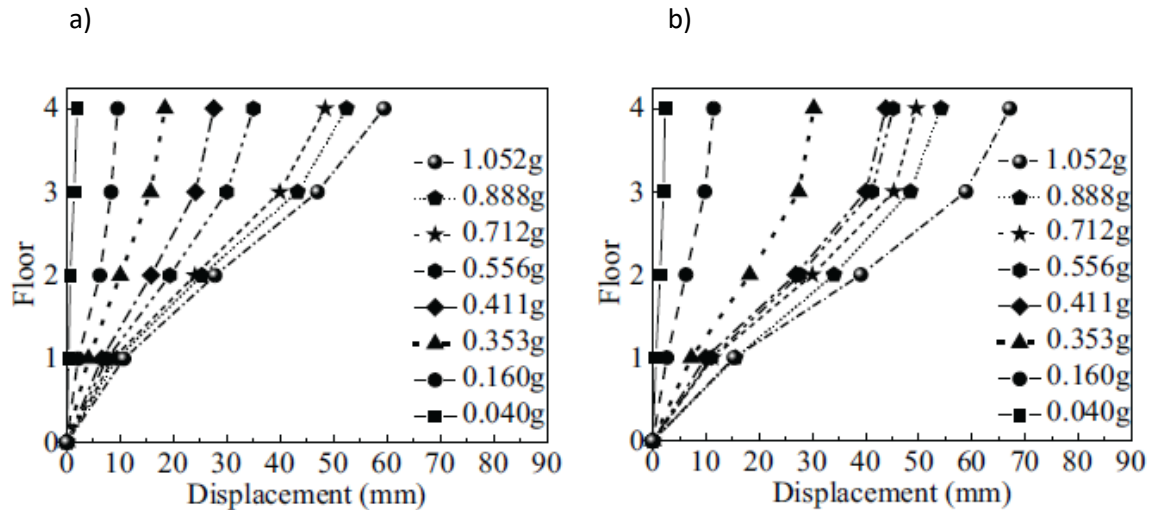


Fig. 2.41 Total global displacement of specimens, a) RC frame and b) ECC/RC frame under different PGA values. [Ref.: 034]

From fig. 2.41 it could be noted than overall trend of the global displacement on both specimen is similar.

### 2.6.2 “Assessment of the seismic design of precast frames with pinned connections from shaking table tests”, [Ref.: 024]

The purpose of this experiment has been to assess performance of the prefabricated frame with beam-to-column pin connection under shaking table loading.

#### a) Specimen details

The experiment has been performed on single-story, one-bay frames constructed of precast column and beam. The elements, beam and column are connected with dowels as a dry pinned connection. Due to limitations in the span length imposed by the shaking table dimensions (4.00m × 4.00 m), only one half of each frame has been tested, fig. 2.42 .At the mid-span in the prototype structure, appropriate boundary conditions were applied.

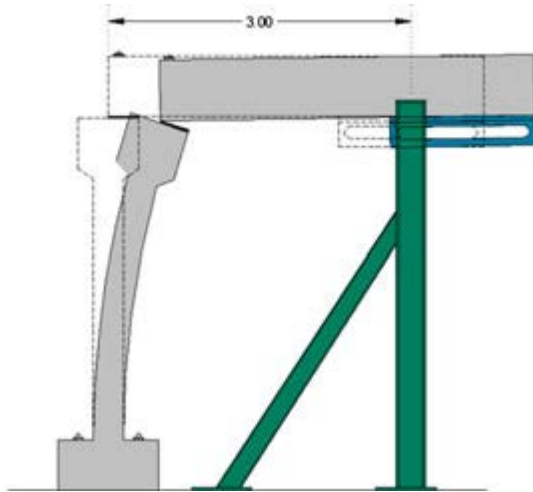


Fig. 2.42 Experimental set-up of a half of frame [Ref.:024]

In total 9 specimens have been tested. These specimens have been distinguished with type of columns in respect to stiffness and strength. In general the types of columns applied on the specimens are as follows:

- Flexible and Weak, type “FW”
- Stiff and Strong, type “SS”
- Flexible and Strong, type FN

The details of the columns in regard to properties and design parameters are presented in the table 2.2

Table 2.2 Detail of specimen of experiment [Ref.: 024]

Column type	Specimen	Dowels	Cover $d$ (m)	Column dimensions <sup>a</sup> / reinforcement <sup>b</sup>	Normal. axial force, $\nu^d$	Design parameters	
						$S \cdot a_g$ (g) <sup>e</sup>	$q^f$
FW	ST-1	2 $\varnothing$ 25	0.10	30×40 / 8 $\varnothing$ 14	0.032	0.40	3.50
	ST-2						
SS	ST-4	2 $\varnothing$ 25	0.10	60×40 / 14 $\varnothing$ 20	0.018	0.50	1.00
	ST-5						
FS	ST-3	2 $\varnothing$ 25	0.10	30×40 / 24 $\varnothing$ 25 <sup>c</sup>	0.031	0.50	1.00
	ST-6				0.032		
	ST-7	2 $\varnothing$ 25	0.20	30×40 / 24 $\varnothing$ 25 <sup>c</sup>	0.048	0.50	1.00
	ST-8	1 $\varnothing$ 25	0.10	30×40 / 24 $\varnothing$ 25 <sup>c</sup>	0.048	0.50	1.00
FN	ST-9	2 $\varnothing$ 25	0.10	30×40 / 12 $\varnothing$ 20	0.032	0.16	3.50

FW flexible–Weak, SS stiff–strong, FS flexible–strong, FN flexible–normal

<sup>a</sup> The first dimension corresponds to the longitudinal direction of the frame (direction of base excitation)

<sup>b</sup> Concerns only the reinforcement placed at the two sides of the cross section that are normal to the direction of shaking

<sup>c</sup> Placed in two rows at each side of the cross section

<sup>d</sup> Axial force normalized to  $A_c f_{cm}$ ,  $f_{cm}$  being the mean concrete strength (Table 2)

<sup>e</sup> Design ground acceleration according to EC8,  $S$  being the soil coefficient

<sup>f</sup> Behaviour factor (also called reduction factor in some codes) used for the dimensioning of the column

**b) Experiment set-up and loading details**

In the fig. 2.43 is presented picture of the experiment set-up.

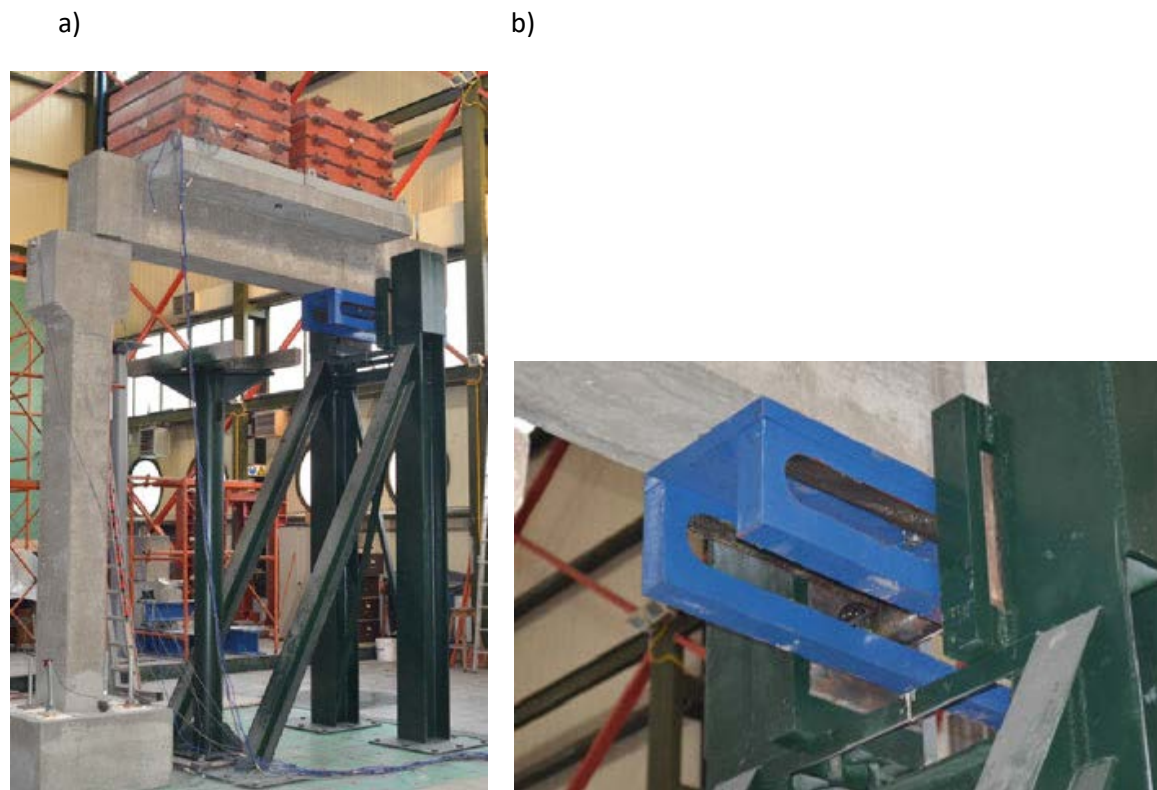


Fig. 2.43 Experimental set-up details; a) Overall specimen, b) detail of sliding achievement on the middle beam [Ref.: 033]

Loading details and concrete strength of the specimen are presented in table....., whereas quality of the reinforcement used is  $f_y=580\text{MPa}$ .

Table 2.3 Loading details and material properties of the specimen [Ref.: 024]

Column type	Specimen	Concrete strength $f_{cm}$ (MPa)	Excitation <sup>b</sup>	Max scaled $pga$ (g)
FW	ST-1	36.17	JFA (H)	0.21
	ST-2	36.17	JFA (HV)	0.21
SS	ST-4	34.30	Petrovac (H)	0.65
	ST-5	34.30	Sine Beat (H)	1.00/0.75 <sup>c</sup>
FS	ST-3	37.68	Petrovac (H)	0.60
	ST-6	36.74	Petrovac (HV)	0.60
	ST-7	24.35	Petrovac (H)	0.65
	ST-8	24.35	Petrovac (H)	0.65
FN	ST-9	36.17	Petrovac (HV)	0.65

FW flexible–Weak, SS stiff–strong, FS flexible–strong, FN flexible–normal

b. H horizontal, HV horizontal and vertical

c. max  $pga = 1.00$  g for  $T = 0.26$  s and  $0.75$  g for  $T = 0.60$  s

### c) Experimental results

The results of shaking table experiment; the overall behavior of the specimen has been compared with the results of similar specimens tested under quasi-static loading and the total strength of the specimen has been compared with analytical calculations of strength of the pin connection.

The results of the experiment, in the form of global force-joint slip diagram are presented as follows:

- in the fig. 2.44 are presented results of specimen ST-4
- in the fig. 2.45 are presented results of specimen ST-6
- in the fig. 2.46 are presented results of specimen ST-8

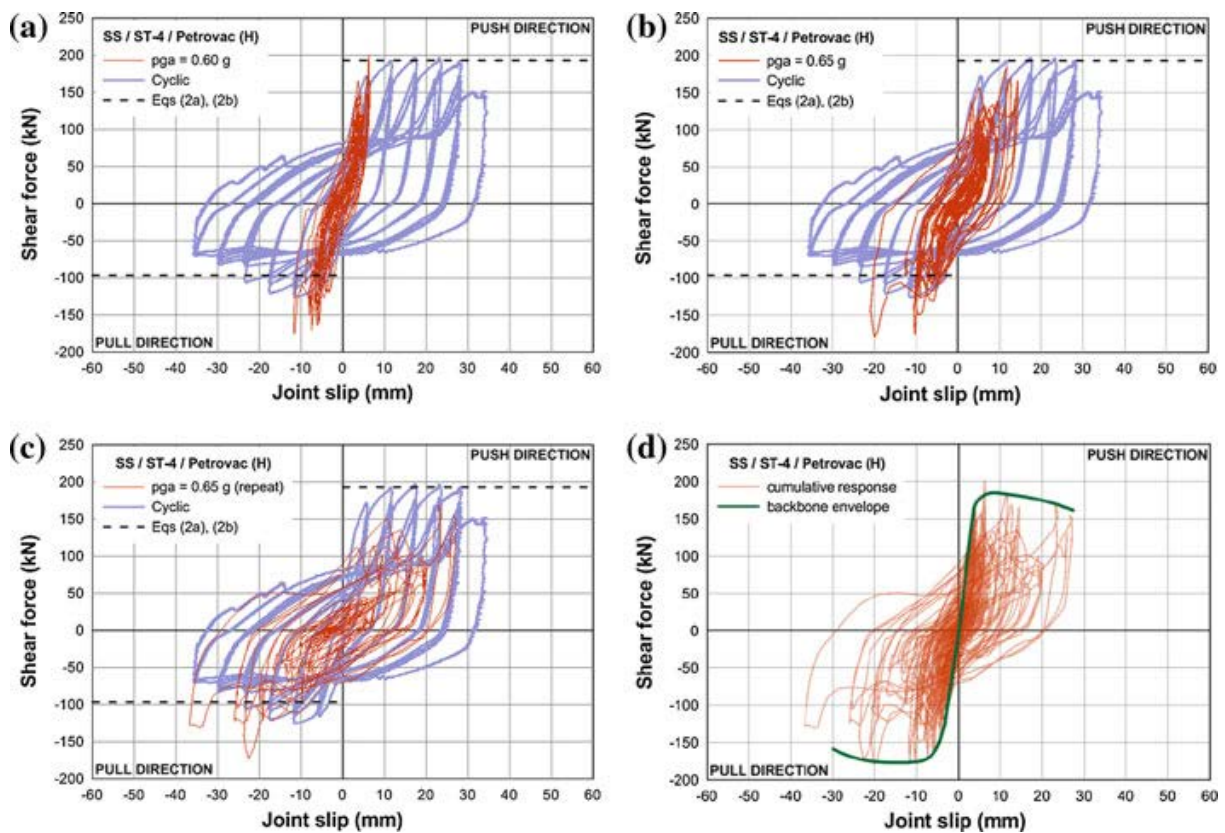


Fig. 2.44 Shear force versus joint slip diagrams for ST-4 specimen (SS column) subjected to Petrovac earthquake in the horizontal direction for stepwise increasing pga and comparison with the corresponding cyclic response (Psycharis and Mouzakis 2012); d backbone envelope of the cumulative response. [Ref.: 024].

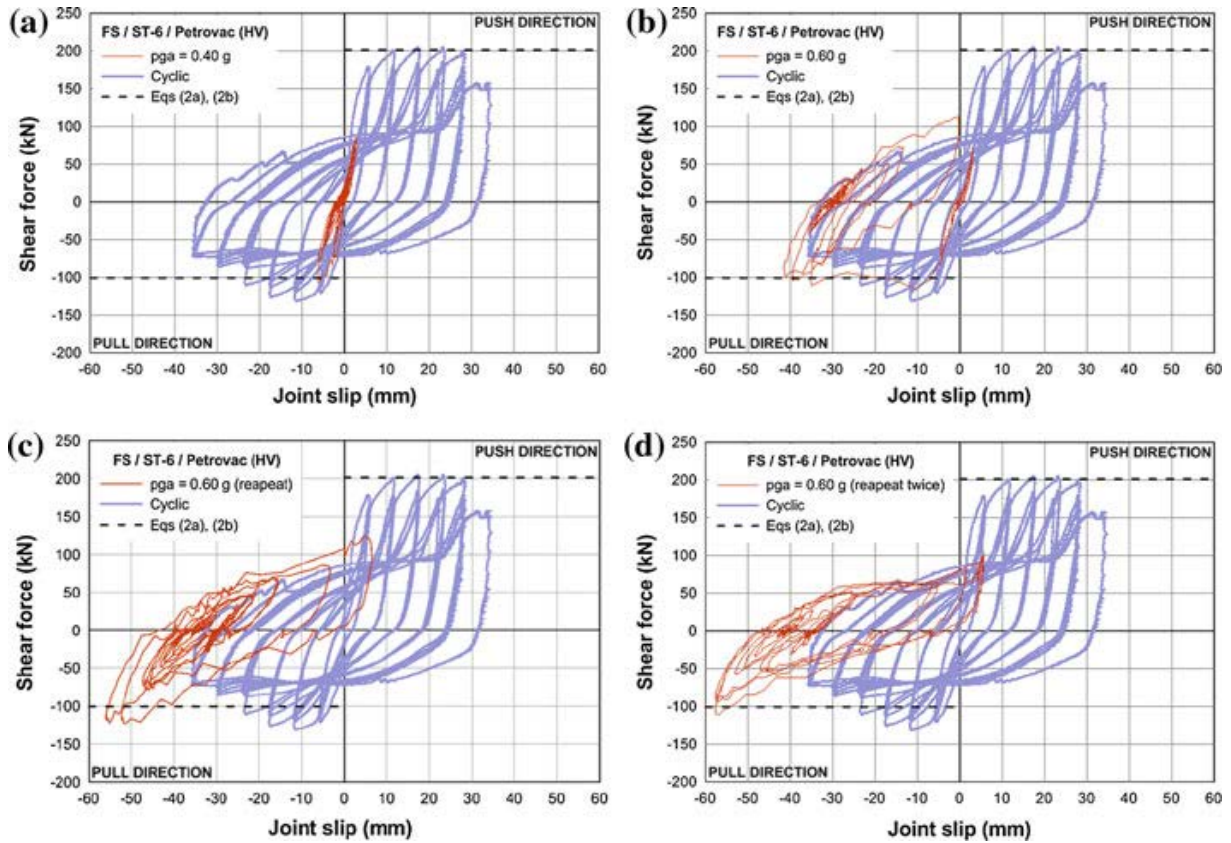


Fig. 2.45 Shear force versus joint slip diagrams for the ST-6 specimen (FS column) subjected to Petrovac earthquake applied in the horizontal and the vertical directions for stepwise increasing pga and comparison with the corresponding cyclic response (Psycharis and Mouzakis 2012). [Ref.: 024].

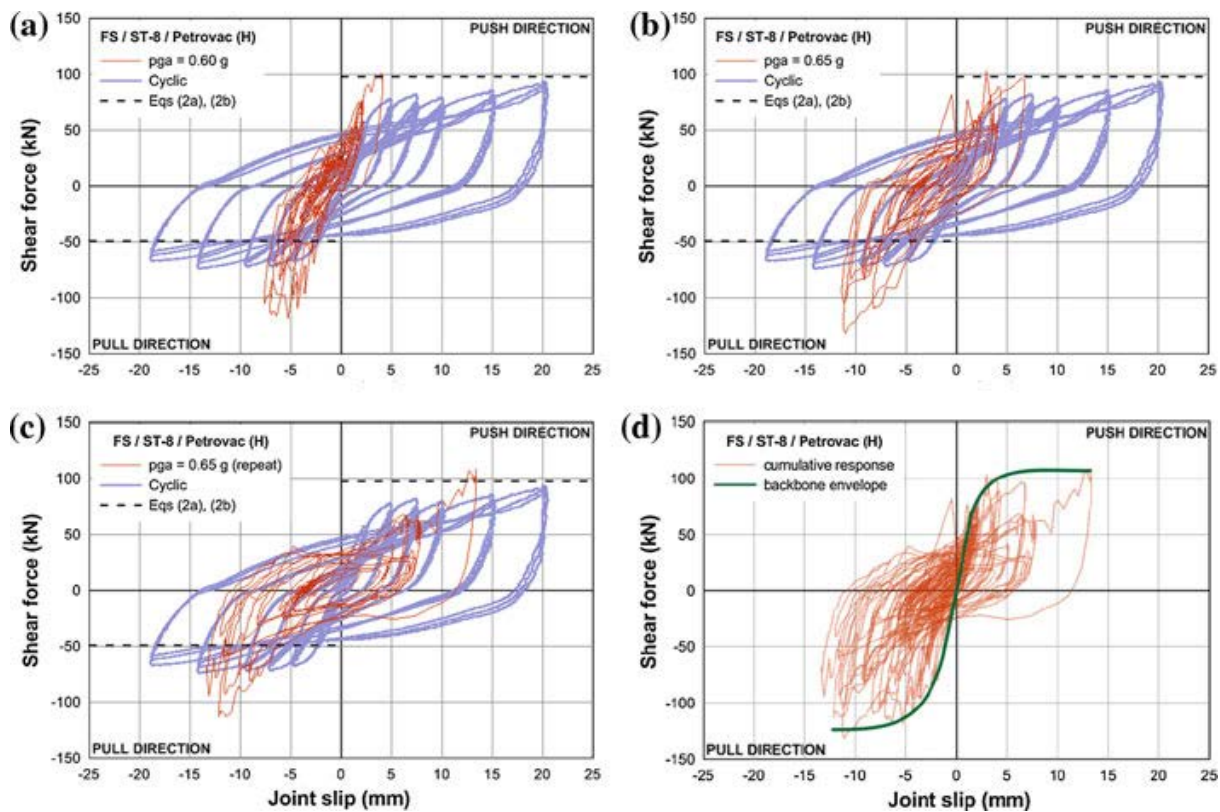


Fig. 2.46 a–c Shear force versus joint slip diagrams for the ST-8 specimen (FS column, connection made of one dowel) subjected to Petrovac earthquake applied in the horizontal direction for stepwise increasing  $p_{ga}$  and comparison with the corresponding cyclic response (Psycharis and Mouzakis 2012); d backbone envelope of the cumulative response. [Ref.: 024]

## 2.7 Gap to be filled

As presented in this chapter, application of moment resisting beam-to-column connection will provide redundancy for a structure which will directly have an impact on the increase of the earthquake resistance capacity of the structure.

In order to enable mass application of precast structures with moment resisting beam-to-column connections, they must be economically feasible, because otherwise, they will not be adopted as a solution by investors.

Presently, connections which can ensure moment resistance are wet connections which are not so much desirable since they require casting-in-situ.

The only dry moment resisting beam-to-column connection that have proved to behave well are the hybrid connections. Despite the good behavior of the hybrid connections, their negative aspects can be a big constraint for their wide use in engineering practice.

The best solution, which can be widely adopted in the precast structure industry is the moment resisting beam-to-column dry connection. The potential solution is to develop a dry moment resisting connection realized with dowel (s) only, with no post tension required. Such a connection can be easy



adopted as a solution for applying seismically resistant precast structures in large span structures, especially industrial buildings.

Developing moment resisting beam-to-column dry connection has been the main research subject of this dissertation with the goal of contributing to further development of more seismically resistant and practical solution.

## CHAPTER 3 - Numerical Modeling of Experiments Performed at UL under SAFECAST Project

### 3.1 Scope

Precast connections realized with single dowels have structurally and generally been considered pinned connections.

The main scope of this chapter is dedicated to verification/confirmation whether precast connections realized with single dowels can be considered as pinned connections for general engineering practices.

In order to make this verification, the results from the experiments performed at UL under SAFACAST Project have been used for further analytical research.

The following approach has been adopted for analytical research:

**First step** - A non-linear modeling of single dowel precast connections has been performed where the respective model parameters of the adopted hysteretic model have properly been calibrated using experimental results as a benchmark.

**Second step** – On the final non-linear model, a non-linear static analysis has been performed, using the properly calibrated non-linear parameters of the adapted hysteretic model, with the purpose of obtaining the member forces at the end column section (connection of the column with the foundation). Specifically, the bending moment at the end column section has been monitored and used as a reference.

**Third step** - Dynamic linear analysis of the same frame has been performed where, at the beam-to-column connection, an elastic hinge has been used. In this analysis, bending moments at the same location as in the non-linear analysis (b) have been obtained and both have been compared.

This verification has been performed on a specimen with centrally positioned dowels since such connection in both directions of force acting (push and pull) exhibits the same behavior, specifically in the elastic range.

Eccentrically positioned dowels have not been considered in this test since, in each direction of force acting, they exhibit different behavior (elaborated in more details further in this chapter).

In addition to the centrally positioned dowels, also for other specimens, a non-linear analysis has been performed for the purpose of calibrating non-linear parameters if needed in engineering practice for any further study.

For this very purpose, the tool/software selected to develop the numerical model has been SAP 2000 software that contains non-linear dynamic modeling which, to an acceptable extent, models the actual behavior of connections, but is also vastly spread out and used among engineers in practice.

The second goal of this chapter has been to determine and elaborate in detail the performance of the tested connection for the purpose of using the acquired knowledge in design of moment resisting connections, as the main goal of this research, and for general engineering practical use.

### 3.2 SAFECAST project, description and goals [Ref.: 027]

The SAFECAST project is a project financed by European Commissions. This project succeeds two other EU funded projects, ECOLEADER and PRECAST EC 8 project, where under these two projects, it was confirmed that precast frames and buildings can experience ductile behavior.

The SAFECAST Project objective was to gain a deeper knowledge on the seismic behavior of precast structures with emphasis on connections. Furthermore, the goal of the project was to develop reliable numerical tools to be used in the design and finally in codifying new criteria for the design of precast structures in seismic regions.

Part of the research under the SAFECAST Project was done at the University of Ljubljana, where the experimental program was carried out.

### 3.3 Description of experiments performed at UL under SAFACAST project

Within the SAFECAST Project, 13 experiments on beam-column connection were performed.

The experiments were focused on behavior of pinned connections with variation of location and number of dowels within the connection. Three types of connections were tested:

- Top centric connection,
- Top eccentric connection, and
- Intermediate story.

The objective of these experiments was to explore, to the best possible extent, the strength and deformation capacity of the existing connections, including of the dowels, considering the large relative rotations between the beam and the column.

The first connection type, top centric connection where the dowel is located in the center of the column, was tested with different column stiffness, with column dimensions 40x40cm and 50x50 cm, and different column strength within the column dimensions 40x40 cm by increasing the strength of the column with longitudinal reinforcement, as presented in table 3.1. For each type of element dimensions, the experiments were carried out by use of two different loading procedures, monotonic (push pull) and cyclic loading in order to explore the possible degradation of stiffness and strength of the connection under cyclic loading.

Fig. 3.1 shows the set-up for the top centric connection.

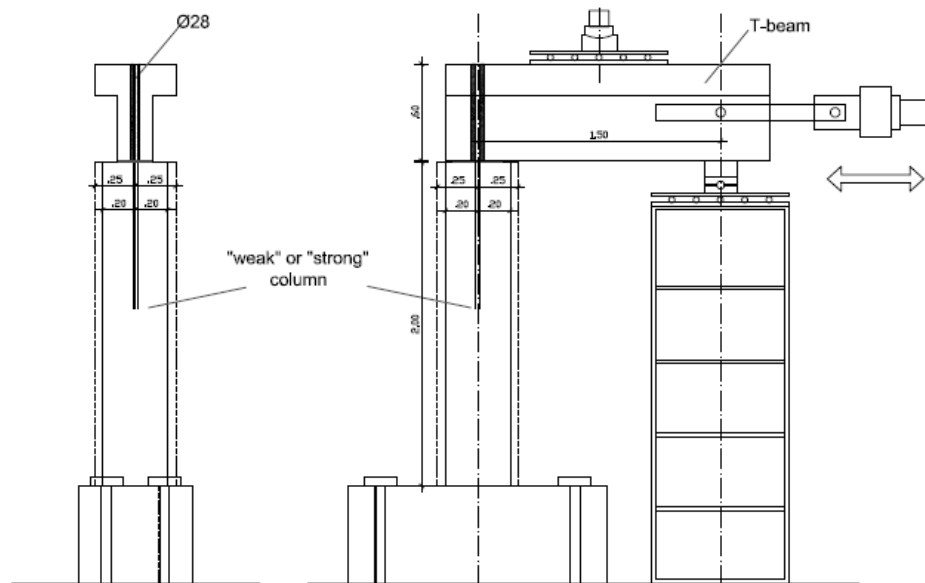


Fig. 3.1 Top centric connection, [Ref.: 027]

For the second connection type, i.e., top eccentric connection with the dowel positioned eccentrically within the column center and near the column face, the experiments were conducted with the same column stiffness and strength, but with two different loading procedures, namely, push pull and cyclic. Presented in fig. 3.2 is the set-up for the top eccentric connection.

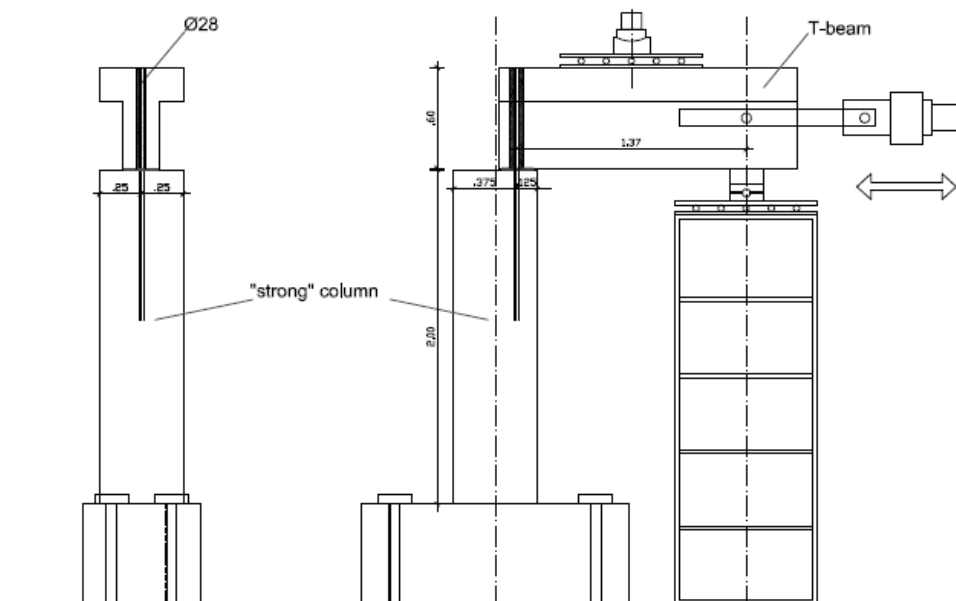


Fig. 3.2 Top eccentric connection, [Ref.: 027]

The third connection, i.e., an intermediate story beam-to-column connection with two dowels, was tested by using the same loading procedure (cyclic loading), but with different column dimensions, namely, one experiment with column dimensions 40x40cm and the other one with column dimensions 50x50cm. Fig. 3.3 shows the set-up for the intermediate story connection.

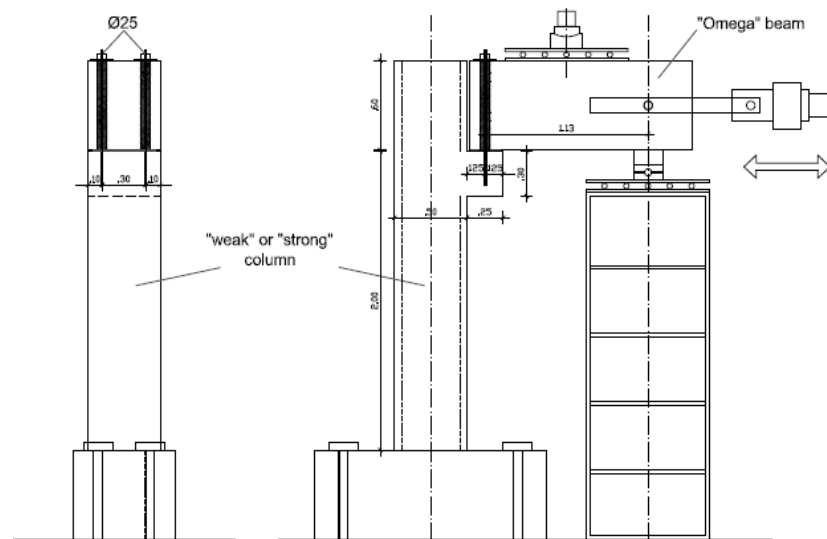


Fig. 3.3 Intermediate story connection, [Ref.: 027]

Table 3.1. Detail of experiments on elements conducted under the UL program, [Ref.: 027]

Exp. No.:	Label	Beam Type	Dowel position	Column type	Column cross-section	Column long. reforc.	Test type			
1	S1-1	T - beam	Top centric	Strong	50x50 cm	16F22	Push-pull			
2	S1-2						Cyclic			
3	S2			Weak	40x40 cm	8F16	Cyclic			
4	S3-1					8F14	Push-pull			
5	S3-2					8F14	Cyclic			
6	S4					8F12	Cyclic			
7	S5-1					8F20	Cyclic			
8	S5-2					4F18+4F20	Cyclic			
9	S6-1					Top eccentric	Strong	50x50 cm	14F22	Push-pull
10	S6-2									Cyclic
11	S7-1	Omega Beam	Intermediate	Strong	50x50 cm	14F22	Cyclic			
12	S7-2									
13	S8			Weak	40x40 cm	6F18+2F14	Cyclic			

### 3.4 Analysis of performance of connections

Understanding the performance of precast dry connections implemented with a dowel is very important for further development of connections of higher performances. Also, the understanding of the failure mechanisms of connections including dowels provided a deeper knowledge for the development of successful moment resisting connections.

#### 3.4.1 Analysis of behavior in experiment S 1-1

The actual strength, the failure point of the connection, was not determined since the maximum loading equator force of 250kN was exhausted and the connection did not fail.

From the detailed force-deformation relationship from the push-pull test of specimen S1 presented in fig.3.4 and from the photos of the broken dowel, the following can be concluded:

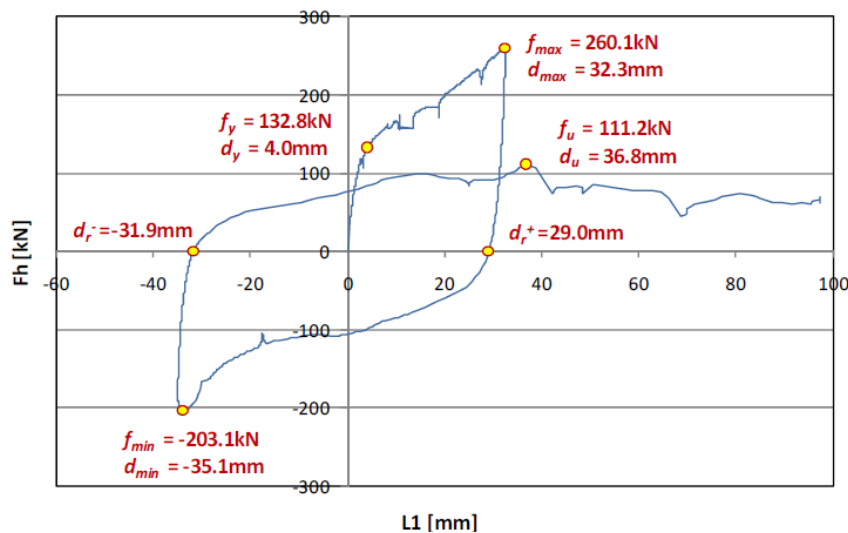


Fig. 3.4 Force-deformation relationship – push/pull test of specimen S1

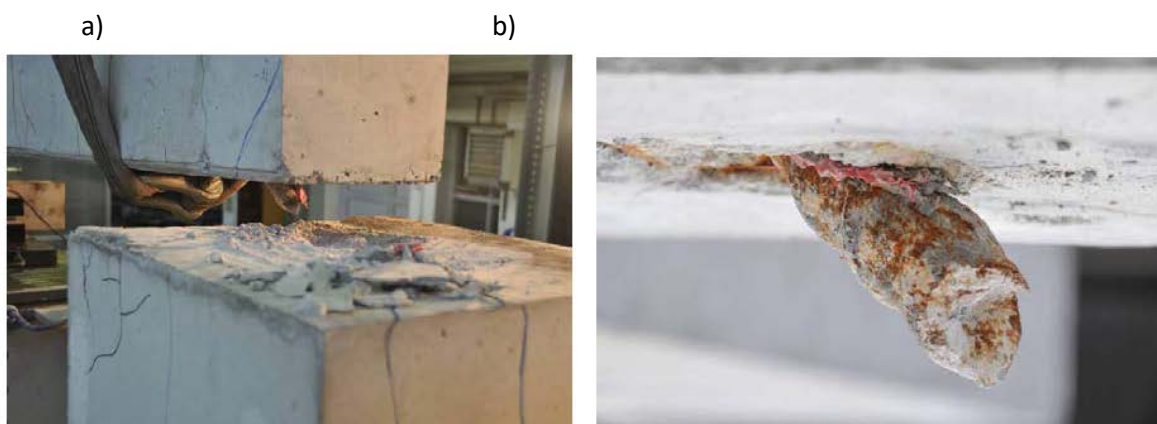


Fig. 3.5. Actual photos of a broken dowel after the test completed for specimen S1, [Ref.: 027]

During the pulling cycle, the initial loading cycle, until the force of around 132kN, the connection/dowel behaved elastically. Following this point, the stiffness of the connection started to degrade. This was when the dowel started to experience inelastic deformation (creation of a hinge).

With the increase of force, at the force of 174kN, the deformation of the connection increased for over 3mm and this was where concrete around the dowel experienced further crushing, which can be noticed in the diagram in fig. 3.4 with the straight line in the deformation line. With further increase of the force, the force-deformation diagram continued with the straight line. This is probably because crushing of the concrete around the dowel was already completed and the force was fully concentrated on the dowel. With the increase of loading, the dowel experienced further bending and since there was no drop in load bearing capacity, the dowel did not reach the ultimate strength.

Observing the standard stress distribution over the steel bars loaded in bending, presented in fig. 3.6, during loading, there was a great possibility for the steel fibers in the compression part to experience a crushing failure.

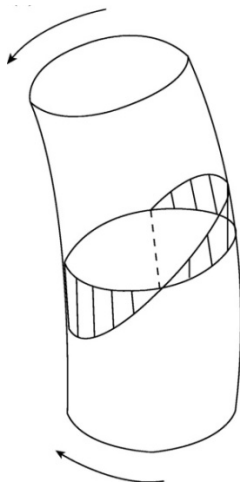


Fig. 3.6. Stress distribution within the dowel loaded in flexure

When the reverse loading began (pulling sequence), the dowel was already with plastic deformation at the hinge location (with possible fiber crushing in compression), few centimeters inside the column wherefore its overall load bearing capacity was reduced.

From the diagram in fig. 3.3, it can be seen that, during the pulling loading sequences, the connection experienced a large deformation at a relatively small amount of force, compared to the push loading sequence. At a load intensity of only 100 kN, the connection, respectively, the dowel experienced deformation, which was the same as for the force of 260 kN during the push sequence. This explains the fact that part of the steel may have crushed (the part that was compressed) during the push loading and now, in the pulling sequence, it was in tension. With the increase of force, the deformation increased as the concrete continued to crush around the dowel in the pull direction and the rotation of the dowel around the hinge increased, as well. At the force of 203kN, the dowel broke.

From the stress distribution in flexure presented in fig. 3.6 and the shape of the broken dowel presented in fig. 3.5.b, it can be concluded that the dowel failed in flexure.

- Damages to the concrete elements

From the photos presented in 3.5 a), it is very well documented that both elements experienced large cracks in the mode of splitting failure presented in Chapter 2.

The beam suffered a splitting crack in orthogonal direction in the direction of loading, as presented in fig. 2.21 a). This crack happened during the pulling sequence where the load intensity was less than that in the pushing direction. The column experienced a splitting crack in two fashions, orthogonal to the direction of loading, fig. 2.21 a) and in an angle fashion in the direction of loading, fig. 2.21 b). Normally, in the cases when the dowel was located in the middle of the column, the angular cracking in the direction of the loading was not something to expect, but in this case, it happened.

Possibly, the reason for angular cracking in the concrete could be the arrangement of the stirrups. In the column, all the stirrups were of the same shape and were positioned perimetrically.

### 3.5 Calibration of non-linear parameters for numerical model

The ultimate goal of calibrating the numerical model of behavior during the experiments was to determine the most feasible and yet accurate procedure for modeling the behavior of the connection that could be used, with a certain liability, for verifying whether the connections can be considered as simplified hinge connections and whether it is possible to be used by engineering community for design and analytical purposes.

#### 3.5.1 Selection of non-linear model, type of hysteresis for numerical model

The connections were modeled though a link element. The hysteretic model of non-linear behavior of the connections available in SAP2000, whose modeling results are considerably reliable, was the Pivot Model. Fig. 3.7 graphically shows the selected Pivot Model.

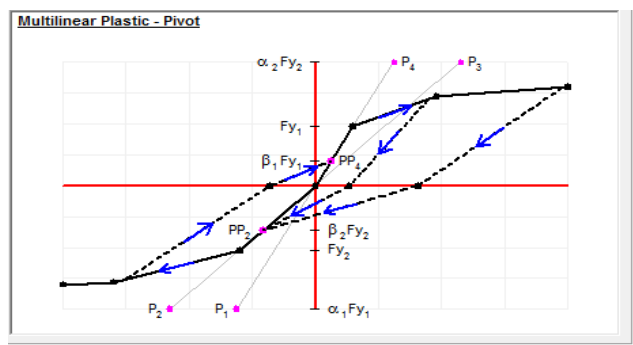


Fig. 3.7 Pivot Model shape

#### a) The strengths of the Pivot Model are:

- Simplicity of use. The Pivot Model is relatively simple to be used and easy to be governed by practitioner engineers.



- Ability to capture the dominant nonlinear characteristics of a member (in our case, the connection) that ensures acceptable results from the analysis compared to the actual behavior. The following are the key characteristics of the Pivot Model from observation of experimental investigations:
  - o The unloading stiffness decreases as displacement ductility increases. In Pivot Model, this can be well captured by parameters " $\alpha_1$ " and " $\alpha_2$ ".
  - o Following the nonlinear excursion in one direction, upon load reversal, the force-displacement path crosses the idealized initial stiffness line. Experimental observation shows that unloading is generally guided toward a single point in the force-displacement plane on an idealized stiffness line. In the Pivot Model, this can be well captured by parameters " $\beta_1$ " and " $\beta_2$ ".
- The force-deformation presented in the Pivot Model is general and can be used for moment-rotation response of the hinge, for force-displacement response of an element or entire structure, or force-displacement response of a link element (as in our case).
- The Pivot Model enables presentation of stiffness degradation.

#### **b) Weakness of the Pivot Model**

The current version of the Pivot Model incorporated in SAP2000 does not include:

- Continued strength degradation for multiple cycles to the same displacement level.
- Strength degradation in one loading direction caused by a sudden strength loss in the opposite loading direction.

#### ***Acceptance of results achieved by the Pivot Model.***

One of the biggest setbacks of the Pivot Model is the fact that it cannot capture the cycles during the strength degradation (cycles beyond the peak in the force-displacement diagram). This setback means that the Pivot Model does not provide:

- The force at the failure point of the connection;
- The total energy dissipation of the connection, considering that, in many situations, failure does not happen right after the maximum force-displacement is achieved.

However, despite these important elements desired/required for the most accurate analysis, the Pivot Model could be used for the purpose of this research since the purpose of this research was calibrating the numerical model with the ultimate goal of using it in practice for design purposes, and the following that the Pivot hysteretic Model offers is sufficient for that:

- The yielding point of the connection is crucial for the design purpose since, for the design, the yielding point for the connection (being material or the section) is the maximum allowable point for the serviceability limit state of the structure;
- The ultimate point (maximum bearing capacity) is the point to be used for determining the maximum load bearing capacity of an element and this is important for determining the performance of the structure at the collapse prevention state as well as for the Capacity Design Approach.

Capturing further behavior of the connection, pass the ultimate point for other potential analysis (such as total deformability capacity of a connection, actual collapse point, total energy absorption) is very important, but for the purpose of this research, these parameters are not needed.

### 3.6 Calibration of non-linear parameters of numerical model

For verification of the accuracy and the appropriateness of the non-linear parameters adopted of the numerical model, results obtained from the numerical model were compared with the experimental ones. For this purpose, the force & global deformation of the beam at the connection point was followed and used as a reference.

The subsequent sub-paragraphs show the best results from the adopted numerical model and also the main features that were calibrated and their respective values.

#### 3.6.1 Experiment S1-1, pinned connection with single centric dowel, push-pull loading

This experiment was conducted with “strong column” of dimensions 50x50cm and longitudinal reinforcement 16Ø22mm.

Fig. 3.8 provides a graphic presentation of the result of the numerical model vs the result from the experimental program in experiment S1-1, top center dowel with push-pull loading.

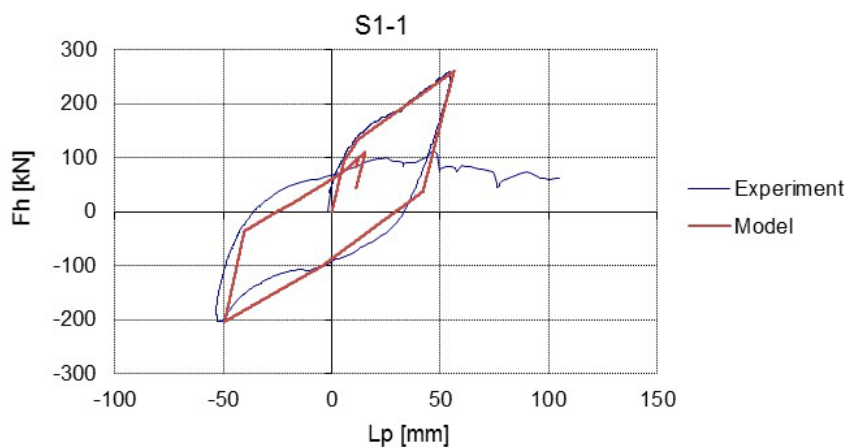


Fig. 3.8 Graphical presentation of numerical model vs experimental results from S1-1 experiment.

From fig. 3.5 showing the comparison of the force-deformation diagram, it can be concluded that the adopted hysteretic model with the respective parameter and frame modeling gives very good results and as such can be used for any kind of analysis desired.

#### 3.6.2 Experiment S1-2, pinned connection with single centric dowel, cyclic loading

This experiment was conducted with “strong column” of dimensions 50x50cm and longitudinal reinforcement 16 Ø22mm.

Fig. 3.9 shows graphically the result of the numerical model v.s. the result from the experimental program of experiment S1-2, top center dowel with cyclic loading.

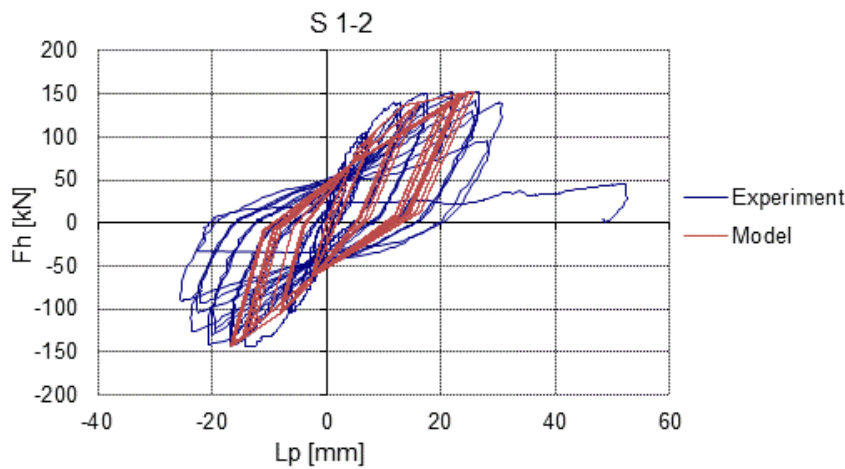


Fig. 3.9 Graphical presentation of numerical model vs experimental results from S1-2 experiment.

Form fig. 3.9 of the comparison of the force deformation diagram, it can be concluded that the adopted hysteretic model with the respective parameter and frame modeling gives very good results.

### 3.6.3 Experiment S-2, pinned connection with single centric dowel, cyclic loading

This experiment was conducted with “weak column” of dimensions 40x40cm and longitudinal reinforcement 8  $\varnothing$ 16mm.

Fig. 3.10 shows graphically the result of the numerical model vs the result from the experimental program of experiment S2, top center dowel with cyclic loading.

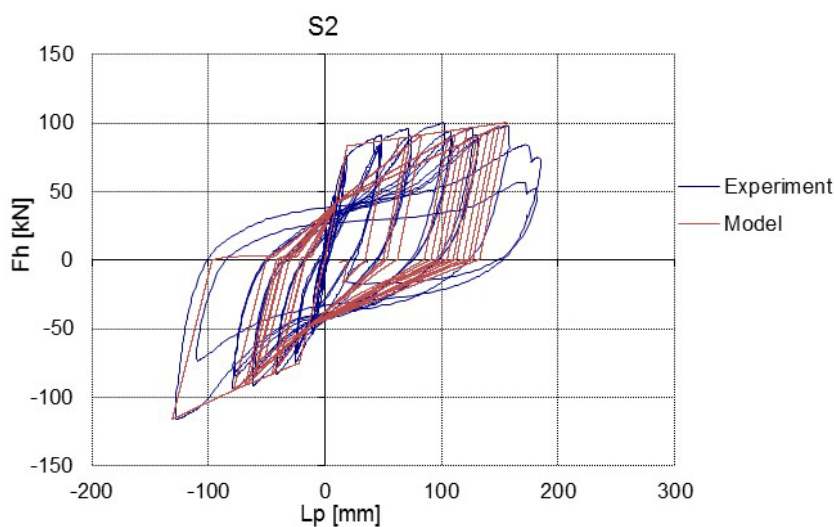


Fig. 3.10 Graphical presentation of numerical model vs experimental results from S2 experiment.

*In this experiment, the connection was stronger than the column, respectively, the column failed before the connection.*

### 3.6.4 Experiment S3-1, pinned connection with single centric dowel, push-pull loading

This experiment was conducted with “weak column” of dimensions 40x40cm and longitudinal reinforcement 8  $\varnothing$ 14mm.

Fig. 3.11 shows graphically the result of the numerical model vs the result from the experimental program of experiment S3-1, top center dowel with cyclic loading.

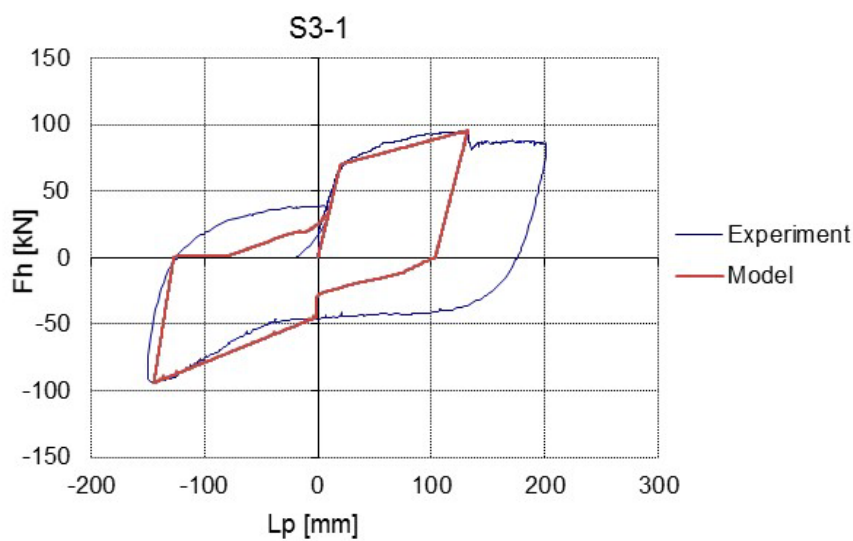


Fig. 3.11 Graphical presentation of numerical model vs experimental results from S3-1 experiment.

*Similarly to experiment S2, also in this experiment, the connection was stronger than the column, respectively, the column failed before the connection.*

### 3.6.5 Experiment S3-2, pinned connection with single centric dowel, cyclic loading

This experiment was conducted with “weak column” of dimensions 40x40cm and longitudinal reinforcement 8  $\varnothing$ 14mm.

Fig. 3.12 displays graphically the result of the numerical model vs the result from the experimental program of experiment S3-2, top center dowel with cyclic loading

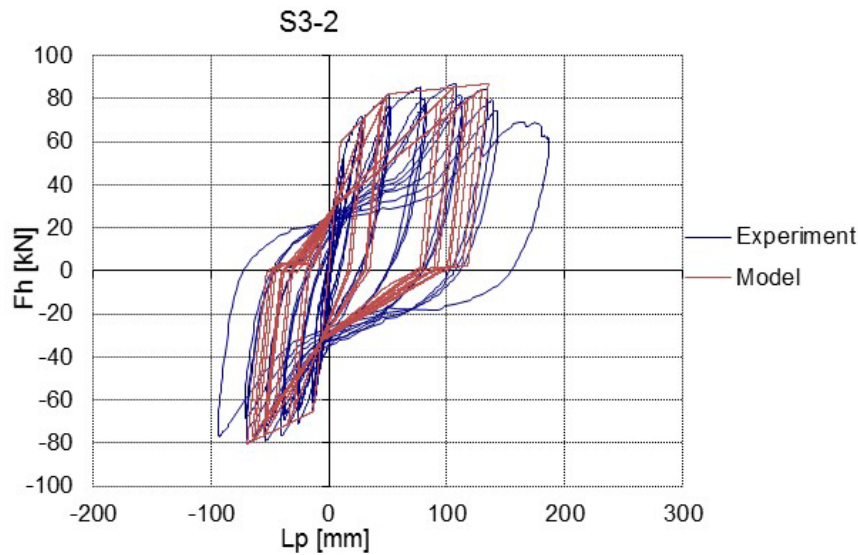


Fig. 3.12 Graphical presentation of numerical model vs experimental results from S3-2 experiment.

**Similarly to other weak column experiments, also in this experiment, the connection was stronger than the column, respectively, the column failed before the connection.**

### 3.6.6 Experiment S4, pinned connection with single centric dowel, cyclic loading

This experiment was conducted with “weak column” of dimensions 40x40cm and longitudinal reinforcement 8  $\emptyset$ 12mm.

Fig. 3.13 shows graphically the result of the numerical model vs the result from the experimental program of experiment S3-2, top center dowel with cyclic loading.

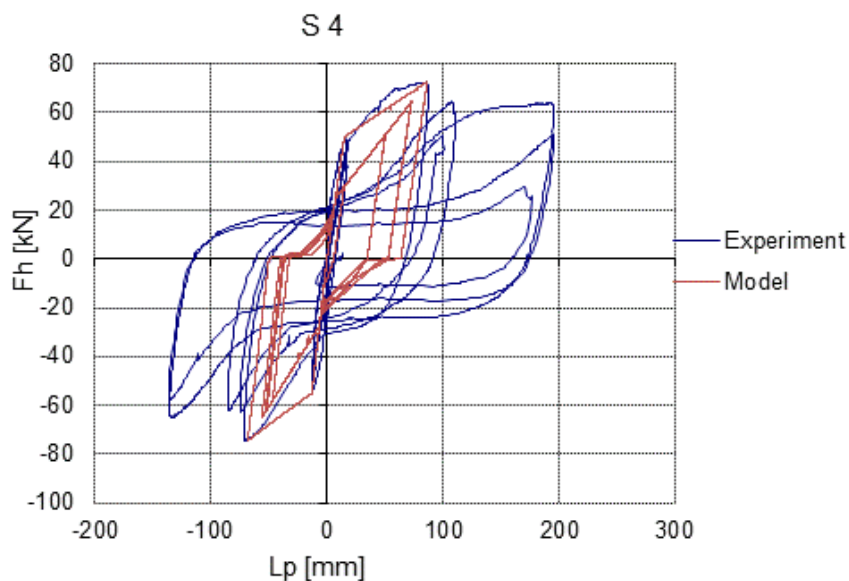


Fig. 3.13 Graphical presentation of numerical model vs experimental results from S3 experiment.

*Due to the very weak column, also in this experiment, the connection was stronger than the column, respectively, the column failed before the connection.*

### 3.6.7 Experiment S5-2, pinned connection with single centric dowel, cyclic loading

This experiment was conducted with “relatively strong column” of dimensions 40x40cm and longitudinal reinforcement of 4  $\varnothing$ 18+4  $\varnothing$ 20 mm.

In comparison with other experiments with column dimension 40x40, the column of these experiments, even of the same dimensions, was characterized by a high reinforcement ratio, which increased the strength capacity rotation ductility of the column, allowing the connection to exhaust its load bearing and deformation capacity.

Since experiments S5-1 and S5-2 were very similar, the only difference being that, in S5-1, all 8 longitudinal bars were of 20mm, it was decided to model and analyze only one of these two.

Fig. 3.14 provides a graphic presentation of the result of the numerical model vs the result from the experimental program of experiment S3-2, top center dowel with cyclic loading.

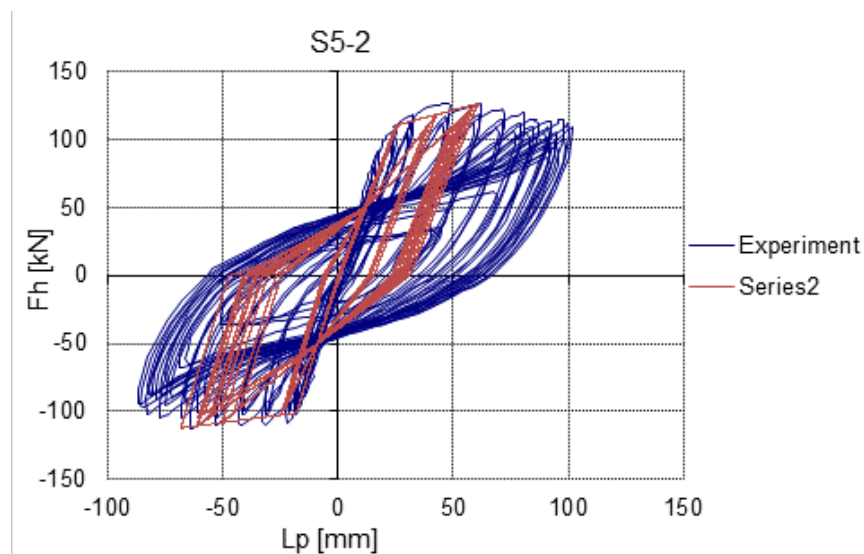


Fig. 3.14 Graphical presentation of numerical model vs experimental results from S3 experiment.

Unlike other experiments with column dimensions 40x40, in this experiment, the connection failed.

### 3.6.8 Experiment S6-1, top eccentric connection, push-pull loading

This experiment was conducted with “strong column” of dimensions 50x50cm and longitudinal reinforcement 16  $\varnothing$ 22mm.

Fig. 3.15 presents graphically the result of the numerical model vs the result from the experimental program for experiment S6-1, push-pull loading.

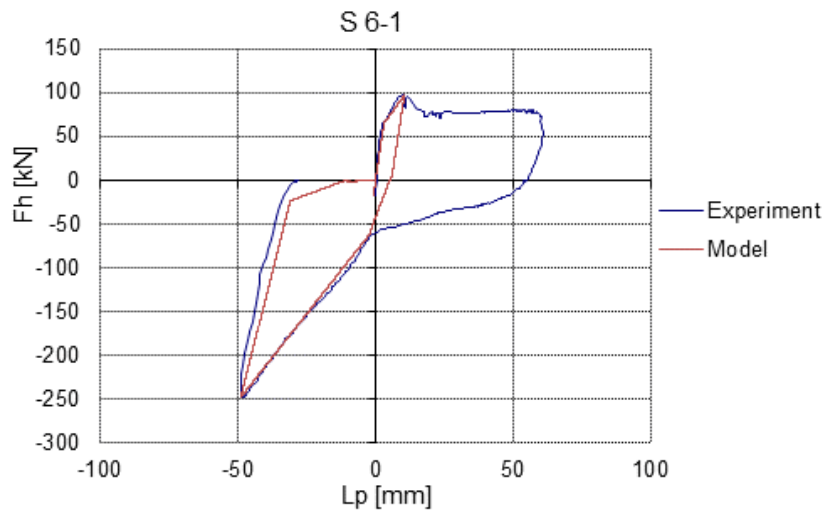


Fig. 3.15 Graphical presentation of numerical model vs experimental results from S6-1 experiment.

### 3.6.9 Experiment S6-2, top eccentric connection, cyclic loading

This experiment was conducted with “strong column” of dimensions 50x50cm and longitudinal reinforcement 16  $\varnothing$ 22mm.

Fig. 3.16 shows graphically the result of the numerical model vs the result from the experimental program of experiment S6-2, cyclic loading.

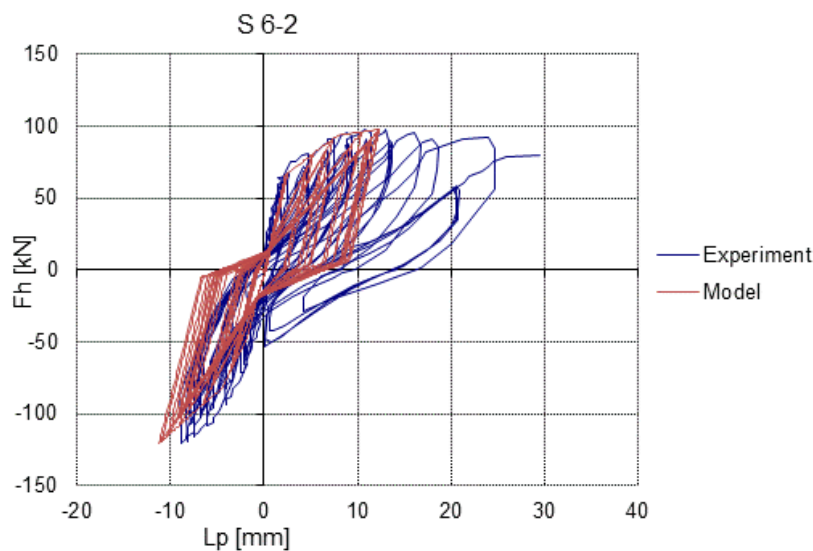


Fig. 3.16 Graphical presentation of numerical model vs experimental results from S6-2 experiment.

### 3.6.10 Experiment S7-2, intermediate story connection, strong column, cyclic loading

This experiment was conducted with “strong column” of dimensions 50x50cm and longitudinal reinforcement 14  $\varnothing$ 22mm. Fig. 3.17 shows graphically the result of the numerical model vs the result from the experimental program of experiment S7-2, cyclic loading.

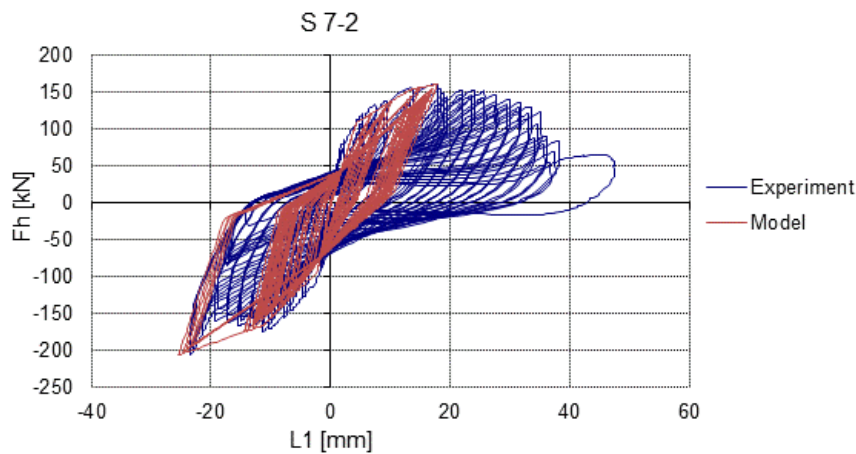


Fig. 3.17 Graphical presentation of numerical model vs experimental results from S7-2 experiment.

### 3.6.11 Experiment S8-1, intermediate story connection, weak column

This experiment was conducted with “weak column” of dimensions 40x40cm and longitudinal reinforcement 6  $\varnothing$ 18+2  $\varnothing$ 14mm.

Fig. 3.18 presents graphically the result of the numerical model vs the result from the experimental program of experiment S8-1, cyclic loading.

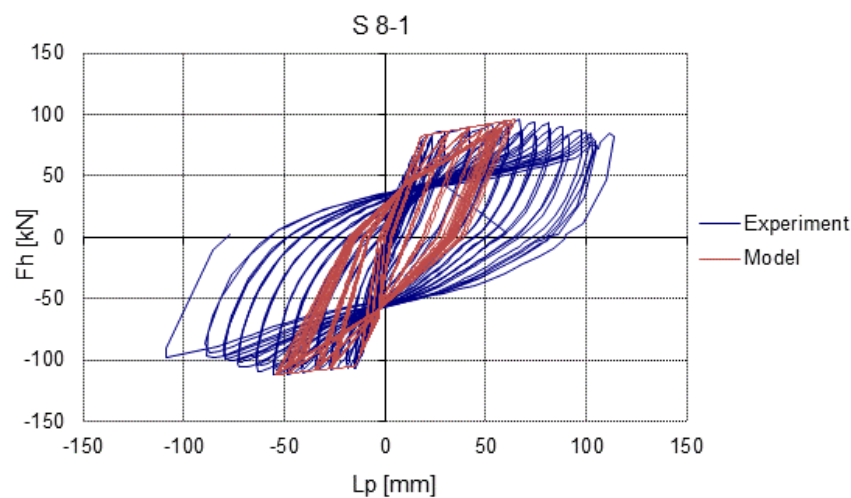


Fig. 3.18 Graphical presentation of numerical model vs experimental results from S7-2 experiment.

As in the previous experiments with weak column, also in this experiment, the strength of a connection was not determined since there were significant damages to the column base wherefore the experiment was stopped at 30mm displacement.

Therefore, assessment of the connection strength and comparison of the experimental connection strength vs analytical strength was not possible.

Here, it should be mentioned that the connection strength was determined and the comparison was made in experiment S7-2.



### 3.7 Verification of application of simplified linear hinge for beam-to-column connection with single dowel

In order to determine the accuracy of linear static analysis modeling parameters and procedures, the member forces were followed and compared, as required output data for the design.

In this case,, the bending moments of the column at the contact point with the foundation were compared with the ones from the non-linear analysis with the respective calibrated non-linear link element.

Initially, a non-linear dynamic analysis using the non-linear link parameters of the models presented in paragraph 3.5 was performed. Then, on the same frame model, a linear dynamic analysis was performed, in which case, the beam-column connection was modeled as a simplified linear hinge. From both models, non-linear and linear, the bending moments at the base column section were obtained and compared.

Verification of the appropriateness of using a simplified hinge element was performed in experiments in which the beam-to-column connection was performed with a centric dowel.

The verification was possible to be performed in experiments S1-1 and S1-2 since in the case of the other centrally positioned dowels, experiments S2, S3-1, S3-2 and S4, the strength of the connection could not have been explored since the column at the connection with the foundation failed before.

Therefore, the results from the analysis of experiment S1-1 and S1-2 could be considered sufficient for verification of application of simplified hinge connection for static analysis of precast beam-to-column connections performed with a single centric dowel.

#### 3.7.1 Verification of application of hinge in experiment S1-1

Fig. 3.19 graphically shows the bending moments at the base of the column which are time dependent in both cases, linear and non-linear dynamic analysis.

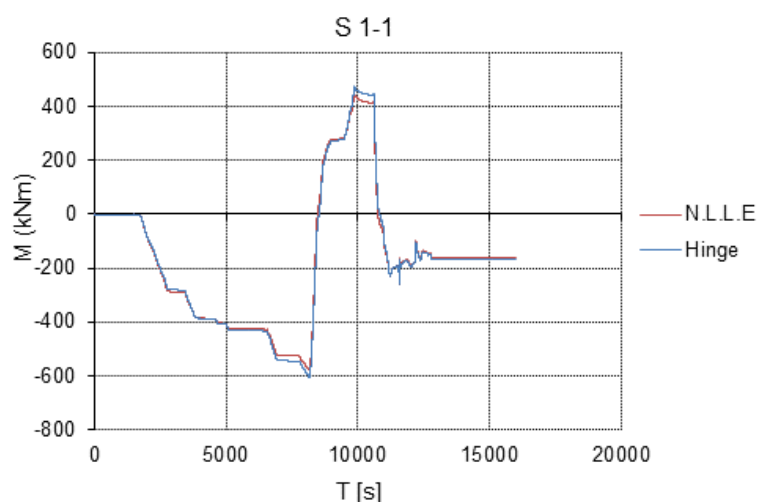


Fig.3.19 Comparison of bending moments at the base of column in experiment S1-1 from non-linear analysis with non-linear link element (N.L.L.E.) vs linear analysis with elastic hinge element.

As presented in fig3.16, the following are the maximum positive and negative results of bending moments at the bottom of the column from the non-linear analysis and linear analysis and the difference.

a) Values of bending moment in the case of the non-linear model with a link element

maxM=445.45 kNm

minM=-578.95 kNm

b) Values of bending moment in the case of the linear model with elastic hinge

maxM=473.23 kNm

minM=-605.94 kNm

c) The difference between the bending moments from both analyses is:

maxM=4%

minM=6%

From the comparison of the member forces (bending moments), it can be concluded that it is completely appropriate and accurate to use an elastic hinge at the beam-column connection and the elastic analysis is appropriate for the design purpose.

### 3.7.2 Verification of application of hinge in experiment S1-2

Similarly to experiment S1-1, in order to determine the accuracy of the linear static analysis, modeling parameters and procedures, the member forces were followed and compared, as required output data for the design. The bending moments at the column base were compared. The force input was the same (time dependent). Fig.3.20 shows graphically the bending moments at the base of the column which are time dependent.

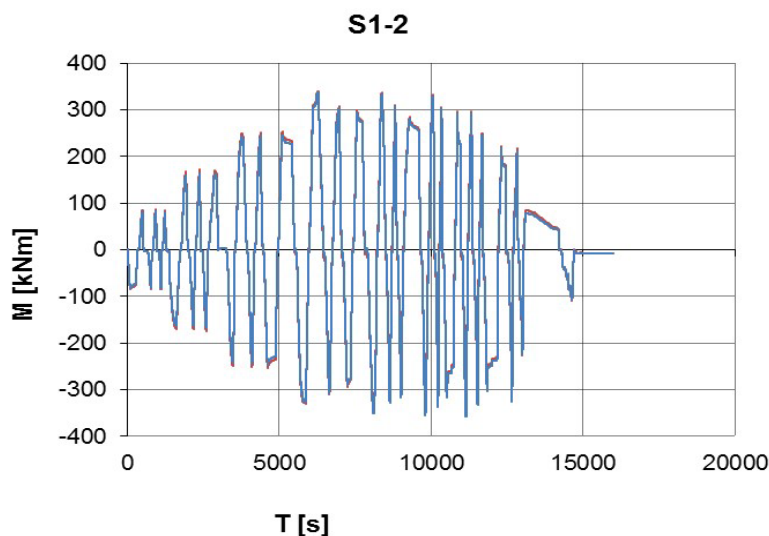


Fig.3.20 Comparison of bending moments at the base of the column in experiment S1-15 from non-linear analysis with non-linear hinge element vs linear analysis with elastic hinge element.

a) Bending moments in the case of the non-linear model with a link element

maxM=339.47 kNm

minM=-350.11 kNm

b) Bending moments in the case of the linear model with a simple hinge

maxM=336.40 kNm

minM=-356.98 kNm

c) The difference between the bending moments from both analyses is:

maxM=0.9%

minM=1.9%

From the comparison of the member forces (bending moments), it can be concluded that the results are almost identical, that it is completely accurate to use a simple elastic hinge at the beam-column connection and that the elastic analysis is appropriate for the design purpose.

## CHAPTER 4 – Design and testing of innovative moment resisting beam to column dry connection

### 4.1 Objective

The objective of this research was to develop a precast beam-to-column dry moment resisting connection. For the developed connection, there had to be a clearly defined design (analytical) procedure as well as a construction methodology. The proposed connections were to be experimentally tested to verify the anticipated behavior.

In order to be able to define a connection that will certainly behave as a fully fixed connection with clearly defined design procedure and construction methodology, a large number of tests had to be done, much higher than the number of tests that can be covered within the scope of one dissertation. However, the main goal of this research was to test several moment resisting beam-to-column connections in order to identify the connection that behaved as full moment resisting connection and then to layout the path for experimental verification of the design procedures and construction methodology.

### 4.2 Proposed moment resisting beam to column dry connections

#### 4.2.1 Brief description of application of beam-to-column connections

For the last few decades, precast buildings have extensively been used in Europe and beyond.

Most of the multi-story buildings that are constructed with precast elements have structural system composed of RC walls and slabs, whereas in single story buildings, which are mainly used as industrial buildings, a precast frame structural system is used.

As to the frame structural systems, in most, if not all buildings that have been constructed until now, the used types of connections have been as follows:

- Column-to-foundation, which are constructed mainly as fixed connections;
- Beam-to-column connections, which are constructed mainly as pinned connections.

The realization of fixity in column-to-foundation connection is not difficult, as described in Chapter 2.3.1, whereas the realization of beam-to-column fixed connection has appeared to be very difficult and with many uncertainties regarding the performance of such connections. Furthermore, for fixed beam-to-column precast connections, there is no standardized procedure for design and construction which makes their application even more complicated.

While observing damages caused to precast industrial buildings with pinned beam-to-column connections, it has been noticed that these structures, even though they are statically stable and behave well under gravity loads, experience considerable damages during earthquakes since they lack the required redundancy to provide a sufficient energy absorption capacity (chapter 2.4). Due to this fact, in recent years, many studies and experiments have been focused on achieving moment resisting beam-to-column connections.

#### 4.2.2 Justification of investigating dry connections

The challenge for designing a moment resisting precast beam-to-column dry connection is an ongoing process worldwide and the goal of this research has been to develop different design solutions for a moment resisting beam-to-column dry connection. In addition, the goal has been to develop not only a fixed connection, but rather a fixed connection that could be widely used in the construction industry. In order to achieve this, the proposed connection had to be as simple as possible. The simplicity had to arise from the design aspects, defined analysis and detailing procedure, as well as, simplicity in construction.

From observing the behavior of the already tested beam-to-column dry moment resisting connections, it is evident that there are many ways of developing a moment resisting connection and each way has its own specificities and factors that have a direct impact on the performance of the connection. A large number of influencing factors on the studied moment resisting connections makes it very difficult to layout a design and construction procedure for a moment resisting connection with the desired outcome.

Chapter 2 presents the types of fixed connections that are recommended and have mostly been investigated. Item 2.5.3 shows details of the positive and negative sides of these types of fixed connections. Further on, item 2.8 displays the wide gap in precast moment resisting beam-to-column connections and the possibility of contributing to the closing of this gap by a dry fixed beam-to-column connection.

The best connection would be the connection with lesser number of influencing factors and simple construction methodology. The simplest dry beam-to-column moment resisting connection is the connection performed by dowels only, should this behaves as a moment resisting one. If a connection implemented with dowels does not behave as a moment resisting connection, then adequate measures for improvement should be taken. In order for the connection to be desirable, due to its simplicity, to be used in the construction industry, the improvement method should be simple and clear.

#### 4.2.3 Overview of proposed connections

The proposed and tested moment resisting beam-to-column connections that were the subject of this research, were:

- dry connections performed by dowels;
- innovative connections;
- up to the best knowledge of author were also unique and not tested before

In the review of existing literature performed during the work on this thesis, there was not found any dry moment resisting connection constructed by dowels applicable in single story structures.

Developing a moment resisting (potentially with full fixity) beam-to-column dry connection implemented with dowels only is a clear gap to be filled in the field of moment resisting connections for single story precast structures.

Most important, the connection implemented by dowels only is also the most simple connection. Because of this, the proposed connections could have a high potential for application in engineering practice.

- Type of connections regarding position of dowels

The developed and tested connections are connections constructed with vertically positioned dowels and horizontally positioned dowels, (fig. 4.1 a), b) and c)). Even though the most feasible type of connection in single story structures is the connection with vertical dowels, in some situations, horizontally positioned dowels could be more appropriate.

Moreover, the findings from the experiments on specimens with connection performed with horizontally positioned dowels could be, in that case, used as a basis for further investigation of the performance of beam-to-column moment resisting connections in multi-story structures. For multi-story buildings, the only way to implement dry connections of beam-column elements is with horizontally positioned dowels.

The potential moment resisting beam-to-column connection with horizontally positioned dowels could be a reliable solution in multi-story structures, especially for internal columns, where moments and shear are not a risk factor.

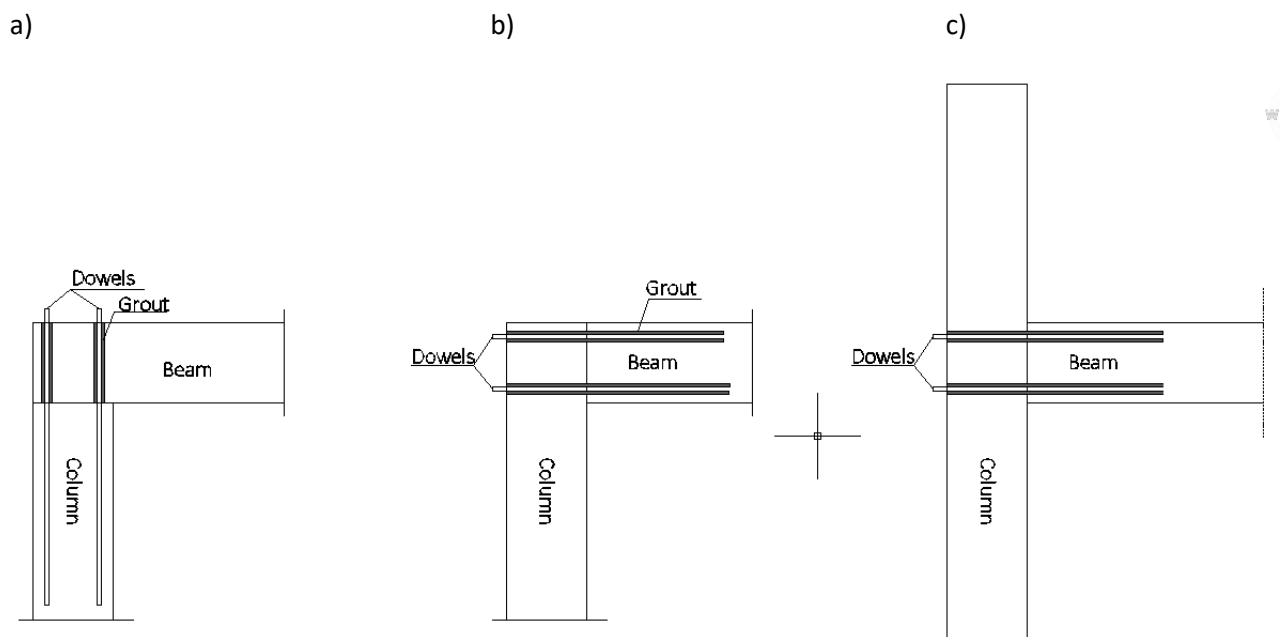


Fig. 4.1. Possible use of connection performed with a) vertical dowels and horizontal dowels in b) single story structure and c) multi-story structures.

#### 4.2.3.1 Anticipated behavior of precast beam-to-column dry connection constructed by dowels

The best way of understanding possible behavior of moment resisting connections constructed by dowels is by observing the behavior of pinned connections with dowels. The behavior of dowels alone and the behavior of pinned connections in general, under different loadings and with different position

of dowels within the section can provide a good overview of possible failure mechanism of the moment resisting beam-to-column connections with dowels. Studying in details the experiments performed at UL under the SAFECAST project [1], it can be seen that precast beam-to-column pinned connections enable understanding of the possible failure mechanisms and provide knowledge on the requirements for preventing such failures. This knowledge can be used to develop a potential moment resisting beam-to-column connection with dowels.

The most simple beam-to-column precast connection is the connection in which two elements are connected with dowels only and the dowels are anchored, through grout, to an already preserved sleeve, (fig. 4.1 a). The anticipated behavior of this type of connection will depend on which type of stress will be predominant, flexure or shear.

In cast-in-situ elements/structures, stresses that affect cross-sections are flexure stresses. In normal structures, shear does not affect cross-sections except for short elements (corbels). In precast elements, shear stresses are predominant at section level only in pinned connections. In fixed connections, at the cross-section level, flexure is usually predominant, whereas shear could be predominant at the element level.

However, in industrial buildings, load arrangement could be such that shear could also be predominant at the section level.

In the situation when shear is predominant, the strength of a connection will depend on the strength of the dowel and the strength of the concrete around the dowel. In the situation of predominant shear force, the shear force will be equally transferred to all the dowels of the connection and the behavior of the connection will depend on the behavior of the dowels.

If required, the best strengthening methods for connections with dominant shear behavior are very simple:

- Increasing the diameter of the dowel,
- Increasing the quality of materials, dowels and concrete, including the grout for the sleeve.

The challenge is to develop performance improving methods for the flexural behavior of precast elements with dowels. In order to develop potentially successful performance improving methods, first of all, the flexural behavior of the connection with dowels only has to be analyzed.

The anticipated behavior of beam-to-column precast connection with dowels only, is explained as follows:

When flexure is predominant, the precast section will rotate. Flexure stresses can appear as a result of gravity loads and combination of gravity and lateral loads. The combination of gravity loads with lateral loads can lead to various flexure stresses, particularly in single story structures. In combination of gravity loads with lateral loads of push direction (+), (fig. 4.2), flexure stresses from lateral loads and flexural stresses already existing from gravity loads will have the same sign. In such a way, the flexural stresses will become higher. When the lateral loads act in the opposite - pull direction (-), flexural stresses from lateral loads will be opposite to the existing ones from gravity loads and this will reduce and even eliminate the already existing flexural stresses.

Therefore, the most realistic scenario for analyzing the rotational behavior of a connection, is to load a specimen in the push direction.

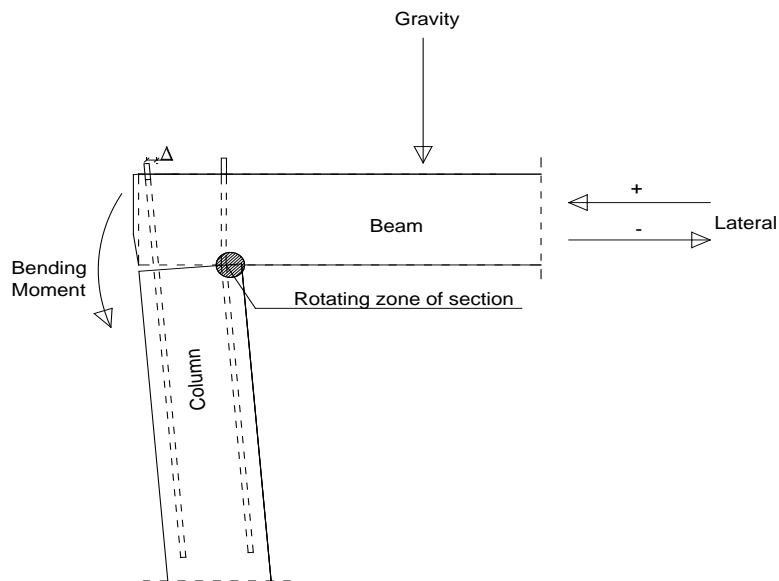


Fig. 4.2 Potential flexural behavior of precast beam-to-column connection

When flexural behavior is dominant, part of the dowels are loaded in tension and part of them are loaded in compression. From the previously analyzed behavior of dowels loaded in tension, Engström et al. (1998), the anticipated failure is the pullout failure, fig. 4.3. [Ref.: 012]

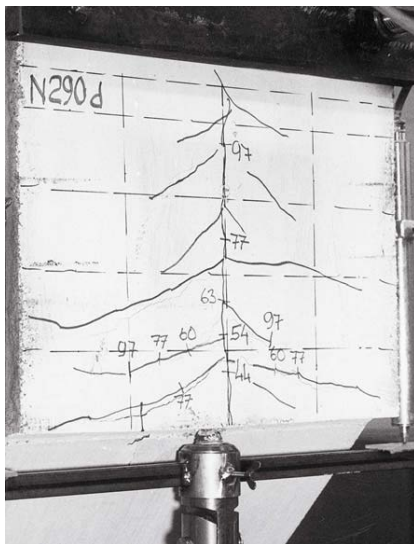


Fig. 4.3 Behavior of dowel in pullout [Ref.: 012]

The situation presented in fig 4.3 is one of the cases when the dowel is fully anchored within the concrete element and thus provides full dowel-concrete bonding strength. Full bonding strength is the situation when the dowel will not fail in pullout, but instead, either concrete will fail in shear as a result of pullout generated force or the dowel will fail in tension at the connection point.

In situations when the height of the element where the dowel is anchored is not sufficient to provide full anchorage, which is usually the case with precast beam-to-column connections and also the



connections studied under this dissertation, in that case, the exact failure of the dowel/connection cannot be completely anticipated.

The possible mode of failure will be:

- Failure of the dowel – concrete bondage

In this situation, the bonding strength between the dowel and the grout/concrete will be much less than the required one, in which case, the dowel will come out completely from the element, fig . 4.4 a).

- Failure of the dowel – concrete bondage in combination with shear failure of concrete due to pullout

Also, in this situation, the bonding strength between the dowel and the grout/concrete will be less than the required one, but higher than that in the case under a). In this situation, the higher the bonding strength, the deeper the cracking pattern will go into the section, (fig. 4.4 b) and the bigger cone will be created.

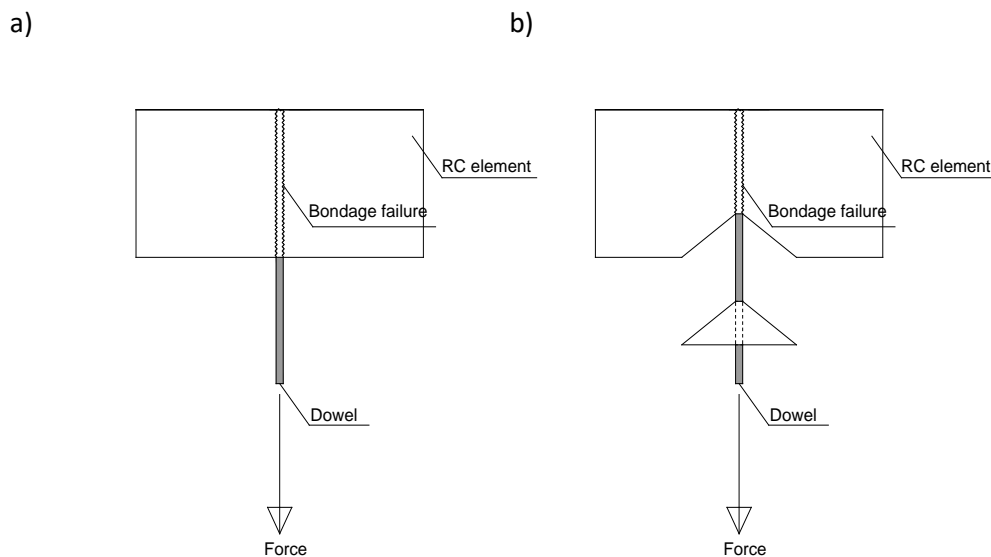


Fig. 4.4 Possible dowel pullout failure in the case of a short anchorage height

#### 4.2.4 Possibilities for improving performance of connections and options adopted for the tests

Methods for improving the flexural performance of connections are a matter of research options, where each researcher may potentially come to particular innovative proposals and solutions. For this research, a number of solutions have been considered and the most feasible ones have been tested.

##### 4.2.4.1 Connection upgrading for preventing dowel pullout failure

One connection upgrading method is to confine dowels that are in tension due to flexure with steel plates. The confinement should be implemented from the top of the dowel as presented in fig. 4.5. These plates should prevent failure of the dowel in pullout. The use of such a plate is noted in pinned connections for positioning of the dowel in the middle of the sleeve. Analyzing the pullout failure

mechanism, it has been noted that the same way of use of the plate may also serve for pullout failure prevention. This use of such a plate has been adopted as one possible method for performance improvement purposes and it has experimentally been tested under this dissertation.

The anticipated behavior of the connection/dowels with this method of strengthening is explained as follows:

During the pullout loading, the dowel-concrete bonding strength will initially start to resist. With the increase of the pullout force, the bonding strength will be reached and this bond will fail, as presented in fig. 4.4 a) or b). Upon bonding failure, all the pullout force will be transferred to the plates and the concrete element will be loaded in shear as a result of the tension force in the plates. In such situation, the strength of the connection will depend on the shear strength of the concrete element.

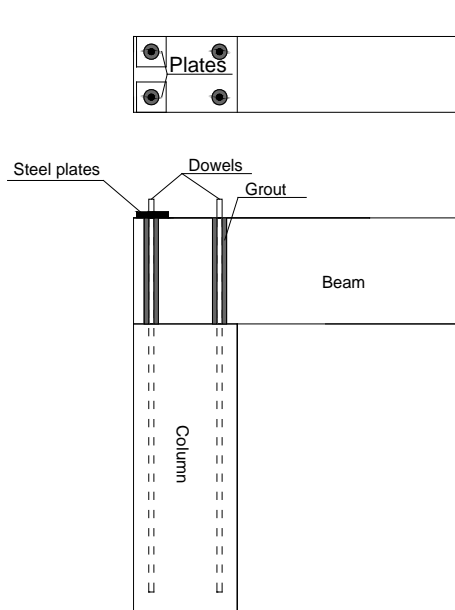


Fig. 4.5 Upgrading of the connection with steel plates to prevent pullout failure

#### 4.2.4.2 Connection upgrading for preventing dowel pullout failure and concrete spalling failure

In addition to pullout, from flexure, the dowels in the tension zone could also be subject to horizontal deflection due to rotation, (fig. 4.2). This horizontal deflection due to rotation can generate shear force on the dowel. This shear force on the dowels, in combination with the shear force from the external loading may result in failure of the concrete, referred to as concrete spalling. When concrete spalling occurs, then the entire connection fails.

Concrete spalling occurs when the shear force on the dowels is greater than the concrete strength in tension.

**a) Preventing concrete spalling failure by stirrups**

There are many possible ways to prevent failure of a connection due to transversal stresses. One of the practical solutions is to insert stirrups in the connection. In this way, even though concrete spalling occurs, the joint will not fail since all the shear force from the dowels will be transferred to the stirrups.

**b) Preventing concrete spalling failure with fiber strips**

Another possible solution to prevent failure of the joint, and even concrete spalling, is by introducing reinforced carbon fiber (of glass fiber) strips, as presented in fig. 4.6.

This type of strengthening presented in fig. 4.6 may potentially strengthen the connection against all possible modes of failure as a result of flexure.

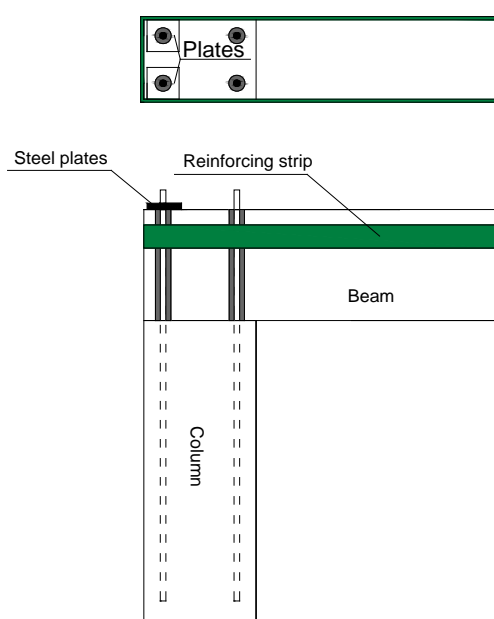


*Fig. 4.6 Upgrading of a connection strength with carbon fiber strips for preventing concrete spalling*

The proposed strengthening method by reinforcing strips has been considered during the performance of the experiments within the frames of the thesis, however, it has not been tested since it has been considered a little bit complicated for wide application in the construction industry.

#### 4.2.4.3 Connection upgrading by a steel plate for preventing dowel pullout failure and concrete spalling failure

The key element for wide application in construction industry is simplicity. Therefore, another simpler method for additional strengthening is proposed. This method consists of applying a large plate bolted to all dowels of the connection, (fig. 4.7).

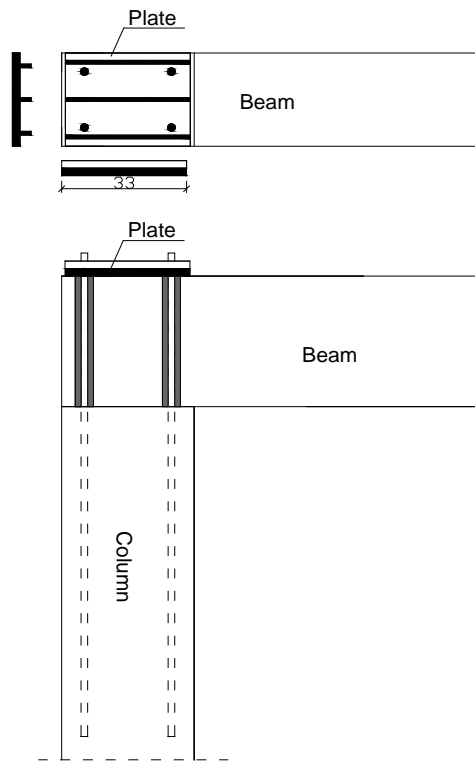


Fig. 4.7 Strengthening dowels by a large steel plate to prevent all failure modes

In addition to preventing pullout failure, this strengthening method should also prevent failure due to transversal forces, as well as, concrete spalling since the transversal force will be transferred to the dowels located in the compression zone of the section.

### 4.3 Experimental program

For verification of the anticipated behavior of precast connections and precast elements in general, with and without additional strengthening, an experimental program has been designed and performed.

#### 4.3.1 Design of the experimental program

Precast connections can experience, depending on the position of the dowel within the connection, one of the following three types of failure mechanisms:

- Pullout failure;

This is a type of failure when the dowel is pulled from the sleeve due to short anchorage length, fig. 4.4.

- Failure of concrete around the dowel,

This is a type of failure that occurs in the case of dowels loaded in shear and when dowels are positioned on the edge of section, fig. 2.6.

- Failure of the dowel due to shear

This is a type of a dowel failure in a connection loaded in shear. This type of failure occurs in the cases when the dowel is positioned in the center of the connection. This type of failure could be very rare in a moment resisting connection, but it is still possible.

Which type of failure will occur depends on the type of loads and consequently the type of stresses (flexure and shear) as well as the position of the dowel within the connection/section. For moment resisting connections, where the dowels have to be positioned eccentrically, at both ends of the section, the connection can be subject to a pullout failure, failure of concrete around the dowel or both types of failure simultaneously.

In a precast connection, which in our case, is the critical section within the element, the bending moments and shear force may have different intensity as a result of the influence of many external factors. The experimental program within this research has been designed to test the proposed connections, presented in paragraph 4.2.4, regarding all failure modes. The specimens were tested for the scenario where flexure was the predominant force, the scenario where shear was predominant and for the scenario where both forces (flexure and shear) acted with equal intensity (a possible situation in which both are predominant).

The type of loads/stresses acting on the element and subsequently on the connection depend on the following factors:

- Span of the frame

The frame with a shorter span will be subject to intensity of shear force at the critical section higher than the intensity of the flexural forces under the same load combination; the opposite holds for a larger span structure. For example, for the frame with a span of 5m, the intensity of shear force at the critical section could be up to twice the intensity of bending moments, i.e., the moment/shear ratio is  $M/V = 0.5$ . With increasing the span, the intensity of bending moments will become higher in respect to the intensity of shear force. For a frame with a span of 15m, the intensity of bending moments could be twice the value of the intensity of shear force, i.e., moment/shear  $M/V > 2.0$  and so on.

- Type of loads acting on the structure

Depending on the location, the building is subject to various types of loads (gravity, high snow, high wind, earthquakes, etc.). For various load combinations with different load intensities of each load type, the moment/shear ratio could vary from a situation when bending moments are higher to the situation when shear is higher. For example, the higher the intensity of gravity loads in respect to lateral loads, the higher the shear force in respect to bending moments, and vice versa.

- Designation of the building

In many situations, industrial buildings could have a moving crane installed within the structure. Usually, a moving crane is placed on the corbel of a column, but there could be a situation when a crane is hooked to the roof elements. The location where the crane is hooked and the maximum weight that the crane can carry may have a direct impact on the moment/shear ratio at the critical section, respectively further increasing shear in respect to flexure.

In real life, the M/V ratio may never be the same in buildings since each building is different in many ways. Even in the same building, this ratio changes in continuity, depending on the variation of load intensity especially during an earthquake.

Consequently, it is not possible to design an experimental program to cover all the situations in real life. Generalization of possible critical situations was adopted that could be representative for many (most of the real life scenarios). The moment/shear ratio, acting on the critical connection (precast connection level), adopted for the testing specimens was:

**a) Higher Moment/Shear ratio,  $M/V= 1.5$**

This experiment covered all the situations where moments are predominant in respect to shear and the behavior of the connection and specimen was anticipated to be a pure flexural behavior. The performance of the connection/specimen under this ratio could be generalized for all real life situations when bending moments are predominant.

**b) Equal Moment/Shear ratio,  $M/V= 1.0$**

These experiments covered situations where the moments and shear are of the same range with the potential of both being predominant forces in the critical section of the specimen. The behavior of the connection was anticipated to be coupled moment/shear behavior. The performance of the connection/specimen under this ratio could be generalized for all real life situations when intensity of bending moment and shear force is similar.

**c) Higher Shear/ Moment ratio,  $M/V= 0.5$**

This experiment covered all situations where shear forces are higher than the flexure forces. The predominant type of behavior of the connection in this case is shear. The performance of the connection/specimen under this ratio could be generalized for all real life situations when the intensity of shear force is much higher than the intensity of the bending moment.

Through these testing combinations, the goal was to get a clear insight into the behavior of the precast connections under the most possible situations in construction practice.

In order to determine if the developed precast connection is behaving as a monolithic connection, the results obtained for a precast connection had to be compared with the ones obtained for a monolithic (cast-in-situ) connection. For proper and reliable comparison, both connections had to be constructed by using the same properties and in such a way as to have same analytical strength.

### 4.3.2 Type of connections tested

Table 4.1 shows the types of tested connections.

Table 4.1. Description of types of experimental tests under this research thesis

Nr.	Label	Moment/Shear ratio at connection level	Description
1	S1, V.D	M/V=1.0	Connection performed with vertical dowels where two dowels in tension are strengthened with individual plates, fig. 4.8 b). M/V=1.0 at the joint face on both sides.
2	S2, V.D	M/V=1.0	Connection performed with vertical dowels where dowels are anchored with grout only, with no additional strengthening, fig. 4.8 a)
3	S3, V.D	M/V=1.0	Connection performed with vertical dowels where two dowels in tension are strengthened with individual plates, fig. 4.8 b).
4	S4, R.M	M/V=1.0	Referent model, cast-in-situ connection, fig. 4.8 c).
5	S5, H.D	M/V=1.0	Connection performed with horizontal dowels where two dowels in tension are strengthened with individual plates, fig. 4.8 d). M/V=1.0 at the joint face on both sides.
6	S6, V.D	M/V=1.5	Connection performed with vertical dowels where dowels are anchored with grout only, with no additional strengthening, fig. 4.8 a)
7	S7, V.D	M/V=1.0	Connection performed with vertical dowels where all four dowels are strengthened with one large plate, fig. 4.8 e)
8	S8, H.D	M/V=1.0	Connection performed with horizontal dowels where all four dowels are strengthened with one large plate, fig. 4.8 f). M/V=1.0 at the joint face on both sides.
9	S9, H.D	M/V=0.5	Connection performed with horizontal dowels where all four dowels are strengthened with one large plate.
10	S10, R.M	M/V=0.5	Referent model, cast-in-situ connection, fig. 4.8 c).

Note:

V.D. – Stands for Vertical Dowels

H.D. – Stands for Horizontal Dowels

R.M. – Stands for Referent Model

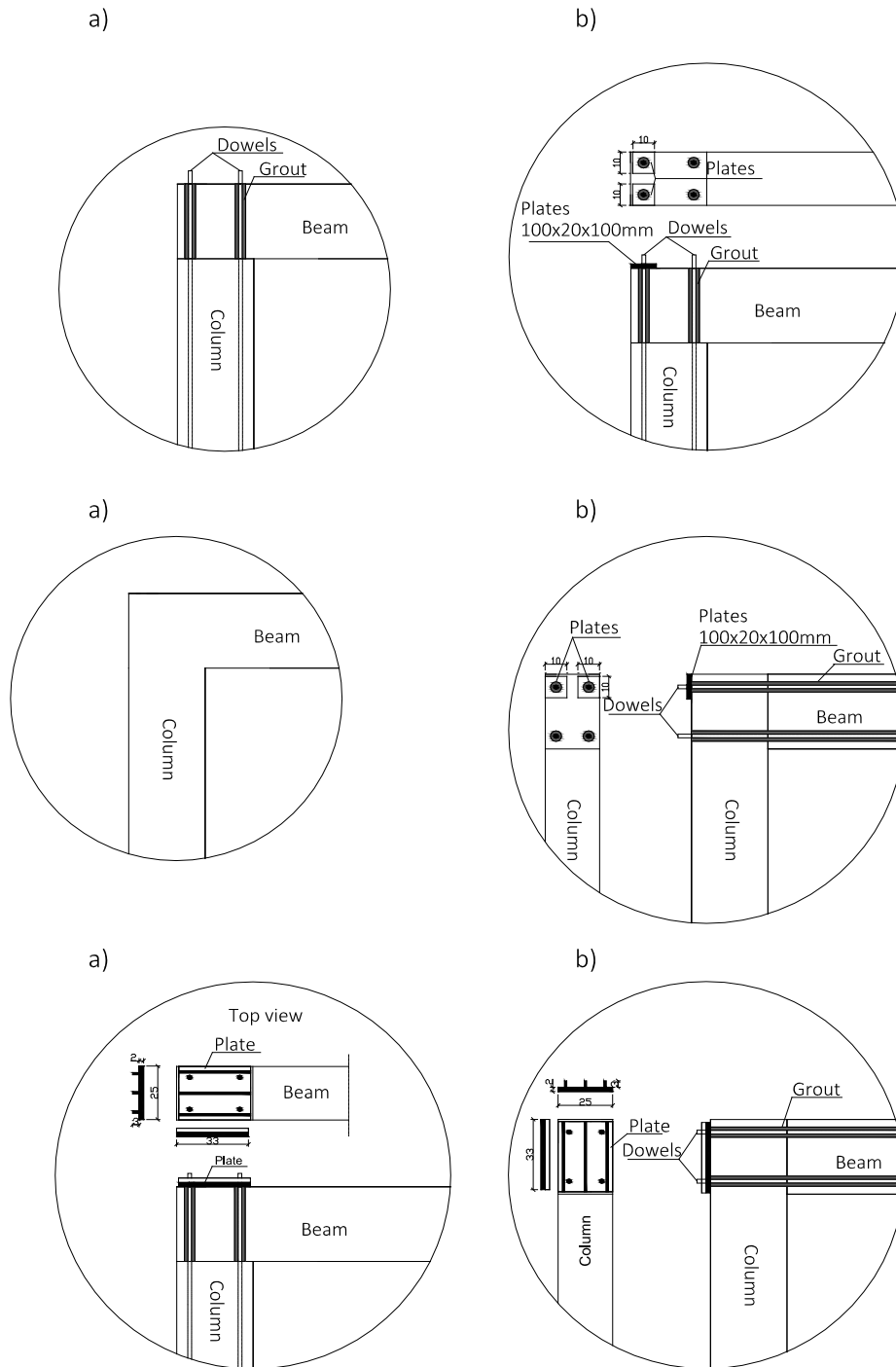


Fig. 4.8. Connection performed with vertically positioned dowels where dowels are anchored with grout only (a), connection performed with vertically positioned dowels where two dowels in tension are strengthened with individual plates (b), cast-in-situ connection (c), connection performed with horizontally positioned dowels where two dowels in tension are strengthened with individual plates (d), connection performed with vertically positioned dowels where all dowels are strengthened with one large plate (e), connection performed with horizontally positioned dowels where all dowels are strengthened with one large plate (f).



#### 4.4 Preliminary design of precast connection

One of the constraints regarding precast connections is the position of the dowel within the cross-section. The dowel has to be positioned inside the stirrups, (fig. 4.9). The exact position of the dowels depends on the type of grout that is used and the requirement for minimum thickness of the grout. This limitation effects clear distance between the dowels in the compressed and the tension zone which, as a result, this distance ( $d_1$ ) is smaller than the distance between the reinforcement in the compressed and the tension zone in the same element. For this reason, in order that the element has the same bearing capacity as the monolithic one, the dowels should have a higher strength than the reinforcement, or if the same material is used, then the dowel diameter needs to be larger than that of the reinforcement bars.

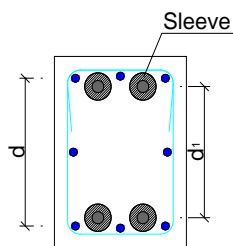


Fig. 4.9. Position of the dowel within the cross-section

Another important factor for consideration in design of precast connections is the approach to flexural strength analysis of the section.

If the connection of two precast elements is constructed with rubber between them, (fig. 4.10 a)), then the strength of the section should be calculated by taking into consideration the dowels only. The dowels should be calculated by converting the bending moment into a pair of forces:

$$F = \frac{M}{d_1} \dots \dots \dots \quad (4.1)$$

Where,

$F$  – force demand for the dowels

$M$  – bending moment acting upon the section

$d_1$  – distance between compressed and tension dowels

If the connection of the precast elements is performed directly through concrete to concrete contact, (fig. 4.10 b)), then the most reliable method for calculating the potential strength of the section is to treat it as a regular reinforced concrete section.

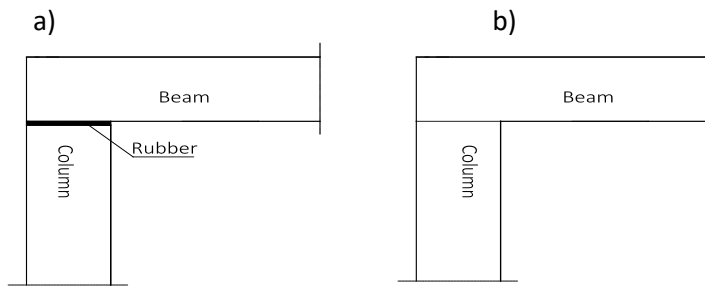


Fig. 4.10 Connection of precast elements, a) with rubber between elements and b) direct contact.

#### 4.4.1 Case study

To obtain the best representative results, a hypothetical case study was considered for analysis and design.

As a case study, a building with a small span, not usual for a prefabricated building, was used for the purpose of having element dimensions that could be experimentally tested.

The reason as to why this building could be considered as representative was that the behavior of its connections could be used as a reference for designing connections of other buildings (with different spans and heights) since the design and analysis method is same regardless the size of a building.

Another reason for adopting this case study is that in regard to the buildings with larger span this building with smaller span represent higher lateral force vs. gravity force ration ( $V/G$ ).

##### a) Details of case study building

For the case study the following was adopted:

- Building geometry, fig. 4.11:
  - o Frame layout 25x5m
  - o Frames spacing of 5m
  - o Height of the building 3m
- Loads
  - o Building is covered with hollow panels with equivalent load of:  $g=2.5\text{kN/m}^2$
  - o Claddings are adopted also to be of hollow panels with the same weight:  $g=2.5\text{kN/m}^2$
  - o Live load from snow:  $Q=1\text{kN/m}^2$
  - o For seismic analysis and design, the provision of EC 8 design criteria are used, with PGA 0.35g
- The same material is used for all the elements, as follows:
  - o Concrete C35
  - o Steel S500 B for the reinforcing bars and the dowels.

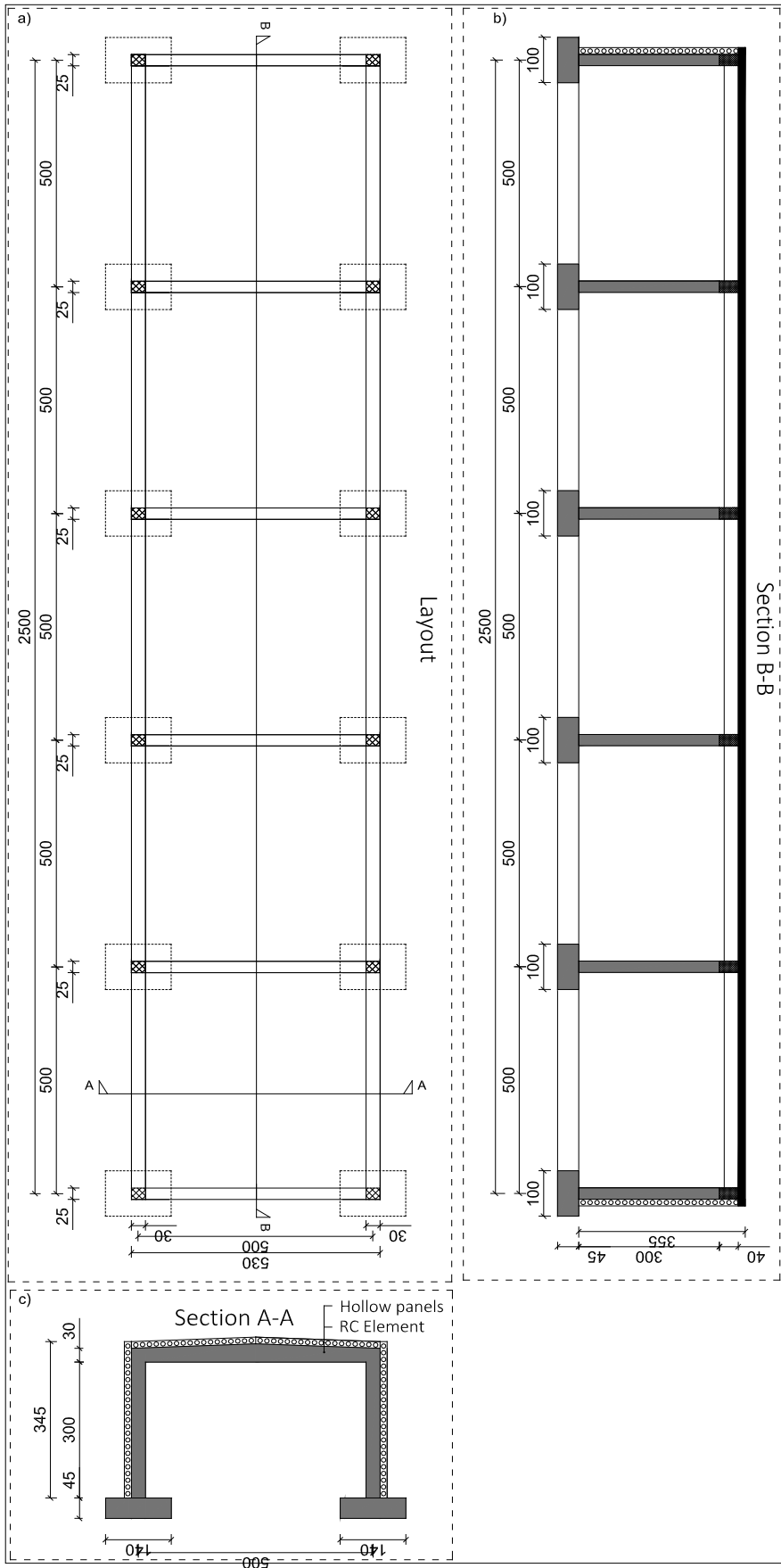


Fig. 4.11 Case study building drawing, a) Layout, b) section B-B, c) section A-A

b) Results from the static analysis of the structure

In the table 4.2 are presented the higher values of member forces under various load combination, based on which forces the frame is designed. Also in this table is presented bending moment at yielding point of the cross-sections based on adopted cross-section properties.

Table 4.2. Maximum member forces on the frame elements and the flexural strength at yielding point of designed section.

	Case study	Cast-in-situ section	Precast section
Design bending moment ( $M_{sd}$ )	54kNm'	N/A	N/A
Design Shear forces ( $V_{sd}$ )	69kN	N/A	N/A
Design axial forces ( $N_{sd}$ )	138kN	N/A	N/A
Yielding flexural strength of designed section	N/A	98kNm'	99kNm'

c) Design details of the frame elements

The following is the outcome of the design of the building:

- a) The cross-section dimensions of the frame elements are adopted 25x35cm. In the real construction scenario, the cross-section dimensions of the same case study can be adopted with different geometrical properties, e.g., 25x40cm. The reason that a 25x35m cross-section is adopted is that, since one of the main failure mode of the precast section, the pullout failure of the anchors, is in direct function of the length of the anchorage, the height of the section has a direct impact on the performance of the connection in regard to the pullout failure. For this reason, the smaller cross-section is adopted for this research because its performance is more critical compared to a bigger cross-section. Therefore, the goal is to test the connection under the most unfavorable conditions.
- b) Since the results from the experiments should be validated with the results on the cast-in-situ connection, the reinforcement amount in the cast-in-situ connection and the dimensions of the dowels in the precast connection are adjusted (regarding strength and position within the cross-section) in such a way that the flexural strength of the cast-in-situ section at the face of the joint and of the precast connection is approximately the same. The flexural strength of both sections (cast-in-situ and precast) is calculated by using the same method, as RC elements, since the precast element is with no intermediate element and it is in direct contact concrete with concrete of the connected elements. For the adopted cross-sections presented in figs. 4.12 a) and b), the flexural strength at yielding point of the cast-in-situ (referent model) and of the precast connection are presented in table 4.2.

The analytical verification of the flexural strength of the cast-in-situ specimen and the specimen with precast connection was done with software "Response 2000" [Ref.: 026]. The flexural behavior of the cross-sections is presented in figs. 4.12 c) and d).

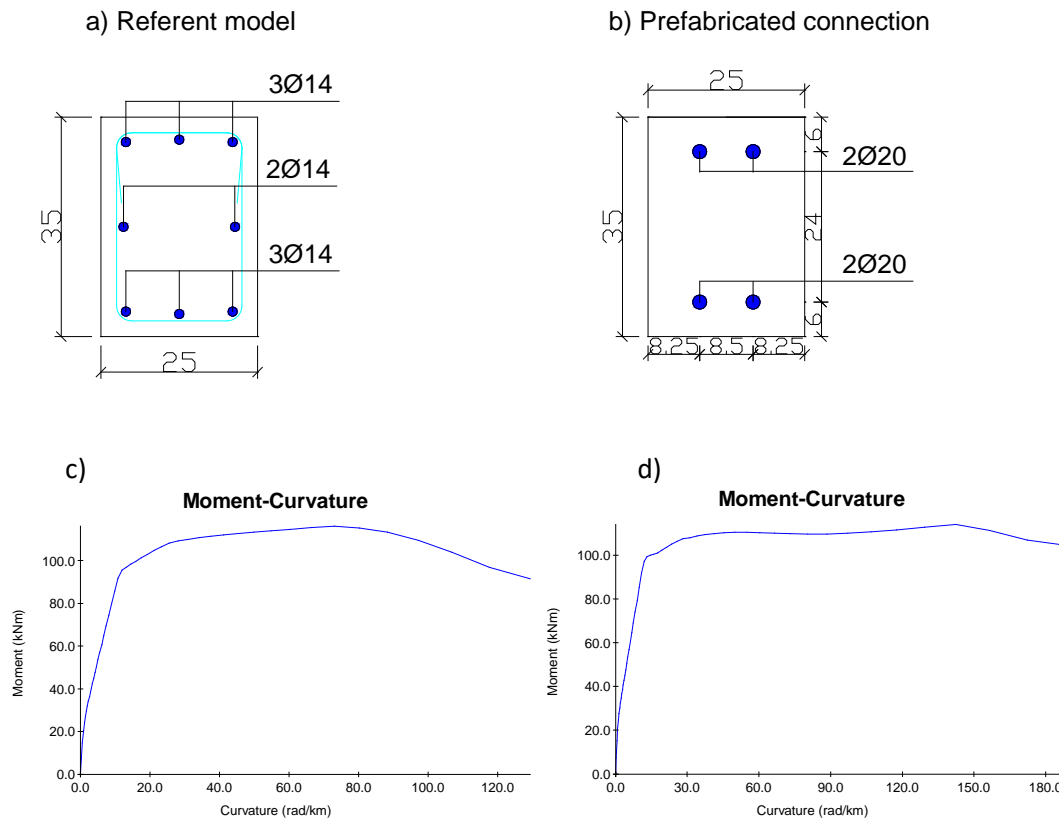


Fig. 4.12. Cross-section properties of the referent model (a), precast model (b), M-f diagram for the referent model (c) and M-f diagram for the precast model (d).

In the construction of the specimen, the monolithic side of the joint, (fig. 4.13) was constructed to have a higher flexural strength than the precast section of the joint in order to explore the strength of the precast connection preventing failure somewhere else.

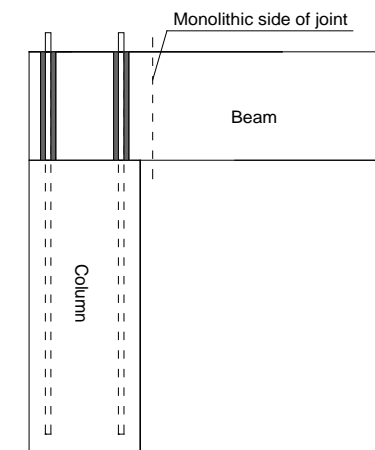


Fig. 4.13 Monolithic side of the joint

#### 4.4.2 Details of the elements for testing

Details of the elements for testing of the referent cast-in-situ model are presented in fig. 4.14, while details of the model with precast connection with vertical dowels and horizontal dowels are given in figs. 4.15 and 4.16, respectively.

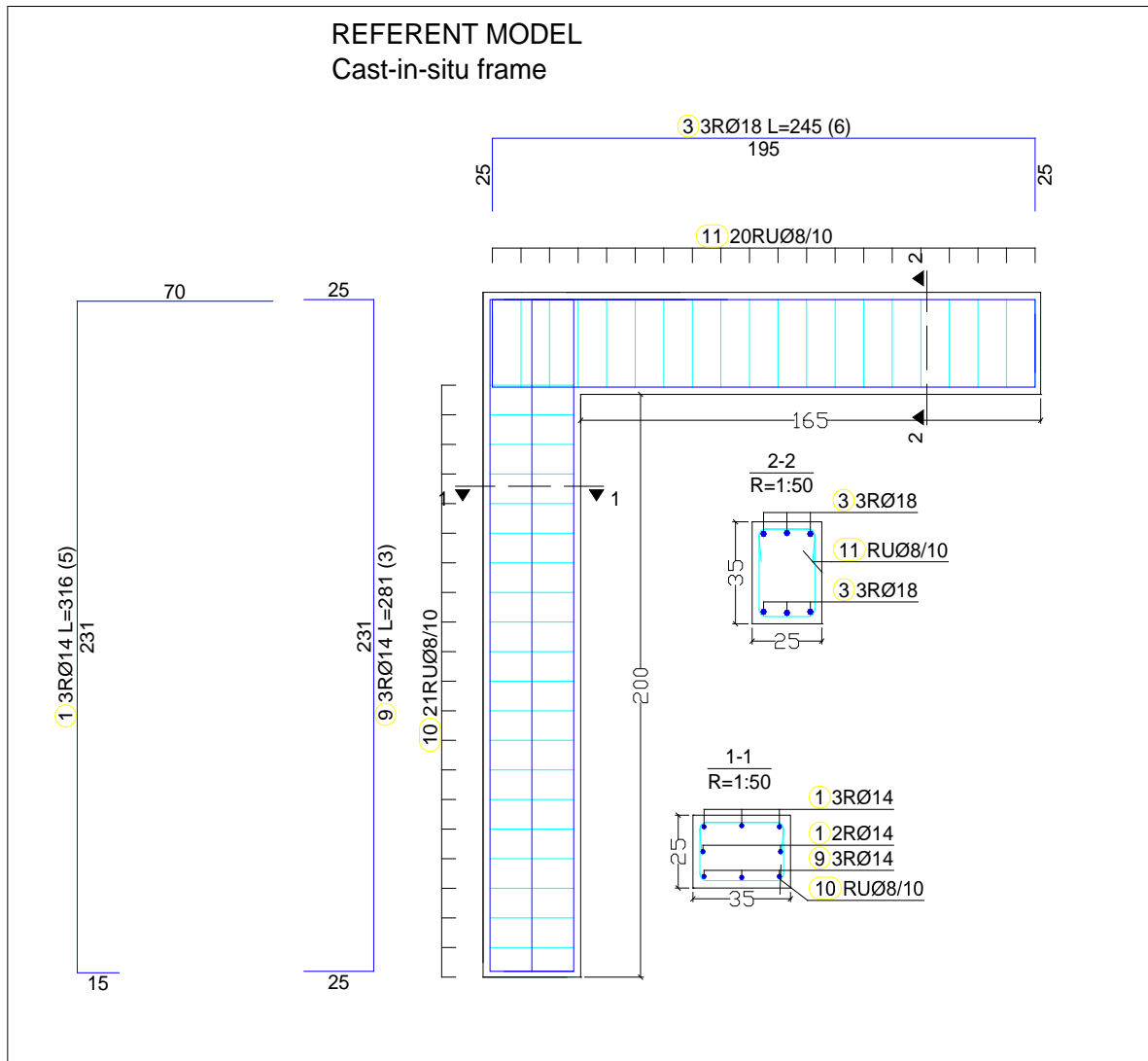


Fig. 4.14. Details of the referent cast-in-situ model.

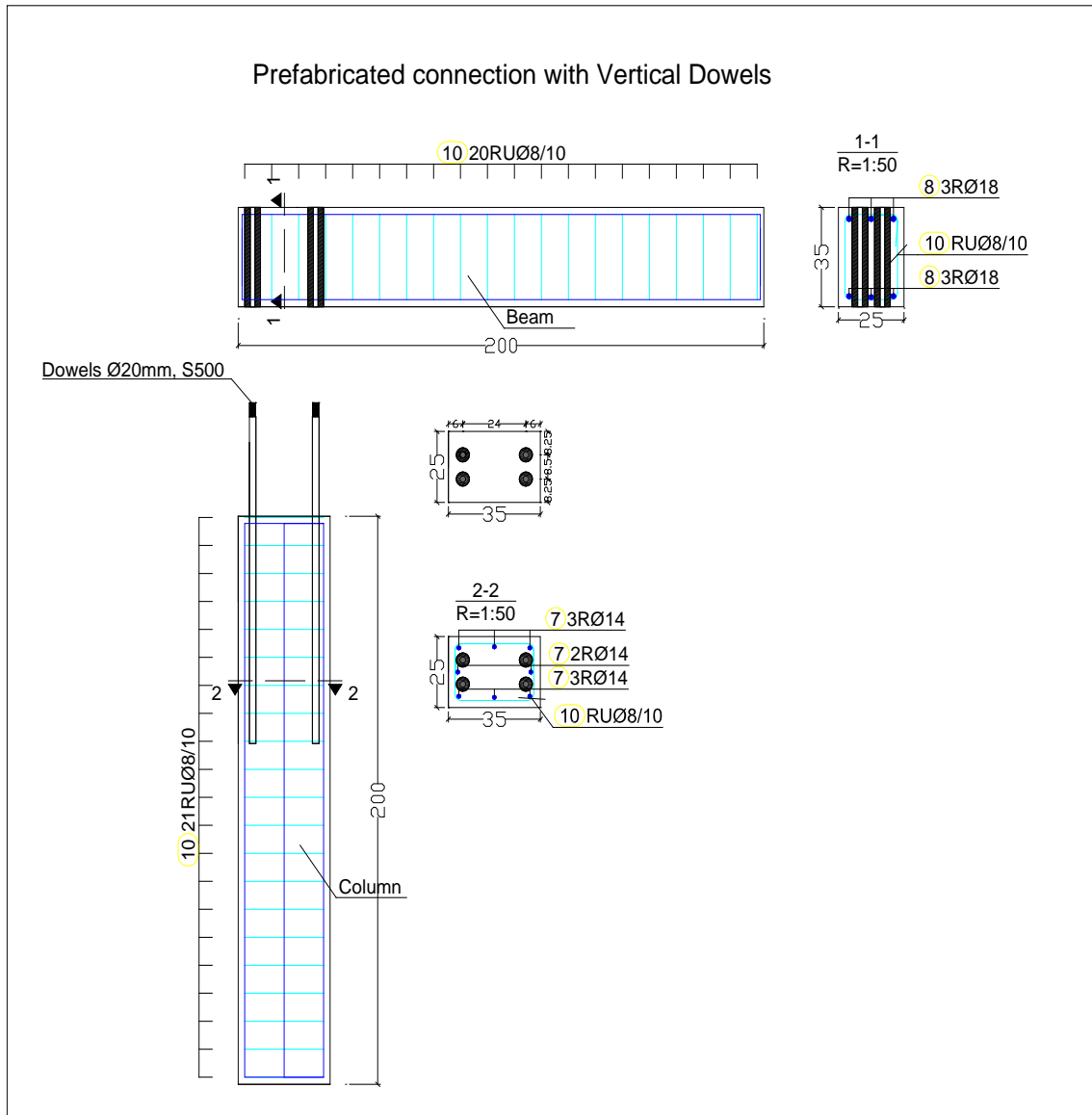


Fig. 4.15. Details of precast element with vertical dowels.

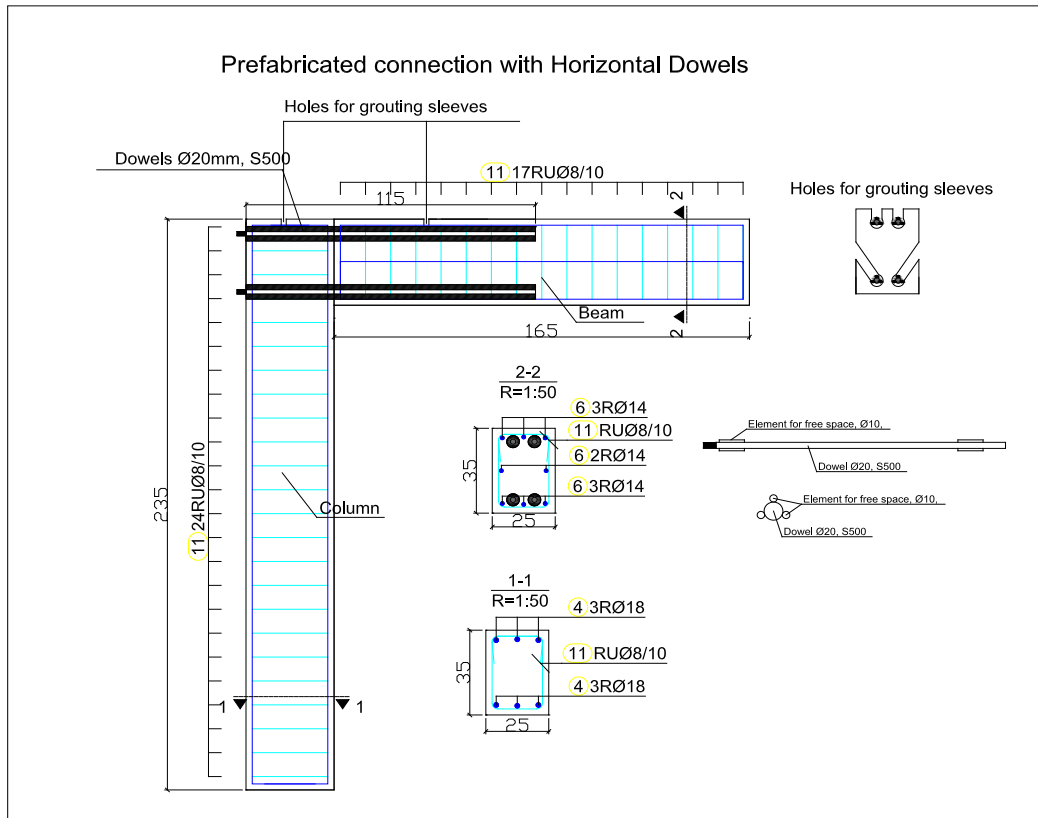


Fig. 4.16. Details of precast element with horizontal dowels.

#### 4.4.3 Construction methodology

It should be noted that the construction of precast elements and connection of the elements are performed on open construction site using standard construction equipment.

An important factor during the construction of the elements is the requirement for minimum temperature of the air and substrate for grout pouring which should be minimum 8°C. This requirement becomes a great constraint since it limits the construction of precast elements only during specific weather conditions otherwise the compression strength and consequently the bonding strength could not reach the maximum that the grout offers.

The process of construction of test specimens is presented further.

##### a) Construction of the referent model

Construction of the cast-in-situ element is performed as it would be in the real life situation. The column is constructed first and the reinforcement from the column is anchored to the beam. Then, the beam is constructed and the beam reinforcement end within the joint. At the potential critical cross-section, the column side (column face) of the joint, there is no overlapping of reinforcement.



**b) Construction of connection with vertical dowels (V.D.)**

Considering the goal of the research, to design and construct as simple as possible connection, the construction has been performed as follows: prior to the concreting, the dowels are inserted in the column and concreted inside the column. The anchorage length is  $35\phi$ . During the construction of the beams, sleeves are preserved by using a steel pipe. The diameter of the sleeve is chosen in correlation with the injected grout. In this case, non-shrinkage cement grout - SIKA 212 of high performances is used for grouting. The compressive strength of the grout is 60MPa and the bonding strength is 13.7 MPa, at full curing time. For this type of grout, the minimum thickness between the dowel and the sleeve should be 1.25cm, and since the dowel diameter is 20mm, in order to meet this requirement, the sleeve diameter is adopted  $(4.0+2\times 1.25=4.5\text{cm})$  5cm.

At the free end of the dowels, threads are formed for bolting, allowing strengthening with plates, (fig. 4.15). The construction of elements with vertically positioned dowels is presented in fig. 4.17.

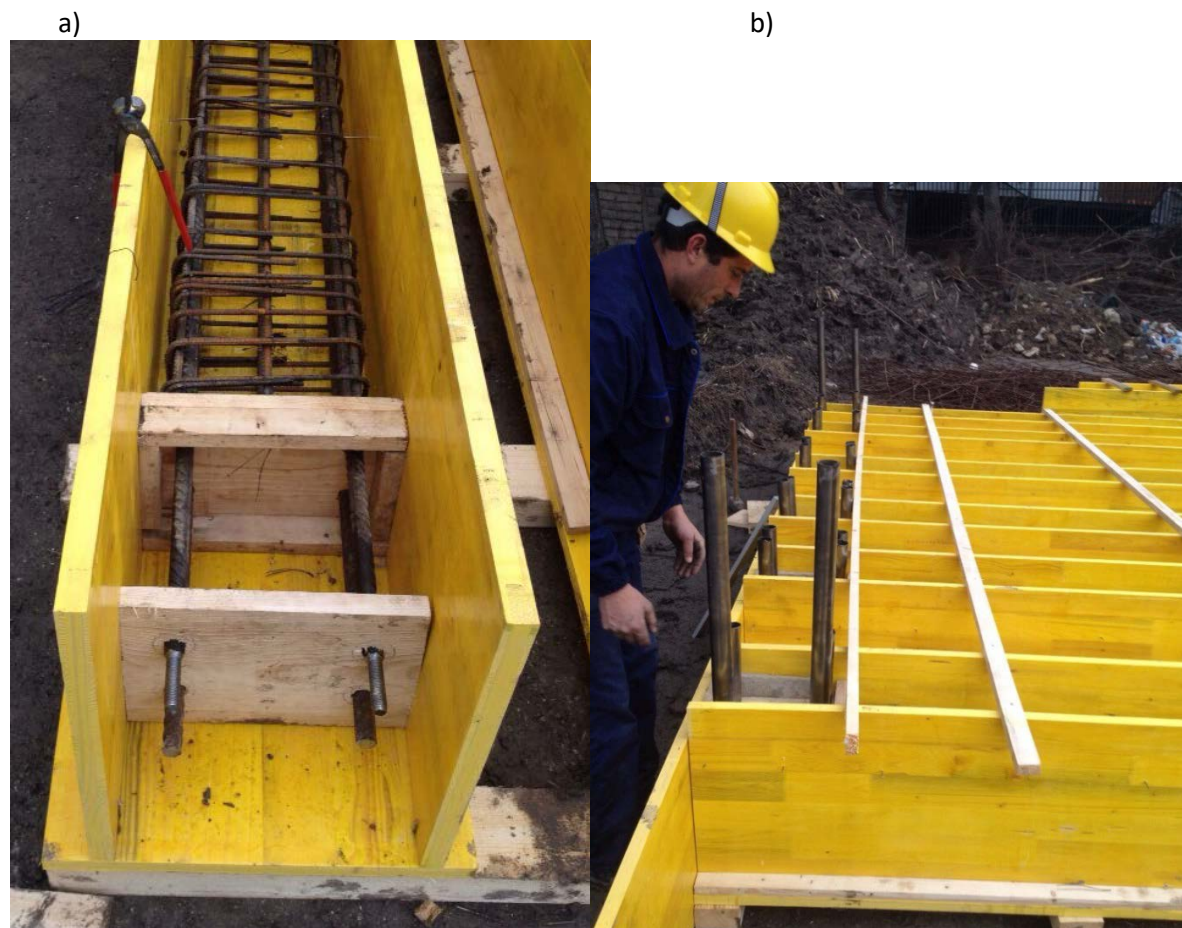


*Fig. 4.17. Photo taken during construction of the column of connection performed with vertically positioned dowel; a) dowels inserted in column prior to concreting, b) sleeves preserved in beam by steel pipes prior to concreting for performing the connection.*

Connection of the elements is performed after the concrete is fully cured and the experiments are performed after the grout is fully cured, too. Initially, the elements are positioned and then the sleeves are filled with grout. Fig. 4.18 shows a photo taken during the connection of the elements with vertically positioned dowels.



*Fig. 4.18. Photo taken during connection of elements with vertically positioned dowels*

The black strips on the photo at the connection level are duct tape for preventing grout flowing off the connection.

**a) Construction of connection with horizontal dowels (H.D.)**

The construction process for elements with horizontal dowels is different than that for vertical connections. This is due to the fact that, for the horizontal connection, the dowels have to be inserted in both elements during the connection phase. For this reason, the sleeve has to be preserved in both connected elements, beam and column. Fig. 4.19 presents a photo of sleeve preservation with removable steel pipes in both elements.



*Fig. 4.19. Photo taken during construction of elements with horizontally positioned dowel, a steel pipe being inserted for sleeve preservation.*

A challenge in connecting elements horizontally is positioning the dowel in the middle of the sleeve as well as filling the sleeve with grout. Positioning of dowels in/or approximately in the middle of the sleeve is a key factor for ensuring adequate anchorage. For this, there could be many different methodologies. It is very important to adopt the methodology that is considered consistent and could be used with certainty for assuring a reliable outcome. For this experiment, the following approach has been adopted:

- For allowing the same diameter of the sleeve, a steel tube of diameter 50mm is used on both elements, column and beam. Proper positioning of the tube is done on both elements, fig. 4.19.
- During actual construction, in order to ensure proper position of the dowel in the sleeve, three short reinforcing bars  $\phi 10$  with a length of 10cm each, are welded on three sides of the dowel, (fig. 4.20). These bars serve for positioning the dowel at the same distance from all sides of the sleeve walls, respectively, in the middle of the sleeve.

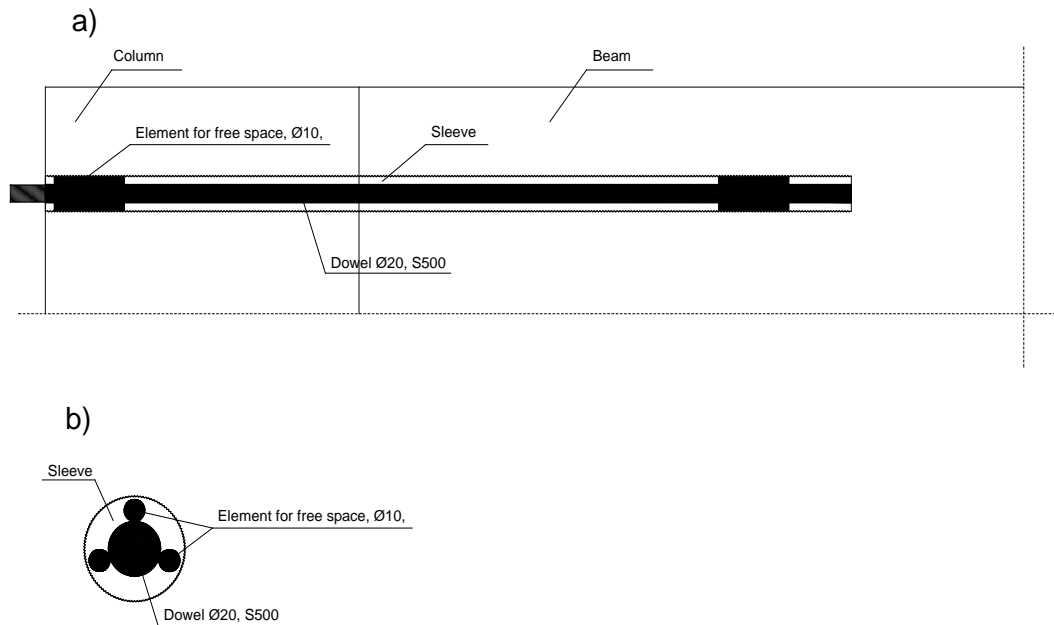


Fig. 4.20. Positioning the dowel within the sleeve; a) longitudinal view of the dowel within the connection, b) cross-section view of the dowel within the sleeve.

Pouring of the sleeve with concrete is performed using four holes which are left open during the concreting (fig. 4.16). Fig. 4.21 shows some photos taken during the actual connection of the element, presenting the process of injection of the grout in the sleeve. For pouring the sleeve, a simple plastic water bottle is used as a funnel.



Fig. 4.21. Photo taken during performance of a connection with horizontally positioned dowels; a) filling of the upper sleeves, b) filling of the upper and the lower sleeves.

- Treating sleeve for adequate roughness.

For proper anchorage, not only the dowel has to be bonded by the grout, but also the grout mass has to be bonded by the concrete element. For proper bondage of grout with concrete element, the

surface/walls of the concrete have to be rough enough, otherwise the grout mass could be pulled out and the connection could fail in pullout. For this activity, there could be different methodologies adopted. For this experiment, the following has been adopted:

Two and a half hours after pouring the concrete in the elements, just at the moment when the process of concrete hardening is started (the concrete is hard enough not to yield but still soft for scratching), the steel tubes are removed. The hardness state of the concrete is observed on spot and, at the right timing, a plastic brush (fibers of which are previously trimmed to meet the sleeve diameter) is used to make the roughness of the inside sleeve by twisting the same in and out one time, as presented in fig. 4.22.



*Fig. 4.22 Method used for treating sleeve walls for adequate roughness.*

## **4.5 Experiment set-up**

### **4.5.1 Boundary conditions**

The boundary conditions of the tested specimens are presented in fig. 4.23. The element is simply supported.

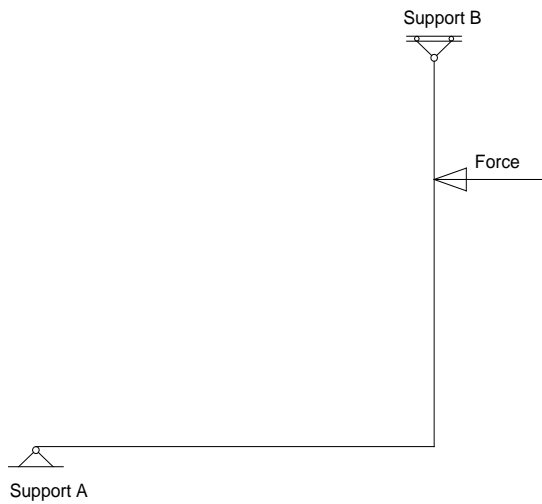


Fig. 4.23. Boundary conditions

Since the goal of the research is to test a connection, due to this boundary condition, all flexural deformations are concentrated in the joint. In this way, all deformation resulting from the experiment will be attributed to this connection/joint only.

The test set-up and scheme of instrumentation are presented in fig.4.24.

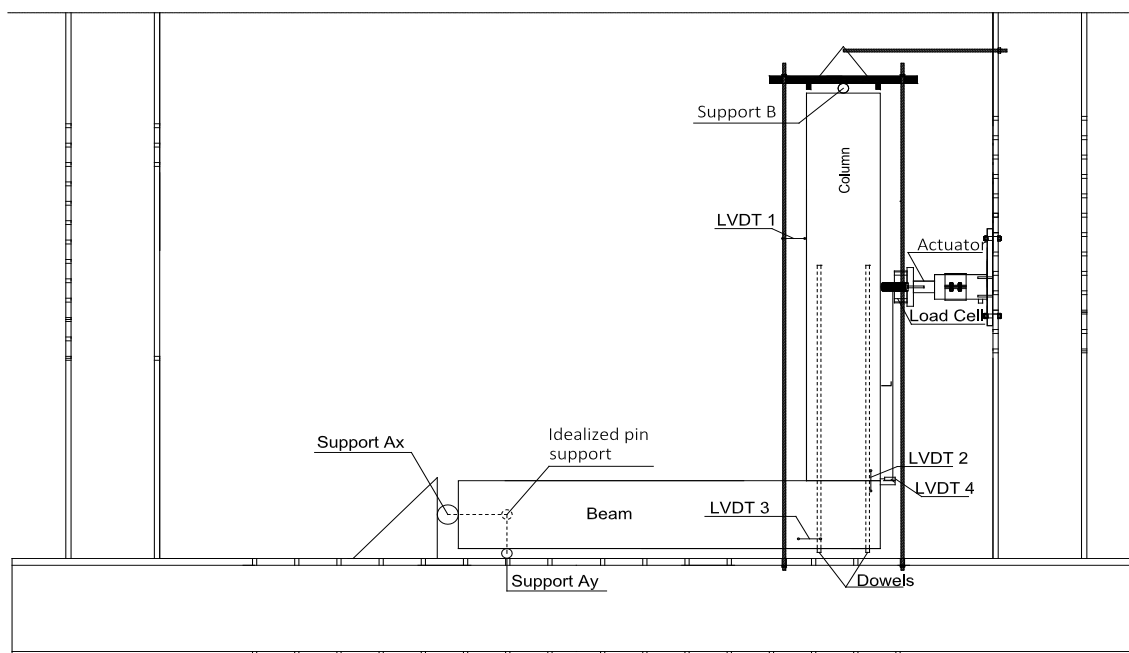


Fig. 4.24 Test set-up of the specimen with vertical dowels

The position of support Ay and the position of the actuator are flexible and they are used to achieve different moment/shear ratio at the section. In the case of vertically positioned dowels, for achieving  $M/V=1.0$  at the connection level, the distance of the actuator from the connection level is  $L=1.0\text{m}$  whereas for achieving  $M/V=1.5$ , the equator is positioned  $1.5\text{m}$  from the connection level. All other supports remain at the same locations for all experiments. Table 4.3 shows data on the location of the supports and the actuator for all experiments.

In the case of horizontally positioned dowels, to simulate the real life situation, the element is placed with the dowels positioned horizontally, (fig. 4.25). On horizontally positioned dowels, support Ay is used to achieve the respective M/V ratio whereas the actuator remains at the same location. For achieving  $M/V=1.0$  at the connection level, support Ay is positioned at distance  $L=1.0\text{m}$  from the connection level, whereas for achieving the  $M/V=0.5$  ratio, the Ay support is positioned at a distance  $L=0.5\text{m}$  from the connection.

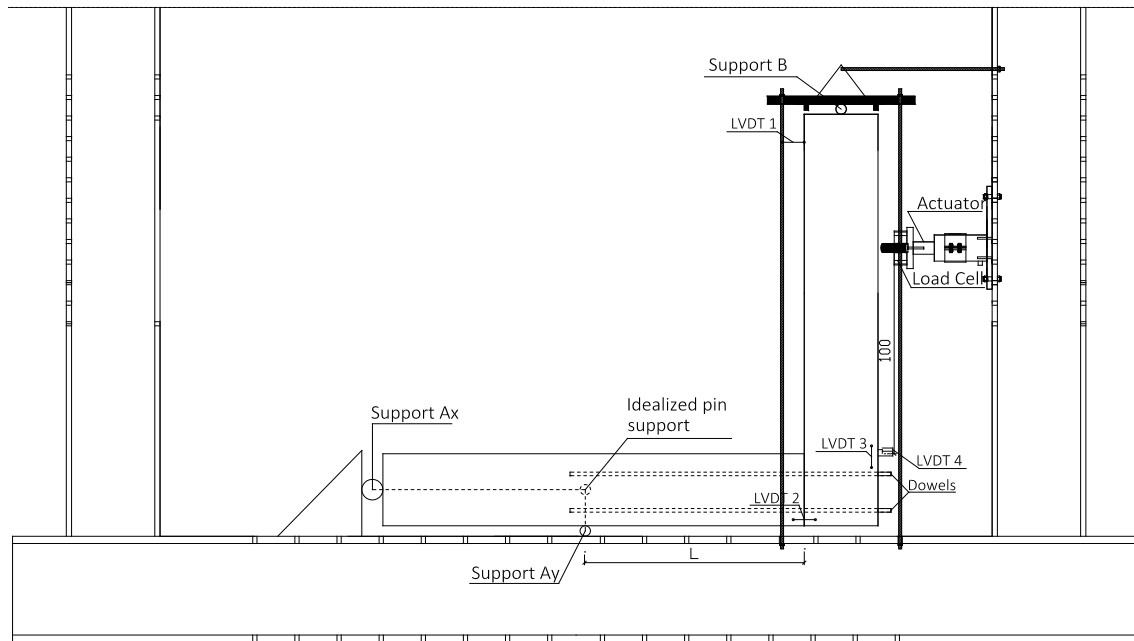
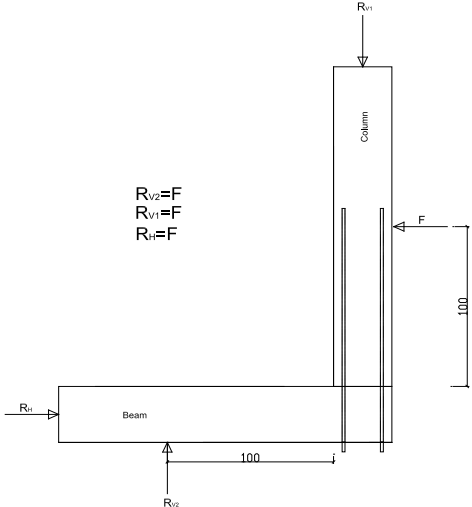
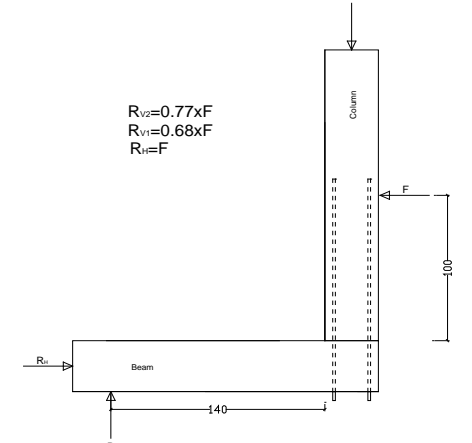
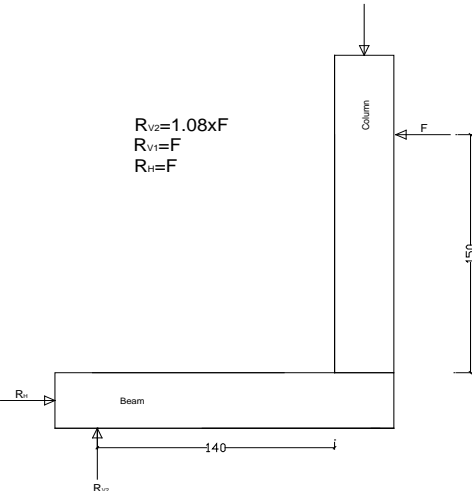


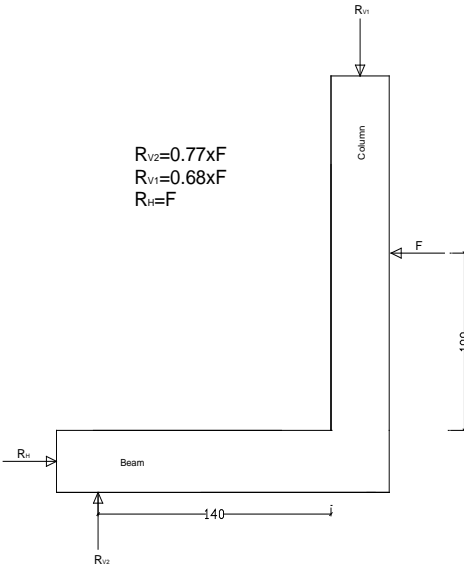
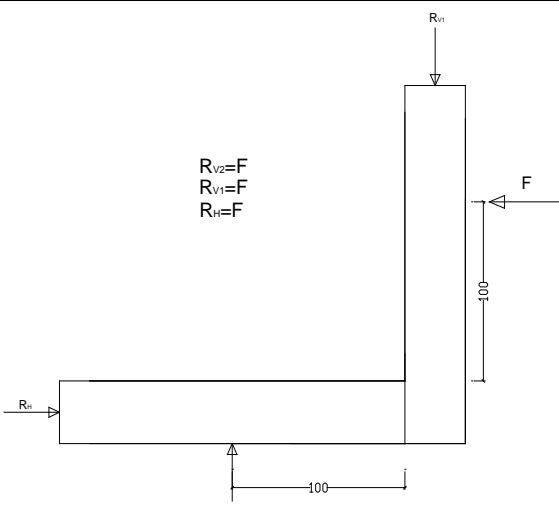
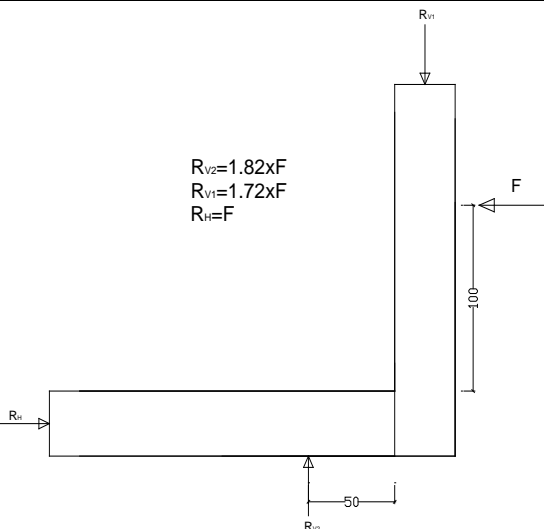
Fig. 4.25 Test set-up for the specimen with horizontal dowels

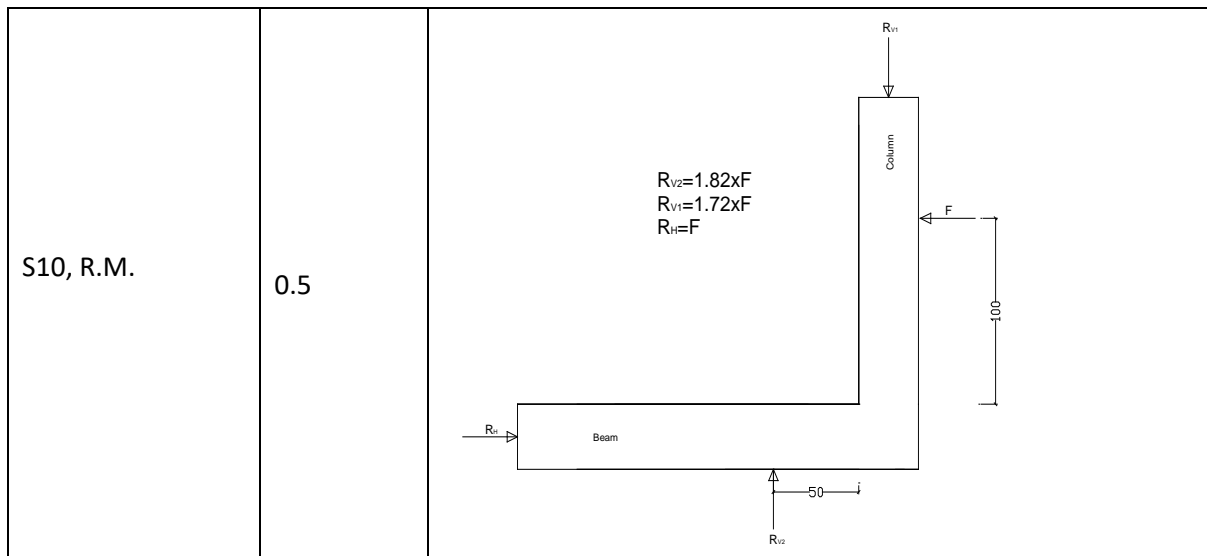
Table 4.3 shows details of boundary conditions of the tested specimens.

Table 4.3 Boundary conditions for the specimens tested under this research thesis

Experiment/Label	M/V ratio	Position of actuator and supports
S1, V.D.	1.0	 <p> <math>R_{V2}=F</math>  <math>R_{V1}=F</math>  <math>R_{H}=F</math> </p>
S2, V.D. S3, V.D. S7, V.D.	1.0	 <p> <math>R_{V2}=0.77 \times F</math>  <math>R_{V1}=0.68 \times F</math>  <math>R_{H}=F</math> </p>
S6, V.D.	1.5	 <p> <math>R_{V2}=1.08 \times F</math>  <math>R_{V1}=F</math>  <math>R_{H}=F</math> </p>



<p>S4, R.M.</p>	<p>1.0</p>	 <p> <math>R_{v2}=0.77xF</math>  <math>R_{v1}=0.68xF</math>  <math>R_H=F</math> </p>
<p>S5, H.D. S8, H.D.</p>	<p>1.0</p>	 <p> <math>R_{v2}=F</math>  <math>R_{v1}=F</math>  <math>R_H=F</math> </p>
<p>S9, H.D.</p>	<p>0.5</p>	 <p> <math>R_{v2}=1.82xF</math>  <math>R_{v1}=1.72xF</math>  <math>R_H=F</math> </p>



#### 4.5.2 Loading Programme

For technical reasons and practical purposes the following loading programme is adopted:

Until the anticipated yield point of the specimens force controlled loading program is applied. After the yielding point the loading programme is continued in deformation control mode. The graphic of loading programme adopted is presented in fig. 4.26

The designed flexural yielding strength presented in table 4.3 is in the level of the section. In cast-in-situ frames this also is considered as flexural yielding of the element and also of the joint. The behavior of precast connections are different from the behavior of the cast-in-situ joints and the strength properties of the section of the precast connection cannot be considered to be strength properties of the connection as an element. The flexural yielding strength of the precast connections to be experimentally tested is anticipated to be lower than flexural yielding strength of the section. For this reason the flexural yielding strength, for purposes of planning the experimental programme, is reduced. The adopted flexural yielding strength of the precast connections is adopted  $M_y = 75 \text{ kNm}$ .

For loading programme the anticipated yielding flexural strength is divided in 5 equal increments ( $\Delta y / 5 = \Delta$ ) and three loading cycled are performed for each increment ( $\Delta = 15 \text{ kN}$ ,  $2\Delta = 30 \text{ kN}$ ,  $3\Delta = 45 \text{ kN}$ ,  $4\Delta = 60 \text{ kN}$ ,  $5\Delta = \Delta y = 75 \text{ kN}$ )

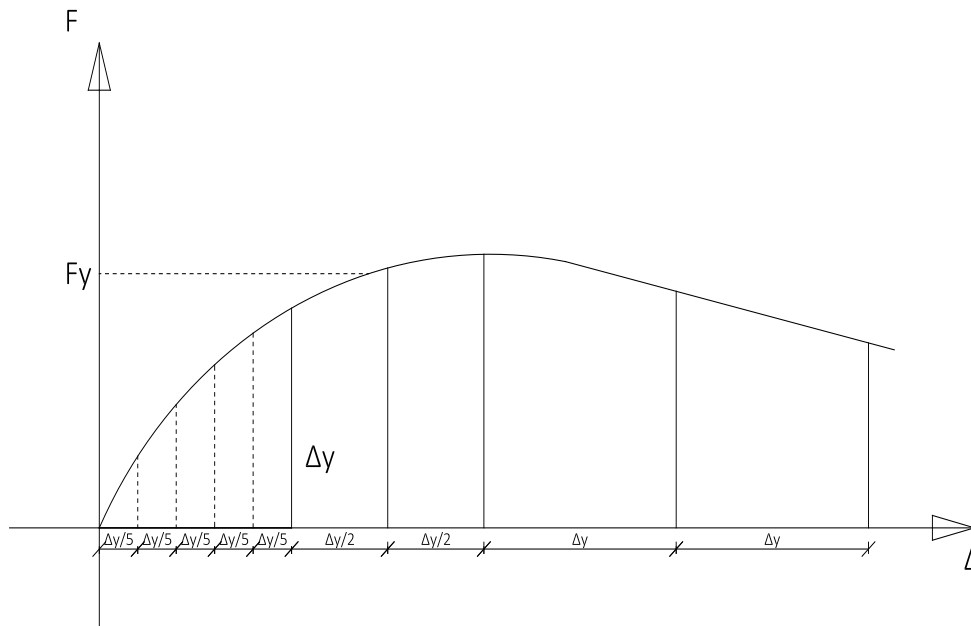


Fig. 4.26 Loading programme adopted for performing experiments

### 4.5.3 Description of equipment and sensors used in the experimental program

The equipment used for the performance of the tests and the processing of the results has been the following:

#### a) Multifunctional Control Console (MCC 8)

Multifunctional Control Console (MCC 8), fig. 4.27 a), with the following characteristics has been used as equipment for conducting the testing program:

- General description: Automatic hydraulic systems for static and low frequency dynamic tests on building materials under control of Load/Stress, Displacement, Strain;
- Hydraulic Group: dual stage pump, 700 bar max. pressure, 2 hydraulic outputs extendable to 4 with the accessories 50-C7022/UP1 and /UP2 (see Upgrading Options), servo-control system for load control with proportional valve;
- Hardware and on board firmware:
  - o Resolution 132000 divisions, closed loop control with high frequency PID,
  - o 4 channels for deformation sensors used in Elastic Modulus determination (normally strain gauges or digital compressometers),
  - o Diagnostic menu to identify possible problems,
- Saving of calibration curves of different sensors;
- Digital linearity of calibration curves with automatic selection of coefficients;
- User interface: The system is controlled via the PC. An alphanumeric keyboard and an icon driven display are also provided for factory settings and use of unit in local mode;
- Graphical display 320x240 pixel;
- Software: automatic execution of fully customized tests under load/stress, displacement strain rate control which are for materials such as fiber reinforced concrete (FRC), Shotcrete, concrete

elements lined with polymeric membranes, structural reinforcement elements. It is also possible to program a sequence of steps with different feedback parameters. All test parameters can be easily modified to meet the Standards requirements.

**b) Hydraulic Cylinder (fig. 4.27 b)**

- Single Acting Cylinder – ENERPAC
- Stroke 159mm
- Capacity 500kN

**c) Force Transducer (AEP Italy) – TC 4 (fig. 4.27 c)**

- Force transducers for the measurement of static and dynamic loads in COMPRESSION and TENSION
- Load capacity 500kN
- Class (ISO 376) 1
- Linearity and hysteresis 0.05%
- Output 2mV/V

**d) Linear potentiometer transducer (fig. 4.27 d)**

- Input voltage 10 V DC
- Nominal displacement 100 mm
- Repeatability: better than 0.002 mm
- Accuracy: better than 0.002 mm
- LDT standard output 2mV/V

**e) Displacement Transducers (AEP Italy) – LDT (fig. 4.27 e)**

- Input voltage 10 V DC
- Nominal displacement 50 mm
- Resolution: Infinite
- Linearity: 0.5%



Fig. 4.27 Photo of items used for the experiments; a) Multifunctional Control Console (MCC 8), b) Hydraulic Cylinder, c) Force Transducer, d) Linear Potentiometer Transducer and e) Displacement Transducer

#### 4.5.3.1 Positioning of LVDT's

A total of four LVDS-s were available and they were positioned to best capture the global and local performance of the specimens. In fig. 4.24 and fig. 4.25 are presented positions of the LVDT-s in the specimen with a vertical dowel and the specimen with a horizontal dowel respectively.

- LVDT 1, is positioned to measure the global deformation of the specimen, which deformation is solely attributed to the deformability of the joint where the connection is performed. This LVDT measured the deformation on one element (column) in respect to the other element (beam). In this way, all other outside factors that could affect the deformation are eliminated.
- LVDT 2, is positioned at the connection level to measure the deformation (gap opening) of the connection section.
- LVDT 3, is positioned on the other side (monolithic part) of the joint, at the location where the biggest potential flexural crack would perform with the intention to follow the deformability of the connection in respect to this anticipated crack formation in the element.
- LVDT 4, is positioned to measure the shear displacement of the beam in respect to the column at the connection level, respectively to measure the shear split of the connection.

## 4.6 Results from experiments

In this item, the results from the experiments and comments on the performance of each specimen during the testing are presented.

### 4.6.1 Specimen “S 1, V.D”

This experiment was performed on a connection with vertical dowels strengthened by individual plates, (fig. 4.8b).

In this experiment, the M/V ratio at the precast connection section as well as at the monolithic side of the joint face was  $M/V=1.0$ .

The results for the behavior of this connection are presented in figs. 4.28 – 4.31.

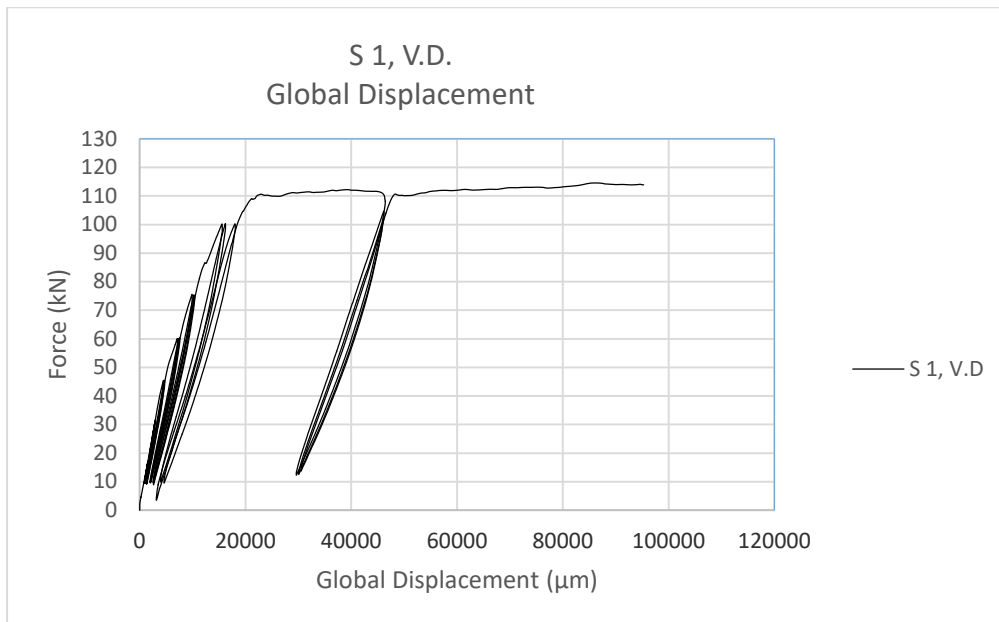


Fig. 4.28 F-D diagram of global displacement of specimen “S.1 V.D.”

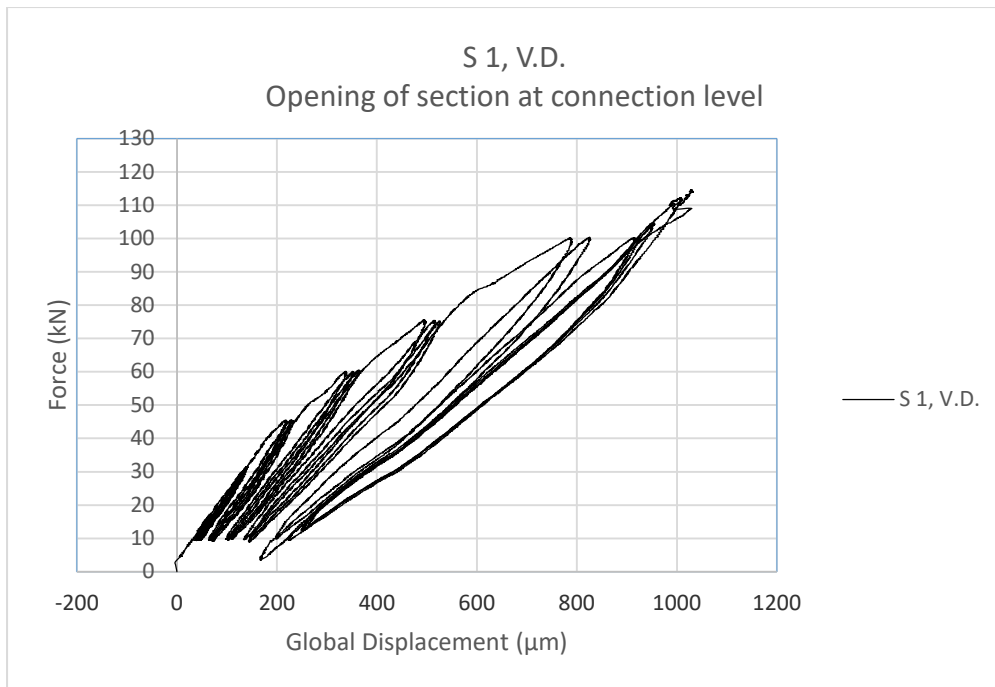


Fig. 4.29 F-D diagram of opening of section at the connection level of specimen "S.1 V.D."

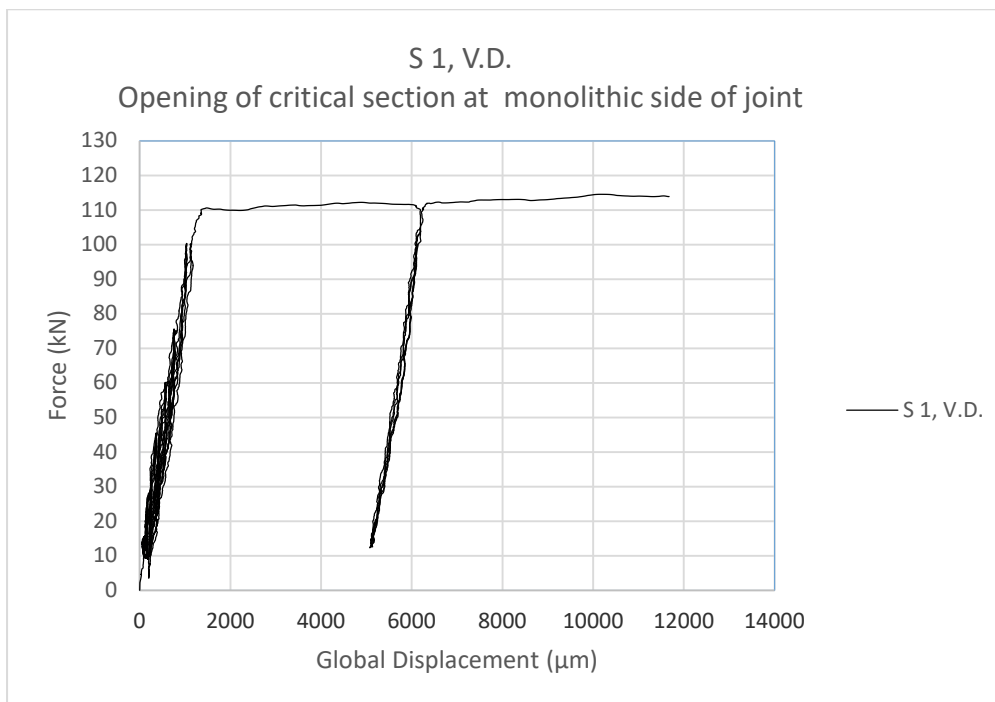


Fig. 4.30 F-D diagram of opening of section at the monolithic part of the joint (beam face) of specimen "S.1 V.D."

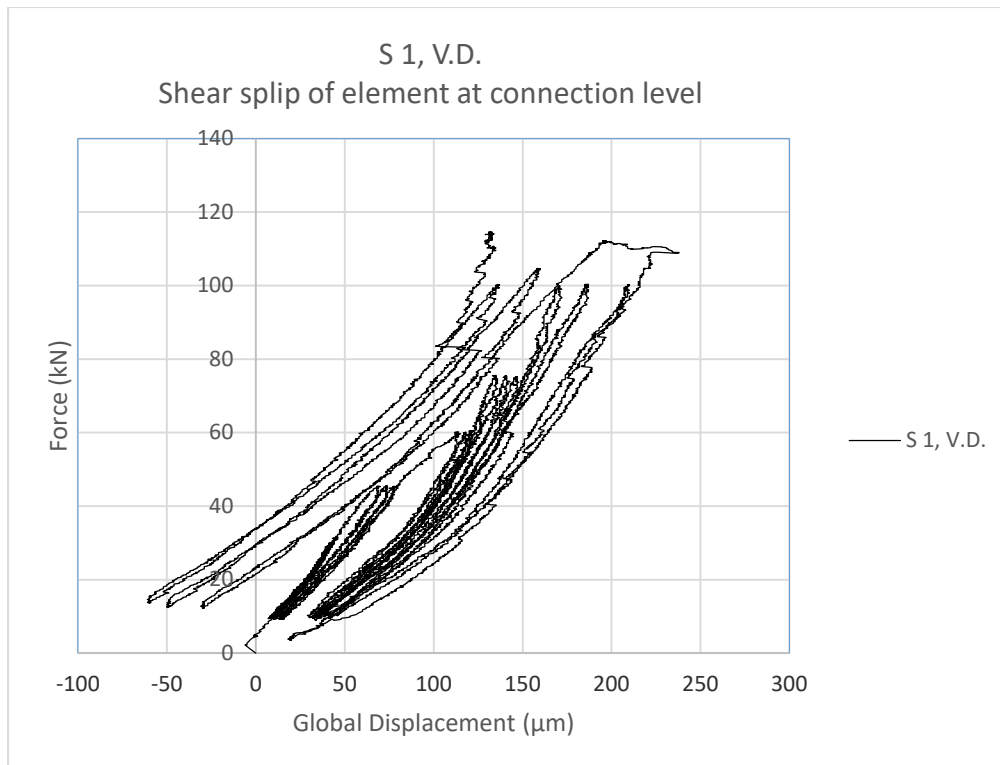


Fig. 4.31 F-D diagram of shear slip of the connection of specimen "S.1 V.D."

#### **Observation during the experiment**

At the last loading cycle, the global deformation of the specimen exceeded the LVDT measuring capacity. Even though the readings of the LVDT 1 stopped, the loading continued. At the moment when the LVDT 1 reached the maximum, the curve was already in slow descending. With the continuation of the experiment, the force was decreasing. Since LVDT 1 was not able to perform the measuring, it was impossible to register the descending curve.

#### **4.6.1.1 Description of the specimen performance**

Until force  $F=110$  kN, the specimen experienced the following behavior, (figs. 4.32 and 4.33):

- a) The joint of the specimen behaved in shear due to the tension force from the plates due to the dowel pullout (this is covered in more details further in text).
- b) The beam exhibited a pure flexure behavior, namely, there were no shear cracks until that force.
- c) The global behavior of the specimen, until force  $F=105$  kN, was mainly governed by the behavior of the precast section, and to a certain extent, also by the beam-joint section. This is clearly evident by observing the F-D diagram of global displacement (fig. 4.28) and the F-D diagram of the precast section (fig. 4.29). With the increase of force on the beam, a large shear crack started to be developed in it, (fig. 4.33). Following the formation of this crack, all flexural deformations started to be concentrated on the beam only and at two places, both slightly away from the joint face. The crack that was initially formed on the joint face did not propagate further after the force exceeded the intensity of 105kN. Both of these other cracks



that governed the behavior of the specimen (section that failed) were cracks that were initially formed due to flexure and then, with the increase of force (over 105kN) and hence, increase of shear stresses, the same section experienced further shear cracks. After the concrete failed in shear, the longitudinal reinforcement started to behave like a dowel in shear. From that moment, this section started to behave like a precast section loaded by a shear/flexure combination. While in the other cracked section, the longitudinal reinforcement was loaded in tension due to flexure, in this section, the reinforcement started to rotate due to the kinking effect. As a result of this, it could be concluded that the specimen failed by a shear/flexure combination which occurred on the beam.

The resistance of the precast beam-to-column section was bigger than that of the other element (beam) of the connection. This is because shear/flexure interaction proved to be more critical than pure flexure. The reason that the column did not experience any damage at all, except for the few hairline flexure types of cracks, (fig 4.32), was that there were also four dowels in addition to the longitudinal reinforcement in the column. This made the column (except for the connection section) much stronger than the other element of the precast specimen. In this way, due to the construction methodology requirements for precast structures, the element of the structure where the dowels were anchored became much stronger than the other element of the precast structure. For the same flexural capacity and under flexure/shear ratio of  $M/V=1.0$ , the precast connection was not a critical section of the structure.

The total deformability of this specimen was very high  $D>10\text{cm}$ .

**Note:**

**As total deformability were considered the global deformation values of the specimen at the force 80% of the ultimate force pass the ultimate point.**

All the deformability of the specimen was provided by the beam (the element with no dowels anchored in it). This is due to the fact that the strength of the column is much higher than that of the beam, which was also confirmed with the experiment. This is a very good outcome because, in the standard seismic design approach, the goal is just this, namely, the column to be stronger than the beam, and this was achieved in this specimen (in this type of connection).



Fig. 4.32 Cracks in the specimen after the sixth loading cycle applied on specimen "S.1 V.D."



Fig. 4.33 The specimen after the last loading cycle, failure state of specimen "S.1 V.D."

#### 4.6.2 Specimen "S 2, V.D."

This experiment was performed on the element with vertical dowels (VD) where the connection was done by grout only. The M/V ratio at the beam-to-column connection level was 1.0. By observing the behavior of specimen "S 1, V.D.", where the beam failed in the shear/flexure mode, by which the properties of the connection could not be explored, in order to prevent such failure of the other specimens, the boundary conditions were changed to allow this element to behave in flexure. Instead of 100cm from the joint face, the support was placed at a distance of 140cm, as presented in table 4.2.

The experimental results represented through F-D diagrams are given in figs. 4.34 – 4.37.

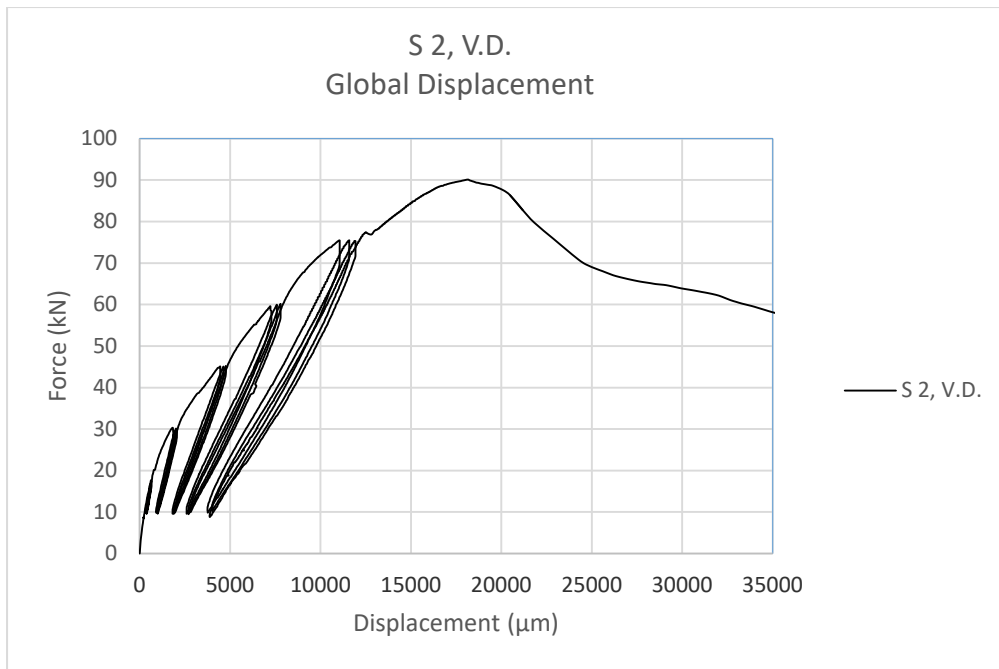


Fig. 4.34 F-D diagram of global displacement of specimen "S.2 V.D."

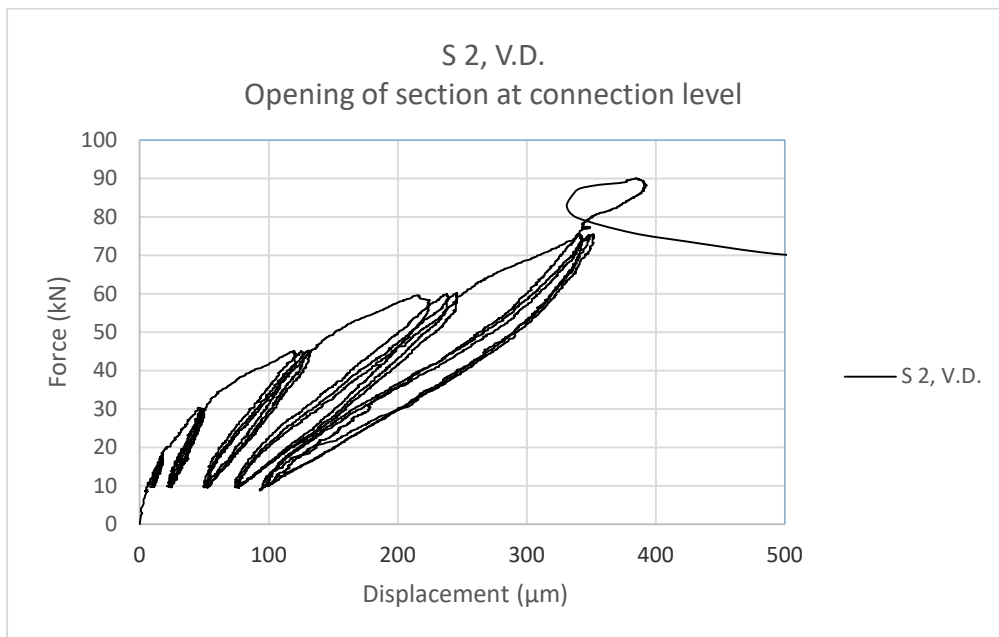


Fig. 4.35 F-D diagram of opening of section at connection level of specimen "S.2 V.D."

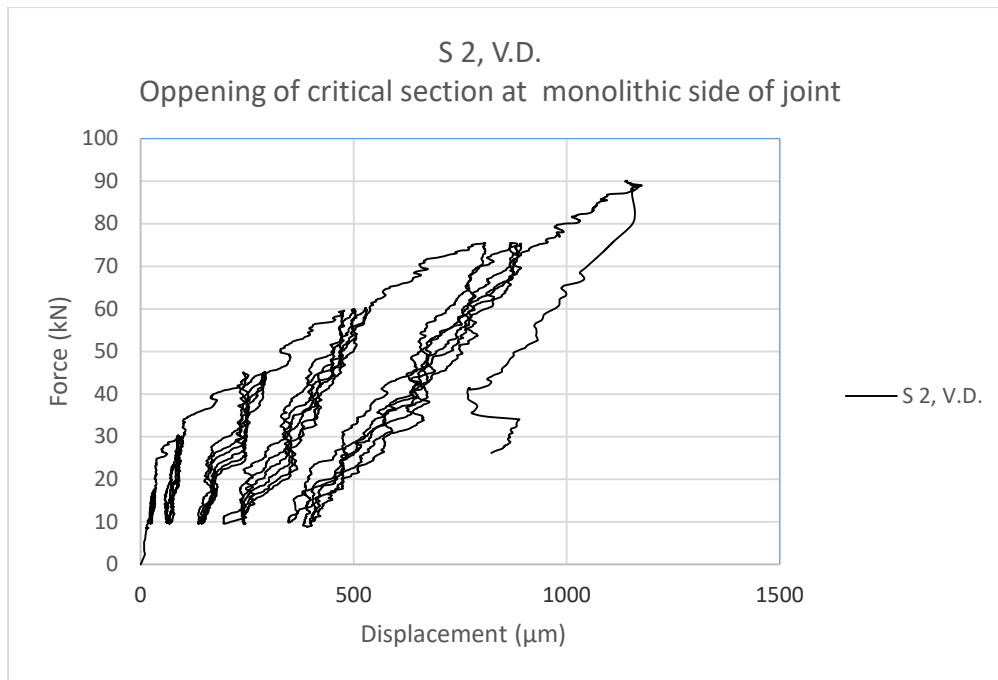


Fig. 4.36 F-D diagram of opening of section at the monolithic part of the joint (beam face) of specimen “S.2 V.D.”

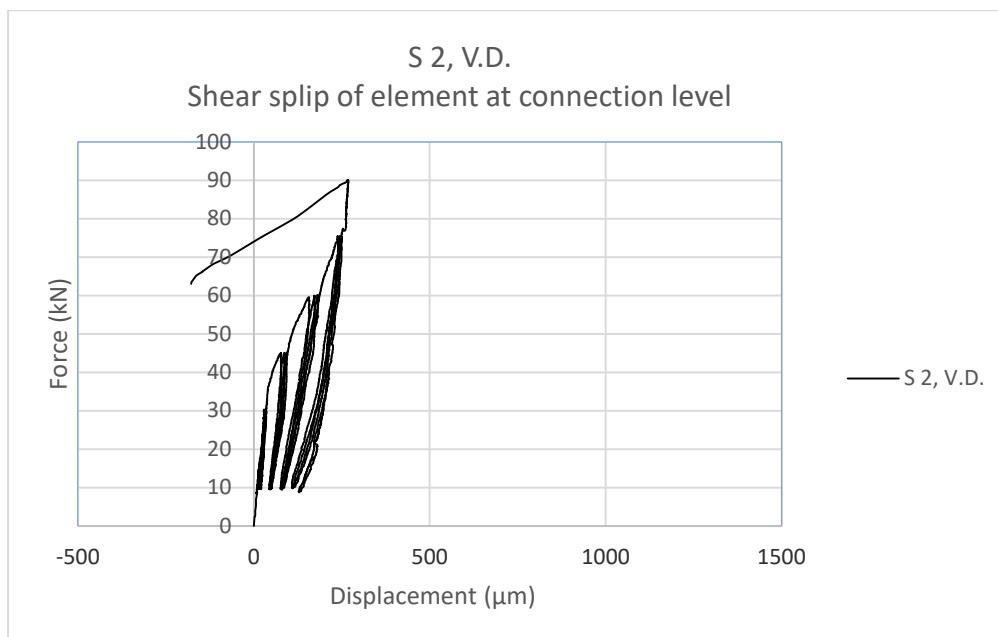


Fig. 4.37 F-D diagram of shear slip of the connection of specimen “S.2 V.D.”

#### 4.6.2.1 Description of the specimen performance

During the first five cycles, up to the load of 75kN, the specimen exhibited a flexural performance. This is shown in the F-D diagram on global displacement, (fig4.34). During these cycles, all parts/sections of the specimen were still in the elastic range. At the sixth cycle, under a load of 77kN, the joint of the specimen experienced the first shear crack from pullout of the dowel. This crack is also detectable in the F-D diagram of global displacement, (fig 4.34).

With further increase of the load, the F-D curve increased under a different (smaller) angle which was an evidence of the drop of the stiffness of the specimen (joint) at this load intensity ( $F=77\text{kN}$ ). However, this degradation of stiffness was due to concrete shear crack occurrence, wherefore this point was not to be considered as a yielding point of the joint since no section (longitudinal reinforcement) of the specimen passed the yielding point. This is evident from observing the F-D curves presented in fig.4.35 and fig. 4.36 where none of the potential critical sections exceeds the elastic range.

With the increase of the load, there appeared another shear/pullout crack in the joint. These shear/pullout cracks appeared due to rotation of the section presented in fig. 4.39. At the force of  $F=90\text{kN}$ , the joint underwent a shear brittle failure caused by pullout of the dowels loaded in tension. This is evident from the F-D diagram presented in fig 4.34 as well as in fig 4.38. The pullout of the dowels was visible at the end of the experiment.

After the pullout failure occurred at two dowels loaded in tension, due to rotation of the section, the dowels in tension also started to rotate and caused concrete spalling. This is also evident in the F-D diagram showing the measured slip of the connection, (fig 4.37) where, at load  $F=90\text{ kN}$ , the deformations started to develop on the opposite side of the slip, indicating concrete spalling.

The overall behavior of this connection, "S 2 V.D.", constructed with vertical dowels and grout only, was dowel pullout failure with small deformability and limited ductility.

The total deformability of specimen "S 2 V.D." was  $D=2.4\text{cm}$ .



Fig. 4.38 Crack pattern of the specimen at the last loading cycle -photo from experiment of specimen "S.2 V.D."

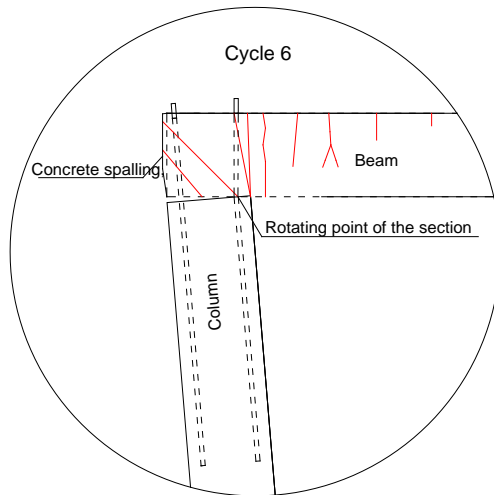


Fig. 4.39 Rotation of the section of specimen "S.2 V.D."

#### 4.6.3 Specimen "S 3, V.D"

This experiment was performed on the connection with vertical dowels strengthened by individual plates. This specimen was the same as specimen "S 1, V.D", the difference being only in the boundary conditions. The boundary conditions of this specimen and all other specimens are presented in Table 2. The results on the behavior of this connection are presented in figs. 4.40 – 4.43.

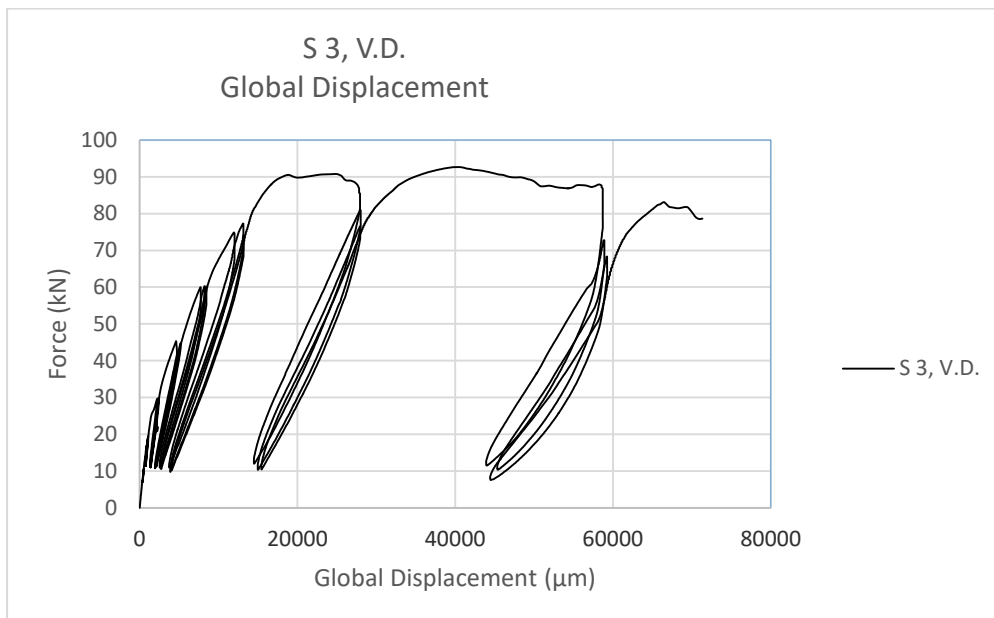


Fig. 4.40 F-D diagram of global displacement of specimen "S.3 V.D."

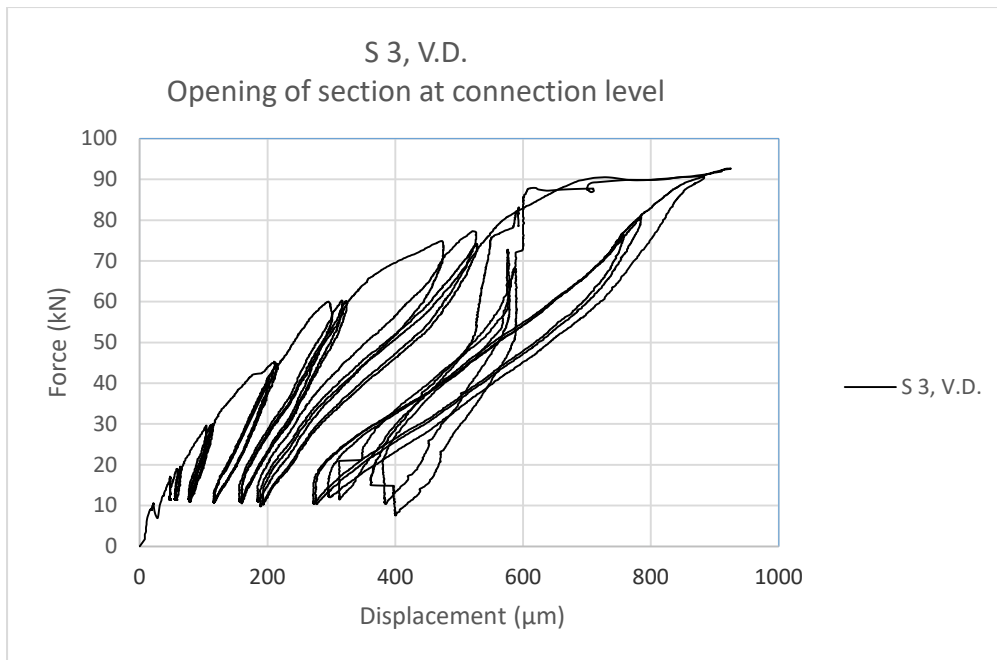


Fig. 4.41 F-D diagram referring to the connection level of specimen "S.3 V.D."

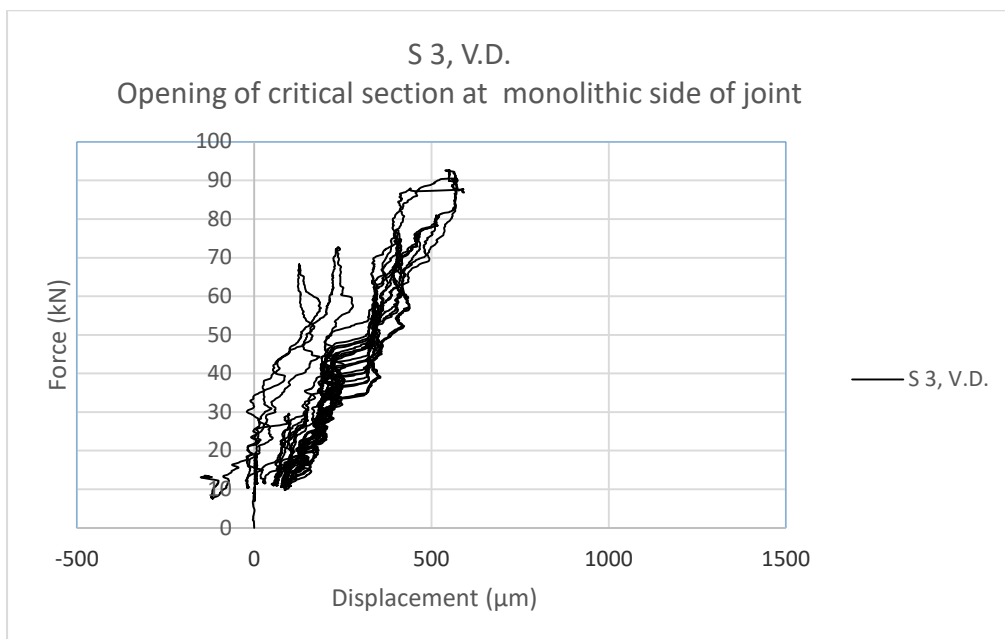


Fig. 4.42 F-D diagram referring to the monolithic part of the joint (beam phase) of specimen "S.3 V.D."

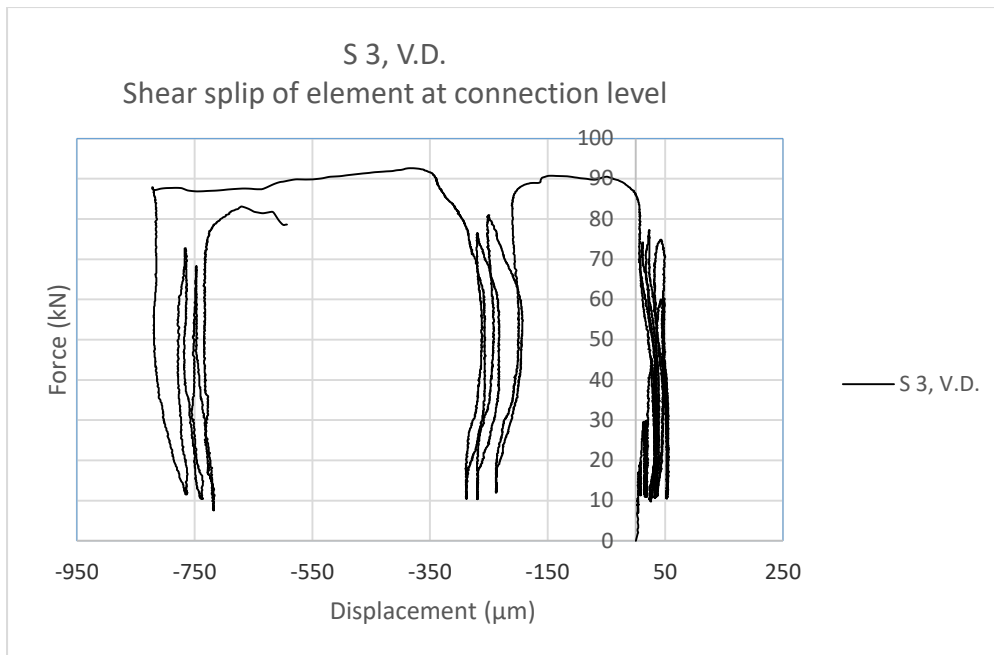


Fig. 4.43 F-D diagram of shear slip of the connection of specimen "S.3 V.D."

#### 4.6.3.1 Description of the specimen performance

The overall performance of the joint can be considered as a shear/flexural performance.

During the sixth loading cycle, up to the load of 90kN, most of the cracks were concentrated on the joint. These cracks were not from the pullout force of the dowel, but rather from the shear force generated from the strengthening plate as a result of pullout prevention. These cracks did not propagate throughout the joint, but stopped at around 85% of the joint depth. This was an indication that this crack was initiated as a shear crack due to the shear force from the plate, but then continued to propagate further as a flexural crack due to rotation of the section.

At the load of  $F=90\text{kN}$ , the specimen reached the yielding point, and the monolithic section of the joint, started to yield. The yielding is evident in the F-D diagram of global displacement (fig. 4.40).

Yielding of longitudinal reinforcement did not occur as expected in the regular flexural behavior section. In the regular flexural behavior of the section, the longitudinal reinforcement would be loaded in tension only due to rotation of the section. In this particular situation, the forces acting on the section are:

- a) shear force from the strengthening plates acting on the joint that caused the shear crack marked in red in fig. 4.45 which force is generated on the plate as a result of tension force on the dowel, and
- b) transversal force acting perpendicularly to the dowel axis generated due to rotation of the dowel as presented in fig. 4.45.

The combination of these forces caused the longitudinal reinforcement of the beam to be loaded in bending and tension at the same time. This kind of loading of the longitudinal reinforcement also



occurred in Specimen "S 1, V.D.". Similar to Specimen "S 1, V.D.", this specimen also failed due to the shear/flexural stresses, but in this case, the failure occurred at the joint.

This specimen provided a considerable amount of total deformability,  $D = 7.1\text{cm}$ .

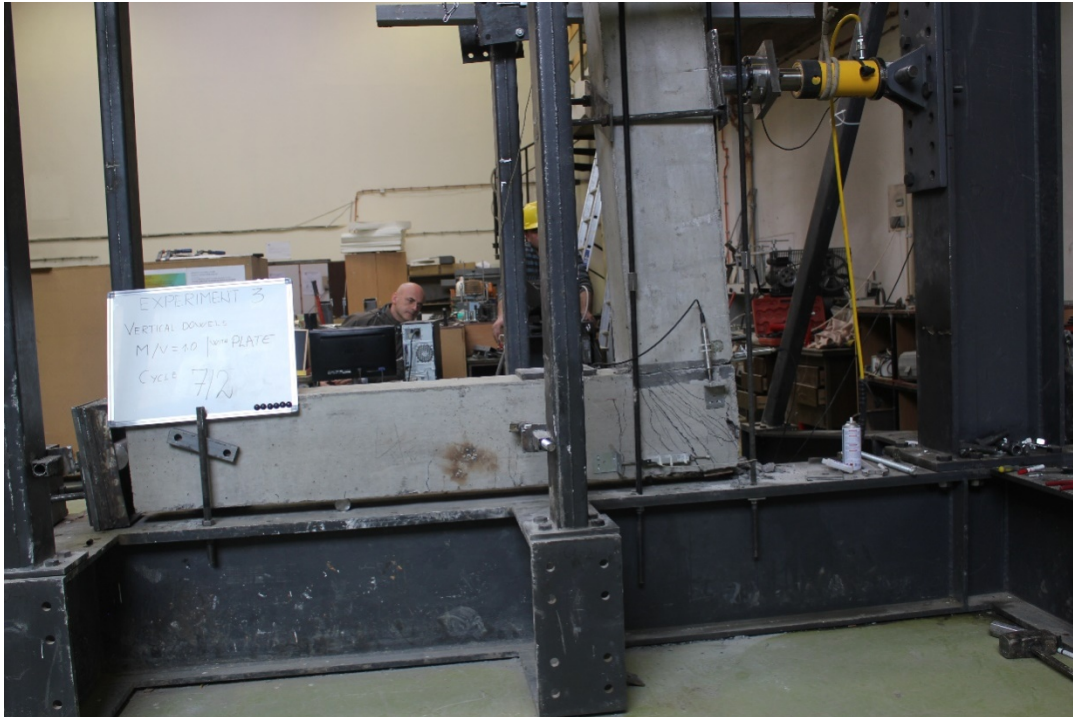


Fig. 4.44 Crack pattern of the specimen under the last loading cycle - photo from the experiment on specimen "S.3 V.D."

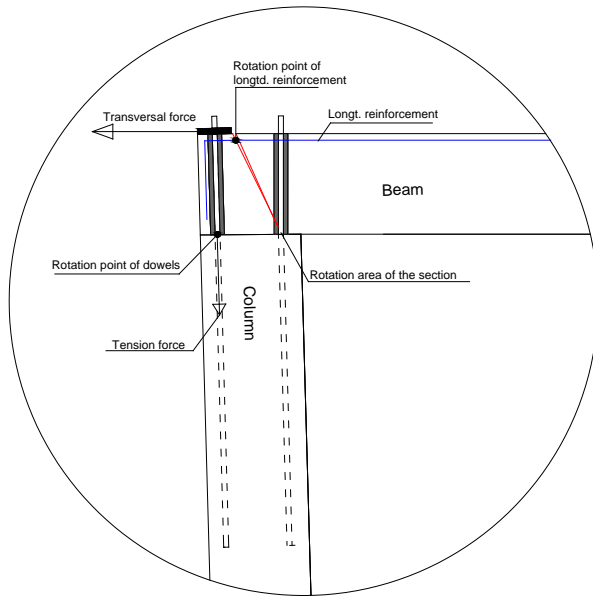


Fig.4.45 Deformation of the connection/joint at the last loading cycle applied on specimen "S.3 V.D."

#### 4.6.4 Specimen "S 4, R.M"

This experiment was performed on the referent cast-in-situ specimen. The results of the experiment "S 4, R.M." are presented in figs. 4.46 – 4.49.

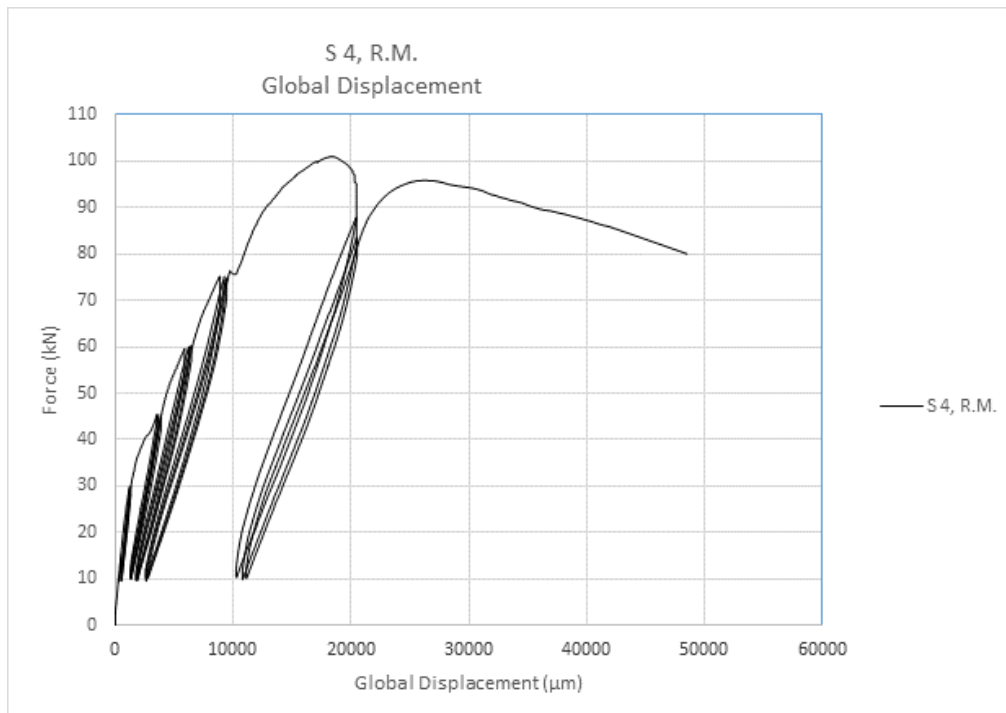


Fig. 4.46 F-D diagram of global displacement of specimen "S.4 R.M."

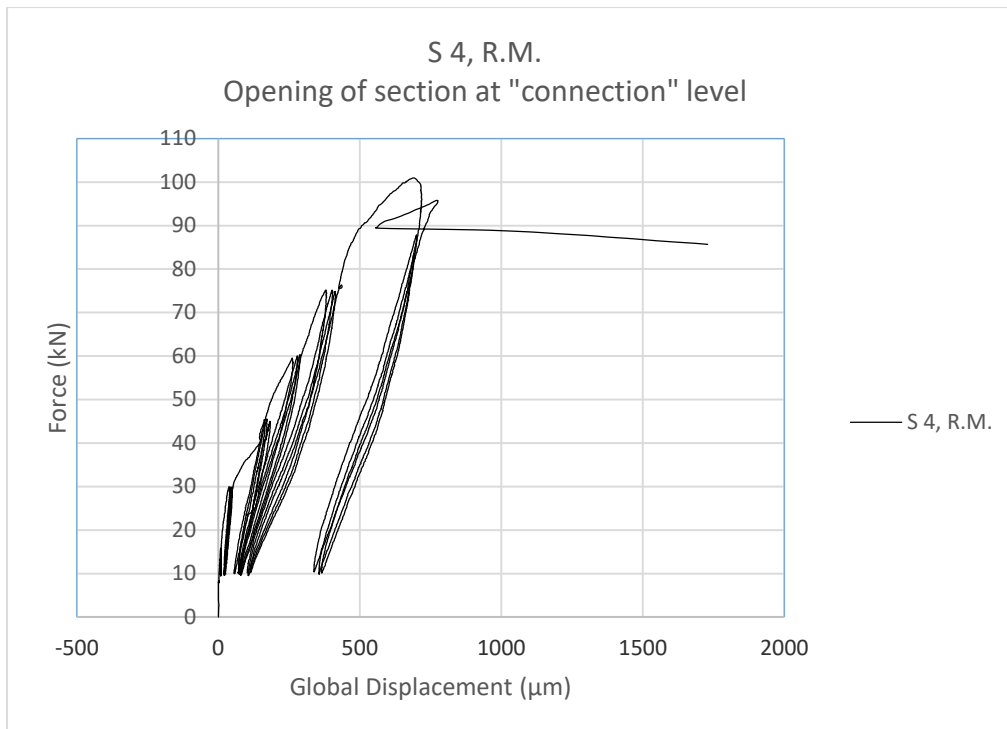


Fig. 4.47 F-D diagram referring to the column face of the joint of specimen "S.4 R.M."

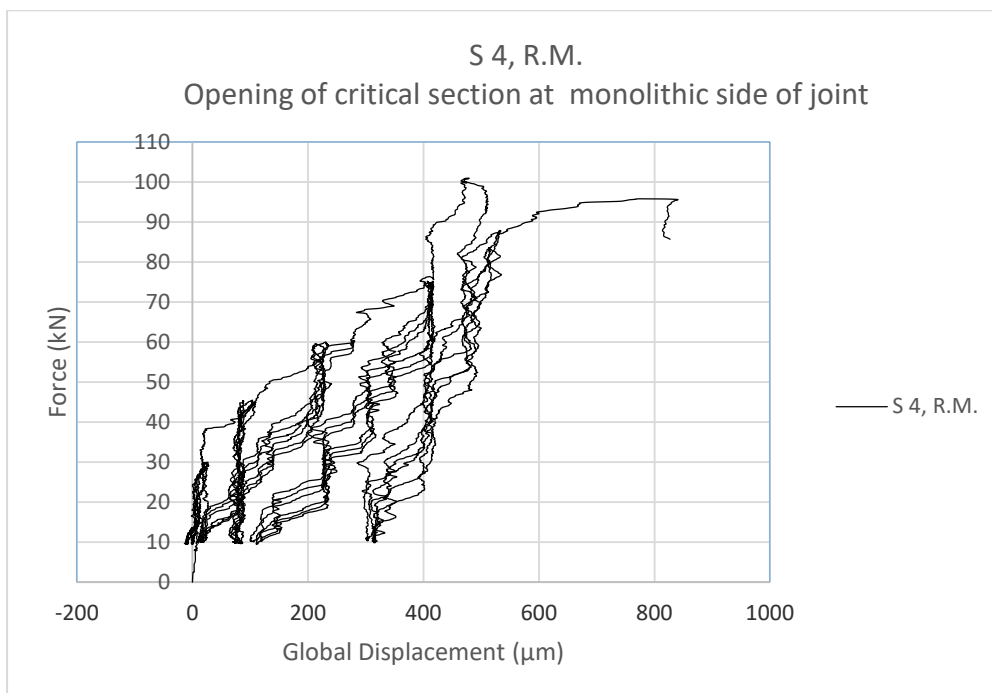


Fig. 4.48 F-D diagram referring to the beam face of the joint of specimen "S.4 R.M."

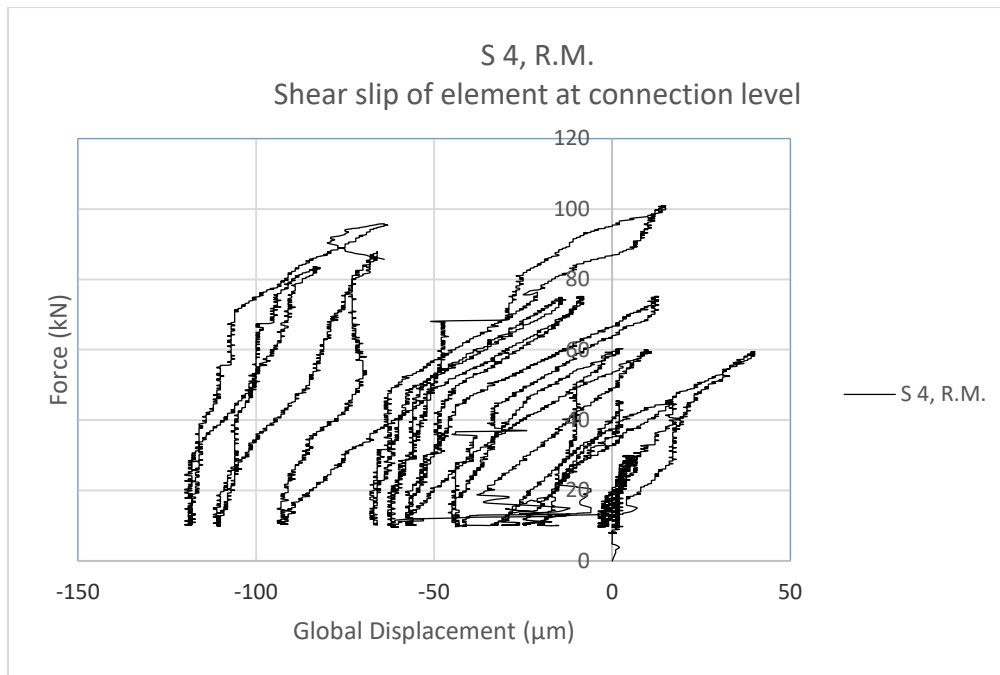


Fig. 4.49 F-D diagram of shear slip of the joint (column face vs joint) of specimen "S.4 R.M."

#### 4.6.4.1 Description of the specimen performance

The overall performance of the joint can be considered as a flexural type of performance.

At the load of 75kN, during the sixth loading cycle, the joint experienced concrete cracking (start of concrete spalling) because of the rotation of the section. This is noticed in the F-D diagram of global displacement as well as in the shear slip diagram, (fig. 4.46 and fig. 4.49).

With further increase of the load, during the sixth cycle, a new flexural crack was formed in the joint, and it appeared to be the critical one. At the load of 102kN, this section achieved the maximum bearing capacity. Due to the cross-section properties, including arrangement of the longitudinal reinforcement of the column and the loads acting on the section (axial and shear), the section provided a limited ductility, since the compressed concrete crushed as soon as the longitudinal reinforcement started to cross the elastic range. This is presented in the F-D diagram of global deformation by an abrupt curve declination.

At the last loading cycle, the tensile reinforcement continued to yield, however, under continuous strength degradation. The critical section and its rotation are presented in fig. 4.51.

The total deformability of this specimen was  $D=4.8\text{cm}$ .

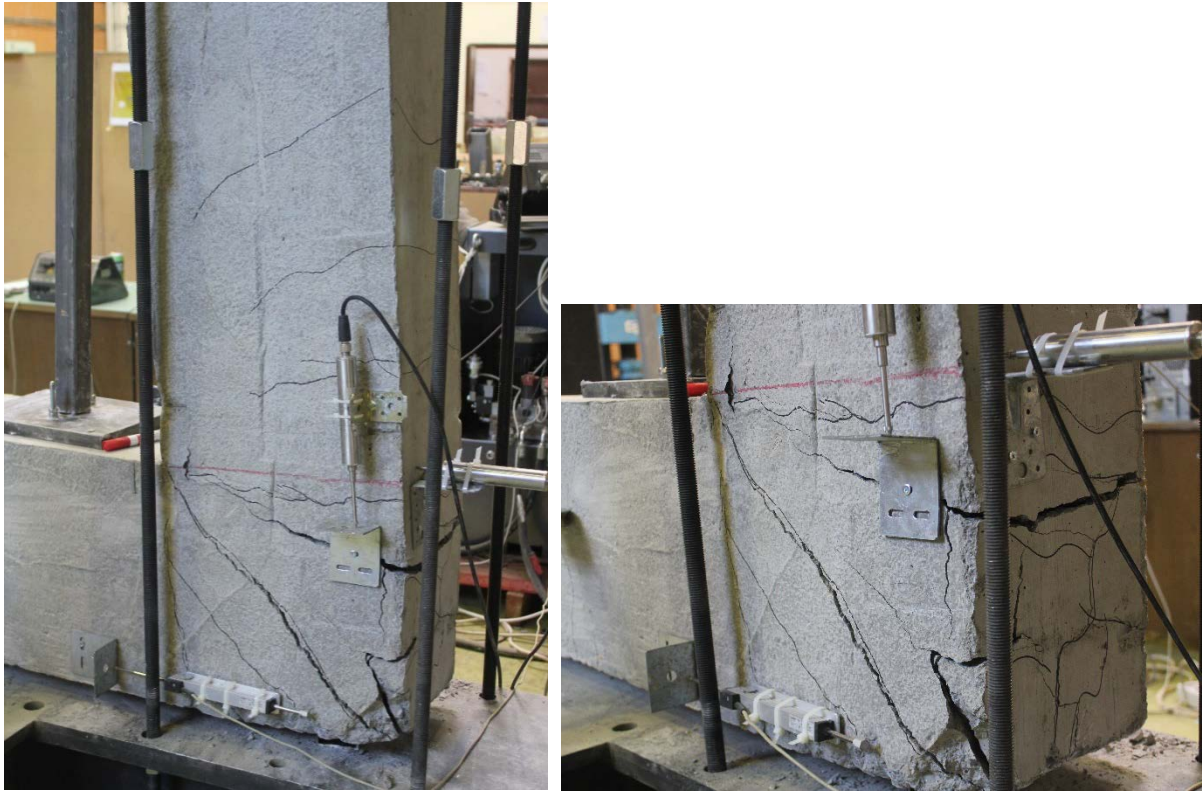


Fig. 4.50 Photo of the specimen after the last loading cycle applied on specimen "S.4 R.M."

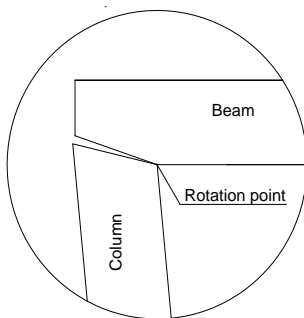


Fig.4.51. Deformation of the connection/joint at the last loading cycle applied on specimen "S.4 R.M."

#### 4.6.5 Specimen "S 5, H.D."

This specimen was constructed with horizontal dowels and strengthened by individual steel plates. It was tested under the same boundary conditions as the "S 1, V.D." specimen.

Figs. 4.52 and fig. 4.53 display the force-deformation diagrams referring to the element with horizontally positioned dowels (H.D).

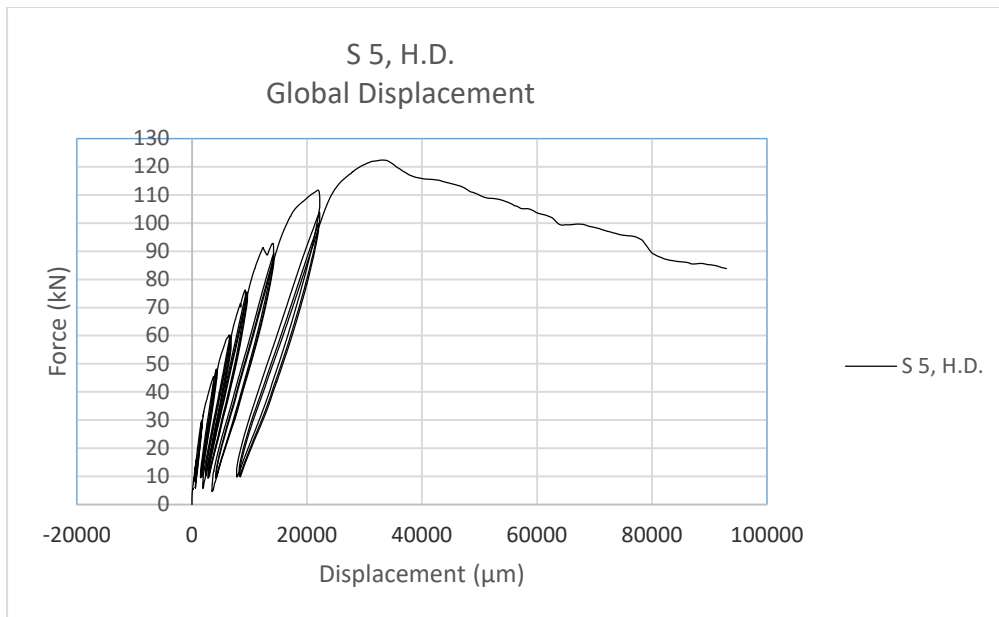


Fig. 4.52 F-D diagram of global displacement of specimen "S.5 H.D."

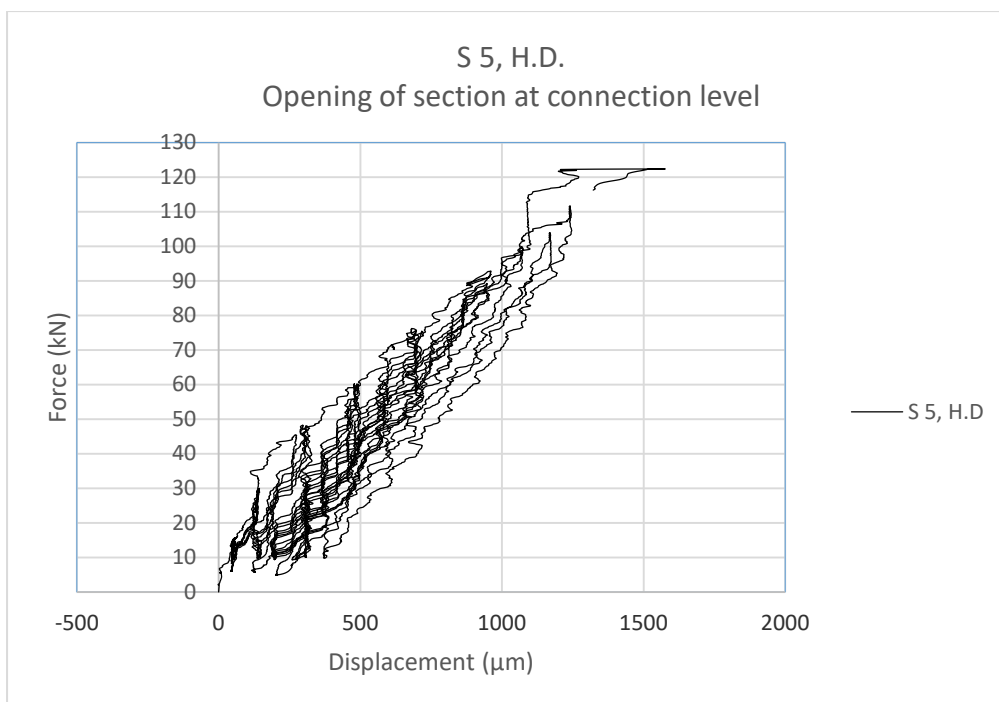


Fig. 4.53 F-D diagram referring to the connection level of specimen "S.5 H.D."

In this experiment, the LVDT 3 did not capture the main crack wherefore the readings of this LVDT are not relevant. The measurements from LVDT 4 during this experiment failed.

#### 4.6.5.1 Description of the specimen performance

Fig. 4.54 shows the crack patterns after the last loading cycle applied on the joint of the element with H.D strengthened by individual steel plates.

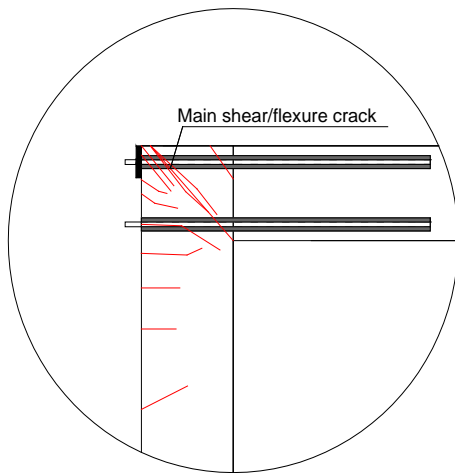


Fig. 4.54 Crack pattern of a joint of an element of specimen "S.5 H.D."

The overall performance of the joint can be considered as a shear/flexural type of performance.

At the load of 90kN, during the sixth loading cycle, the joint experienced concrete cracking (start of concrete spalling) from rotation of the section, respectively, the first shear slip.

At the load of  $F=105\text{kN}$ , the joint reached the yielding point, which can be seen from the F-D diagram of global displacement (fig. 4.52).

At the load of 122kN, this section achieved the maximum bearing capacity. As a result of observation during the experiment and investigation of the specimen after the test, it can be noticed that the specimen experienced shear/flexure failure, not at the beam, as in the case of element "S 1, V.D", but at the joint.

This specimen provided a considerable amount of the total deformability,  $D= 7.3\text{cm}$ .

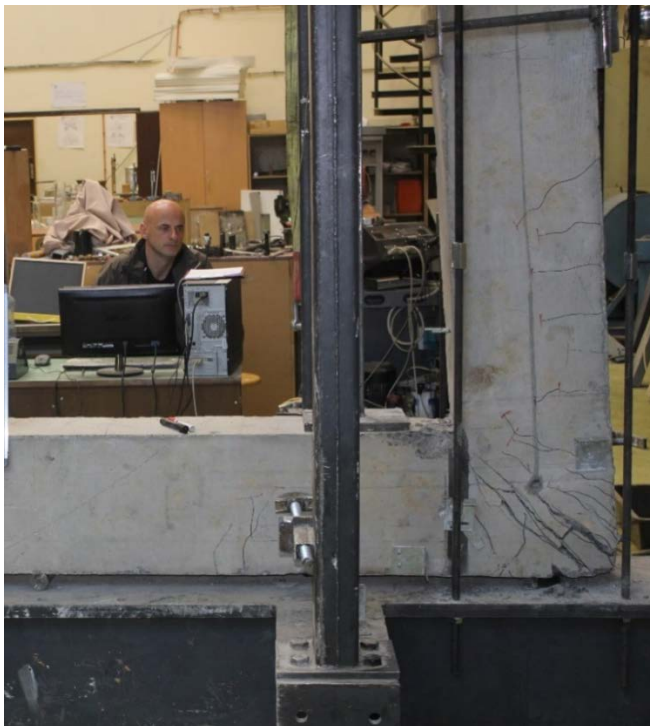




Fig. 4.55 Photos after the last loading cycle applied on specimen "S.5 H.D."

#### 4.6.6 Specimen "S 6, V.D."

This experiment was performed on the specimen with vertical dowels (VD) in the case when the connection was performed by grout only, the same as experiment "S 2, V.D.", with the only difference being that, in this experiment, the M/V ratio at the connection level was 1.5. The experimental results are given in figs. 4.56-4.58.

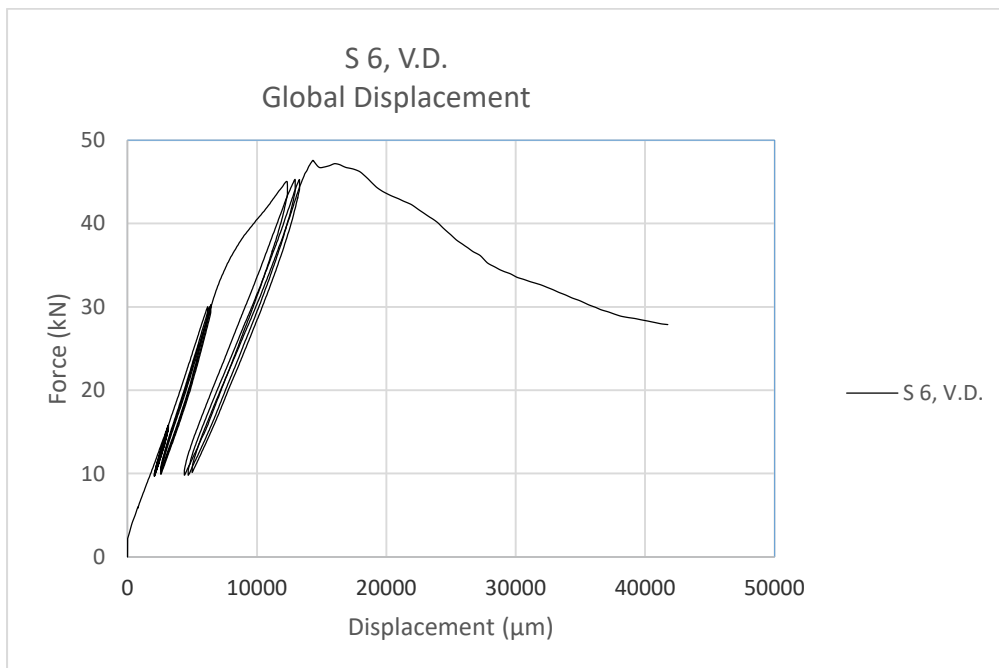


Fig. 4.56 F-D diagram of global displacement of specimen "S.6 V.D."



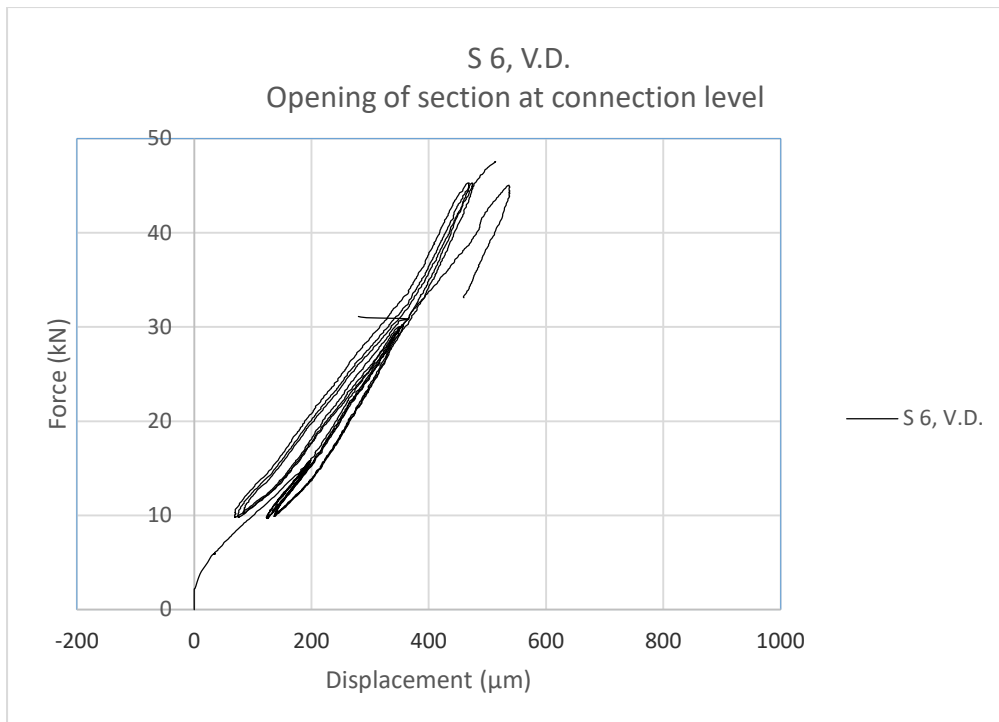


Fig. 4.57 F-D diagram referring to the connection level of specimen "S.6 V.D."

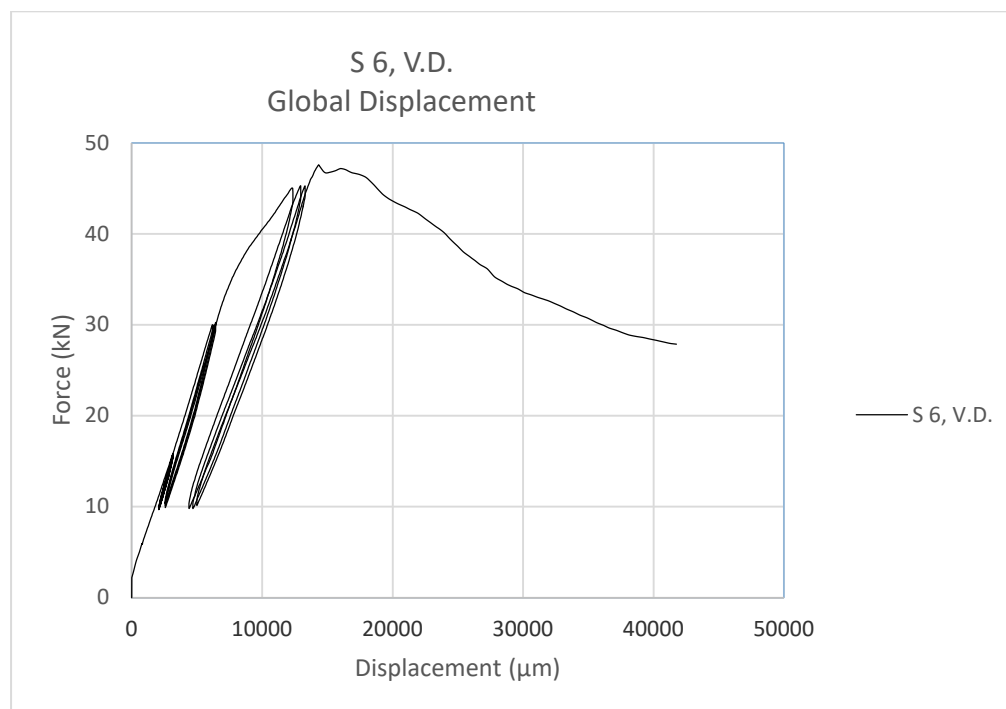


Fig. 4.58 F-D diagram referring to the monolithic part of the joint (beam phase) of specimen "S.6 V.D."

The measurements from LVDT 4 are not available since this LVDT was displaced during the first steps of the experiment.

#### 4.6.6.1 Description of the specimen performance

Fig. 4.59 shows the crack pattern after the last loading cycle.

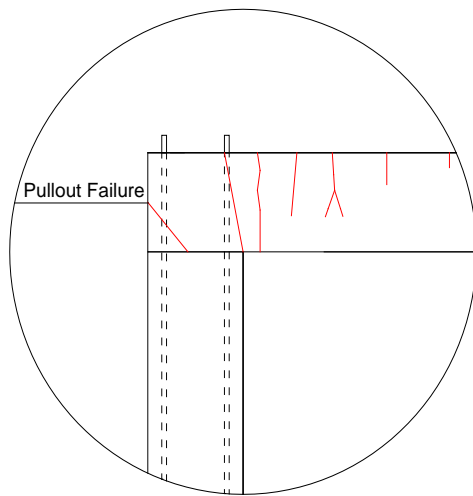


Fig. 4.59 Crack pattern of specimen "S.6 V.D."

During the first loading cycle, the specimen started to experience flexural performance. This can be best identified from the cracking pattern presented in fig.4.60 which, for better presentation, is figuratively illustrated in fig. 4.59

At the fourth loading cycle, at a load level of 46kN, the joint of the specimen experienced shear failure due to pullout of the dowels. This crack is presented in fig. 4.59, but is also detectable in the F-D diagram of global displacement, (fig 4.56).

After inspecting the specimen, it was noticed that the dowels (the dowels in tension) were eccentrically positioned within the sleeve, (fig. 4.61). Due to this, the thickness of the grout on that side of the dowel was smaller than the minimum required (1.25cm) and did not provide full anchorage.

Therefore, the full length/perimeter of the dowels was not fully active against pullout, which caused lower anchorage strength.

The total deformability of the specimen "S6, V.D." was  $D= 2.4\text{cm}$ .



Fig. 4.60 Photo taken after the last loading cycle applied on specimen "S.6 V.D."

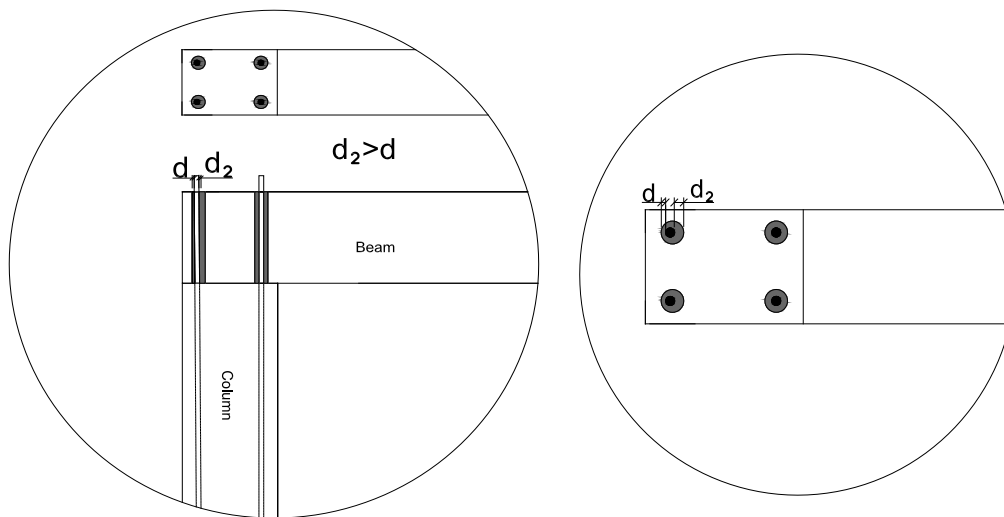


Fig. 4.61 Eccentric position of the dowels in the sleeve of specimen "S.6 V.D."

#### 4.6.7 Specimen "S 7, V.D."

This experiment was performed on the specimen with vertical connections/dowels strengthened by a large steel plate.

The experimental results are presented in figs. 4.62-4.65.

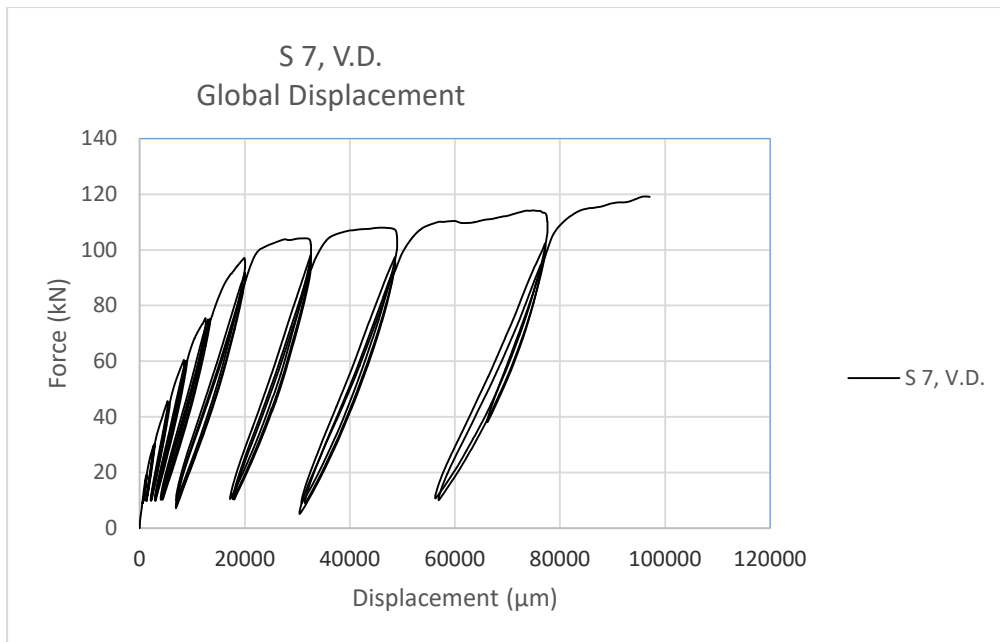


Fig. 4.62 F-D diagram of global displacement of specimen "S.7 V.D."

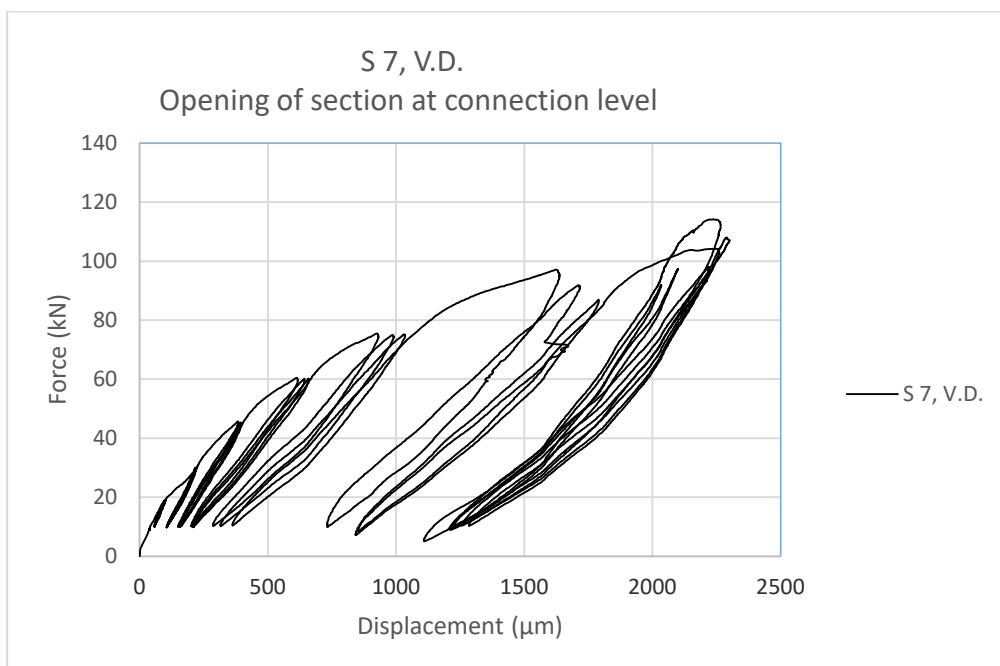


Fig. 4.63 F-D diagram referring to the connection level of specimen "S.7 V.D."

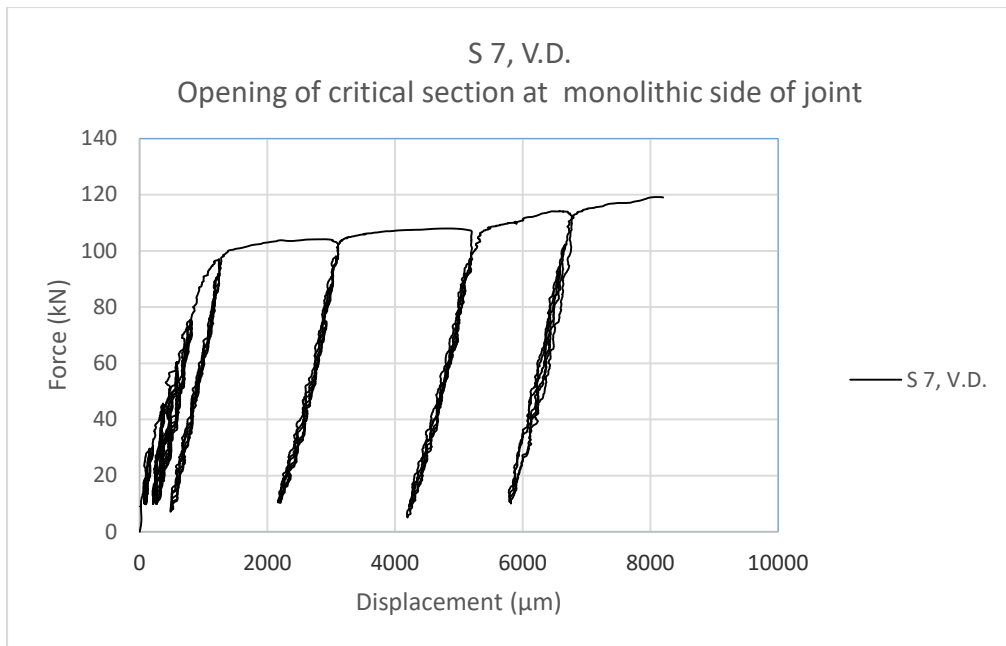


Fig. 4.64 F-D diagram referring to the monolithic part of the joint (column face) of specimen "S.7 V.D."

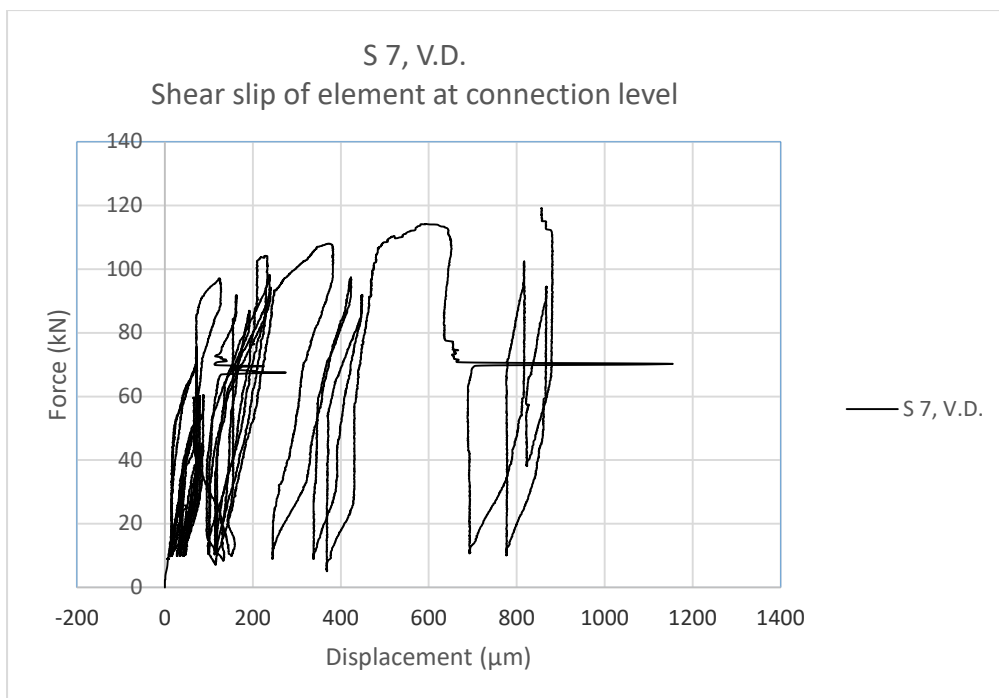


Fig. 4.65 F-D diagram of shear slip of the connection of specimen "S.7 V.D."

#### 4.6.7.1 Description of the specimen performance

Fig. 4.66 shows the main crack after the last loading cycle.

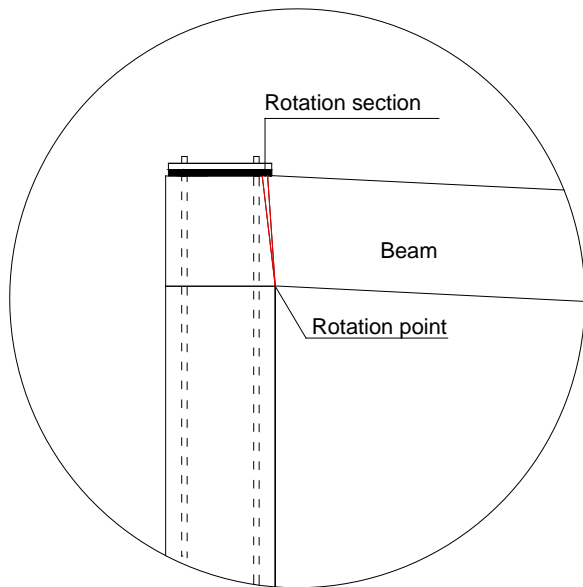


Fig. 4.66 Main crack after the last loading cycle applied on specimen "S.7 V.D."

With the application of a large plate as a strengthening element, the unfavorable failure modes of the specimen with precast connections with grout only and failure modes of the specimens strengthened by individual steel plates were eliminated.

The performance of the specimen was of a typical flexural performance type. This is evident from the F-D diagram (fig 4.62) and the crack formation presented in fig. 4.67.

From observing the F-D diagram at the connection level, (fig 4.63), and the critical section at the monolithic part of the joint, (fig. 4.64), it can be noticed that both sections reached the yielding point at a force of 96kN. However, with further increase of the load, the deformation was concentrated in the monolithic section (beam face) (fig. 4.62 and fig. 4.64) and this section governed the behavior of the specimen.

The total capacity of the specimen and the bearing capacity of the sections was not achieved due to the limitations of the testing equipment (10cm was the limit of the LVDT and the available free stroke of the actuator).

The yielding point of the specimen could be considered to have taken place at the force of 98kN, respectively, for the monolithic part of the joint face -  $M_y=105\text{kNm}$ , whereas for the precast connection -  $M_y=96\text{kNm}$ .

Due to the limitations mentioned above, the total deformability of the specimen could not be explored, but it could be concluded that total deformability was over  $D>10\text{cm}$ .



Fig. 4.67 Photos of the specimen after the last loading cycle applied on specimen "S.7 V.D."

#### 4.6.8 Specimen "S 8,H.D."

This experiment was performed on the specimen with precast connection conducted by horizontal dowels strengthened by a large steel plate.

The measured results are presented in fig. 4.68-4.70.

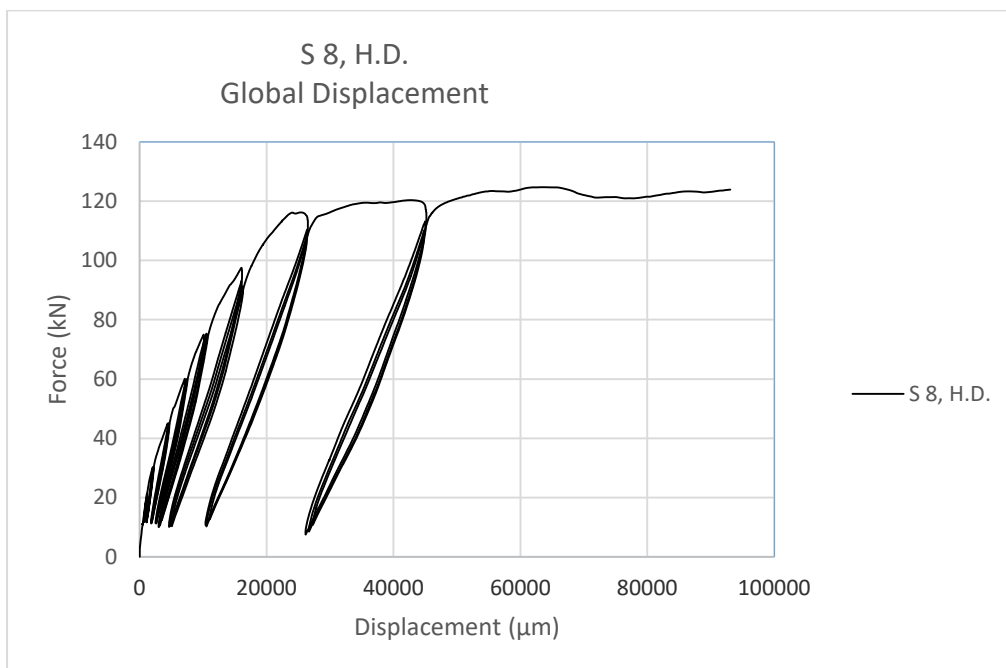


Fig. 4.68 F-D diagram of global displacement of specimen "S.8 H.D."

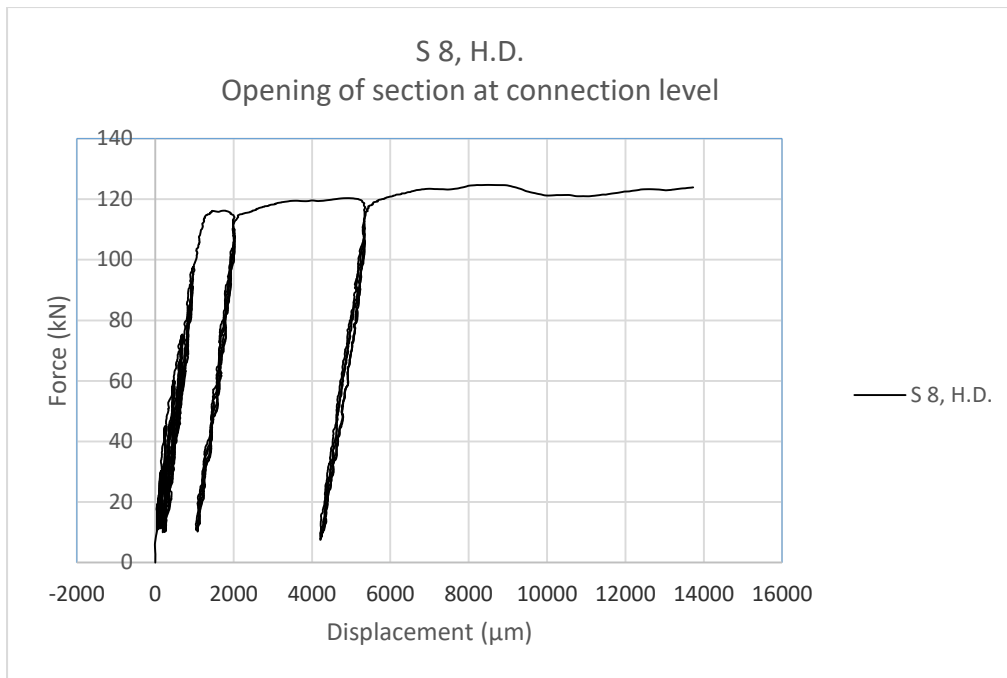


Fig. 4.69 F-D diagram referring to the connection level of specimen "S.8 H.D."

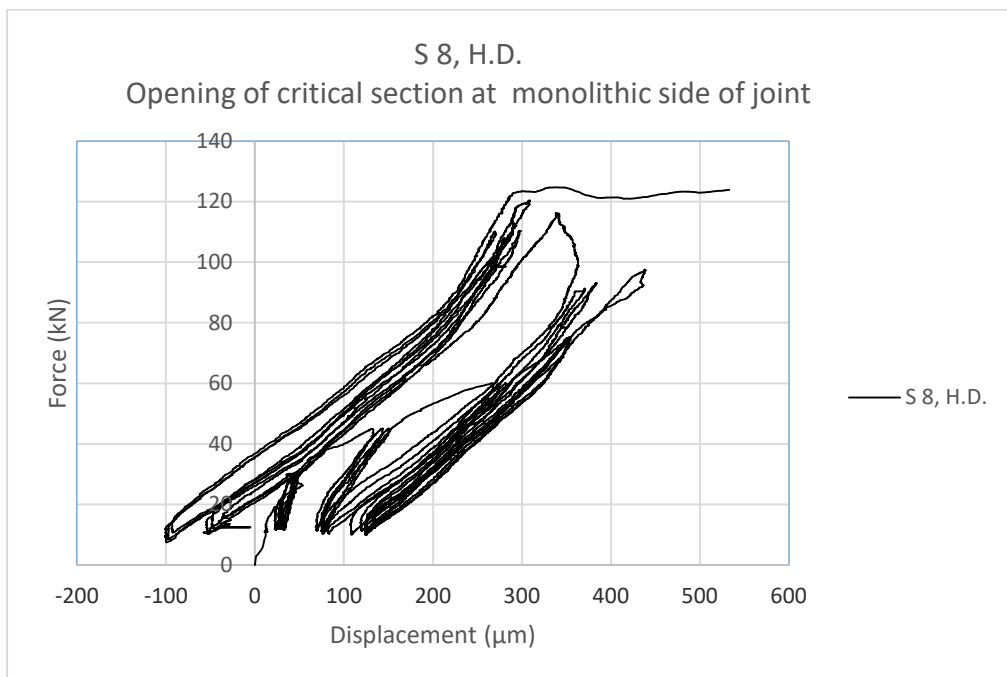


Fig. 4.70 F-D diagram referring to the monolithic part of the joint (column face) of specimen "S.8 H.D."

#### 4.6.8.1 Description of the specimen performance

The performance of the specimen was of a typical flexural performance type. This is evident from the F-D diagram of global displacement, (fig 4.68), and from observing the behavior of the element during the experiment (crack pattern as well as failure mode, figs. 4.71 and 4.72).

Even though the global and ultimate behavior of the specimen was to be considered as flexural behavior, shear cracks from dowel pullout were formed in the joint during the experiment. This was



because, in order that the force from the dowels be transferred to the plate, first, the bonding between the dowel and the grout had to fail and only then the force started to be sustained by the plate. During the loading process, while the bonding was active due to the pullout force, these cracks appeared in the joint.

The yielding point of the specimen could be considered to have taken place at the force of 115kN, respectively, the flexural strength at yielding point was  $M_y=115\text{kNm}$  at the critical section, the joint face.

The ultimate strength of the specimen could be considered to have taken place at the force of  $F=124\text{kN}$ , respectively, the ultimate flexural strength of the section was  $M=124\text{kNm}$ .

At the last loading cycle, the dowels failed in tension inside the bolt which was used for tightening the dowel to the strengthening plate, (fig. 4.73). Since reinforcing bars were used for the dowels in order to tighten them to the plate, the bars had to be threaded, which reduced the effective diameter of the dowel from 20mm to 18mm, meaning that the strength of a connection was in function of the tension strength or the reinforcing bar with a diameter of 18mm.

From the behavior of this specimen strengthened with such plate, it was evident that the total strength of the connection depended on the strength of the dowel, which meant that the anchorage strength of the grout (bonding strength) did not have any effect on the connection strength. This is very important since for this strengthening method, the bonding strength is not crucial for the strength of the connection. Therefore, the application of this type of strengthening will avoid any possible defects during anchorage, which proved to be very important in experiment  $M/V=1.5$ , (S6, V.D) in the case of a connection made with grout only. This kind of strengthening will provide full fixity of the connection.

The deformability of this specimen was also very high. The total deformability of this specimen was  $D=9.3\text{cm}$ .

The pattern of the main critical crack is given in fig. 4.71.

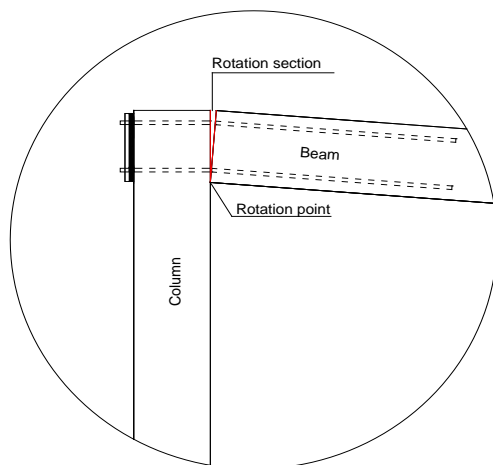


Fig. 4.71. Main critical crack of specimen "S.8 H.D."



Fig. 4.72 Photos of the specimen at the last loading cycle applied on specimen "S.8 H.D."



Fig. 4.73 Failure of the joint after the last cycle applied on specimen "S.8 H.D."

#### 4.6.9 Experiment "S 9,H.D."

This experiment was performed on the specimen with precast connection conducted with horizontal dowels strengthened by a large plate and  $M/V=0.5$  at the precast connection level.

The  $M/V=0.5$  ratio was predefined for the precast section only, whereas for the monolithic side of the joint, the  $M/V$  ratio was left  $M/V=1.0$  in order to eliminate any possibility for the monolithic element to fail in shear, as was the case with specimen "S 1, V.D."

The purpose of this experiment was to test the connection in the case where shear is predominant but also flexure is present, which is realistic for moment resisting (fixed) beam-to-column connections.

The experimental results are given in figs. 4.74-4.77.

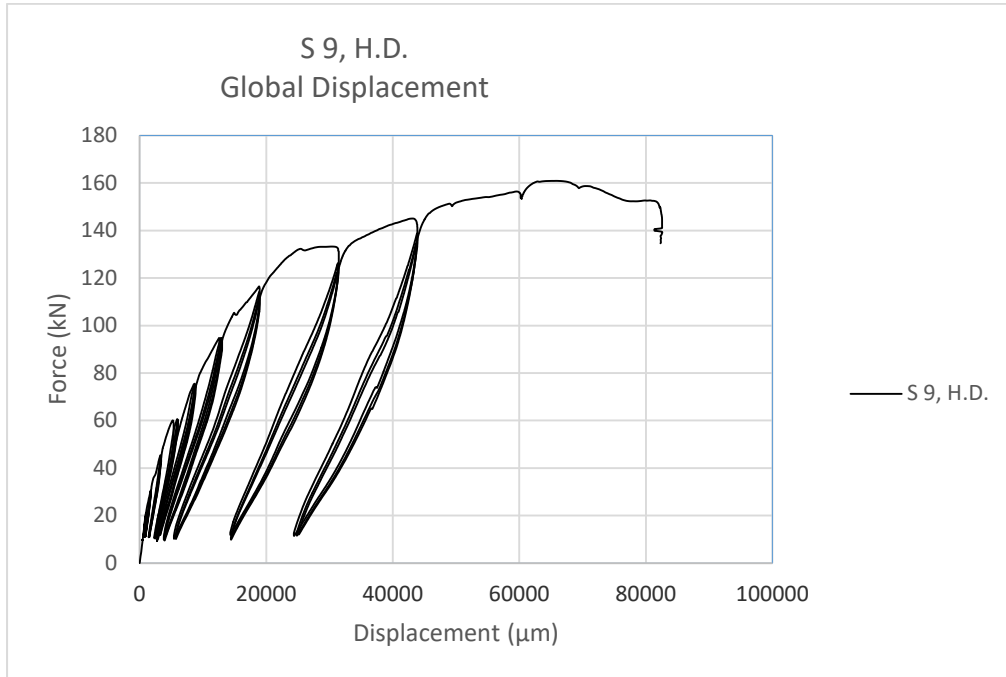


Fig. 4.74 F-D diagram of global displacement of specimen "S.9 H.D."

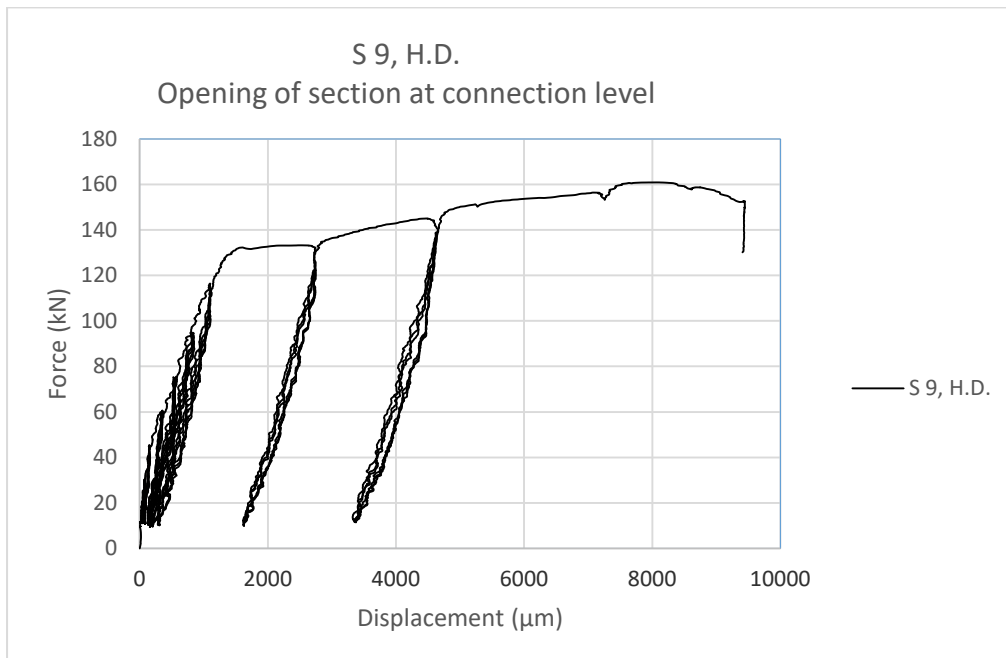


Fig. 4.75 F-D diagram referring to the connection level of specimen "S.9 H.D."

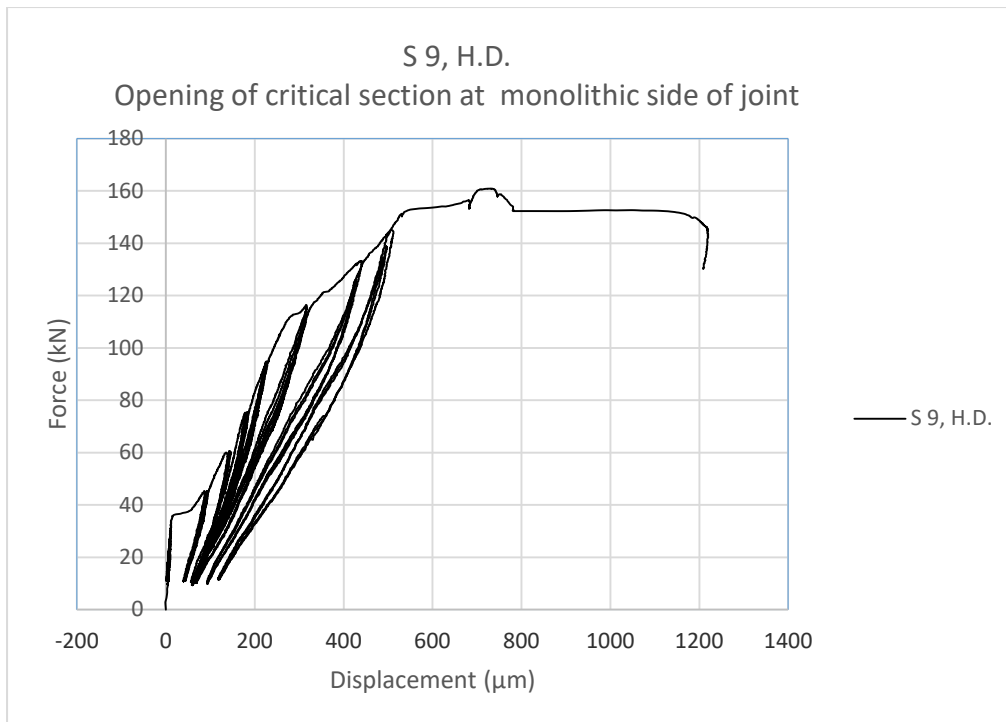


Fig. 4.76 F-D diagram referring to the monolithic part of the joint (column phase) of specimen "S.9 H.D."

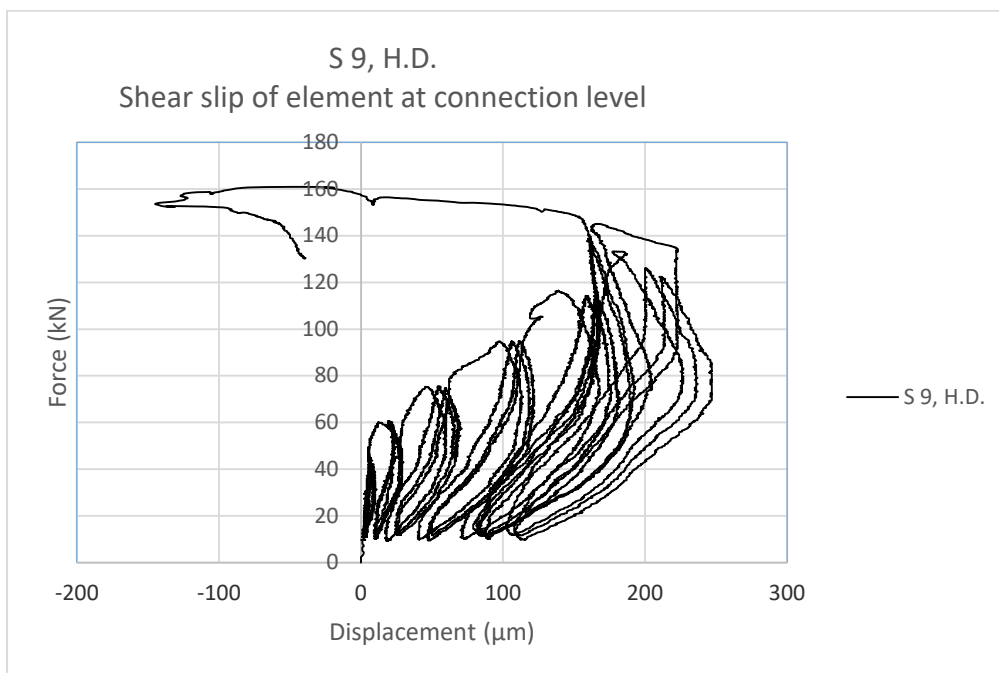


Fig. 4.77 F-D diagram of shear slip of the connection of specimen "S.9 H.D."

#### 4.6.9.1 Description of the specimen performance

Besides the M/V ratio being equal to 0.5, the performance of the specimen was of a typical flexural performance type. This is evident from the crack formation presented in fig. 4.78 and from observing the behavior of the specimen during the experiment (crack pattern as well as failure mode). The behavior of this specimen was almost the same as that of specimen S 8, H.D.

The yielding point of the specimen could be considered to have taken place at the force of 131kN and displacement  $d_y=25\text{mm}$ , respectively, the flexural strength at the yielding point was  $M_y=119\text{ kNm}$  at the critical section, which was a precast section.

The ultimate strength of the specimen could be considered to have taken place at the force of  $F=160\text{kN}$  and displacement  $d_u=65\text{mm}$ , respectively, the ultimate flexural strength of the section was  $M=145\text{ kNm}$ .

The behavior of this specimen was governed mainly by the behavior of the precast section. This can be concluded by analyzing the F-D diagram of global displacement (fig. 4.74) and the F-D diagram of the precast section, (fig. 4.75).

The total deformability of this specimen was  $D=8.2\text{cm}$



*Fig. 4.78 Photo of the specimen after the last loading cycle applied on specimen "S.9 H.D."*

#### **4.6.10 Specimen "S 10, R.M."**

This experiment was performed on the cast-in-situ specimen for  $M/V=0.5$  ratio at the joint face. This experiment was performed to serve as a reference for comparison of the performance with that of "S 9, H.D." specimen.

This experiment was performed with the same boundary conditions as "S 9, H.D." The results from the tests are presented in figs. 4.79-4.80.

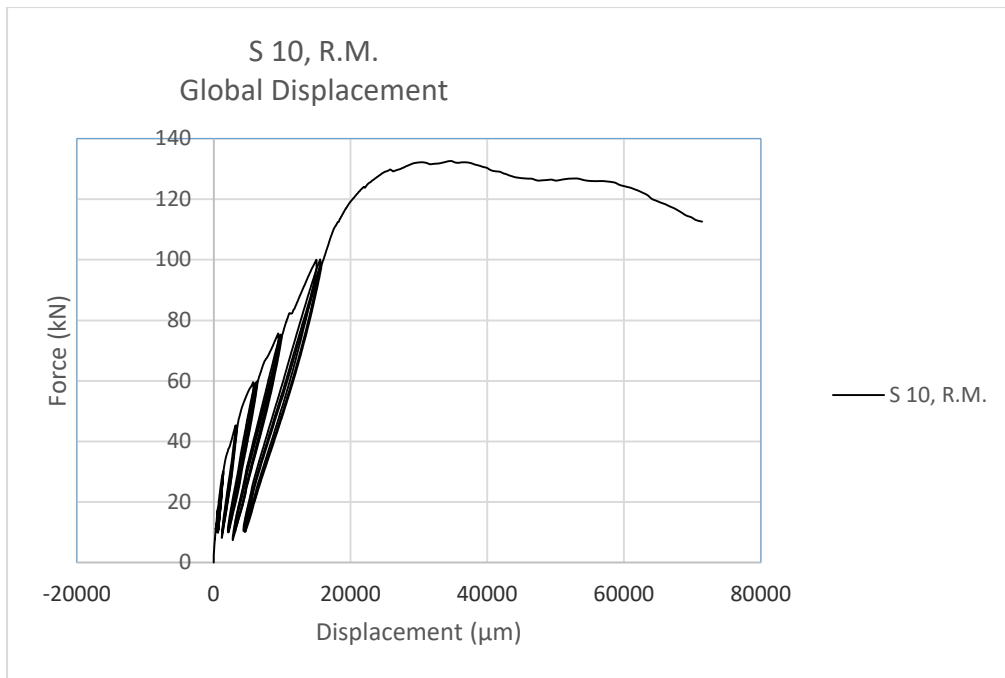


Fig. 4.79 F-D diagram of global displacement of specimen "S.10 R.M."

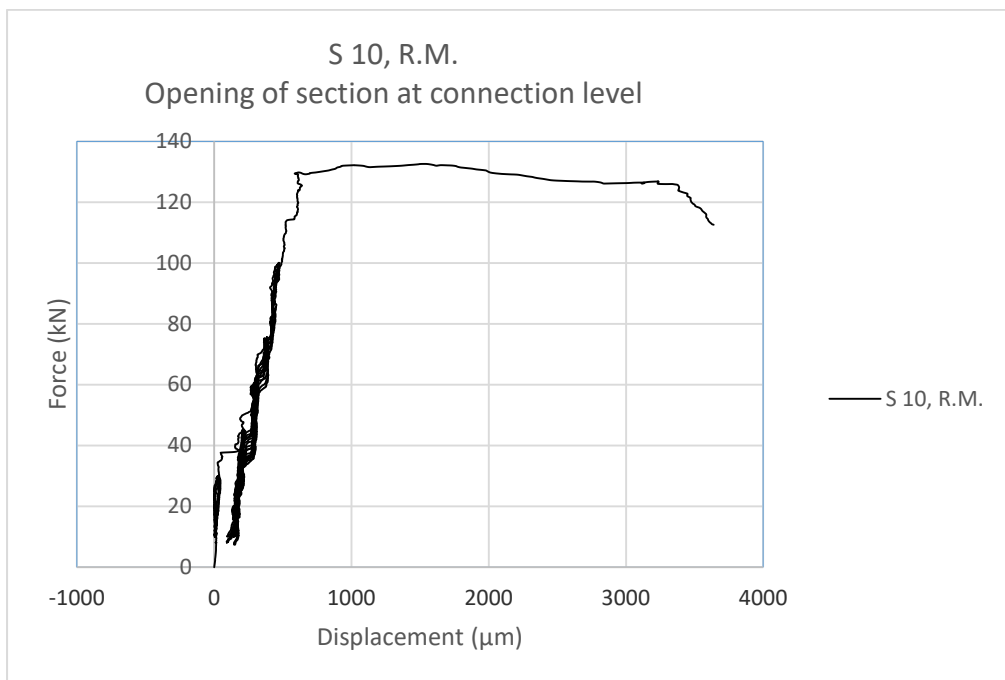


Fig. 4.80 F-D diagram referring to the connection level of specimen "S.10 R.M."

During the experiment, LVDT-s 3 and 4 were displaced by a crack wherefore their readings are not relevant.

#### 4.6.10.1 Description of the specimen performance

The performance of the specimen with M/V ratio 0.5 was of a typical flexural performance type, almost similar to "S 4, R.M" (cast-in-situ specimen with M/V=1.0).

The yielding point of the specimen could be considered to have taken place at the force of 125kN and displacement  $d_y=23\text{mm}$ , respectively the flexural strength at the yielding point was  $M_y=125\text{ kNm}$  at the critical section, which was a precast section.

The ultimate strength of the specimen could be considered to have taken place at the force of  $F=131\text{kN}$  and displacement  $d_u=31\text{mm}$ , respectively the ultimate flexural strength of the section was  $M=132\text{ kNm}$ .

The total deformability of this specimen was  $D=7.2\text{cm}$



Fig. 4.81 Photo of the specimen after the last loading cycle applied on specimen "S.10 R.M."

#### 4.7 Comparison of the performance of the tested specimens

The results obtained during the testing of the specimens were compared as follows:

- The overall behavior of the specimens. The specimens with the same boundary conditions were compared since the boundary conditions have an impact on the F-D relation;
- The total flexural strength of the specimens measured at the critical section;
- The total deformability capacity, elastic and inelastic/ductility.

##### 4.7.1 Comparison of overall performance of the specimens

###### 4.7.1.1 Comparison of specimens "S 2, V.D.", "S 3, V.D.", "S 4, R.M." and "S 7, V.D."

This comparison was performed among specimens constructed with vertical dowels and with:

- cast-in-situ specimen, referent specimen, "S 4, R.M.";
- connection performed by grout only, "S 2, V.D.";

- connection with grout and strengthening of the two tension dowels by an individual steel plate, "S 3, V.D."; and,
  - connection with grout and strengthening of all four dowels by a large steel plate, "S 7, V.D."
  -
- a) **Comparison between the specimen with connection performed by grout only, "S 2, V.D.", and the specimen with strengthening of the tension dowels by individual steel plates, "S 3, V.D."**

Specimen "S 2, V.D." exhibited a pullout/shear behavior, whereas specimen "S 3, V.D." exhibited flexure behavior (fig. 4.82).

Both specimens had the same stiffness, the same yielding strength and the same ultimate strength.

Specimen "S 2, V.D." provided a limited total deformability ( $d=2.4\text{cm}$ ), whereas specimen "S 3, V.D." provided a considerable total deformability ( $d=7.1\text{cm}$ ), respectively around 300% higher than that of specimen "S 2, V.D."

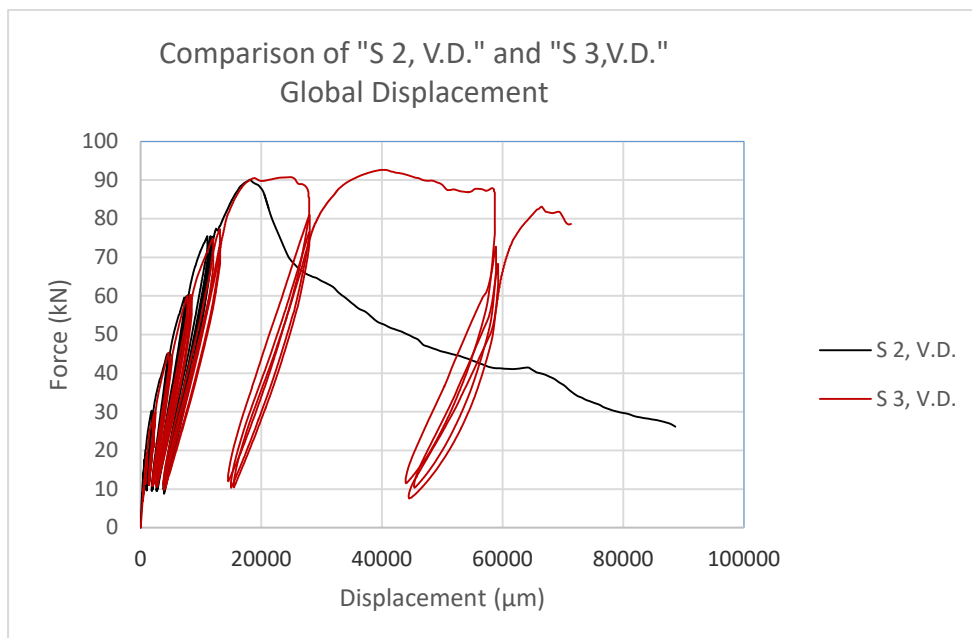


Fig. 4.82 Comparison of global behavior of specimens "S2, V.D." and "S3, V.D."

- b) **Comparison of the specimen with connection performed by grout only, "S 2, V.D." and the strengthened specimen by steel individual plates, "S 3, V.D." with the referent cast-in-situ specimen "S 4, R.M."**

The strength of the precast specimen "S 2, V.D." and the strength of the precast specimen "S 3, V.D." were about 90% of the strength of the referent cast-in-situ specimen, "S 4, R.M." (fig. 4.83).

The elastic stiffness of the precast specimen "S 2, V.D." and of the precast specimen "S 3, V.D." was 80% of that of the referent cast-in-situ specimen, "S 4, R.M.". The reason that the precast element had less elastic stiffness than the referent model was that the position of the dowels within the cross-section was farther from the edge of the section and due to this, the opened gap of the section was larger than that of the referent model. This larger gap created larger global deformations.



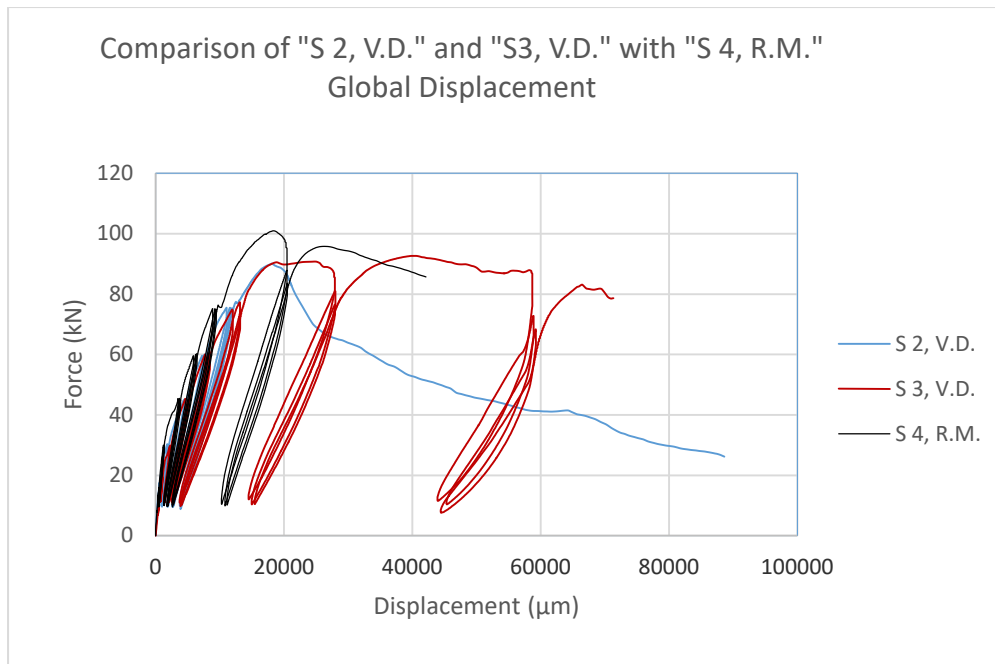


Fig. 4.83 Comparison of global behavior of specimens "S2, V.D." and "S3, V.D." with "S4, R.M."

- c) **Comparison of the specimen with strengthening of tension dowels by individual steel plates, "S 3, V.D." and the specimen strengthened by a large steel plate, "S 7, V.D." with the referent cast-in-situ specimen, "S 4, R.M."**.

Since specimen "S 7, V.D." was not able to be tested to its ultimate capacities due to the limitations of the testing equipment, only the following could be concluded (fig. 4.84):

The strength of specimen strengthened by a large plate, "S 7, V.D.", was:

- over 20% higher than the strength of the referent cast-in-situ model;
- over 30% higher than strength of specimens "S 2, V.D." and "S 3, V.D." performed under the same boundary conditions.

The total deformability of the specimen strengthened by a large plate, "S 7, V.D." was over 10cm, which was over 140% higher than the total deformability of specimen "S 3, V.D." performed under the same boundary conditions.

The initial/elastic stiffness of the specimen with precast connection "S 7, V.D." was the same as that of the other two specimens with precast connections, "S 2, V.D." and "S 3, V.D."

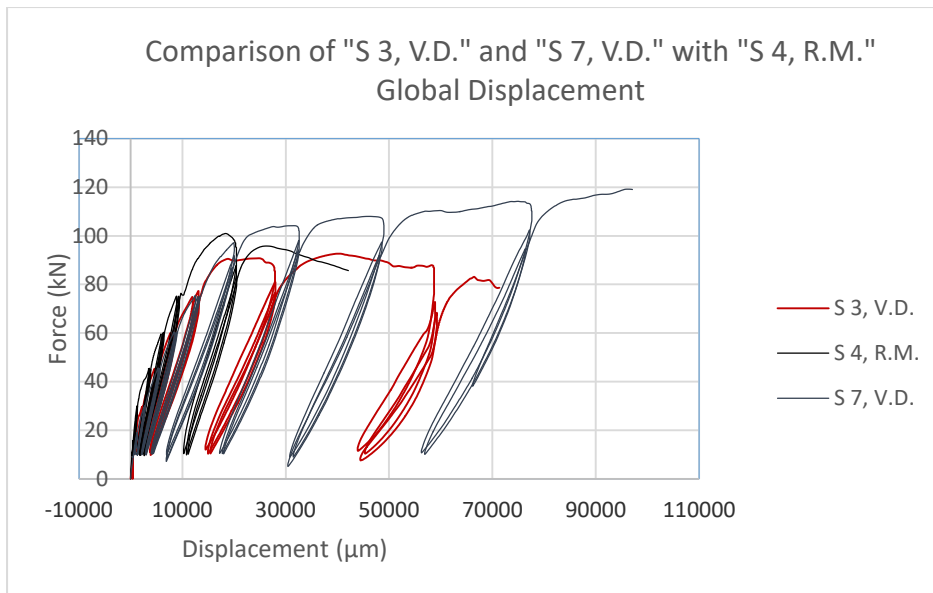


Fig. 4.84 Comparison of global behavior of specimens "S3, V.D." and "S7, V.D." with "S4, R.M."

#### 4.7.1.2 Comparison of specimens "S 1, V.D.", "S 5, H.D." and "S 8, H.D."

Comparison was done among specimens constructed with:

- connection by grout and with strengthening of the two vertical tension dowels by individual steel plates, "S 1, V.D.";
- connection by grout and strengthening of the two horizontal tension dowels by individual steel plates, "S 5, H.D.";
- connection by grout and strengthening of all four horizontal dowels by a large steel plate, "S 8, H.D."

All these specimens were tested under the same boundary conditions, presented in table 4.3, enabling comparison of their global behavior.

- a) **Comparison between the specimen with the connection with strengthened vertical tension dowels by individual steel plates, "S 1, V.D.", and the specimen with the connection with horizontally positioned dowels strengthened by individual steel plates, "S 5, H.D."**

The beam of specimen "S 1, V.D." experienced shear/flexure failure, but under considerable total deformability, whereas in the case of specimen "S 5, H.D.", the beam experienced a joint shear/flexure failure with limited deformability, fig. 4.85.

Even though the beam of specimen "S 1, V.D." and the column of specimen "S 5, H.D." had the same reinforcement and cross-section properties and forces acting on them, still the performance of these two elements of the specimens was not the same. The beam of specimen "S 1, V.D." experienced shear/flexure failure, whereas the column of "S 5, H.D." experienced flexure behavior.

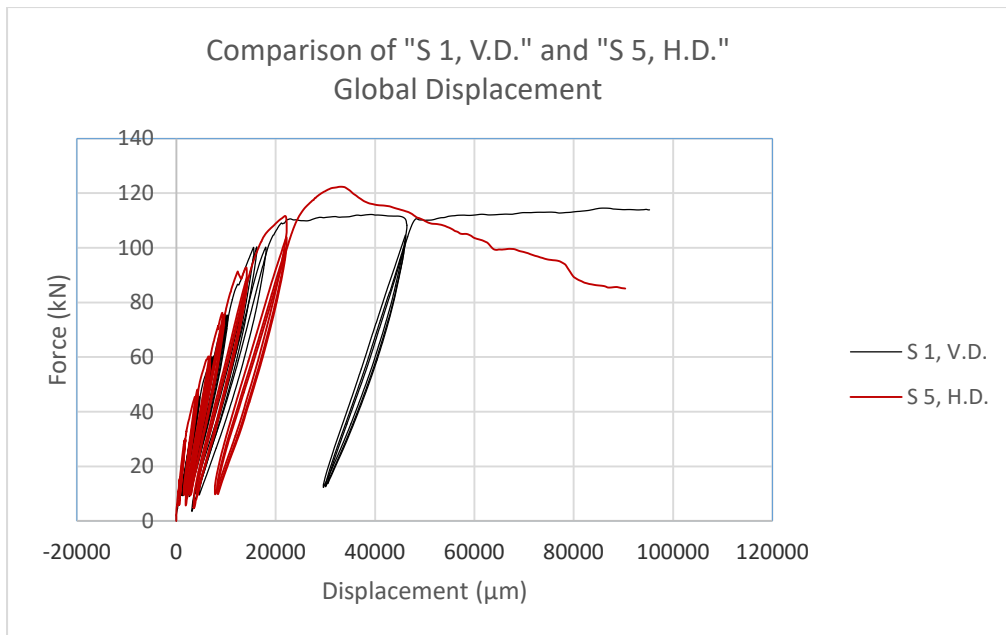


Fig. 4.85 Comparison of global behavior of specimens "S1, V.D." and "S5, H.D."

- b) Comparison between the specimen with connection with two horizontal tension dowels strengthened by an individual plate, "S 5, H.D." and the specimen with horizontal dowels strengthened by a large steel plate, "S 8, H.D."

The strength of the specimen strengthened by a large plate, "S 8, H.D.", was almost the same as that of specimen "S 5, H.D."(fig. 4.86).

The total deformability of the specimen strengthened by a large plate, "S 8, V.D." was  $d=9.3\text{cm}$ , whereas that of specimen "S 5, H.D." was  $d=7.3\text{cm}$ . For comparison, the total deformability of specimen "S 8, V.D." was higher than that of specimen "S 5, H.D." for 1.27.

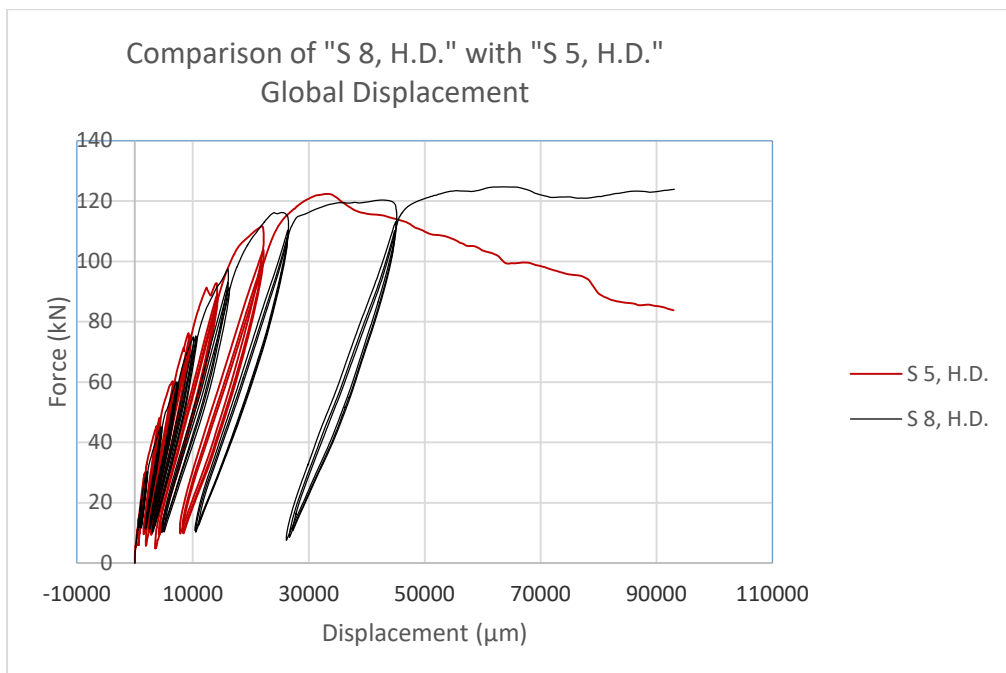


Fig. 4.86 Comparison of global behavior of specimens "S5, H.D." and "S8, H.D."

#### 4.7.1.3 Comparison between specimens "S 9, H.D." and "S 10, R.M."

This comparison was performed between specimens, under  $M/V=0.5$ , constructed with:

- connection with grout and horizontal dowels strengthened by a large steel plate, "S 9, H.D."
- cast-in-situ specimen, referent specimen, "S 10, R.M.",

Specimen "S 10, R.M.", at the critical section, experienced crushing of concrete in compression before the longitudinal reinforcement was loaded to its ultimate strength, wherefore, in addition to no ductility, this specimen provided less ultimate strength.

The strength of the specimen strengthened by a large plate, "S 9, H.D.", was 20% higher than that of the specimen "S 10, R.M."(fig. 4.87).

The total deformability of the specimen strengthened by a large plate, "S 9, H.D." was  $d=8.2\text{cm}$ , whereas that of specimen "S 10, R.M." was  $d=7.2\text{cm}$ . For comparison, the total deformability of specimen "S 8, V.D." was higher than that of specimen "S 5, H.D." for 1.14.

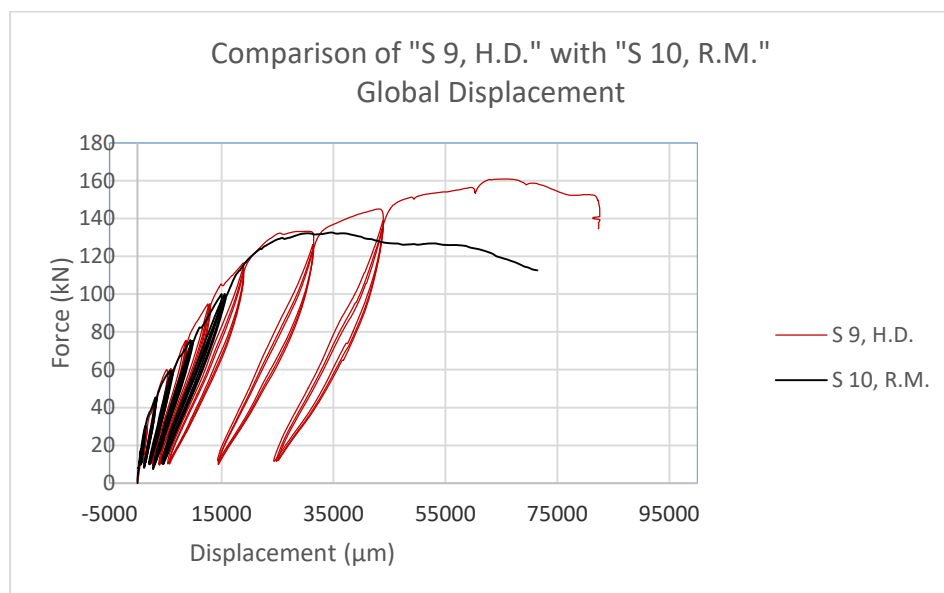


Fig. 4.87 Comparison of global behavior of specimens "S9, H.D." and "S10, R.M."

#### 4.7.2 Summary of the results

For presenting the behavior of the connections the followed parameters were followed:

- Flexural strength of the connection
- Lateral displacement

Since all specimens were not tested under the same boundary conditions, the best way to compare the strength of the specimens, respectively, the precast connection, was to compare their flexural strength rather than the applied force intensity. The flexural strength was calculated by using the forces from the F-D Diagram of global displacement of the specimen and was computed at the respective critical

section. The relations of the reaction forces in regard to the acting force, presented in table 4.2, were used for calculating flexure at the critical section.

Taken as total deformability was the global deformation value of the specimen at the force amounting to 80% of the ultimate force pass the ultimate point.

**The horizontal drift was calculated based on the total deformability and the distance from the axis of the horizontal element to the position global displacement is measured, LVDT 1, which was 142 cm.**

Table 4.4 shows summary of results of all tested specimens, whereas table 4.5 shows the comparison results. The comparison was done between the results of each precast specimen tested in regard to respective cast-in-situ specimen.

Table 4.4. Summary of results, flexural strength (at yielding and ultimate points), total deformability and the lateral displacement of the specimens.

Summary of the results from experiments						
Specimen	M/V Ratio	N/M Ratio	My (kNm')	Mu (kNm')	$\Delta$ (%)	General comments on performance of the connection
S1, V.D.	1	1	100	115	>7	In general the specimen has experienced flexure behavior. The specimen failed outside of the connection in shear/flexure failure mechanism.
S2, V.D.	1	0.77	90	90	1.7	Specimen failed in the connection. Mode of failure is brittle pullout failure
S3, V.D.	1	0.77	90	92	5	In general the specimen has experienced flexure behavior. Specimen failed in the connection. Failure mode is flexure.
S4, R.M.	1	0.77	96	102	3.4	In general the specimen has experienced flexure behavior with limited ductility.
S5, H.D.	1	1	106	122	5.1	In general the specimen has experienced flexure behavior with limited ductility. Specimen failed in the connection. Failure mode is shear/flexure failure.
S6, V.D.	1.5	1	72	72	1.7	Specimen has failed in the connection. The connection has experienced brittle pullout failure. The failure is to be considered as premature due to faults during the construction.
S7, V.D.	1	0.77	95	120	7	The specimen has experienced flexure behavior with high ductility. The specimen has failed outside the connection, therefore the connection is considered with the strength of cast in situ.
S8, H.D.	1	1	118	124	6.5	The specimen has experienced flexure behavior with high ductility. The specimen has failed outside the connection, therefore the connection is considered with the strength of cast in situ.
S9, H.D.	0.5	1.7	121	145	5.7	The specimen has experienced flexure behavior with high ductility. The specimen has failed outside the connection, therefore the connection is considered with the strength of cast in situ. Hi shear force did not have impact on inducing shear failure.
S10, R.M.	0.5	1.7	125	132	5.1	In general the specimen has experienced flexure behavior with limited ductility.

Table 4.5. Comparison of results of precast connections vs cast-in-situ connection.

Comparison of the results of the precast connection with cast-in-situ reference connections Values presented in percentage in respect to cast-in-situ reference model						
Specimen	M/V Ratio	N/M Ratio	My (kNm')	Mu (kNm')	$\Delta$ (%)	General comments
S1, V.D.	1	1	104%	113%	206%	Overall behavior of the connection can be considered as cast-in-situ connection, in regard to strength and the deformability.
S2, V.D.	1	0.77	94%	88%	50%	The strength of the connection is near to cast-in-situ connection, whereas there is no deformability capacity of the connection.
S3, V.D.	1	0.77	94%	90%	147%	Overall behavior of the connection can be considered as cast-in-situ connection. The strength of a connection is slightly less whereas the deformability capacity is higher than of a cast-in-situ connection.
S5, H.D.	1	1	110%	120%	150%	Overall behavior of the connection can be considered as cast-in-situ connection, in regard to strength and the deformability.
S6, V.D.	1.5	1	75%	70%	47%	The specimen experienced brittle pullout failure. The construction flaws on mis-positioning of the dowels within the sleeve have been noted on the specimen.
S7, V.D.	1	0.77	99%	118%	>206%	Overall behavior of the connection can be considered as cast-in-situ connection, in regard to strength and the deformability.
S8, H.D.	1	1	123%	122%	191%	Overall behavior of the connection can be considered as cast-in-situ connection, in regard to strength and the deformability.
S9, H.D.	0.5	1.7	97%	110%	112%	Overall behavior of the connection can be considered as cast-in-situ connection, in regard to strength and the deformability.

- My, bending moment at yielding point
- Mu, bending moment at ultimate point
- $\Delta$ , total horizontal displacement of the specimen

**Note:**

The yielding point is read from F-D diagram of global displacement by personal judgment. There may be a possibility for other viewer to consider some other point as a yielding point. For the purpose of this research similar approach is followed in all the cases, therefore comparison results could be considered reliable.

## CHAPTER 5 - Numerical modeling of moment resisting beam to column dry connections

### 5.1 Objective

The objective of the investigations presented in this chapter has been to develop a numerical model that can be used in further research programs and most important, to define a modeling procedure that can be used in engineering practice with an acceptable reliability.

For application in practice, considering that practical engineers do not need to have deep knowledge on complicated nonlinear modeling procedures, the ultimate goal has been to develop models that have a great chance to be easily adopted and used by practical engineers. For this reason, the model should be such that it will present, in an acceptable manner, the behavior of the connection, but should also be user friendly.

### 5.2 Challenges in modeling precast beam-to-column connections and possible options

Each precast connection, especially moment resisting beam-to-column precast connection, is independently unique.

To achieve fixity at monolithic elements, there is only one requirement, which is respecting the reinforcement lap splices. For this reason, for as long as this requirement is met, monolithic connections are easily generalized, which means that an adopted principle of any kind in one case can be applied in all cases with an acceptable reliability.

In moment resisting beam-to-column connections, especially dry connections, from previous experimental research on behavior of such connections and from the observation of the behavior of the connections tested under this thesis, presented in Chapter 4, it is evident and it can be concluded that:

- a) Moment resisting beam-to-column connections are very specific connections and their realization can be performed in many different ways. This makes each individual connection specific and with unique behavior.
- b) Achieving moment resisting beam-to-column dry connections requires application of additional construction procedures and materials for strengthening purposes, where each developed connection proposal requires the use and application of unique elements and materials. For this reason, the behavior of beam-to-column moment resisting dry connections is complex, involving joint and simultaneous behavior of each element taking part in the connection, such as the concrete element, the reinforcement of the element within the part of the joint, the dowels implemented in the connections, the sleeve composition tying the dowels with the concrete element, and any adopted strengthening/improving element.

Since there are many ways of achieving moment resisting beam to column dry connections (subject to design innovation), each connection design has its own specificities so that the general approach that is used for monolithic connections cannot be applied to precast dry connections. This implies that a modeling procedure to be applied in all cases cannot be established, wherefore the development of each connection requires unique modeling procedures and parameters.



To model the behavior of any connection, including also moment resisting beam-to-column connections, there are currently two available general options:

- a) Macro-modeling, and
- b) Micro-modeling

### **5.2.1 Application of macro-modelling for beam-to-column moment resisting connections**

The procedure for application of macro-modelling to beam-to-column connections is the same as the one presented in Chapter 3 which means that two precast elements, beam and column, will be connected with non-linear link elements. For moments resisting connections, the displacement in both directions of the link element would be restricted whereas the behavior of the connection would be determined by applying a hysteretic model to the rotation degree of freedom.

This method is very simple to be used and could provide very satisfactory results for each individual connection.

However, since each connection is unique, the modelling parameters for one connection cannot be applied for another connection.

This fact has its own positive and negative sides.

- The positive side is that the calibrated parameters of the model can be used, with high reliability, for modeling structures where that specific connection is used;
- The negative side is that there is no way of determining, even preliminarily, the parameters of a connection which has not been tested before. An additional negative side is that the behavior of moment resisting precast connections depends on the behavior of each constitutive element of the connection and with macro-modeling, there is no way of presenting the behavior of each element.

This negative side of macro-modeling, especially in industrial buildings where the structures have one span, has no specific practical use. The reason for this is that each designed connection is unique and in order to know the behavior of the connection, an experimental program has to be performed. Once the experimental program is performed, we can use the experimental data to obtain the behavior of the connection (maximum capacity and degree of fixity), which for practical design purposes, is sufficient to design a structure by applying linear elastic analysis only.

Considering the above mentioned, it can be concluded that macro-modeling of precast connections is not something that can have a wide range of application.

### **5.2.2 Application of micro -modelling for beam-to-column moment resisting connections**

Micro-modeling with 3D finite element is a modeling approach that has recently begun to be widely used, especially in mechanical engineering connections since through micro-modeling, there is a possibility to follow the stress and deformation including the failure mechanism of each of the elements that constitute a connection.

Since moment resisting beam-to-column connection is a connection that is composed of many elements and factors, such a connection can easily be considered as a “mechanical connection” and as such, an approach to modeling of mechanical connection is appropriate to be applied here.

Ability to follow stress distribution over the elements composing the connection can be a very good indication of the possible behavior of each specific moment resisting beam-to-column connection by observing the behavior (stress distribution) of each element constituting the connection.

In this way, application of micro-modeling can be useful in research programs where, prior to conducting an experiment, a researcher may have an indicative information on the possible behavior of the designed connection and make potential improvement and strengthening before even the experiment is performed. In such a situation, a researcher can exclude from testing, connections with no promising outcome and focus on the ones with a high potential. Micro-modeling can also be applied in everyday engineering practice for obtaining the potential behavior of modifications of the already tested connections (if the number of dowels is changed, or the type or size of dowels is changed, other specific material is used for grouting, additional strengthening elements are changed, etc.) and indicating the behavior of new innovative connections and applying these connections without any previous experimental verification.

### **5.3 Micro-modelling procedure adopted for this research program**

As indicated in article 1 of this chapter, the ultimate goal of this research program in regard to modeling has been to identify a modeling procedure that will provide satisfactory results and, at the same time, be reasonable in respect to simplicity of use so that it can be applied by the wide engineering community.

Considering the complexity of the moment resisting beam-to-column connections and the importance of having, as an output result, the stress distribution on the connection and on each element of a connection (concrete, reinforcement, dowels, gout sleeve), Abaqus V14 has been used for developing micro-modeling of moment resisting beam-to-column connection.

The reason for using this software has been:

- a) It is widely used in different fields of engineering especially in mechanical engineering, including also structural engineering;
- b) It has a friendly users' interface for modeling preparing and output results reading;
- c) There are tutorials available for application of such software, which makes it easy to be learned and applied by the engineering community;

- d) It contains many analysis and output choices which can provide many kinds of results needed for practical use;
- e) The results obtained by Abaqus in many engineering fields are of a high reliability, including structural engineering; and,
- f) It is developed such that it will allow building up a connection in the same way as it has been constructed, by applying all materials and elements as used for constructing the connection.

### **5.3.1 Procedure of modeling specimens in Abaqus [Ref.: 001]**

The modeling procedure in Abaqus is performed in such a way as to reflect, to the best possible extent, the real situation in regard to material properties as well as connection elements interaction.

Since the connections studied have been composed of more than two elements, and since the behavior of the connection is in direct dependence on the interaction between the elements, the model in Abaqus has been prepared and the elements have been connected with each other in the same pattern as in the real situation.

#### **a) Connection assembly approach adopted**

In principle, there are many ways of preparing a model, bringing together all elements and specifying their interaction. For this research, the following approach has been used:

- Each element, beam and column, is initially modeled as a volume independent element, fig. 5.1;
- Reinforcement of each element is modeled as line elements, including stirrups, which are lined with an axis of longitudinal reinforcement, creating, in this way, a “mini frame” structure, fig. 5.2. Further, this “mini frame” is then embedded in the concrete element where the concrete elements are defined as a host element. This is the best way to ensure proper steel reinforcement and concrete interaction;
- The dowels, part of which, in the real case, are concreted in the column, are embedded in the column, the same as the reinforcement;
- As to the beam element, sleeves are preserved by creating a hole in the elements, with the same dimensions as in the real scenario.

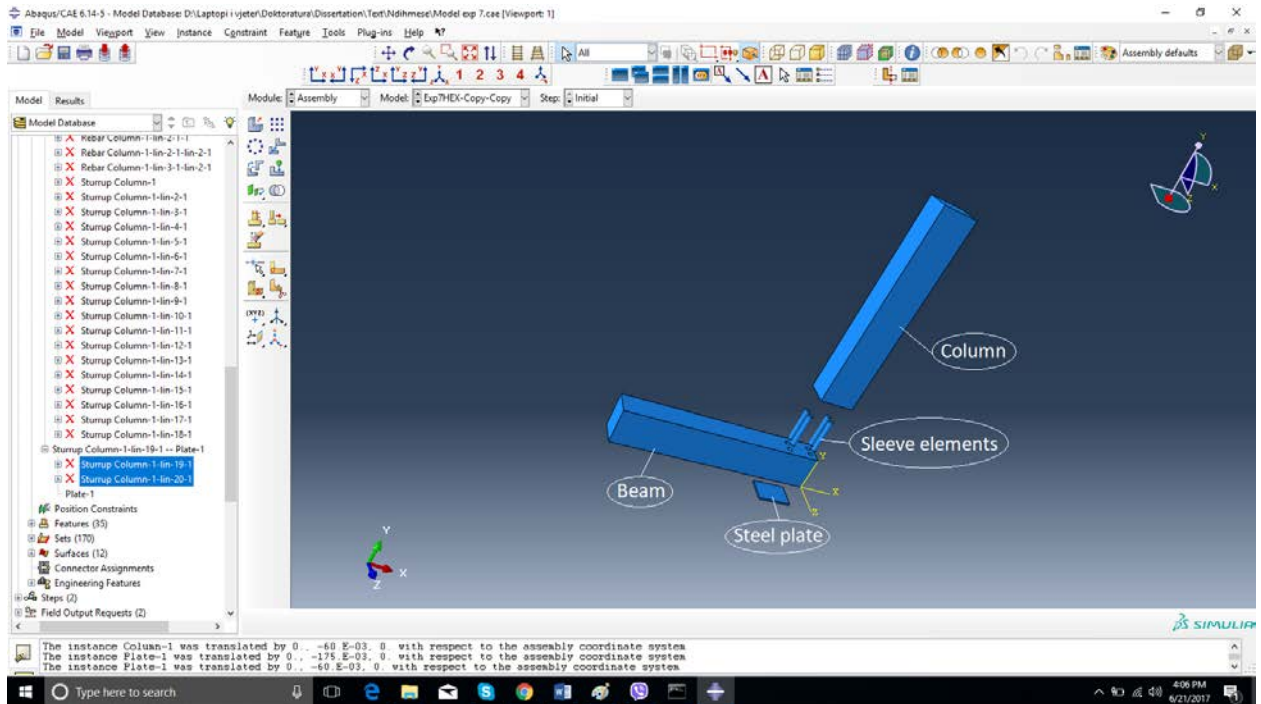


Fig. 5.1 Presentation of independent elements, column, beam, steel plate and sleeve elements for composing the model.

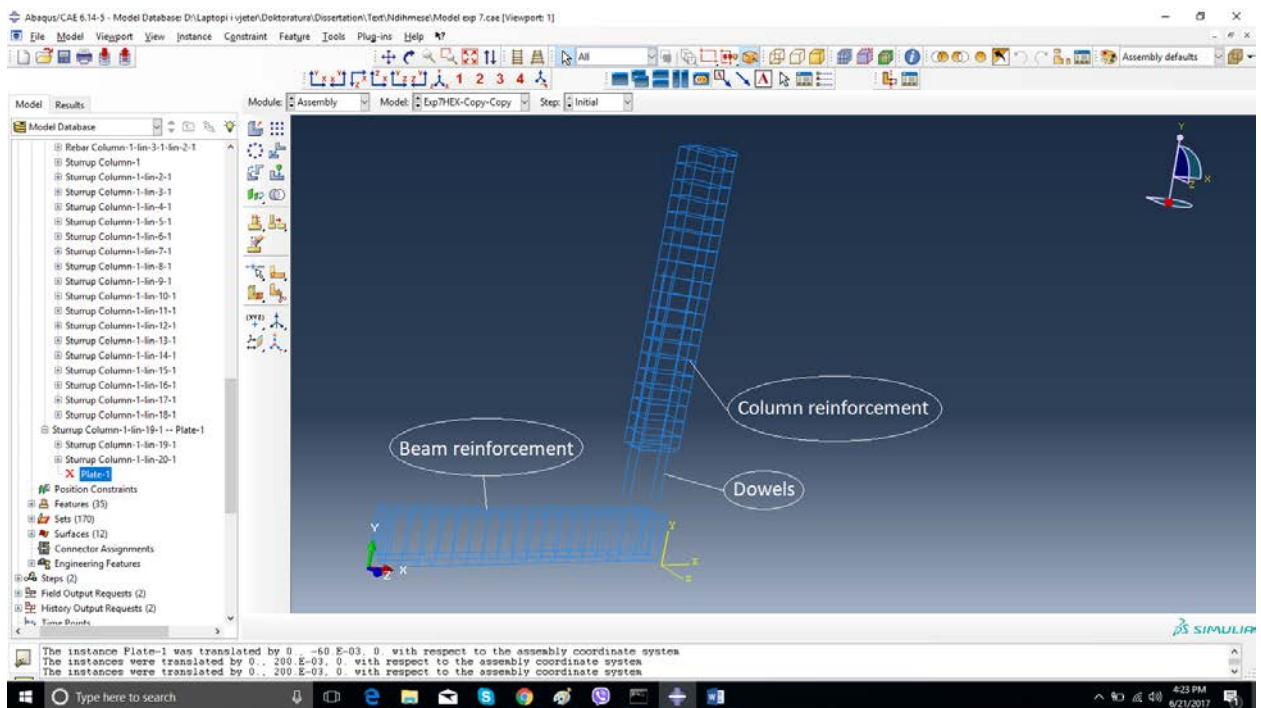


Fig. 5.2 Presentation of reinforcement assembling.

The main challenge in developing the model in the way to best reflect the real scenario has been proper connections of dowels, sleeve, column, beam and strengthening plates. During the development of the models, few options have been tried and the option that has been analyzed successfully and has also provided the best results has been the following:

- The cement grout that is used to fill the sleeve in the real scenario is modeled as a separate element, the “sleeve element in the model”, fig. 5.1;
- In the real scenario, the connection of the column with the beam is done through a dowel in the way that, in one part, the dowels are concreted inside the column where, with the beam, the dowels are connected through the cement grout of the sleeve. For the model, the following has been adopted:
  - o The “sleeve elements” are merged with the columns creating one element, fig. 5.3. In this way, when the dowels are embedded in the concrete element, they are also embedded in the sleeve element. In this way, the dowel-sleeve connection is solved.
  - o Sleeve elements are tied with a surface tie mechanism enabled by the “surface-to-surface tie” software. Since, in the real scenario, all precautions are taken to ensure full connection of the cement grout with the concrete beam element, the “surface-to-surface” connection is modeled as a full connection, with no limitations nor constraints.
- For the models strengthened with steel plates, where in the real scenario, the steel plates are tied with dowels only through bolts, for the model, the following has been adopted.
  - o Initially, the steel elements are merged with the beam elements, since no other way is enabled by the software, fig. 5.4. This merge cannot have any negative impact since, in the real scenario, the plates are loaded in tension where, even if they are to be concreted inside the beam element, the overall behavior of the connection will be the same.
  - o Finally, the dowels are connected with the plate by the point-to-surface tie method, which is enabled by the software. Since, in the real scenario, the connection of these elements is done by bolts, ensuring full connection, in the model, the tie connection is performed also as a full connection, with no limitation nor constraints.

The above steps constituted the full model in Abaqus, fig. 5.5

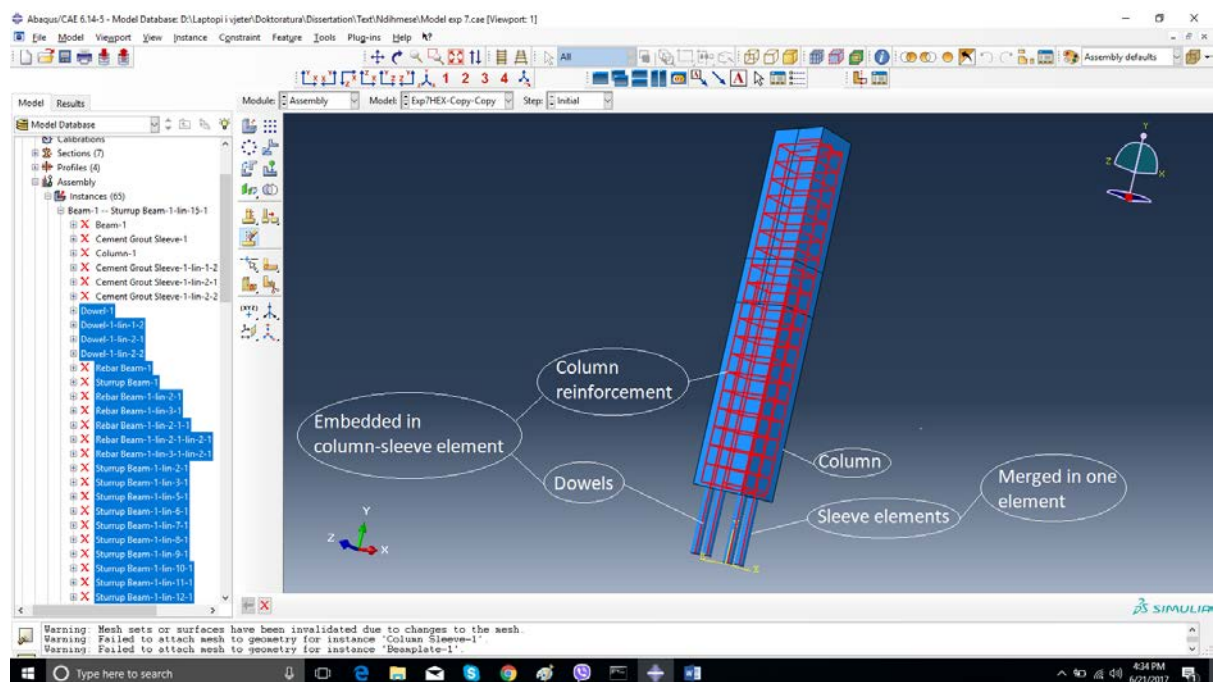


Fig. 5.3 Graphic presentation of assembling column, sleeve elements, column reinforcement and dowels.

# Doctoral Dissertation: Performance of innovative beam-to-column connections in precast industrial buildings

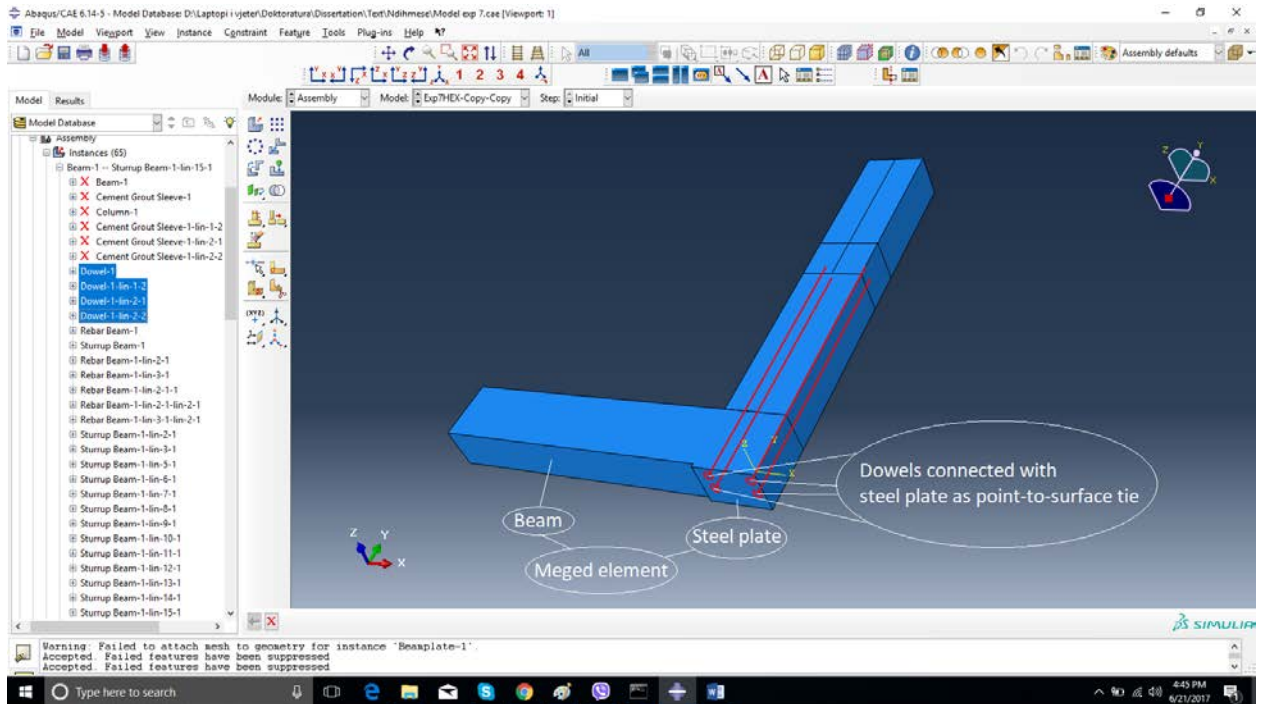


Fig. 5.4 Graphic presentation of assembling beam, steel plate, and their connection with dowels.

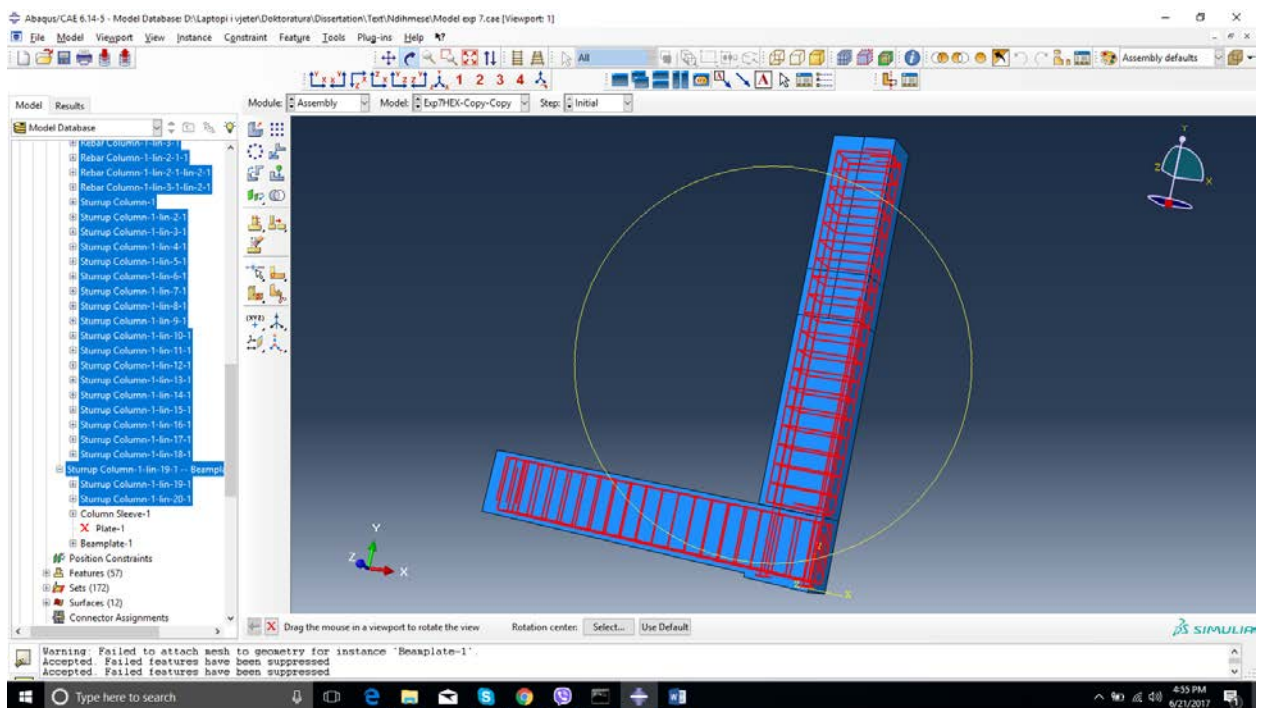


Fig. 5.5 Graphic presentation of the complete assembled model, the column-sleeve element and the beam-plate element are presented in blue color, while the steel reinforcement rebar and the dowels are presented in red color.

**b) Material properties input data**

For the dynamic explicit analysis and the option chosen for running the analysis, the following material properties have been entered as input data:

- The concrete elements, beam and column have been modelled to have the following properties:
  - o Density..... 24 kN/m<sup>3</sup>
  - o Concrete yield strength 35MPa
  - o Concrete tensile strength 3.2MPa
  - o Young’s Module..... 20 GPa
  - o Concrete Damage Plasticity parameters
    - Dilatation angle ..... 37
    - Eccentricity..... 0.1
    - Ratio  $f_{b_0}/f_{c_0}$ ..... 1.16
    - K.....

Where,

$f_{b_0}$  – initial biaxial compressive yield stress

$f_{c_0}$  – initial uniaxial compressive yield stress

K - ratio of the second stress invariant on the tensile meridian to compressive meridian at initial yield with default value of 2/3 (Abaqus User Manual, 2008). This material has been defined based on full triaxial test of concrete.

- Reinforcement steel including the dowels:
  - o Density..... 78 kN/m<sup>3</sup>
  - o Yield strength..... 500MPa
  - o Ultimate strength..... 560MPa
  - o Young’s Module..... 200 GPa
  - o Plastic strain..... 0.12
  
- Cement grout for sleeve element:
  - o Density..... 21 kN/m<sup>3</sup>
  - o Compressive strength..... 60MPa
  - o Tensile strength..... 8MPa
  - o Young’s Module..... 40 GPa

**5.4 Theoretical background of features of applied model [Ref.:002], [Ref.:003]**

The elements composing connection are used in the following formulation:

- Reinforced concrete elements (column and beam), sleeve element and the steel reinforcing plates are adopted as “SOLID, Homogeneous” elements. In the fig. 5.6 is presented print screen shot of the modeling of the beam with respective assignment.

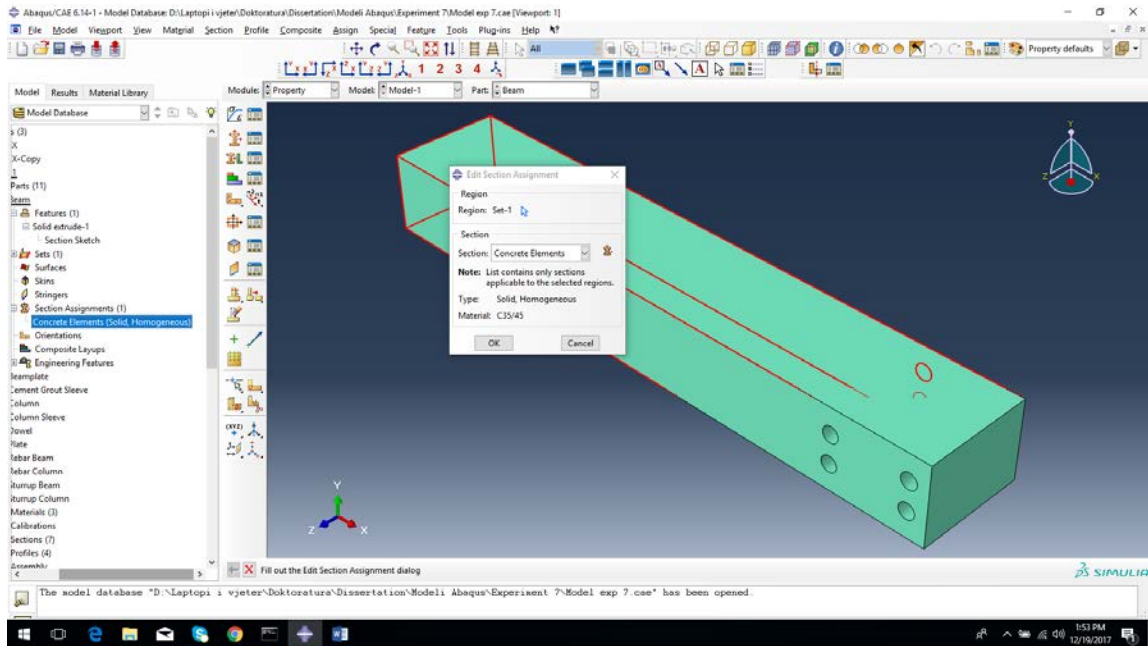


Fig. 5.6. Print screen shot of the modeling of the beam element.

- The reinforcements of the elements and the dowels are adopted as “BEAM” elements, fig. 5.7.

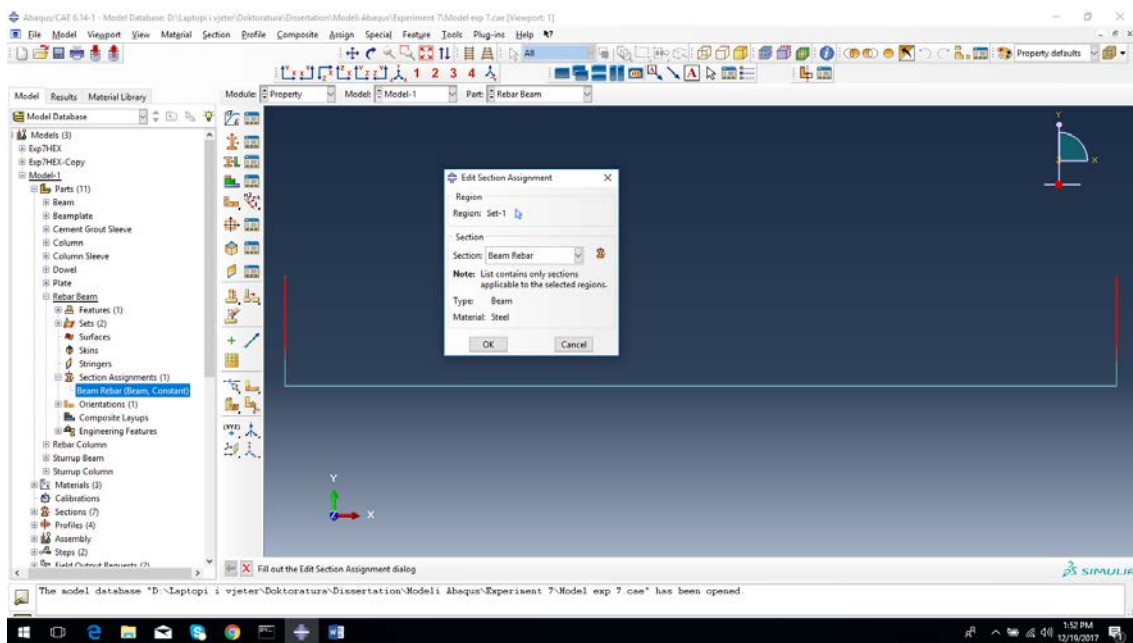


Fig. 5.7. Print screen shot of the modeling of the rebar element.

#### 5.4.1 Solid Elements

The principle of finite elements is to formulate the problem in to the system of algebraic equations.



In the library of ABAQUS application of solid elements are of two and three dimensional application. The solid element library includes isoparametric elements: quadrilaterals in two dimensions and "bricks" (hexahedra) in three dimensions which are more often preferred.

In fig.5.8 are presented isometric parametric elements

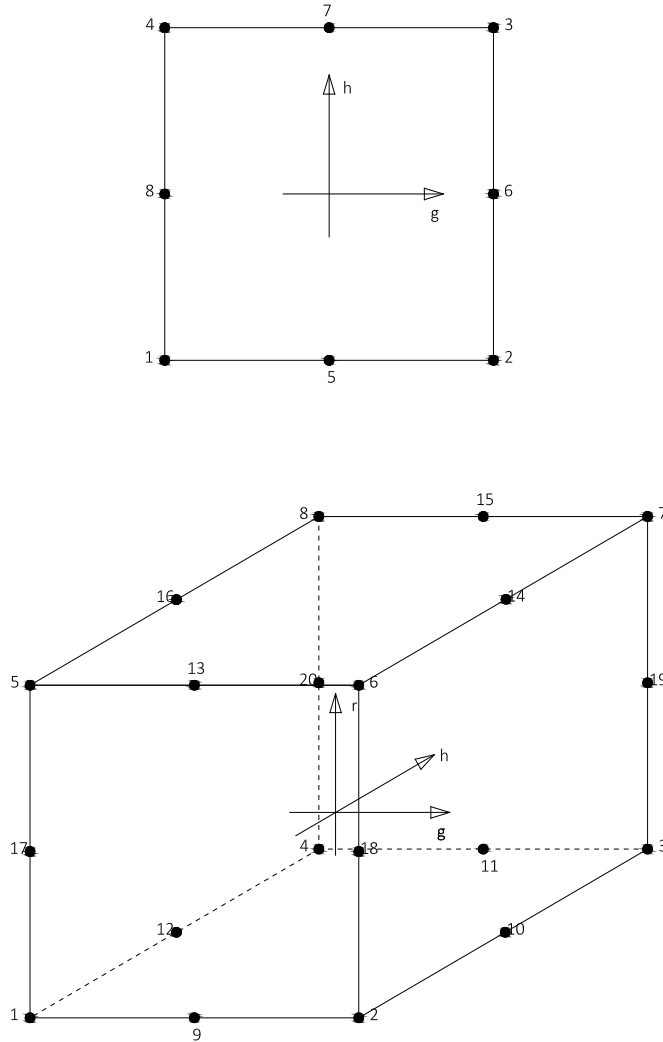


Fig. 5.8 Isometric parametric elements

Isoparametric interpolation is defined in terms of the isoparametric element coordinates,  $g, h, r$ , fig.5.8 since ABAQUS is a Lagrangian code. They each span the range -1 to +1 in an element.

Bellow are presented interpolation functions for first-order quadrilateral, second order quadrilateral and 20 nods brick:

a) First-order quadrilateral:

$$u = \frac{1}{4}(1-g)(1-h)u_1 + \frac{1}{4}(1+g)(1-h)u_2 + \frac{1}{4}(1+g)(1+h)u_3 + \frac{1}{4}(1-g)(1+h)u_4 \quad (5.1)$$

b) Second –order quadrilateral:

$$u = -\frac{1}{4}(1-g)(1-h)(1+g+h)u_1 - \frac{1}{4}(1+g)(1-h)(1-g+h)u_2 - \frac{1}{4}(1+g)(1+h)(1-g-h)u_3 - \frac{1}{4}(1-g)(1+h)(1+g-h)u_4 + \frac{1}{2}(1-g)(1+g)(1-h)u_5 + \frac{1}{2}(1-h)(1+h)(1+g)u_6 + \frac{1}{2}(1-g)(1+g)(1+h)u_7 + \frac{1}{2}(1-h)(1+h)(1-g)u_8 \quad (5.2)$$

c) 20 nods brick:

$$u = -\frac{1}{8}(1-g)(1-h)(1-r)(2+g+h+r)u_1 - \frac{1}{8}(1+g)(1-h)(1-r)(2-g+h+r)u_2 - \frac{1}{8}(1+g)(1+h)(1-r)(2-g-h+r)u_3 - \frac{1}{8}(1-g)(1+h)(1-r)(2+g-h+r)u_4 - \frac{1}{8}(1-g)(1-h)(1+r)(2+g+h-r)u_5 - \frac{1}{8}(1+g)(1-h)(1+r)(2-g+h-r)u_6 - \frac{1}{8}(1+g)(1+h)(1+r)(2-g-h-r)u_7 - \frac{1}{8}(1-g)(1+h)(1+r)(2+g-h-r)u_8 + \frac{1}{4}(1-g)(1+g)(1-h)(1-r)u_9 + \frac{1}{4}(1-h)(1+h)(1+g)(1-r)u_{10} + \frac{1}{4}(1-g)(1+g)(1+h)(1-r)u_{11} + \frac{1}{4}(1-h)(1+h)(1-g)(1-r)u_{12} + \frac{1}{4}(1-g)(1+g)(1-h)(1+r)u_{13} + \frac{1}{4}(1-h)(1+h)(1+g)(1+r)u_{14} + \frac{1}{4}(1-g)(1+g)(1+h)(1+r)u_{15} + \frac{1}{4}(1-h)(1+h)(1-g)(1+r)u_{16} + \frac{1}{4}(1-r)(1+r)(1-g)(1-h)u_{17} + \frac{1}{4}(1-r)(1+r)(1+g)(1-h)u_{18} + \frac{1}{4}(1-r)(1+r)(1+g)(1+h)u_{19} + \frac{1}{4}(1-r)(1+r)(1-g)(1+h)u_{20} \quad (5.3)$$

Solid elements are provided with first-order (linear) and second-order (quadratic) interpolation where the second order is preferred.

All solid elements are written to include fine-strain elements. The strain are calculated as integral of the rate of the deformation:

$$D = sym\left(\frac{\partial v}{\partial x}\right) \quad (5.4)$$

, where  $D$  is rate of deformation,  $v$  is velocity and  $x$  is spatial coordinates of the point.

For kinematic linear analysis the strain is defined as:

$$\varepsilon = sym\left(\frac{\partial u}{\partial X}\right) \quad (5.5)$$

, where  $u$  is displacement and  $X$  is spatial position

#### 5.4.2 Beam Elements

The “beam” element is used in the contest where the problem is reduced to one dimensions where the primary solution variables are function along the axis only.

For the assumptions where the plane cross section initially normal to the axis of the means remains normal Euler-Bernoulli classic theory is applied. For the beam elements that use linear and quadratic interpolation that also allow "transverse shear strain"; the cross-section are not normal to the beam axis. In such a case Timoshenko beam theory (Timoshenko, 1956) is applied.

For the numerical modeling of the specimens of this research the Euler-Bernoulli classic theory is applied. In the elements it is assumed that the internal virtual work rate is associated with axial strain and torsional shear.

The internal virtual work associated with axial stress is:

$$\partial W_1^I = \int_{L^f} \int_A \sigma^f \partial \varepsilon^f dA f L^f \quad (5.6)$$

, where  $\sigma^f$  and  $\partial \varepsilon^f$  are material stress and strain associated with axial deformations of the beam.

Following application of Green strain and further development the expression of the virtual work is:

$$\partial W_1^I = \int_L [\delta \varepsilon \int_A \sigma^f dA - \delta K_2 \int_A g \sigma^f dA + \delta K_1 \int_A h \sigma^f dA + \delta e_1 \int_A \tau^f r dA] dL \quad (5.7)$$

, where  $K_1$  and  $K_2$  are axial strain,  $e_1$  is torsional strain.

### 5.4.3 Rebar modeling in three dimension solid element

The rebar is integrated using 2x2 or 1x1 Gauss points. The volume of integration at a Gauss point is:

$$\Delta V = \frac{A_r}{S_r} \left| \frac{\partial X}{\partial r_1} \times \frac{\partial X}{\partial r_2} \right| W_N \quad (5.8)$$

, where  $A_r$  – is cross-sectional area of each rebar,  $S_r$  is the rebar spacing,  $W_N$  is the Gauss weighting associated with the integration point,  $X$  is the position of the Gauss point.

$$\frac{\partial X}{\partial r_\alpha} = \frac{\partial X}{\partial g_i} \frac{\partial g_i}{\partial r_\alpha} \quad (5.9)$$

The strain in the rebar is:

$$\varepsilon = \frac{1}{2} \ln\left(\frac{g}{G}\right) \quad (5.10)$$

, where

$$g = \frac{\partial x}{\partial t} * \frac{\partial x}{\partial t} \quad (5.11a)$$

and

$$\frac{\partial x}{\partial t} = \frac{\partial x}{\partial r_i} * \frac{\partial r_i}{\partial t} \quad (5.11b)$$

### 5.4.4 Procedure for modeling reinforced concrete elements model used for reinforcement and concrete

The reinforced concrete elements in ABAQUS are modeled by combining standard elements by using plain concrete with rebar elements as one dimensional elements that are solved with one dimensional theory. The rebar are embedded in the plain concrete where are superposed on the mesh of the plain concrete. Behavior of the rebar is described by standard metal plasticity models. This modeling approach allows concrete behavior to be considered independently.

#### 5.4.4.1 Metal elasto-plasticity model

In ABAQUS main options for modeling metal plasticity are between rate-independent and rate-dependent plasticity, Mises yield surfaces for isotropic materials and Hills yield surfaces for anisotropic materials and a option between isotropic and kinematic hardening.

Rate-independent plasticity is used in modeling response of metal with low temperature and low strain.

For rate-dependent there are two types of modeled. In the first model the yield strength is introduced in material model. This model is to be used for high strain rate application such as dynamic loading.

Hardening theory is presented with two models. Isotropic hardening with Bauschinger effect that is used for dynamic problems involving large plastic strains. Another model that is used for low strain amplitude is kinematic hardening model.

##### a) Isotropic elasto-plastic material model

This material model is used for common metal plasticity calculations for either rate-independent or rate-dependent models.

The strain rate decomposition is:

$$\varepsilon = \varepsilon^{el} + \varepsilon^{pl} \quad (5.12)$$

The elasticity of metals is written with parameters bulk module K and shear module G.

$$K = \frac{E}{3(1-2\nu)} \quad (5.13)$$

and

$$G = \frac{E}{2(1+\nu)} \quad (5.14)$$

The elasticity can also be written in deviatoric components.

$$S = 2Ge^{el} \quad (5.15)$$

Following further development of expressing, the final expressions for uniaxial stresses is:

$$\sigma = \frac{3}{2}S \quad (5.16)$$

Final expression for stiffness for uniaxial stress is:

$$\partial\sigma = \left[\frac{3}{2}Q - R\sigma^2\right]\partial\varepsilon \quad (5.17)$$

#### 5.4.4.2 Inelastic model for concrete – Concrete damage plasticity

##### a) Stress-strain relation

Stress-strain relation are governed by scalar damage plasticity:

$$\sigma = (1 - d)D_0^{el} : (\varepsilon - \varepsilon^{el}) = D^{el} : (\varepsilon - \varepsilon^{el}) \quad (5.18)$$

, where  $D^{el}$  is undamaged elastif stiffness of material ,  $D^{el} = (1 - d)D_0^{el}$  is degraded elastic stiffness and d is scalar stiffness degradation variable.

Following continuum damage mechanics the effective stress is:

$$\bar{\sigma} = D_0^{el} : (\varepsilon - \varepsilon^{pl}) \quad (5.19)$$

The Cauchy stress is related to effectivr stress through the scalar degradation relation:

$$\sigma = (1 - d)\bar{\sigma} \quad (5.20)$$

, where the factor  $(1 - d)$  represent the ratio of effective load carrying area to overall section area.

##### b) Hardening variable

The expression of hardening variable is:

$$\tilde{\varepsilon}^{pl} = \begin{bmatrix} \tilde{\varepsilon}_t^{pl} \\ \tilde{\varepsilon}_c^{pl} \end{bmatrix}; \quad (5.21a)$$

$$\dot{\tilde{\varepsilon}}^{pl} = h(\sigma, \tilde{\varepsilon}^{pl}) \cdot \dot{\varepsilon}^{pl} \quad (5.21b)$$

The elastic-plastic response of concrete damaged plasticity model is described in terms of the effective stress and the hardening variables:

$$\bar{\sigma} = D_0^{el} : (\varepsilon - \varepsilon^{pl}) \in \{\bar{\sigma} | F(\bar{\sigma}, \tilde{\varepsilon}^{pl}) \leq 0 \} \quad (5.22)$$

$$\dot{\tilde{\varepsilon}}^{pl} = h(\sigma, \tilde{\varepsilon}^{pl}) \cdot \dot{\varepsilon}^{pl} \quad (5.23)$$

$$\dot{\tilde{\varepsilon}}^{pl} = \lambda \frac{\partial G(\bar{\sigma})}{\partial (\bar{\sigma})} \quad (5.24)$$

, where the  $\lambda$  and F obey Kuhn-Tucker conditions:  $\lambda F=0, \lambda \geq 0, F \leq 0$

##### c) Damage and stiffness degradation of uniaxial conditions

Stress-strain curves can be converted into stress versus plastic strain curves of the form:

$$\sigma_t = \sigma_t(\tilde{\varepsilon}_t^{pl}, \dot{\tilde{\varepsilon}}_t^{pl}, \theta, f_i) \quad (5.25)$$

$$\sigma_c = \sigma_c(\tilde{\varepsilon}_c^{pl}, \dot{\tilde{\varepsilon}}_c^{pl}, \theta, f_i) \quad (5.26)$$

, where t refers to tension and c refers to compression, whereas  $\dot{\tilde{\varepsilon}}_t^{pl}$  and  $\dot{\tilde{\varepsilon}}_c^{pl}$  are equivalent plastic strain rates

$$\bar{\varepsilon}_t^{pl} = \int_0^t \dot{\varepsilon}_t^{pl} dt, \text{ and} \quad (5.27)$$

$$\bar{\varepsilon}_c^{pl} = \int_0^t \dot{\varepsilon}_c^{pl} dt \quad (5.28)$$

Under uniaxial loading conditions the effective plastic strain are given:

$$\dot{\varepsilon}_t^{pl} = \dot{\varepsilon}^{pl}, \text{ in uniaxial tension and}$$

$$\dot{\varepsilon}_c^{pl} = \dot{\varepsilon}^{pl}, \text{ in uniaxial compression.}$$

In the fig. 5.9 is presented diagram of response of concrete to uniaxial tension (a) and compression (b)

As shown in figure 5.9, when the concrete specimen is unloaded from any point on the strain softening branch of the stress-strain curves, the unloading response is observed to be weakened: the elastic stiffness of the material appears to be damaged (or degraded).

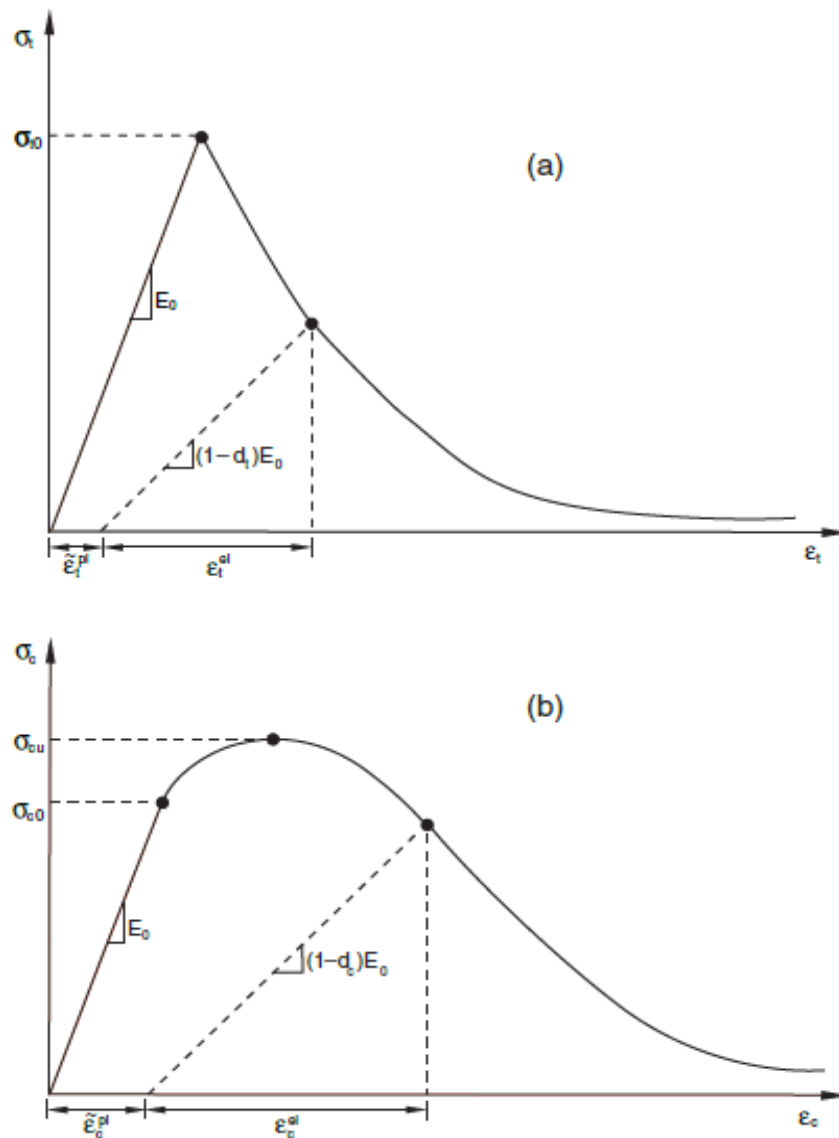


Fig.5.9 Response of concrete to uniaxial loading in tension (a) and compression (b).

If is the initial (undamaged) elastic stiffness of the material, the stress-strain relations under uniaxial tension and compression loading are, respectively:

$$\sigma_t = (1 - d_t)E_0(\varepsilon_t - \bar{\varepsilon}_t^{pl}) \quad (5.29)$$

$$\sigma_c = (1 - d_c)E_0(\varepsilon_c - \bar{\varepsilon}_c^{pl}) \quad (5.30)$$

The effective uniaxial cohesion stresses  $\bar{\sigma}_t$  and  $\bar{\sigma}_c$ , after crack propagation and reduction of load bearing capacity and the considerable amount of concrete crushing, are:

$$\bar{\sigma}_t = \frac{\sigma_t}{(1-d_t)} = E_0(\varepsilon_t - \bar{\varepsilon}_t^{pl}) \quad (5.31)$$

$$\bar{\sigma}_c = \frac{\sigma_c}{(1-d_c)} = E_0(\varepsilon_c - \bar{\varepsilon}_c^{pl}) \quad (5.32)$$

The effective uniaxial cohesion stresses determine the size of the yield (or failure) surface.

#### 5.4.5 Contact modeling

The contact pressure is defined as Hard Contact. The contact is defined between two surfaces at the point,  $p$ , as a function of over closure,  $h$ , of the surfaces.

In the case of hard contact is the following:

$$p = 0 \text{ for } h < 0 \text{ (open), and}$$

$$h = 0 \text{ for } p > 0 \text{ (closed)}$$

The contact constrain is enforced with Lagrange multiplier where the virtual work contribution is:

$$\delta\Pi = \delta p h + p \delta h \quad (5.33)$$

### 5.5 Results from micro-modelling and comparison with experimental results

The models in Abaqus are built up in the same way as they are constructed. The included material properties have been as of the elements used in the experiment and also the strengthening elements, the individual plates and the large plate in the respective specimens.

As the main output results the stress distribution in the connection and the connection elements has been considered. The results of stress distribution have been compared with the performance of the connection from the experiment, the crack pattern and the failure mode. Through observation of the stress development and propagation and their comparison with the experiment, there is a possibility to determine the accuracy of the output results from the modelling and the reliability of the results for the given modeling procedure for further application.

Additional output results is global force-deformation curve plot of specimens, which have been compared with the results from the experiment.

### 5.5.1 Results of stress distribution

Modeling has been performed for each representative case and the stress distribution results are obtained for following specimens:

- For the referent cast in situ specimen, on the specimen
- For the precast connection implemented with grout only
- For the precast connection strengthened with individual plate, and
- For the precast connection strengthened with one large plate

For better illustration, the tension stresses have been left on in order to follow the propagation of these stresses, whereas the compression stresses have been turned off and are shown in the figures with light grey color.

#### a) Comparison of stress distribution on specimen "S 4, R.M."

Fig. 5.10 shows the tension stresses in the referent model. Observing the main crack (failure crack) from the experiment, presented in fig. 5.11, it can be noted that the stresses in the Abaqus model are very close to the ones from the experiment and as such the modelling procedure performed in Abaqus is providing reliable results.

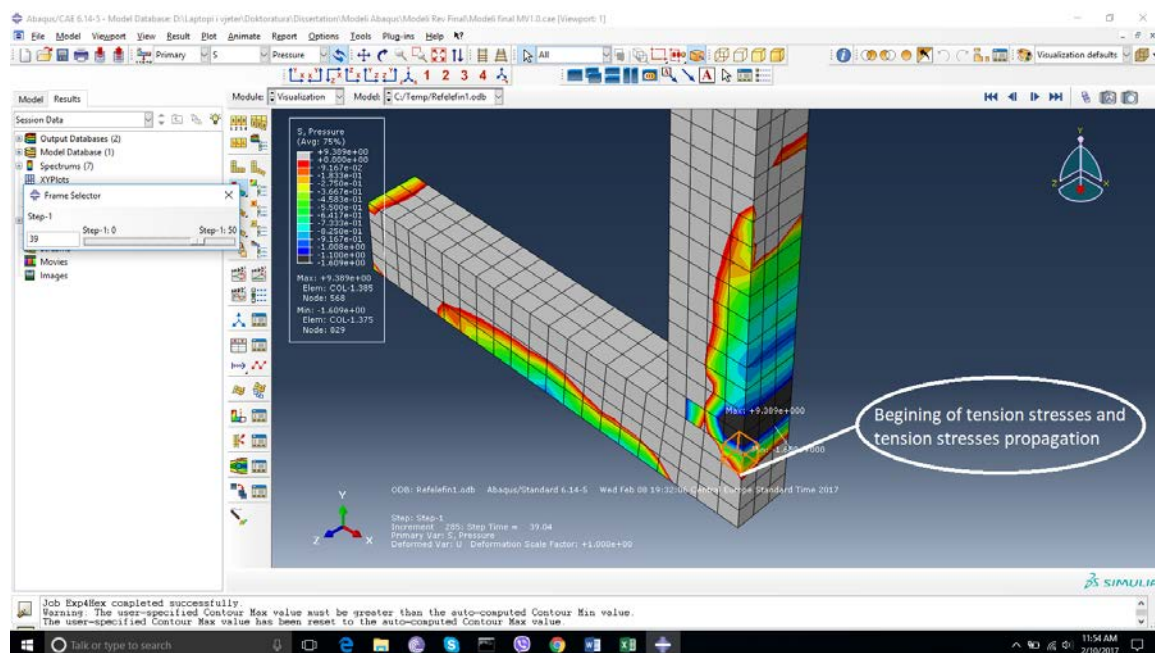


Fig.5.10 Tension stress distribution on referent model specimen S4



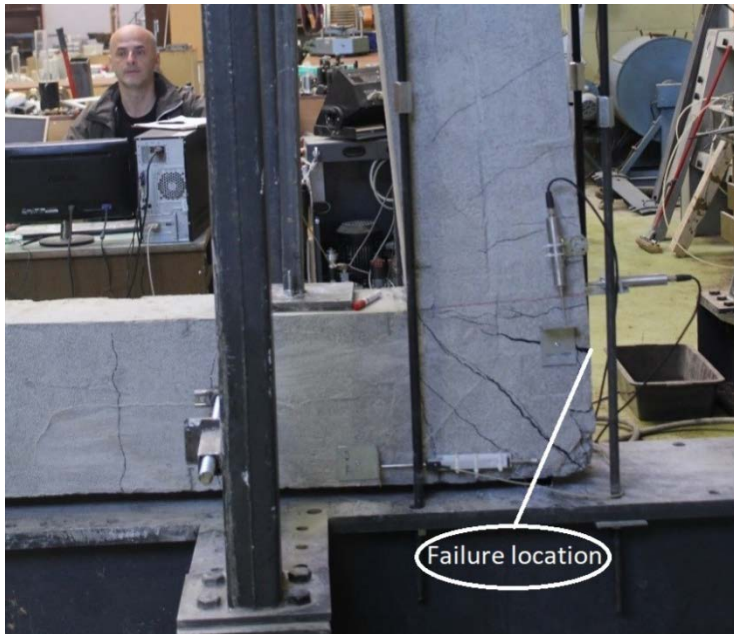


Fig.5.11 Crack distribution on Specimen S4 after failure.

**b) Comparison of stress distribution on specimen "S 2, V.D."**

This is a beam-to-column precast connection realized with dowels only.

Fig. 5.12 shows the stress distribution on the cross-section of the connection, at the dowel level, with force intensity of 92kN. This is the force intensity at which the specimen failed in the experiment.

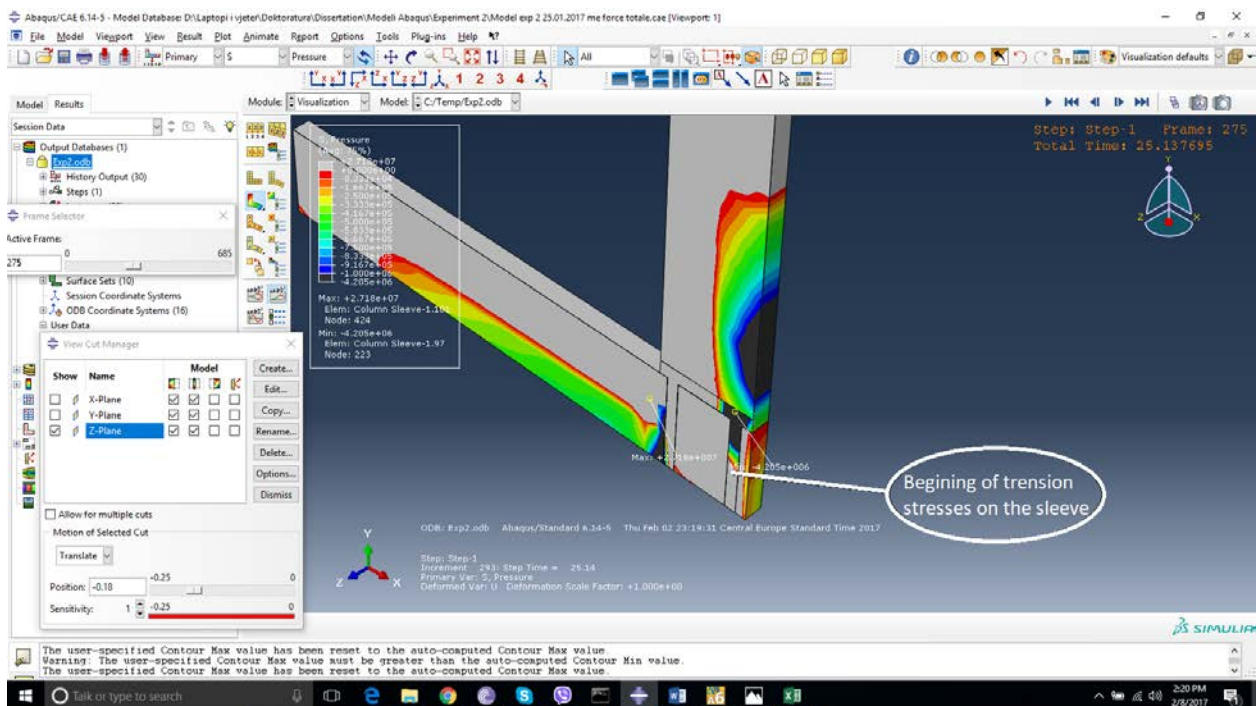
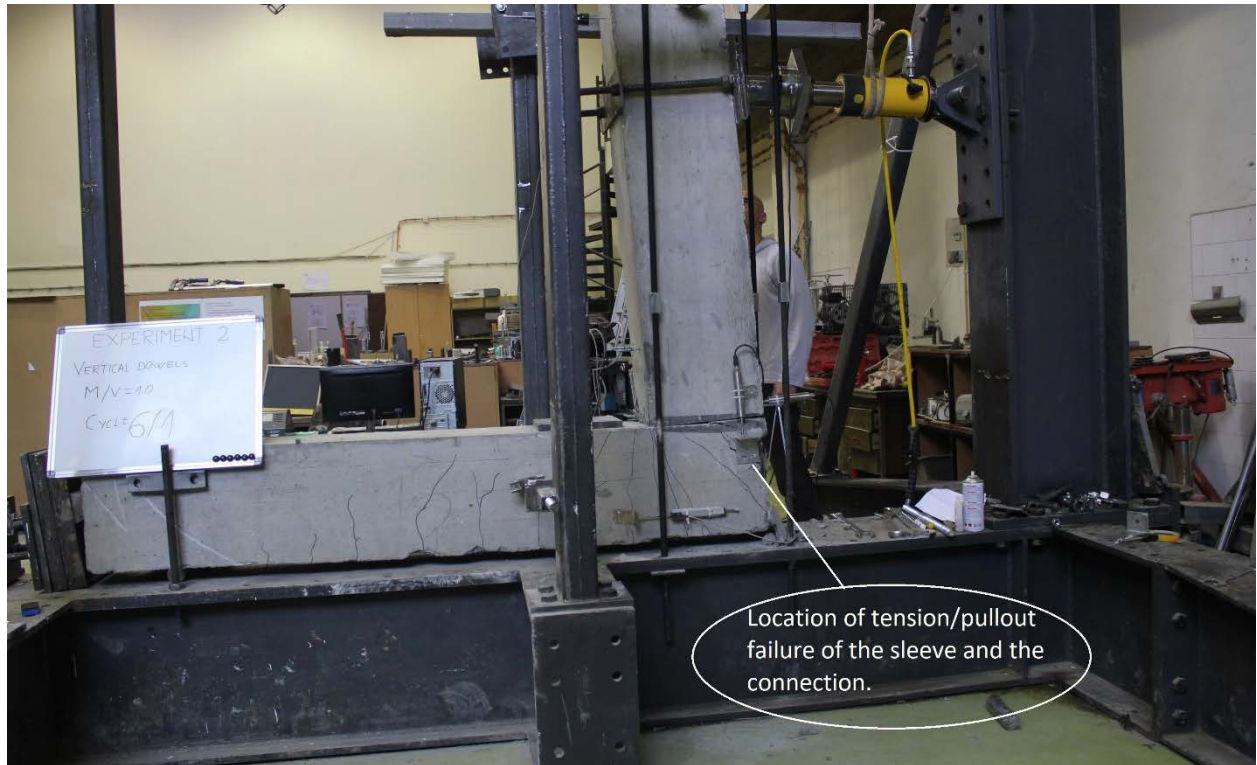


Fig. 5.12 Stress distribution on the cross-section of connection of specimen "S 2, V.D."

While observing the stress distribution in the models, it can be noticed that maximum tension stresses have been built up in the sleeve due to the dowel pull out.

Observing the photo from the experiment on the same specimen, fig. 5.13, we see that there is a similar pattern of stress distribution in the experiment and the model.



*Fig.5.13 Photo of specimen "S 2, V.D." after failure indicating the failure mode of dowel pullout.*

By further observation of damages from the experiment on Specimen S2, it has been noticed that concrete spalling also occurred due to the rotation of the dowels as a result of the rotation of the section. This is presented in fig 5.14.



*Fig.5.14. Concrete spalling in specimen "S 2, V.D." due to rotation of the dowel*

Stress distribution on the model at the cross-section from top view, fig. 5.15, is showing the same pattern as that from the experiment.

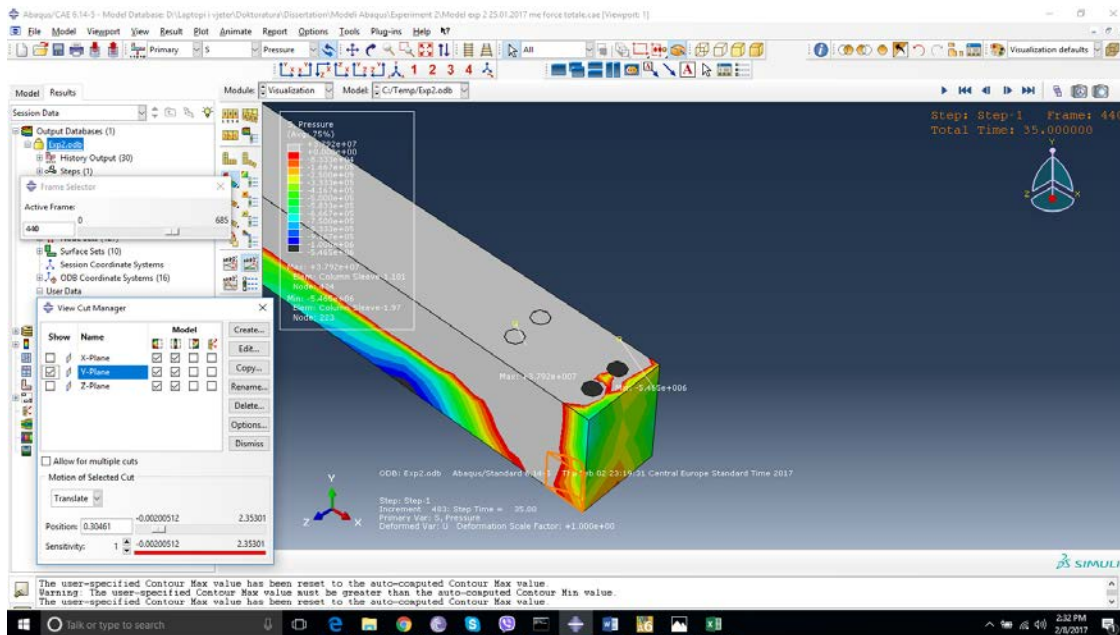


Fig.5.15 Tension stress distribution on specimen “S 2, V.D.” due to rotation of the dowel

**c) Comparison of stress distribution on specimen “S 3, V.D.”.**

This is a beam-to-column precast connection realized with dowels and strengthened with individual plates.

This experiment has been performed on a connection with vertical dowels strengthened by individual plates.

Similar to specimen S2, this connection also failed at the force of 92kN, but the failure mechanism has been completely different. As described in Chapter 4, specimen S3 has not failed due to dowel pullout since this failure has been prevented by implementation of individual strengthening plates on the tension dowels.

Observing the tension stress distribution on the connection at force 92kN, presented in fig.5.16, and comparing with the tension stress distribution presented in fig.5.12 it is noticed that the effect of the strengthening plate preventing the dowel pullout also appears in the Abaqus model. In fig. 5.16, it is visible that the sleeve grout is now almost completely in compression due to the compression applied on the connection from pulling of the plate by the dowels.

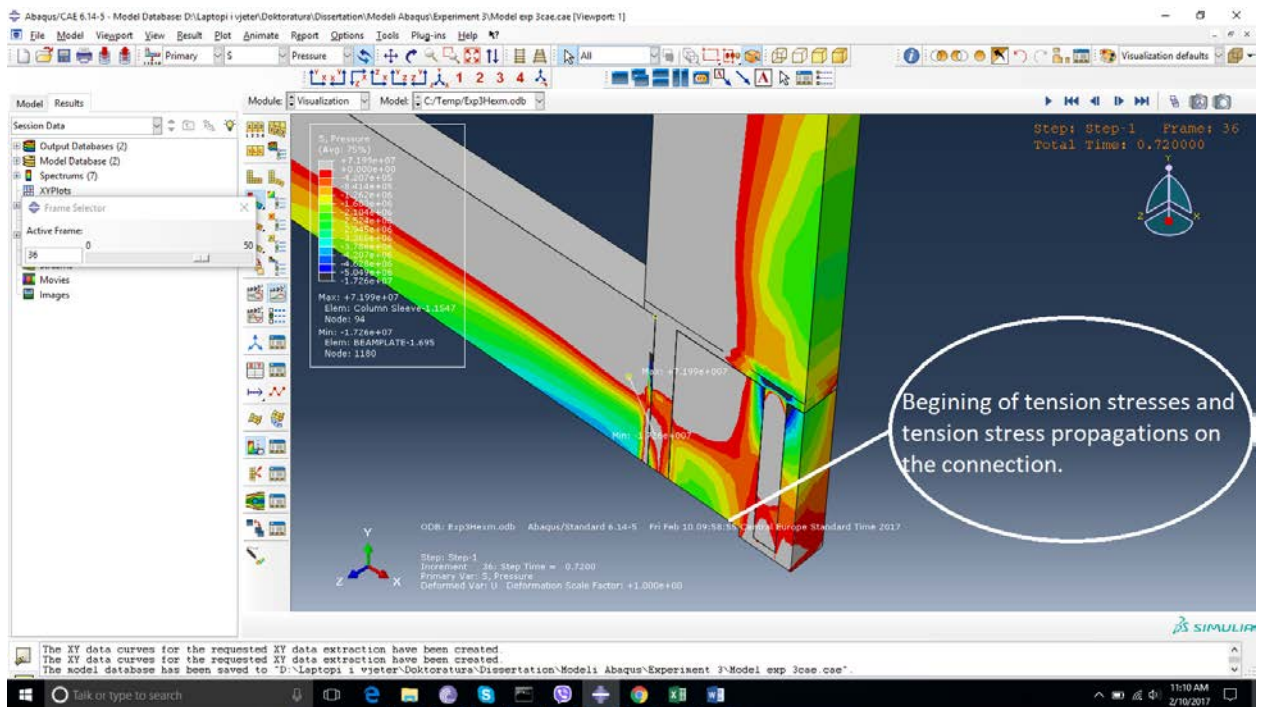


Fig.5.16 Tension stress distribution on specimen "S3, V.D." in x-y cross-section plane.

By observing the photo from the experiment, fig.5.17, on Specimen 3, after failure, one can see the pattern of tension stress distribution on the model, fig. 5.16, with cracks, from the experiment.



Fig.5.17 Crack distribution on specimen "S 3, V.D." after failure.

d) Comparison of stress distribution on specimen "S 7, V.D."

Fig. 5.18 shows the stress distribution on the model of connection strengthened with one large steel plate.

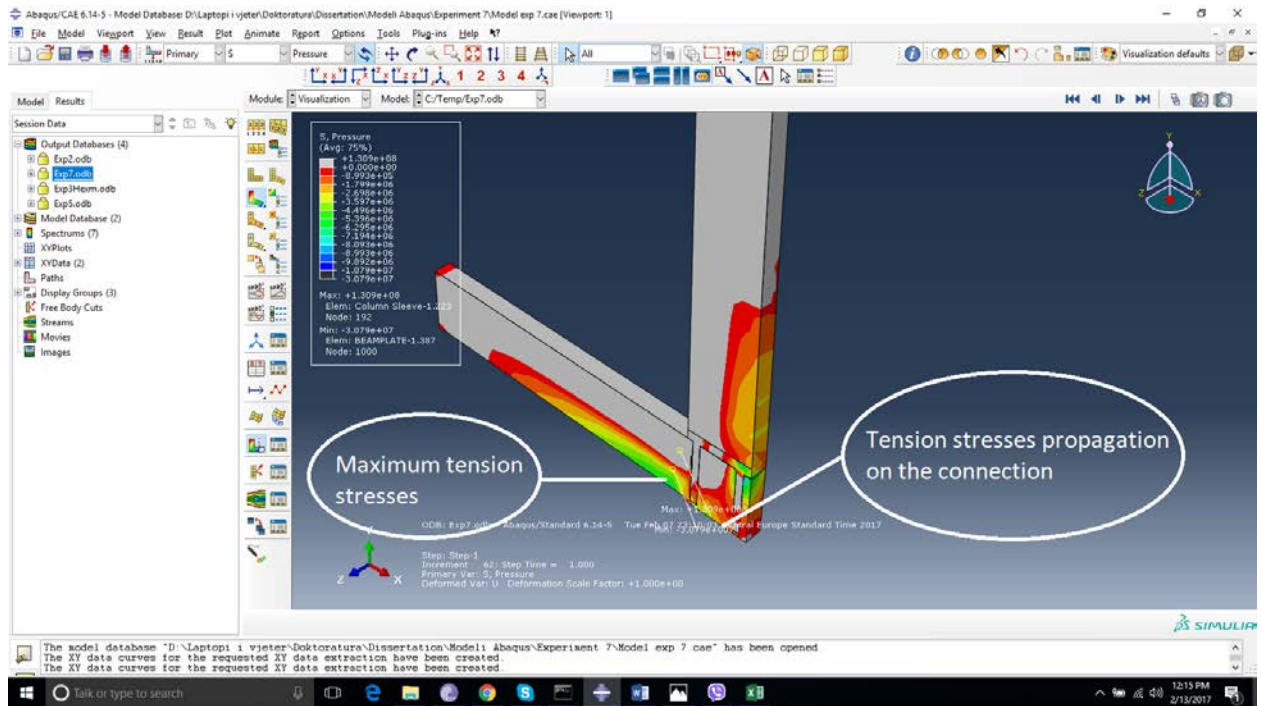


Fig.5.18 Tension stress distribution on concrete element of specimen "S7, V.D." at the grout sleeve cross-section.

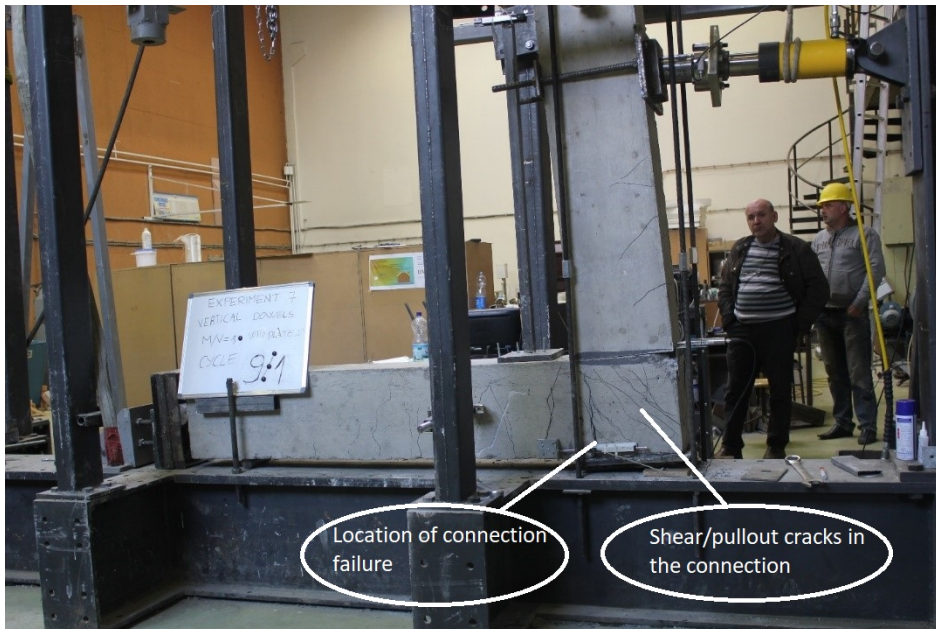


Fig.5.19 Crack distribution on specimen "S 7, V.D." after failure

From comparing the stress distribution on the model, fig. 5.18, with cracks developed in the experiment, fig. 5.19, there are notable similarities on the stress distribution patterns and the crack development patterns on the tested specimen. Also, the maximum tension presented in the model, fig. 5.18, has occurred at the same location as that of the main crack, failure location.

Also in this case the results of modeling are showing the sleeve grout been in compression.

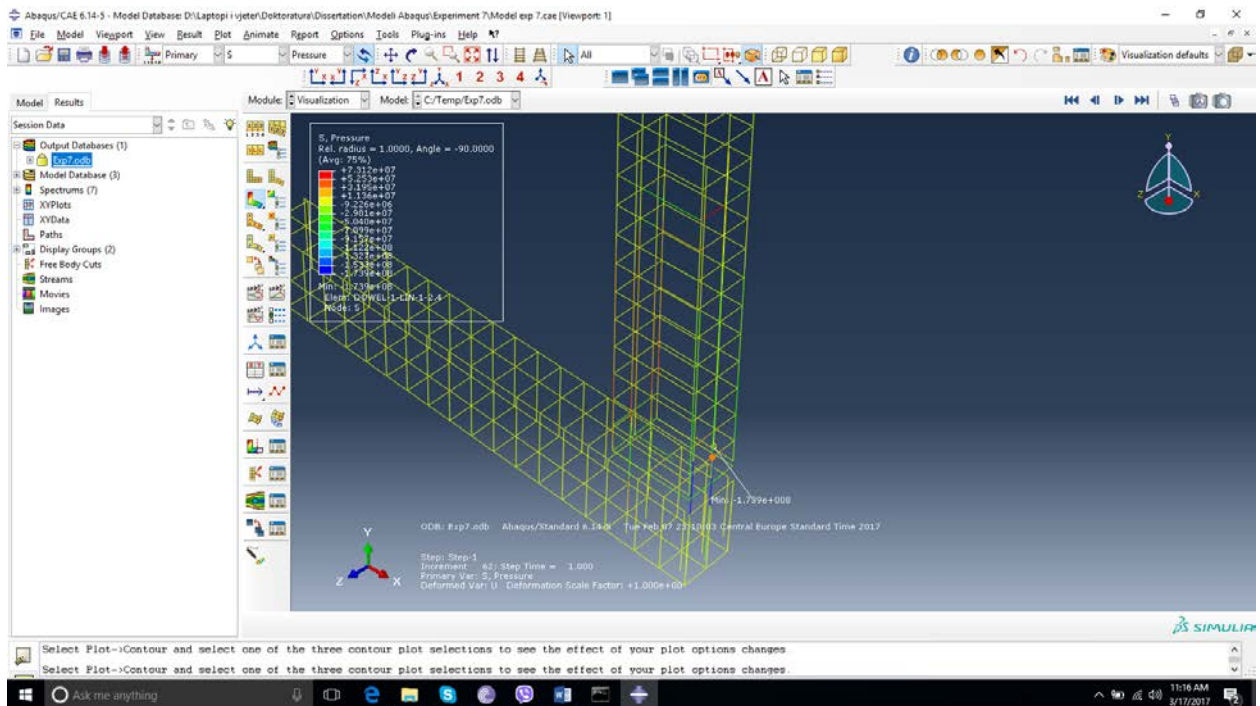


Fig.5.20 Tension of dowels on model specimen "S 7, V.D."

Apart from the accuracy of stress distribution on the concrete element, when stress distribution on the reinforcement and the dowels is observed, fig. 5.20, it is easily noticeable that the maximum stresses develop in the dowels (blue color).

**e) Comparison of stress distribution on specimen "S 9, H.D."**

The tension stress distribution on Specimen S9, H.D - connection strengthened with a large plate and tested with  $M/V=0.5$ , is presented in fig. 5.21. Compared with the crack development at the failure mode, fig. 5.22, there is a similarity in stress distribution in this case, too.

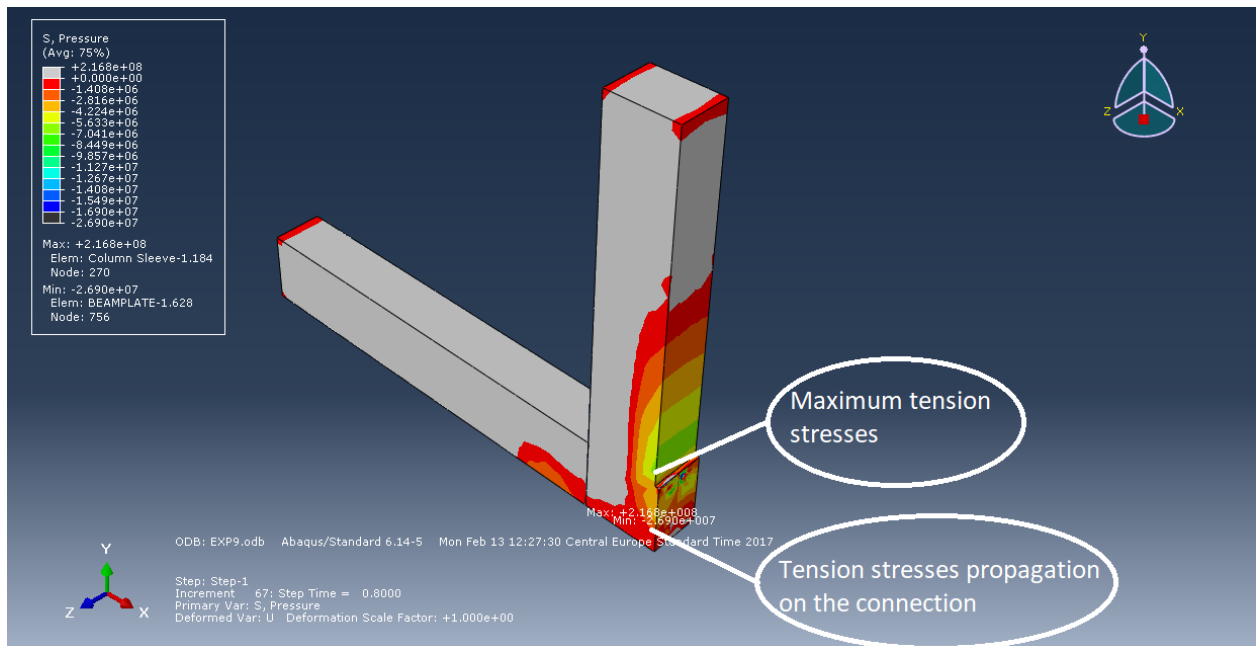


Fig.5.21 Tension stress distribution on concrete element of specimen "S 9, H.D."

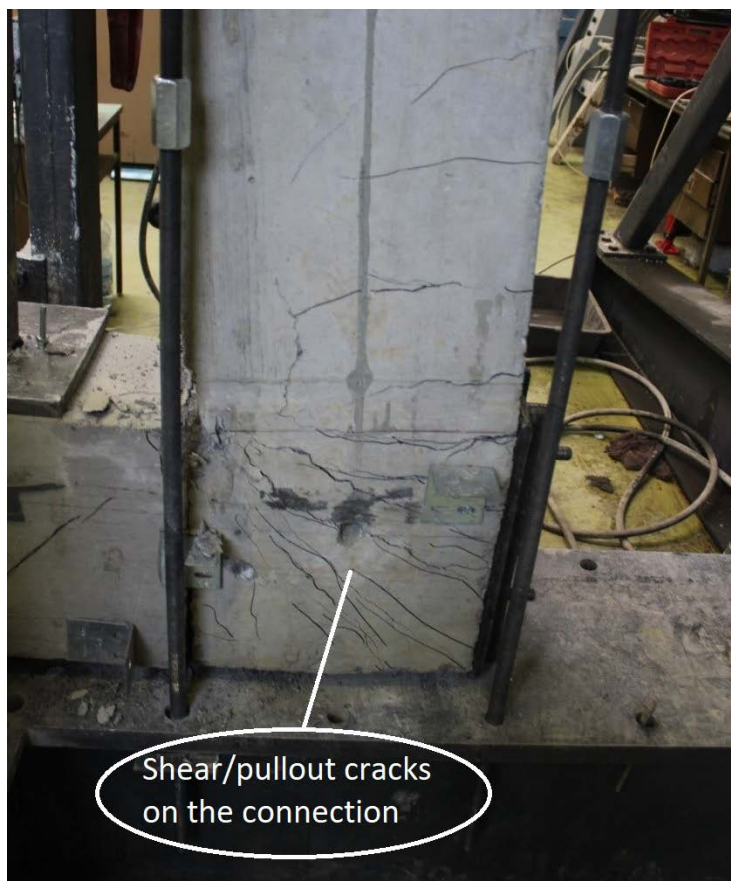


Fig.5.22 Crack distribution on specimen "S 9, H.D." after failure

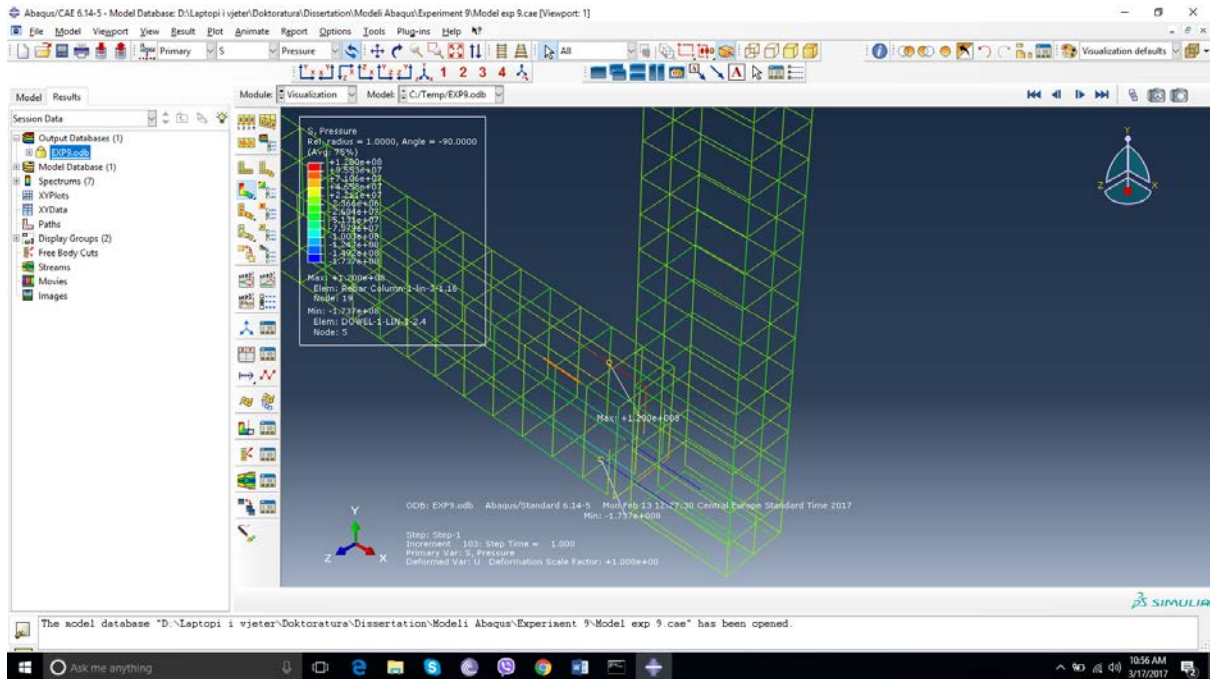


Fig.5.23 Stress on tension and compression dowels of specimen "S 9, H.D."

Also, by observing the stress distribution on the reinforcement and the dowels, fig. 5.23, it can easily be noticed that maximum stresses develop in the dowels (blue color- tension stresses and red color- compression stresses).



### 5.5.2 Results of global behavior

The global behavior results, force-deformation plot, is obtained for two specimens, "S2 V.D" and "S10 V.D" and the same are compared with the results from the experiment. In the fig. 5.24 and fig.5.25 are presented results of model vs. results from experiment for specimen "S2 V.D" respectively for specimen. "S10 V.D".

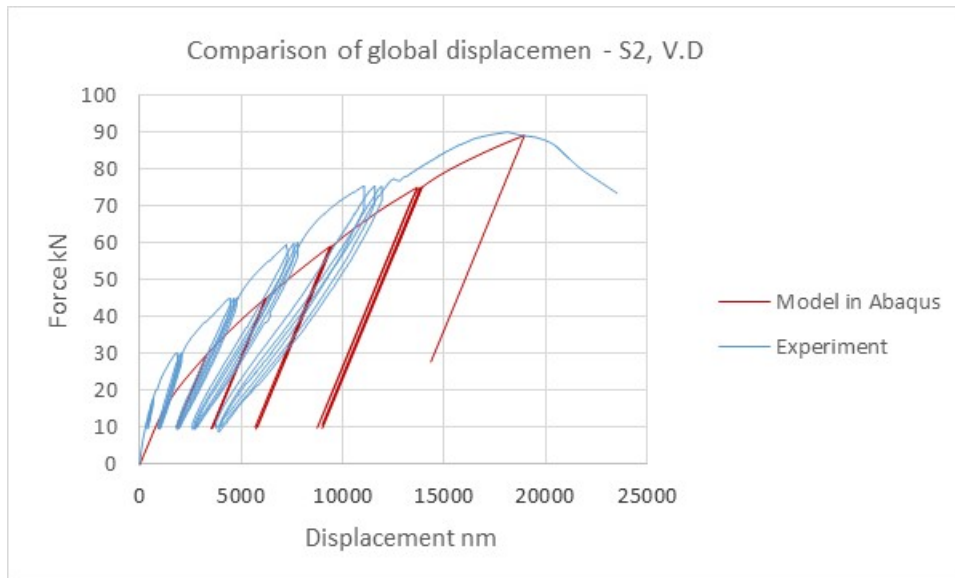


Fig.5.24 Results of force-deformation plot of global displacement from modeling and comparison with results from experiment of specimen "S2, V.D"

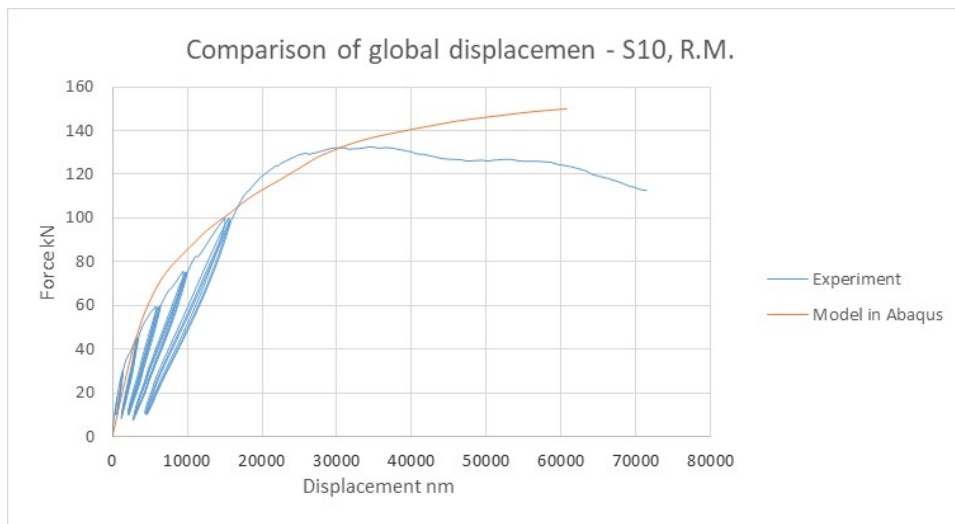


Fig.5.25 Results of force-deformation plot of global displacement from modeling and comparison with results from experiment of specimen "S10, R.M"

## CHAPTER 6 - Conclusions and Recommendations for Further Research

The main goal of the research within the doctoral dissertation has been to investigate performance of dry precast beam-to-column connections, especially moment-resisting ones, by applying scientific approach and using science tools. Practitioner engineers in the field of precast structures and the construction industry in general, should benefit from the outcomes of this research.

The objective of this research are focused on experimental and numerical analysis of innovative moment resisting dry precast beam-to-column connections. Additionally, in order to give better insight in the performance of the most frequent distributed pinned beam-to-column connections in the existing structures, numerical analysis of such connections were carried out, also.

The following investigations were carried out:

- 1) Determining proper modeling for general design purposes of beam-to-column connections realized with centrally positioned dowels. For this research the results of experiments on pinned beam-to-column connections realized in University of Ljubljana (UL), under the SAFECAST Project [Ref.: 027], have been used as input data for calibration of the numerical model.
- 2) Develop innovative moment resisting dry beam-to-column connections simple enough for practical use in engineering practice in precast structures and reliable as monolithic RC joints. For developing such a connections a full scale quasistatic testing of ten specimens, were carried out.
- 3) Determine the most appropriate numerical modeling procedure that will reflect, as accurately as possible, the performance of the connections developed under item 2) as a whole and the behavior of the each separate element in the connection. For this purpose micro modeling is applied and one of the most advanced existing software packages for numerical simulation has been used.

### 6.1 Conclusions referring to modeling procedure of connections realized with single centrally positioned dowel

The goal of this part of the research was to verify whether the connections realized with single centrally positioned dowel could be considered as a hinge connections, from structural point of view, and could this assumption continue further to be applied in engineering practice for design purpose, with necessary reliability.

For proper verification of whether this type of connection should be considered as hinge connection the following is conducted:

- Non-linear modeling of single dowel precast connections has been performed where respective numerical model parameters of the adopted hysteretic model have been properly calibrated using the experimental results conducted in UL under the SAFECAST Project [Ref.: 027]

- Nonlinear dynamic analysis of a beam-to-column connections (under same loading conditions as in experimentally tested within SAFECAST Project) using calibrated non-linear model were carried out and the bending moments of columns at base point were obtained.
- Linear dynamic analysis with elastic hinge element for modeling beam-to-column connection were carried out under same loading history as in the case of non-linear dynamic analysis and the bending moments on the same location column at base point were obtained.
- Finally, analyzing the results from both, non-linear dynamic analysis with non-linear model for the connection and linear dynamic analysis with applying elastic hinge as a beam-to-column connection, comparing time history of the calculates bending moments the following conclusion was drawn:

***Beam-to-column connections implemented with a dowel positioned vertically and in the center of the connection in regards to structural modeling are to be considered as hinge connections.***

In addition to the above conclusion, from analyzing the behavior of the beam-to-column connections implemented by dowels positioned vertically and eccentrically in respect to a plane, it could be concluded that such a way of realizing a connection cannot be considered as pinned connection (hinge). This type of connection should be considered as fixed connection since these dowels prevent rotation of the section. Depending on the actual location of the dowel, fig. 2.6 a) and b), and the strength and deformability of the dowel the degree of fixity of this connection could vary. Whenever such a connection is selected, during the design of precast structure the following should be considered:

- i. In the vicinity of a connected element, the upper zone of the element will be loaded with bending moments and will have to be designed and detailed to resist these bending moments. If the connection is realized as in fig.2.6 b), then the beam in the upper zone will have to be reinforced with proper longitudinal reinforcement to resist moments due to fixity that is provided by the dowel.
- ii. These connections are subject to failure mechanisms of moment resisting connections, such as dowel pullout failure, (similar to Specimen "S 2, V.D") and concrete spalling due to rotation of the dowel wherefore, in order to provide moment resistance to the connection, proper measures against potential failures must be taken.

## **6.2 Conclusions on developed innovative dry moment resisting beam-to-column connections**

The ultimate goal of this part of the research was to develop a moment resisting dry beam-to-column connection whose performance is quite similar to the performance of a moment resisting monolithic beam-to-column connection. In addition, the proposed innovative moment resisting dry beam-to-column connection should be simple enough for construction and application in everyday engineering practice.

For purpose of developing such innovative moment resisting beam-to-column connection a full scale experimental programme has been undertaken, where eight precast specimens were tested. In addition to them and in order to determine whether a proposed connection could be considered as a moment resisting one, two moment resisting cast-in-situ connections have been constructed and

tested. The results of these two cast-in-situ connections, “S4 R.M” and “S10 R.M”, have been used as a reference for developed precast connections.

The precast industrial buildings in real engineering applications could be constructed in different seismic hazard zones, with different frame spans and various loadings, thus beam-to-column connections could be exposed to various ratios of member forces. Depending on these circumstances, there could be a situation when on the precast connection the flexural forces are predominant one, situations when shear forces could be predominant ones and there could be situations when both flexure and shear are equally present. In order to cover these potential situations the experimental programme has been extended to test the developed moment resisting dry beam-to-column connection under different loading situations:

- Flexure/Shear=1.5, where flexure forces are predominant
- Flexure/Shear=0.5, where shear forces are predominant, and
- Flexure/Shear=1.0, where potentially both flexure and shear forces are equally predominant

## 6.2.1 Conclusions based on experimental results

### 6.2.1.1 Connections implemented by dowels only

Two specimens of a connection implemented by dowels only have been tested. One is tested with M/V ratio of 1.0 (S2, V.D.) and the other one is tested with M/V ratio of 1.5 (S6, V.D.). Both connections are designed with vertical dowels (V.D.)

#### a) Specimen S2, V.D.

Specimen S2, V.D. has experienced brittle failure. The flexural strength of the specimen is considerable whereas the deformation capacity is very limited due to nature of failure. The specimen failed since the tension dowels failed in pullout. Below are provided the strength and deformation properties of the specimen S2, V.D. compared by the referent model (S4 R.M.):

- Yielding strength..... **94%** of the referent model
- Ultimate strength..... **88 %** of the referent model
- Total deformability ..... **50 %** of the referent model

#### b) Specimen S6, V.D.

Specimen S2, V.D. has experienced brittle failure. Both, the flexural strength and deformation capacity have been very limited due to nature of failure. The specimen failed since the tension dowels failed in pullout. After close look to the failed specimen it has been noted that mistake was made during the construction of the specimen. The dowels were not completely positioned in the middle of the sleeve. This caused that the area of the dowels that should resist the pullout has been reduced. Below are provided the strength and deformation properties of the specimen S6, V.D. compared by the referent model (S4 R.M.):

- Yielding strength..... **75%** of the referent model
- Ultimate strength..... **70 %** of the referent model
- Total deformability ..... **47 %** of the referent model

- c) General conclusions of connections implemented by dowels only
  - Positive side of connections implemented by dowels only  
If properly constructed, the connections implemented by dowels only could have flexural strength high enough to be considered as similar to cast-in-situ connections,.
  - Negative side of connections implemented by dowels only
    - i. The connections implemented by dowels only have very limited or no deformability capacity.
    - ii. For implementing such a connection, a high construction precision is required where there is a great chance for faults during construction. Very small mistake in construction could result with drop in flexural strength and significant decrease of deformability capacity.

### 6.2.1.2 Connections with dowels strengthened by individual steel plates

Regarding the moment resisting dry beam-to-column connections with dowels and strengthened by individual steel plates on the tension dowels, three specimens have been tested, two with vertically positioned dowels "S1 V.D.", "S3 V.D." and one with horizontally positioned dowel "S5 H.D.". The overall behavior of these three specimens could be considered as flexure behavior with shear force influence. In general these three specimens are characterized with good flexural strength and high deformability capacity. The detailed results of comparison of these connections with referent model are presented in table 4.5.

Comparing the results it could be concluded that strengthening tension dowels with individual steel plates eliminates pullout failure since it transfers tension force on top of the connection, which force then acts as compression force on the connection. This type of performance improvement method has been shown as successful and the performance of such a connections could be considered similar as of a cast-in-situ connection.

- **General conclusions**

- Positive side of these connections
  - i. These connections have both flexural strength and deformability capacity very similar to a reference cast-in-situ connection and as such could be considered as moment resisting.
  - ii. Construction method is very simple and does not require special precision.
- Negative side of these connections  
The tension force that is transferred on top of the connection as compression force on the connection could have negative impact by action as shear force in combining with flexural force. In such a combination connection could experience shear failure of initially flexural behaved section, as did the specimen "S3, V.D.". It should be point out that this consideration is based on observation of single specimen only and shouldn't be taken as general one.

### 6.2.1.3 Connections with dowels strengthened by single large steel plate

Regarding the moment resisting dry beam-to-column connections with dowels and strengthened by a single large steel plate, three specimens have been tested, "S 7 V.D", "S 8 H.D." and "S 9 H.D.",.

All three specimens have experienced pure flexural behavior. In general, these three specimens have provided considerably high amount of flexural strength as well as deformability capacity. The detailed results of comparison of these connections with referent model are presented in table 4.5.

This type of performance improvement method has shown successful and the performance of such a connections could be considered as of a cast-in-situ connections. By applying this method of performance improvement all the negative sides of two previous types of connections, connection implemented by dowels only and connection with dowels strengthened by individual steel plates, are eliminated.

- **General conclusions**

Based on the obtained results the above connections can be considered as full moment resisting connections and can be treated as cast-in-situ connections.

With the application of this strengthening method, the performance of a connection becomes simpler, having in mind that all the forces on the connection are transferred onto the dowels as pair of force. This is a very good attribute since it offers the possibility of calculating the strength of such a connection with a high accuracy and desirable reliability for practical use.

An additional benefit of the connections strengthened by a large plate is the fact that this strengthening method does not require high precision for construction and eliminates the consequences of any possible mistake during the construction of connection, such as, treating the sleeve wall for adequate roughness, miss-positioning the dowel in the center of the sleeve, etc.

### 6.2.1.4 Impact of flexure/shear ratio on precast dry moment resisting beam-to-column connections

In all the connections tested during this research, the effect of  $M/V$  (flexure/shear) haven't any significant impact on the performance of a connections. It could be concluded that the proposed innovative moment resisting dry beam-to-column connections are not affected by shear force and their performance could be considered as flexural.

### 6.2.1.5 Impact of axial force on the precast dry moment resisting beam-to-column connections

Based on conducted testing it has been noted that the increase of axial force caused increasing of the flexural strength of the connection in a similar way as in monolithic reinforced concrete elements.

This fact is important to underline and to consider since with increase of the span of the precast structure frame the  $N/M$  ratio decreases. For proper design of connection and to benefit from positive influence of increasing  $N/M$  ratio on the flexural strength of the connection, the  $M-N$

interaction diagram should be determined. Whenever the N/M ratio passes “balance point” than for vertically positioned dowels the appropriate strengthened method could be implementation of single large steel plate.

### **6.2.2 Conclusions based on numerical analyses**

Moment resisting dry beam-to-column connections are composed of several intermediate elements, such as dowels, sleeve grout and strengthening elements. This composition of connection elements makes these connections rather “mechanical” than typical “structural” connections. Therefore, for the purpose of numerical analysis it is more appropriate to treat these connections as mechanical ones.

The behavior of a connection depends directly of the all elements as an assemblage, as well as of the behavior of each element, taken separately.

The best way for numerical modeling of these innovative moment resisting dry precast beam-to-column connections is micro-modeling since it enables following of the stress distribution within each individual element of the connection. In this way, there is a possibility to map the weak elements in the assemblage and possible failure mechanism of a connection.

The micro-modeling procedure adopted within this research using Abaqus software [Ref.: 001], as presented in chapter 5 of this dissertation, has provided very good results in regard to stress distribution within the connection and the connecting elements when comparing them to the experimental results. Therefore, the modeling procedure adopted herein is appropriate for understanding the overall behavior of a connection and the behavior of each connecting element, separately and the use of such modeling procedure in further innovative developed connections could provide a good indication of their performance and thus reduce the need for experimental testing/verification.

### **6.3 Limitations of the drawn conclusions**

The experimental program is conducted in quasi-static conditions in half cyclic tests. This procedure of half cyclic test could be considered appropriate for outer beam-to-column connections of the frame for the following reason:

In real engineering applications the connection is constantly loaded with gravity loads. When the connection is additionally loaded with lateral loads than the influences from gravity loads and lateral loads will be superimposed. For lateral loads acting in one direction the member forces (bending moments) will have the same “sign” as the bending moments from gravity loads and this will further increased total bending moments, at the location of the connection. When the lateral loads act in opposite direction than the bending moments from lateral loads, at the same considered location, will have different “sign” than the ones of gravity loads which lead to the decreasing of the total bending moment.

Precast industrial structures could be considered gravity load governed structures where the bending moments from gravity loads are usually higher than the ones from lateral loads. Therefore the moments from lateral loads in combination with the ones from gravity loads usually are never high enough to push the connection in reverse cycle. Considering this practical fact, the half cyclic tests

have been considered to be more appropriate and closer to real loading of a connection under real engineering situation in practice.

The one possible situation when there could be a full cycling loading (deformation in both directions) of the connection from lateral loads is in the continuous connections that are located in the middle of the frame in multi-bay frames. Usually, in such a case bending moments from gravity loads are very low. So, the bending moments from lateral loads are predominant and will govern behavior of the connection where the effect of full cyclic loading will be present.

It should be noted that very often precast industrial buildings are one bay frames. Also, in a case of multi-bay frames, most of the inner connections aren't continuous connections but rather the beams are simply supported. In such a case again the principle of outer connection applies.

Based on the above stated the following are the limitations of the tested precast beam-to-column connections:

1. The results and conclusions presented herein couldn't be applied for continuous middle beam-to-column connections.
2. Connections under this research are tested under half cycle quasi-static conditions and despite the fact that in practice outer connections might not be exposed to reverse cycling loads, still their actual performance under real seismic conditions remains assumptive.

## **6.4 Recommendations for further research**

### **6.4.1 Recommendation for further investigation of connections strengthened by a single large steel plate**

Among the proposed innovative connections, this type of connection shown best performance. The connection with this type of strengthening could be considered as full moment resisting connection (structurally fully fixed connection). Considering the importance of moment resisting connections in a structure and the improvement of the seismic performance that a moment resisting connection could offer to precast structures, it is of a great importance to define, with undoubted certainty, a connection that will act as a full moment resisting connection. Nevertheless the performed tests shown that the connection strengthened by a single large steel plate behaved as a full moment resisting connection, it is highly advisable to confirm its behavior with additional experiments in order to prove its moment resisting capacity.

It is of high interest to determine an expression for calculating the strength of a connection which will include the strength of the dowel and the minimum requirements for the strengthening plate. If and when such an expression will be defined as a result of more extensive experimental programme, then this connection could be easily and successfully applied by practitioner engineers in the construction industry.

In this research, through investigation of the behavior of connections strengthened by a single large steel plate, i.e. specimens "S 7 V.D", "S 8 H.D." and "S 9 H.D.", it become obvious that, when the elements are connected face to face, then the factor of surface imperfection can play a role in the



strength capacity of a connection by transferring different loads to the tension dowels. Since faces of elements cannot be treated to have a perfect flat surface, this imperfection in the flatness may have an impact on the location of rotation of the section (neutral axis). Since, in each case, the surfaces of the elements may have a slightly different imperfection, this may affect the position of the neutral axis and consequently it may transfer different force to the tension dowels, each time differently. This is an uncertainty that may become a big obstacle in defining an expression for calculating the strength of a connection and design of a connection.

In order to eliminate this obstacle, a possible investigation could be performed for the case when an intermediate element is placed in-between structural elements, namely, the beam and the column. This intermediate element could be rubber (plain or reinforced rubber) allowing pure transfer of force to the dowels, equally to tension and compressing dowels. However, in this approach, the moment will be transferred to the joint as a pair of forces. Performing experiments with this approach, there is a possibility to confirm an expression for the relation between the moment and the pair of forces and adopt it as an expression for calculating the strength of the dowels in this type of moment resisting connections.

#### **6.4.2 Recommendation for further investigation of connections strengthened without any steel plates**

There could be a situation in structures where a strengthening plate might complicate the construction of the claddings and the roof covering where the dowels should not extend outside the sleeve, respectively, outside the face of the structural elements. In such a situation, the pullout dowel is the potential failure mechanism.

From observation of the performance of the tested specimens and analyzing the failure modes in each case, the following improving methods that could be applied to provide a desired moment resisting behavior:

##### **a) Strengthening performed by a bolt placed inside the sleeve**

Observing the behavior of specimen "S5 H.D." which behaved differently than specimen "S 3 H.D.", there is high possibility that reinforcement bars of a smaller diameter, welded to the dowel for ensuring centering of the dowel within the sleeve, may have an impact on the transferring of the load from the dowel to the connection. These elements, when placed away from the connection section, as in the case of the experiments within this research, may eliminate dowel pullout failure since they transfer the load to the connection from the top of the connection, similar to the strengthening plate.

For simplicity of construction, for preventing pullout failure, the bolt could be placed on the top of the dowel, instead of the three rebar pieces presented in fig. 4.19, by which the tension force would be transferred to the top of the dowel and, in this way, pullout failure will be prevented. This approach could make easier centering of the dowel and simplify overall construction of the connection.

**b) Increasing anchorage length of the dowel**

Anchorage strength of a dowel is in direct function of the length of an anchorage, respectively, the  $l_b/\Phi$  ( $l_b$  – length of anchorage,  $\Phi$  – diameter of dowel) ratio.

For this research, the  $l_b/\Phi=17.5$  ratio has been adopted.

The increasing of this ratio, respectively, the height of the beam elements in the case of vertically positioned dowels and the depth of the column in the case of horizontally positioned dowels, may have a direct impact on improvement regarding the pullout failure.

**c) Use of sleeve grout reinforced with fibers**

Observing damages to connections performed by grout only, specimen “S 2, V.D”, the main cause of failure of the connection was the pullout failure. This failure occurred due to concentration of tension forces in the sleeve due to dowel tension and consequently their transfer from the sleeve to the concrete in the adjacent area.

Application of cement grout reinforced with fibers could eliminate concentration of tension forces in the sleeve by transferring the force from the tension dowel to all the sleeves. This approach may eliminate pullout failure.

**6.4.3 Recommendation for further investigation of connections regarding their seismic performance**

Half-cycling quasi-static testing protocol of the outer beam-to-column connections was adopted within this research. As already explained in item 6.3 above, performance of outer beam-to-column connections of the single story precast industrial structures is governed mainly by gravity loads. When these type of connections are additionally exposed to lateral loads, also the following situation might appear:

- a) When lateral loads act in one direction (e.g positive direction) their flexural effect will superimpose with already existing flexural force from gravity loads, and
- b) When lateral loads act in opposite direction (e.g negative direction) their flexural effect will decrease already existing flexural force from gravity loads.

However, in order to have better understanding of performance of dry precast moment resisting beam-to-column connections exposed to actual seismic loads, full scale shaking table experiments is recommended to be carried out. By performing such type of experiments complete insight in the seismic behavior of these innovative beam-to-column connections will be accomplished.

As a first phase of research it is recommended that the same connections (same geometry, materials and construction methodology) already tested within this dissertation to be investigated under simulated earthquake loads. Further research, as second phase, could cover scaled (2D or 3D) models of frames where these innovative beam-to-column connection will be applied. In such a way a solid base for more relevant conclusion regarding seismic performance of these connections (structures) will be created.

### List of references

Ref.: No.	Reference details
001	ABAQUS. 2014. Finite Element Analysis, V. 6.14. ABAQUS Inc.
002	ABAQUS Theory Manual. Hibbitt, Karlsson & Sorensen, Inc.
003	ABAQUS Theory Manual. SIMULIA
004	Daniel Abrams, Brian Bell, Nick Hyatt, Sharon Wood.(2006). Dynamic Response of Precast Concrete Frames CIVIL ENGINEERING STUDIES Structural Research Series No. 615. A report on research sponsored by the National Science Foundation. Grant Number NSF BCS 93-07666
005	M.H. Arslan, H.H. Korkmaz, F.G. Gulay (2005). Damage and failure pattern of prefabricated structures after major earthquakes in Turkey and shortfalls of the Turkish Earthquake code. Engineering Failure Analysis 13 (2006) 537–557. ELSEVIER.
006	Ninel Alver, Mehmet Efe Selman, Osman Burak Akgun. (2012). The effect of short cantilever beam formation on the structural behavior of precast post-tensioned connections. Construction and Building Materials. ELSEVIER.
007	Dionysios A. Bournas, Paolo Negro, Fabio F. Taucer (2014). Performance of industrial buildings during the Emilia earthquakes in Northern Italy and recommendations for their strengthening. Bull Earthquake Eng (2014) 12:2383–2404 DOI 10.1007/s10518-013-9466-z
008	V. Capozzi, G. Magliulo, G. Fabbrocino and G. Manfredi. (2008). Experimental tests on beam-column connections of precast buildings. 14th WCEE, October 12-17, 2008, Beijing, China.
009	J.J. Castro, H. Imai. 1997. Seismic performance of precast concrete beam-column joints. Earthquake Engineering, Ten World Conference, Balkema Rotterdam.
010	H.-K. Choi, Y.-C. Choi , C.-S. Choi. (2013). Development and testing of precast concrete beam-to-column connections. Engineering Structures . ELSEVIER
011	Mizam DOGAN, Hakan ÖZBAŞARAN, Ayten GÜNAYDIN. (2010). Effect of seismic loading to prefabricated connections. ANADOLU UNIVERSITY JOURNAL OF SCIENCE AND TECHNOLOGY –A; Applied Sciences and Engineering; Cilt/Vol.:11-Sayı/No: 1 : 47-58.
012	Engström, B., Magnusson, J. and Huang Z. (1998). Pull-Out Bond Behavior of Ribbed Bars in Normal and High-Strength Concrete with Various Confinements ACI-International SP-180, Page. 215-242
013	Guidelines for the Use of Structural Precast Concrete in Buildings. Second Edition. Report of a Study Group of the New Zealand Concrete Society and the New Zealand Society for Earthquake Engineering.
014	Neil M. Hawkins, Ph.D.; S. K. Ghosh, Ph.D., FPCI. (2004). Requirements for the Use of PRESSS Moment-Resisting Frame Systems. PCI Journal, March-April 2004.

015	Husain M.Husain, Nazar K. Oukaili, Hakim S. Muhammed. (2009). Dowel action between two concretes. Journal of Engineering, Volume 15 June 2009, Number 2.
016	Manoj K. Joshi, C.V.R. Murty and M. P. Jaisingh. (2004). Cyclic behaviour of precast RC connections. The Indian Concrete Journal (ICJ).
017	F.Karadogan, E.Yuksel, I.E.Bal. (2012). The Seismic Behavior of An Asymmetric Exterior Precast Beam-Column Connection. 15thWCEE Lisboa.
018	Jubum Kim, at al. (2004). Cyclic load testing of precast hybrid frame connections. 13thWCEE, Paper No. 1671
019	C. Mazzotti, L. Vincenzi. (2010). Experimental Investigation on a Beam-Column Node of a Multi-Story, Precast RC System. 14th ECEE.
020	G. Metelli and P. Riva. (2008). Behaviour of a beam to column “dry” joint for precast concrete elements. 14th WCEE.
021	T. Öztürk and Z. Öztürk (2008). Seismic damage observed on prefabricated industrial structures after 1999 earthquakes in Turkey and the protecting mesures. The 14th WCEE, October 12-17, 2008, Beijing, China.
022	A. Palermo, S. Pampanin. (2008). Analysis and simplified designn of precast jointed ductile connections. 14th WCEE, October 12-17, 2008, Beijing, China
023	M. I. Pastrav, C. Enyedi. (2012). Hybrid Moment Frame Joints Subjected to Seismic Type Loading. 15 World Conference of Earthquake Engineering, Lisboa 2012
024	Ioannis N. Psycharis, Harris P. Mouzakis (2012). Assessment of the seismic design of precast frames with pinned connections from shaking table tests. Bull Earthquake Eng (2012) 10:1795–1817 DOI 10.1007/s10518-012-9372-9. Springer Science+Business Media B.V. 2012
025	Paolo Negro and Giandomenico Toniolo. (2012). Design Guidelines for Connections of Precast Structures under Seismic Actions. By the Joint Research Centre of the European Commission <a href="http://xxx.jrc.ec.europa.eu/">http://xxx.jrc.ec.europa.eu/</a>
026	Response 2000, University of Toronto by Evan Bentz. An analysis software for reinforced concrete analysis.
027	SAFECAS (2010). Performance of innovative mechanical connections in precast building structures under seismic conditions. Research Project financed by EU.
028	SAP2000. V. 18. 2015. Computer and Structures Inc.
029	Hiroshi SATO, Kazunori FUJIKAKE and Sidney MINDESS. (2004). Study on dynamic pullout strength of anchors based on failure modes. 13th World Conference on Earthquake Engineering. Vancouver, B.C., Canada. Paper No. 854.

030	H. Shariatmadar and E. Zamani Beydokhti. (2014). An investigation of seismic response of precast concrete beam to column connections: Experimental study. Asian Journal of Civil Engineering (BHRC) VOL. 15, NO. 1 (2014), Pages 41-59.
031	Study Group of the New Zealand Concrete Society and the New Zealand Society for Earthquake Engineering. (1999). Guidelines for the Use of Structural Precast Concrete in Buildings - Second Edition. Published by Centre for Advanced Engineering.
032	H. Shariatmadar, E. Zamani Beydokhti. 2013. An investigation of seismic response of precast concrete beam to column connections. Department of Civil Engineering, Faculty of Engineering, Ferdowsi University of Mashhad, Mashhad, Iran.
033	Do Tien THINH, Koichi KUSUNOKI and Akira TASAI. (2008). Experimental study on a new precast post-tensioned concrete beam column connection system. 14th World Conference on Earthquake Engineering. Beijing, China.
034	The International Federation for Structural Concrete ( <i>fib</i> - Fédération internationale du béton). (2003). Bulletin 27 – “Seismic design of precast concrete building structures”. State-of-art report prepared by Task Group 7.3. Technical Document.
035	The International Federation for Structural Concrete ( <i>fib</i> - Fédération internationale du béton). (2008). Bulletin 43 – “Structural connections for precast concrete buildings”. Guide to good practice prepared by Task Group 6.2.
036	Marco Valente. (2012). Numerical Investigations of the Seismic Response of Precast Buildings with Beam-to-Column Connections with Steel Dowels. IACSIT International Journal of Engineering and Technology, Vol. 4, No. 6, December 2012.
037	R. Vidjeapriya, K.P. Jaya.(2012). Behavior of precast beam-to-column tie-rod connection under cyclic loading. Iset Golden Jubilee Symposium. Indian Society of Earthquake Technology, Department of Earthquake Engineering Building, IIT Roorkee, Roorkee.
038	R. Vidjeapriya, K.P. Jaya. (2012). Behavior of precast beam-column mechanical connections under cyclic loadings. Asian Journal of Civil Engineering (Building and Housing) Vol.13, No. 2, pages 233-245.
039	Ercan Yuksel, at al. (2015). Seismic behavior of two exterior beam–column connections made of normal-strength concrete developed for precast construction. Engineering Structures. ELSEVIER.
040	Li Xu, Jinlong Pan, CKY Leung andWanyun Yin. (2017). Shaking table tests on precast reinforced concrete and engineered cementitious composite/reinforced concrete composite frames. Advances in Structural Engineering 1-14, DOI: 10.1177/1369433217733759. SAGE